


This item is held in Loughborough University's Institutional Repository (<https://dspace.lboro.ac.uk/>) and was harvested from the British Library's EThOS service (<http://www.ethos.bl.uk/>). It is made available under the following Creative Commons Licence conditions.




creative
commons
C O M M O N S D E E D


Attribution-NonCommercial-NoDerivs 2.5

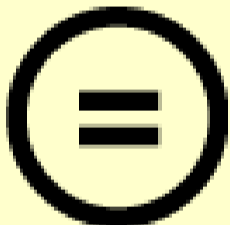
You are free:

- to copy, distribute, display, and perform the work

Under the following conditions:

 **BY:** **Attribution.** You must attribute the work in the manner specified by the author or licensor.


 **Noncommercial.** You may not use this work for commercial purposes.

 **No Derivative Works.** You may not alter, transform, or build upon this work.

- For any reuse or distribution, you must make clear to others the license terms of this work.
- Any of these conditions can be waived if you get permission from the copyright holder.

Your fair use and other rights are in no way affected by the above.

This is a human-readable summary of the [Legal Code \(the full license\)](#).

[Disclaimer](#) 

For the full text of this licence, please go to:
<http://creativecommons.org/licenses/by-nc-nd/2.5/>

ADSORPTIVE STRIPPING VOLTAMMETRIC DETERMINATION OF REACTIVE DYES

BY

AHMAD H. AL-GAMDY

A Ph.D. Thesis
Submitted in Partial Fulfilment of the
Requirements for the Award of

Doctor of Philosophy

**Of
Loughborough University**

August 2000

Supervisor

Dr. Tony E. Edmonds
Senior Lecturer in Analytical Chemistry

Co-Supervisor

Dr. Arnold G. Fogg
Reader in Analytical Chemistry

Department of Chemistry
Loughborough University
UK

© By Ahmad H. Al-Gamdy

ACKNOWLEDGEMENTS

I would like to express my sincere thanks to my supervisor Dr. Tony E. Edmonds for his guidance, invaluable advice, friendly-assistance and attention devoted to this work throughout the period of the study.

Grateful appreciation is also due to my co-supervisor Dr. Arnold G. Fogg for his continuing interest in the research and his helpful discussions, which have contributed greatly to my study.

I am extremely grateful to my wife Suad for her encouragement, emotional support, patience and understanding. Thanks are also dedicated to my children (Sara and Abdulrahman) for their lightening, happiness and inspiration.

I am most thankful to my and my wife's parents and family members for their supplications and prayers for my welfare and success, and for their patience and tolerance during the period my family and I were away from home.

I would also like to thank my colleagues in the analytical laboratory, academic and technical staffs for their kind co-operation and assistance.

I am indebted to King Saud University for its financial support and leave of absence.

Finally, I acknowledge the efforts made by Mrs. Jacky A. Godfrey for word-processing the main text of this thesis.

CONTENTS

CHAPTER ONE: INTRODUCTION TO ADSORPTIVE STRIPPING VOLTAMMETRIC TECHNIQUE	1
1.1 Introduction	1
1.2 Principles of Stripping Techniques	1
1.3 Operational Steps and Stages in Stripping Voltammetry	2
1.3.1 The preconcentration step	2
1.3.2 The equilibration step	3
1.3.3 The analysis step	4
1.4 Stripping Voltammetric Techniques	5
1.4.1 Anodic stripping voltammetry (ASV)	5
1.4.2 Cathodic stripping voltammetry (CSV)	6
1.5 Adsorptive Stripping Voltammetry (AdSV)	7
1.5.1 Principles of AdSV	7
1.5.2 Theoretical basis of quantitative measurements	10
1.5.3 Suitable analytes for AdSV	10
1.5.4 Features and advantages of the AdSV technique	11
1.5.5 Limitations and challenges associated with AdSV	12
1.5.6 Practical applications of AdSV	13
CHAPTER TWO: INTRODUCTION TO REACTIVE DYES	24
2.1 Introduction	24
2.2 History of Reactive Dyes	25
2.3 Classification of Dyes	26
2.4 Structure of Reactive Dyes	27
2.5 Mechanism of Cellulosic Fibre Dyeing (Textile Dyeing)	29
2.6 The Problem of Hydrolysis of Reactive Dyes	30
2.7 Types of Reactive Dyes	31
2.7.1 Azo reactive dyes	31
2.7.2 Anthraquinone reactive dyes	32
2.7.3 Triphenodioxazine reactive dyes	33
2.7.4 Phthalocyanine reactive dyes	34
2.8 Environmental and Health Hazards Associated with Dye Industrial Effluents	35
2.9 Dyehouse Effluent Removal Treatment	36
2.10 Economic Importance of Reactive Dyes	37

CHAPTER THREE: ANALYSIS OF REACTIVE DYES	40
3.1 Introduction	40
3.2 Spectroscopic Methods	40
3.2.1 Visible Spectroscopy	40
3.2.2 UV Fluorescence	41
3.2.3 Infrared Spectroscopy	41
3.2.4 Nuclear Magnetic Resonance Spectroscopy	41
3.2.5 Mass Spectroscopy	42
3.3 Separation Techniques	42
3.3.1 Paper and Thin-layer chromatography	42
3.3.2 HPLC and GLC	42
3.3.3 Electrophoresis	43
3.4 Electroanalytical Determination of Reactive Dyes	43
3.4.1 Amperometric titration	44
3.4.2 Potentiometric titration	45
3.4.3 Coulometric titration	46
3.4.4 Conductivity	46
3.4.5 Polarography	47
3.4.6 Cyclic Voltammetry	49
3.4.7 Adsorptive Stripping Voltammetry	50
CHAPTER FOUR: EXPERIMENTAL	56
4.1 Apparatus	56
4.2 Reagents	57
4.3 Working Procedure	58
CHAPTER FIVE: DIFFERENTIAL PULSE ADSORPTIVE STRIPPING VOLTAMMETRIC DETERMINATION OF REACTIVE BLUE 19 AT THE HMDE	62
5.1 Introduction	62
5.2 Aim of the Study	65
5.3 Mechanism of the Electrochemical Reduction of the Anthraquinone Group	65
5.4 The Differential Pulse-AdSV and Linear Sweep-AdSV Behaviour of RB-19	67
5.5 Cyclic Voltammetric Studies of RB-19	74
5.6 Optimum Experimental Conditions	79
5.6.1 Effect of accumulation time	80
5.6.2 Effect of accumulation potential	80
5.6.3 Effect of pH	82
5.6.4 Effect of reactive dye concentration	84
5.6.5 Effect of supporting electrolyte and boric acid concentrations	84
5.6.6 Effect of scan rate	86
5.6.7 Effect of convection rate	87
5.6.8 Effect of working electrode area	87

5.7 Analytical Application	88
5.7.1 Calibration graph	88
5.7.2 Detection limits	89
5.7.3 Reproducibility	90
5.7.4 Stability	90
5.8 Measurements of the Hydrolysed Reactive Dye	90
5.9 Conclusions	93
CHAPTER SIX: ADSORPTIVE STRIPPING VOLTAMMETRY OF REACTIVE BLUE 19 IN THE PRESENCE OF SURFACTANTS	97
6.1 Introduction	97
6.2 Aim of the Study	99
6.3 Effect of Various Surfactants on the Anthraquinone Reduction Process	99
6.3.1 Effect of Glycerol	100
6.3.2 Effect of Sorbitol	101
6.3.3 Effect of Gelatine	102
6.3.4 Influence of surfactant charge	103
6.4 Influence of Experimental Conditions	108
6.4.1 Effect of pH	108
6.4.2 Effect of supporting electrolytes	111
6.4.3 Effect of T_{acc} and E_{acc} in the presence of surfactant	113
6.5 Analytical Application	115
6.6 Conclusions	117
CHAPTER SEVEN: DETERMINATION OF FLUOROTRIAZINE-BASED AZO REACTIVE DYES BY AdSV AT THE HMDE	120
7.1 Introduction	120
7.2 Aim of the Study	120
7.3 The Electrode Reduction Process of Azo and Fluorotriazine Functional Groups	121
7.3.1 Azo group	121
7.3.2 Fluorotriazine group	122
7.4 The AdSV Behaviour of the Studied Azo-Based Reactive Dyes	123
7.5 Parameters Affecting the Adsorptive Stripping Response	125
7.5.1 Effect of pH	125
7.5.2 Effect of dye molecular structure	128
7.5.3 Effect of accumulation time	130
7.5.4 Effect of accumulation potential	132
7.5.5 Effect of supporting electrolyte constituent	132
7.5.6 Effect of reactive dye concentrations	135
7.6 Analytical Application	135
7.6.1 Calibration graph	135
7.6.2 Detection limits	136
7.6.3 Reproducibility and stability	136

7.7 Hydrolysis Studies	137
7.8 Simultaneous Analysis of Fluorotriazine Dyes in Mixtures	139
7.9 Conclusions	143
CHAPTER EIGHT: CATALYTIC-AdSV DETERMINATION OF FLUOROTRIAZINE-BASED AZO REACTIVE DYES AT A HMDE IN THE PRESENCE OF NICKEL ION	145
8.1 Introduction	145
8.2 Aim of the Study	146
8.3 The Catalytic Reduction Mechanism	146
8.4 Catalytic AdSV Characteristic of Fluorotriazine Dye-Ni (II) Complex	148
8.5 Factors Affecting Catalytic-AdSV of Ni(II)-Dye Complex	152
8.5.1 Effect of pH	152
8.5.2 Effect of accumulation conditions	154
8.5.3 Effect of dye concentration	156
8.5.4 Effect of nickel ion concentration	156
8.5.5 Effect of supporting electrolyte concentration and composition	158
8.5.6 Effect of scan rate	159
8.5.7 Effect of instrumental parameters	160
8.6 Interference	160
8.6.1 Interference by metal ions	160
8.6.2 Interference by surface-active surfactants	161
8.6.3 Interference of complexing agent	161
8.7 Analytical Application	162
8.7.1 Calibration graph	162
8.7.2 Detection limit	163
8.7.3 Reproducibility	163
8.7.4 Stability	164
8.8 Practical Applications	164
8.9 Conclusions	164
CHAPTER NINE: AdSV PROPERTIES OF DOUBLE ANCHOR-BASED BISAZO REACTIVE AT THE HMDE	167
9.1 Introduction	167
9.2 Aim of the Study	167
9.3 Preliminary Studies	168
9.4 Optimum Conditions	174
9.4.1 Effect of pH	174
9.4.2 Effect of accumulation potential	177
9.4.3 Effect of accumulation time	178
9.4.4 Effect of reactive dye concentration	179
9.4.5 Effect of scan rate	181

9.5 Analytical Application	182
9.5.1 Calibration graph	182
9.5.2 Detection limits	183
9.5.3 Reproducibility and stability	183
9.6 Hydrolysis Studies	184
9.7 Conclusions	187
CHAPTER TEN: APPLICATION OF AdSV TO ANALYSIS OF BISAZO REACTIVE DYES BASED ON THEIR COPPER (II) COMPLEXES AT THE HMDE	189
10.1 Introduction	189
10.2 Aim of the Study	189
10.3 Electrode Reduction Process	190
10.4 Adsorptive Stripping Peak of Cu(II)-Reactive Dye	191
10.5 Parameters Affecting Adsorptive Stripping Behaviour	194
10.5.1 Effect of supporting electrolyte constituent	194
10.5.2 Effect of pH	196
10.5.3 Effect of accumulation time and potential	200
10.5.4 Effect of reactive dye concentration	201
10.5.5 Effect of varying Cu(II) concentration	202
10.5.6 Effect of scan rate	203
10.6 Quantitative Utility	205
10.7 Interference Studies	205
10.8 Practical Applications	206
10.9 Conclusions	208
CHAPTER ELEVEN: GENERAL CONCLUSIONS	210
11.1 Final Conclusions	210
11.2 Further Studies	217

ABSTRACT

The present study was mainly devoted to evaluate the applicability of differential pulse adsorptive stripping voltammetry (DPAdSV) for the determination of ultra-trace concentration levels of a range of reactive dyes. The studied reactive dyes were found to adsorb effectively onto the hanging mercury drop electrode (HMDE). This applied electroanalytical method was primarily based on the nonelectrolytic accumulation (adsorption) of the analyte of interest (reactive dye), followed by a cathodic reduction scan measurement. Consequently, the adsorptive stripping voltammograms of the analysed reactive dyes exhibited several useful electrochemical signals, corresponding to the cathodic reduction of the anthraquinone, azo and halo-s-triazine groups.

AdSV has been used successfully for monitoring and studying the electrochemical behaviour of the anthraquinone-based reactive dye (Reactive Blue 19) via its well-developed AdSV peak associated with the two-electron reversible reduction of the anthraquinone moiety. The stripping voltammogram of this reactive dye in alkaline solution displayed a further AdSV peak at a more negative potential, probably related to the cathodic reduction of anthrone product. The reversible characteristic of the first electrochemical wave (anthraquinone wave) was confirmed by cyclic voltammetric studies. Owing to the lack of the AdSV signal for the sulfatoethylsulfone reactive group, the discrimination between the original dye and its hydrolysed form is not feasible. In addition, the present study investigated the influence of several surfactants on the electrochemical response of the anthraquinone group. An inhibition effect arises from the presence of some surface-active molecules, due to the co-adsorption competition for the adsorption sites on the HMDE. In contrast, the addition of Gelatine and anionic surfactant Aerosol OT at low concentrations leads to an enhancement influence on the analytical signal of interest.

Furthermore, the present investigation described an effective means for the analysis of four fluorotriazine-based azo reactive dyes. Two AdSV peaks for the cathodic reduction of the azo functional group and fluorotriazine reactive system were obtained. However, the azo AdSV signal was more analytically useful, due to its well-defined peak shape and large peak current. The variations of the chemical environment around the azo functional centre for these four fluorotriazine reactive dyes have a significant effect on their peak potentials. Moreover, these fluorotriazine reactive dyes

can be monitored indirectly via their catalytic-AdSV response in the presence of nickel (II) ion. The applied procedure is based on the effective accumulation of Fluorotriazine dye/ Ni (II) complex onto the HMDE and the catalytic reduction of this adsorbed complex.

Two double-anchor (bichlorotriazine)-based bisazo reactive dyes (Reactive Orange 12 and Reactive Red 120) were also studied by DPAdSV. In order to evaluate the effect of adding a second azo functional and/or chlorotriazine reactive groups on the AdSV property of these bisazo reactive dyes, their AdSV behaviours were compared with the AdSV behaviours of structurally similar monoazo reactive dyes (Reactive Yellow 84 and Reactive Red 24, respectively). Preliminary studies indicated that for the bisazo reactive dyes, the AdSV signals for the azo and chlorotriazine groups were more enhanced, hence, their stripping voltammetric monitoring is readily achieved. In spite of the direct analysis of these bisazo reactive dyes via their enhanced azo and chlorotriazine AdSV peaks, an indirect analysis of these reactive dyes through their further Cu (II)/Reactive dye complex signals is also possible. Two bichlorotriazine-based bisazo reactive dyes (Reactive Blue 171 and Reactive Red 141) formed Cu(II)/Reactive dye complexes, which effectively adsorbed onto the HMDE. The subsequent stripping voltammetric measurement of the adsorbed complexes yielded a new AdSV peak related to the reduction of Cu (II) in the formed complexes.

List of Abbreviations

AdSV	: Adsorptive Stripping Voltammetry
AQH	: Anthrahydroquinone
AQH ₂	: Anthradihydroquinone
ASV	: Anodic Stripping Voltammetry
B-R	: Britton-Robinson buffer
CB	: Cibacron Blue
CI	: Colour Index
CME	: Chemically Modified Electrode
CSV	: Cathodic Stripping Voltammetry
CV	: Cyclic Voltammetry
CZE	: Capillary Zone Electrophoresis
DC	: Direct current
DMG	: Dimethylglyoxime
DP	: Differential Pulse
EDTA	: Ethylenediaminetetraacetate
GC	: Gas Chromatography
GLC	: Gas Liquid Chromatography
HMDE	: Hanging Mercury Drop Electrode
HPLC	: High pressure liquid Chromatography
IR	: Infrared
LS	: Linear Sweep
MS	: Mass Spectroscopy
NMR	: Nuclear Magnetic Resonance
PB	: Procion Blue
RB-19	: Reactive Blue 19
RB19-OH	: Reactive Blue 19- 2-Hydroxy ethyl Sulfone
RB19-VS	: Reactive Blue 19- Vinyl Sulfone
RB171	: Reactive Blue 171
RO12	: Reactive Orange 12
RR24	: Reactive Red 24
RR120	: Reactive Red 120
RR141	: Reactive Red 141
RY84	: Reactive Yellow 84
RSD	: Relative Standard deviation
SV	: Stripping Voltammetry
TFME	: Thin Film Mercury Electrode
TLC	: Thin Layer Chromatography
TPPC	: Tetraphenyl Phosphonium Chloride
UV	: Ultra Violet

INTRODUCTION TO ADSORPTIVE STRIPPING VOLTAMMETRIC TECHNIQUE

1.1 Introduction

The technique of Stripping Voltammetry has been receiving considerable attention since it is the most sensitive electroanalytical technique, and in recent years it has become a widely used method for trace metal analysis. Actually, interest in stripping analysis has been sparked by its ability to measure simultaneously four to six trace metals at concentration levels down to 10^{-11} M utilising relatively inexpensive instrumentation¹. In fact, the remarkable sensitivity of this approach is attributed to the combination of an effective preconcentration step with advanced measurement procedures that generates extremely favourable signal-to-background measurements in the part per billion range². Usually, in the analysis of very dilute samples, it is often necessary to employ some type of preconcentration step prior to actual analysis, this can be accomplished by the electrochemical deposition of trace analyte from a large volume of solution onto a working electrode, followed by redissolution or “stripping off” the accumulated analyte back to the test solution. Hence, analytical information (quantitative or qualitative) can be obtained during the stripping process.

1.2 Principles of Stripping Techniques

Different versions of stripping analysis can be employed, depending upon the nature of the deposition and measurement steps³⁻⁵. Stripping voltammetric methods encompass a variety of electroanalytical procedures having a common characteristic initial step, in all these procedures, the analyte is accumulated and deposited (preconcentration step) on a working electrode by controlled potential electrolysis and usually with constant convection of the sample solution. After an accurately measured period the electrolysis is discontinued, the stirring is stopped (rest period). This is

followed by the stripping step (measurement step), which involves the dissolution of the deposit. The subsequent stripping of the accumulated species from the electrode occur voltammetrically as a linear voltage ramp is applied to the electrode, generally using one of the direct current, alternating current, or differential pulse modes.

In fact, stripping voltammetric techniques are based on the measurement of current as a function of potential. The current is produced at an electrode surface following the oxidation or reduction of the analyte at a characteristic potential. The current can be considered as the response signal to the potential excitation waveform. By careful interpretation of the peak shape current-potential voltammograms recorded during the stripping step, important and desired analytical information is obtained. The peak potential (position of E_p) is characteristic of the given substance (in analogy to $E_{1/2}$ in classical polarography), and thus it can be used for qualitative identification, whereas the peak current i_p is proportional to the concentration of the corresponding analyte in the test solution. This analytical quantitative information can be obtained from the height (or area) of the stripping voltammetric response signal.

However, a comprehensive treatment and discussion of all aspects and topics effecting stripping voltammetry can be found in several monographs⁶⁻¹².

1.3 Operational Steps and Stages in Stripping Voltammetry

Stripping voltammetric techniques usually involve three operational steps: a preconcentration step (deposition step), an equilibrium step (rest step), and an analysis step (stripping step).

1.3.1 The preconcentration step

In this step the species of analytical interest are reduced or oxidised onto or into an electrode from the bulk of solution to be analysed. The electrolytic preconcentration of the substance is mostly performed at a constant potential. The test solution is usually under reproducible hydrodynamic (mass transport) conditions during the electrolysis to ensure a constant supply of the analyte from the bulk solution. This is usually accomplished by stirring (mainly in conjunction with

HMDE) or flowing (when using mercury film, or solid electrode) the solution, or rotating the working electrode. However, the overall sensitivity and precision are largely dependent on the effectiveness of the hydrodynamic condition.

In general, when mercury electrodes of either type, hanging mercury drop electrode or thin film mercury electrode (HMDE,TFME) are used, the preconcentration step may include deposition into, as well as deposition onto, the surface of the working electrode, whereas, when using a solid inert electrode, deposition is only on the surface of the electrode. However, for the accumulation step, several cases can be considered, depending on the type of electrode reaction: for example; electroplating on solid electrodes, such as the deposition of Ag on a platinum electrode; precipitation of insoluble electrode oxidation products, and amalgam formation as obtained when many of the common metals (lead, cadmium, zinc, nickel, etc.) are reduced onto a mercury electrode¹³. Furthermore, various non-electrolytic (open-circuit) alternative approaches to the deposition step, based on adsorptive accumulation and specific covalent or ion exchange reactions have been used recently⁹.

In stripping measurements, one of the most significant parameters under the control of the analyst is the potential at which the electroactive species are deposited onto the electrode. In addition, the sensitivity of stripping determinations can be increased by prolonging the accumulation time. The duration of the accumulation is selected according to the concentration level of the analyte in question; from less than 1 min at the 10^{-7} mol l⁻¹ level to about 15 min at the 10^{-9} mol l⁻¹ level of analyte.

1.3.2 The equilibration step

After the predetermined time of the preconcentration step, the stirring is stopped and the solution is left to become quiescent to ensure equilibrium and uniform concentration distribution of the analyte in the mercury drop or the thin film working electrode. However, this equilibration step is often omitted, and in a practical analysis is not strictly necessary, but quantitative or theoretical studies on mercury do require it, since a uniform concentration in the mercury or in the solution is necessary.

1.3.3 The analysis step

This step which is also known as stripping or dissolution step, proceeds in the reverse direction to the accumulation method where the analyte of interest is either reduced or oxidised back into the test solution by applying a reverse-scan excitation waveform. During the analysis step, the voltage is ramped to opposite direction, linearly or using another potential-time waveform (differential pulse or square-wave). At the appropriate potential, the accumulated analyte is reoxidised or rereduced. The resulting current-potential curve (see Fig. 1.1) displays a peak with peak potential E_p and peak current i_p , which is proportional to concentration of analyte onto the working electrode and, therefore, to its concentration in the sample solution. The resulting peak current depends upon various parameters of the preconcentration and stripping steps (accumulation time, mass transport, scan rate and accumulation potential), as well as on the characteristics of the analyte (diffusion coefficient) and instrumental adjustment (electrode geometry). Peak potential, on the other hand, serves to identify the analyte in test samples.

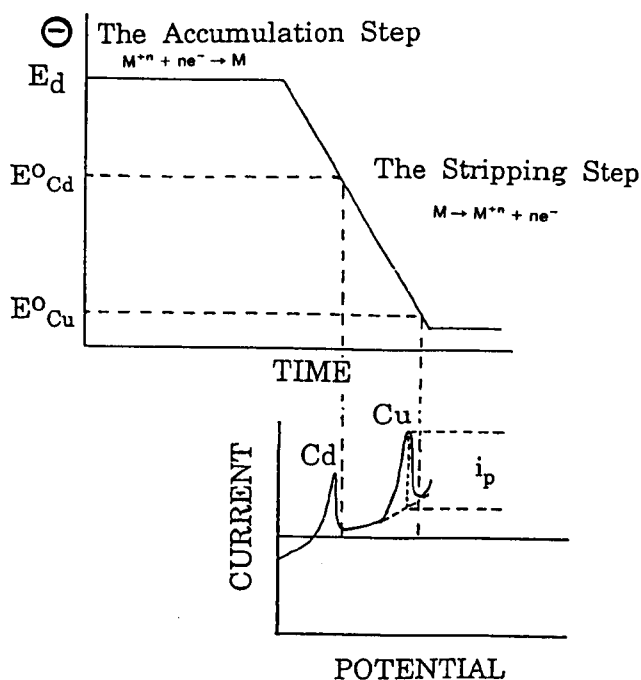
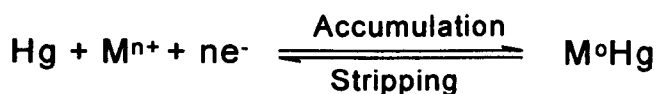


Figure 1.1: The potential-time sequence used in linear scan anodic stripping experiment along with the resulting voltammogram⁹

1.4 Stripping Voltammetric Techniques

1.4.1 Anodic stripping voltammetry (ASV)

This stripping voltammetric method was one of the most known and common versions of stripping analysis, and it has been used for trace analysis with relative ease and success in a variety of analytical applications. The basis of ASV of metals is the electrolytic dissolution of a metal, which previously had been deposited on an electrode⁶. More frequently the metals capable of forming a sufficiently concentrated amalgam with mercury can be preconcentrated by cathodic electrodeposition into a stationary mercury electrode (HMDE or TMFE). The preconcentration is achieved by cathodic deposition at a controlled time and potential. The metal ions reach the electrode surface by diffusion and convection by rotating the working electrode or stirring the solution, where they are reduced and concentrated as amalgams. In the following measurement step, the potential is scanned anodically and linearly. During the anodic scan procedure, the amalgamated metals are stripped out of the electrode, reoxidized, and dissolved back to the bulk of the sample solution. The resulting anodic current is recorded as a function of the applied voltage.



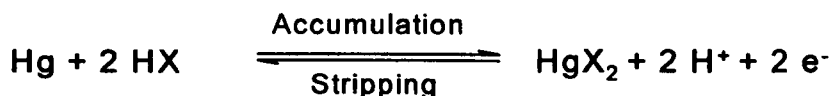
The major disadvantage of ASV is that it only works well for metals that are readily reduced to form amalgams. Materials that are reduced to form insoluble salts on mercury can be tackled with platinum electrodes but less satisfactorily. Moreover, the major types of interferences in ASV are; overlapping stripping peaks caused by a similarity in oxidation potentials, the presence of surface-active organic compounds that adsorb on the Hg electrode, and thus, inhibit the metal deposition, and finally, the formation of intermetallic compounds (e.g. Cu-Zn) which affects the peak size and position. However, various chemical or instrumental strategies have been made available for the elimination or minimisation of these interfering effects.

Applications of ASV: This method is an extremely sensitive electrochemical technique used for trace or ultratrace metals analysis. Those metals, which can be

determined, have high solubility in mercury and form amalgams. About 20 amalgam-forming metals including lead, cadmium, zinc, copper, bismuth, thorium, indium, antimony, tin, manganese, nickel, and gallium are easily measurable by ASV with the mercury electrode. In addition, several noble metal ions such as selenium, arsenic, mercury, gold, and silver are also determinable by ASV using an inert solid electrode (metals such as Ag and Pt or carbon electrode).

1.4.2 Cathodic stripping voltammetry (CSV)

The cathodic stripping voltammetric technique (developed in the mid-1970s) is possible when an anodic reaction can form an insoluble compound (mercury salts or complexes) with the electrode material¹⁴. In this technique, the oxidation of the analyte is used for its preconcentration as an insoluble film on the electrode, subsequently, the concentrated analyte is reduced and measured during a negative-going scan, thus it sometimes known as the “mirror image” of ASV. As in anodic stripping procedures, the solution containing the analyte is usually stirred vigorously during the deposition step. Following the preconcentration step, the deposit is stripped off and measured during the cathodic potential scan. Quantification is accomplished by measuring the height of the resulting reduction peak.



The technique of CSV can be applied to the determination of a wide range of anions (inorganic and organic analytes capable of forming insoluble salts with the electrode material). This is usually requires a mercury working electrodes, although silver electrodes can be used for some species, such as halides or sulfide.

Applications of CSV: This procedure has been applied successfully to sensitive measurements of various organic and inorganic analytes. Among these are ions such as halides, which are measured after forming its precipitation as the silver halides. Sulfide was determined at a rotating silver disk or mercury electrode utilising the formation of Ag_2S and Hg_2S surface compounds, respectively. In addition, iron, manganese, arsenic, copper, phosphate and oxometallates (vanadate, chromate,

tungstate, molybdate) have been analysed indirectly by the technique of CSV. Organic substances can also be determined by this procedure. These are principally sulfur-containing substances, such as thiols (thioureas, thiobarbiturates, thioamides) cysteine, thiourea-containing pesticides, and penicillin. However, various non-sulfur compounds of biological significance such as nucleic acid bases (adenine or guanine), hemoglobin and several drugs have been determined by CSV.

1.5 Adsorptive Stripping Voltammetry (AdSV)

Over the last decade, Adsorptive Stripping Voltammetry (AdSV) has evolved into a very versatile and powerful electroanalytical technique. This method is aimed to extend the scope of the sensitivity and selectivity of stripping analysis toward numerous analytes (organic molecules and metal chelates exhibiting surface-active properties)¹⁶. Based on the wide range of applications reported during the recent years, the adsorptive concept appears to be the most universal stripping approach. When the given substance contains an electrochemically reducible or oxidisable group, the peak current on the voltammetric curve is recorded after completion of the accumulation period. Only tensammetric adsorption peaks are obtained for electroinactive compounds¹⁶.

The adsorption phenomenon of organic compounds onto the electrode surface has traditionally been regarded as a problem that limits voltammetric measurements, and has been blamed for many unexplained results. However, it has been illustrated that controlled adsorptive accumulation of important compounds on the electrode surface can be used to offer certain analytical advantages.

1.5.1 Principles of AdSV

Numerous important analytes are not accessible to conventional stripping measurements because of the electrolytic nature of the preconcentration step (most organic compounds cannot be electrodeposited). Nevertheless, the AdSV method is similar to conventional stripping analysis in that the analyte of interest is initially preconcentrated onto the working electrode prior to its voltammetric measurement, but it differs from the conventional scheme in the way the preconcentration step is

accomplished. In AdSV a spontaneous adsorption at a stationary electrode is purposely utilised as an effective preconcentration step. Hence, for a wide range of surface-active organic and inorganic species that cannot be preconcentrated electrolytically, the adsorption approach allows the analyte to interfacially accumulate on the electrode surface. Therefore, this method is considered as a non-faradaic process i.e. the accumulated analyte does not react with the electrode material and charge is not transferred during the preconcentration step.

The adsorption of the analyte itself is, however, not the only method of accumulation process in AdSV. The reaction of analyte, with a selected reagent added to the sample solution, may lead to the formation of a complex (metal chelates) or a derivative, which is adsorbed, on the electrode. The reaction of the analyte with a reagent, previously adsorbed on the electrode surface (e.g. glassy carbon or carbon paste electrode whose surface has been modified with complexing agents), represent alternative approaches for adsorptive accumulation². In the stripping (measurement) step in AdSV, the adsorbed material is determined by applying a negative or positive going potential scan for reducible or oxidisable species, respectively. Figure 1.2 illustrates the steps involved in AdSV measurement of metal ions, based on the formation, adsorptive preconcentration, and the reduction of its surface-active complex. During the stripping step, different waveforms can be applied including linear scan, differential pulse, alternating pulse, square wave, staircase and subtractive modes. However, Both DP and SW modes are in fact widely used because they increase the signal-to-noise ratio and for their commercial availability.

In AdSV, the amount of the analyte accumulated on the electrode and thus the measured current signal depends on similar factors and parameters as in ASV and CSV techniques such as solution concentration, time of accumulation period, electrolyte composition (ionic strength, pH, solvent), temperature and electrode material. The peak height in this kind of analysis is also dependent on the type of surface-active substance, its structure, and its electrochemical properties¹⁷. Optimum conditions for maximum accumulation of strongly adsorbing species in order to achieve maximum sensitivity are usually found by examining the peak current enhancement using a 10^{-6} - 10^{-7} mol l⁻¹ solution.

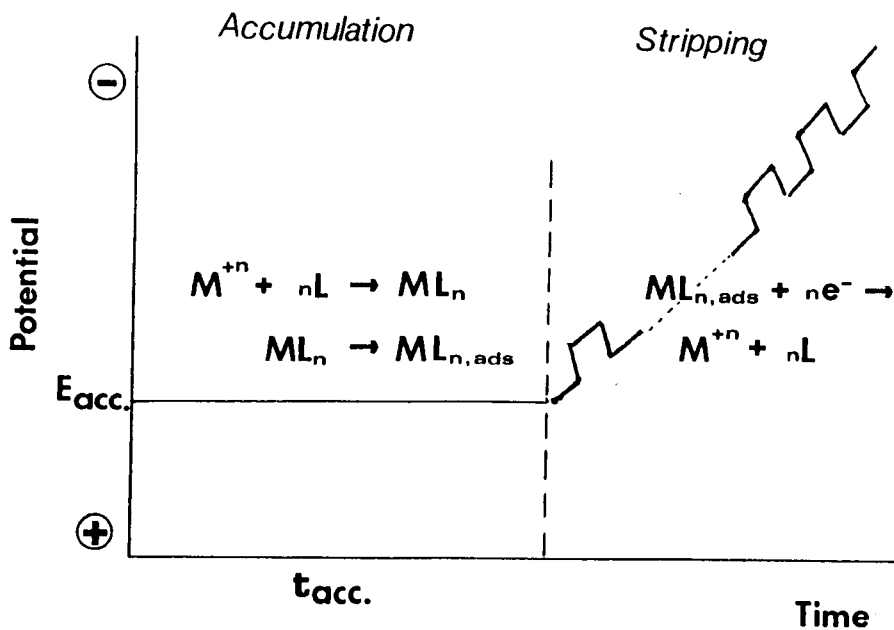


Figure 1.2: Accumulation and stripping steps in adsorptive stripping measurement of a metal ion (M^{+n}) in the presence of appropriate chelating agent (L)³

Since the amount of analyte adsorbed is proportional to the bulk concentration of the analyte, and because the procedure involves a film formation on the electrode surface, a linear response is expected, provided that full coverage of electrode area is avoided, i.e. at concentration less than 10^{-6} mol l^{-1} . Working at carefully controlled solution and instrument conditions, the reproducibility obtained with AdSV is usually good. AdSV can be carried out at practically all types of electrodes employed in voltammetry for which a completely reproducible constant surface area can be ensured. However, the HMDE is widely used for measuring the reducible surface-active species, whereas the carbon paste electrode and platinum disk electrode are used when oxidisable analytes are involved⁹. Similarly, the mercury film electrode (MFE) has also been used for the measurement of several reducible analytes of interest¹⁸. In addition, chemically modified electrodes (CME) have been used for AdSV measurements¹⁶. In this approach, the non-electrolytic (non-faradaic) accumulation process is achieved through a specific chemical interaction and reactions between the analyte and the modified electrode surface¹⁹. The nature of the preconcentration mechanism is determined by the reactivity of the electrode-modifying group. However, complexation, electrostatic attraction or covalent linkages can be used to achieve such goals. Finally, it should be noted that the presence of other surface-active

substances, such as surfactants in the sample solution can affect the accumulation process via a competitive coverage and thus, may interfere in the measurements^{20,21}.

1.5.2 Theoretical basis of quantitative measurements

The amount of substance adsorbed at the working electrode is dependent on its concentration in the solution. For a rapid and diffusion-controlled adsorption, which occurs most often in adsorption accumulation, the voltammetric response of the surface-active species is directly related to their surface concentration. The relationship between the response peak current (i_p) and the concentration of the adsorbed species (C_{ad}) can be given by the following equation:

$$i_p = K A C_{ad}$$

Where K: Proportionality constant

A: Electrode surface area

In fact, the peak current (i_p) is a function of analyte concentration and accumulation time, it increases linearly with both parameters until the electrode surface is saturated. At low analyte levels (10^{-10} – 10^{-7} mol Γ^{-1}) AdSV usually gives rectilinear calibration plots, whereas at higher analyte concentration deviations from linearity are observed. However, in routine AdSV practice, departures from linearity at fairly high concentration are controlled, either by dispensing with the usual stirring of the sample solution during accumulation or by dilution of the sample solution.

1.5.3 Suitable analytes for AdSV

There is a wide range of analytes to which the AdSV technique can be applied. However, several conditions must be met for AdSV to be possible. The formed adsorption product must be insoluble (otherwise it would simply diffuse away back into the solution), must form a coherent layer on the electrode surface and the adsorption substance must be chemically stable and not be attacked by the solution. In

general, neutral organic compounds are adsorbed on an uncharged electrode. The adsorption process decreases as the charge of the electrode is shifted in either negative or positive directions. However, cationic and anionic organic substances exhibit strong adsorption at negative or positive potentials to the zero charge potential respectively. Examples for such substances suitable for AdSV analysis include higher aliphatic alcohols, aliphatic and aromatic sulfonic acids, compounds with π bonds (aromatic rings), and aromatic nitro-compounds. Higher fatty acids, alkaloids, antibiotics, polyamino acids, peptides, proteins, purines, pyrimidines, anionic or cationic detergents, or non-ionogenic detergents²¹, and various biomacromolecules, pharmaceuticals, environmental, and industrial pollutants, in addition, several trace metals after complexation with suitable ligands (chelator) can be analysed by AdSV.

1.5.4 Features and advantages of the AdSV technique

AdSV has greatly improved the application of stripping voltammetric techniques to the determination of numerous analytes that cannot be preconcentrated by an ordinary electrolysis approach²². The list of organic compounds and metal ions, which are accessible to be determined by AdSV analysis, is continuously expanding. The principle of coupling specific chemical reactions with a preconcentration/voltammetric measurement offers high sensitivity, selectivity, versatility, and simplicity. A further significant advantage of AdSV is that all these features can be achieved by utilising relatively inexpensive and simple commercial instrumentation. This approach is distinguished not only by broad possibilities in the accumulation stage, but also allows choosing the method for obtaining the analytical signal, which is most convenient for the specific conditions.

AdSV is a very promising method, the detection limit of metal ions or reducible organic compounds can descend to values as low as 10^{-11} mol l⁻¹ for important metals. However, even lower levels (less than picomolar concentration levels), for example 10^{-13} mol l⁻¹ of platinum²³ can be measured by coupling the adsorption accumulation with catalytic reactions. Furthermore, adsorptive collection of metals, as their surface-active complexes on the HMDE, has been shown to be remarkably useful for ultratrace measurements of some important metals, including aluminum, nickel, molybdenum, vanadium, uranium, lead, and iron, that face some

limitation when measured by conventional stripping analysis (ASV) due to low solubility in mercury, irreversible redox behaviour or formation of intermetallic compound¹⁶. This strategy also offers an effective alternative approach for metals (e.g. gallium, manganese, and tin) which are measurable with certain difficulty by conventional ASV.

Another advantage of this methodology for the direct analysis of complex matrices (blood, urine, body fluids, cattle feed, paint, oil, etc.), is its high degree of selectivity and discrimination over non-absorbable electroactive constituents. This advantage can be obtained when an adsorptive-extractive accumulation at a carbon paste electrode is followed by transferring the electrode from the complex sample to the blank solution where the voltammetric scan is initiated, thus, interferences by large biological macromolecules (as in blood and body fluids) with similar redox potentials are eliminated, and hence analytes of interest can be measured directly without prior separation in such complex samples. Moreover, the adsorptive concentration of metals in the form of complexes can add to the stripping voltammetric selectivity, since the choice of some specific chelating reagents (ligands) and a certain degree of oxidation of metal to be determined can provide for the conditions of the metal measurement when mixed ions of other metals are present.

In conclusion, the AdSV technique appears to be very promising, as it broadens the range of the trace analysis down to (ng l^{-1}) levels. This method is quite universal for both organic and inorganic substances and a further advantage is that it is relatively inexpensive and simple instrumentation (as a classical polarographic arrangement) can be employed.

1.5.5 Limitations and challenges associated with AdSV

Like the majority of analytical techniques, AdSV is subject to various types of limitations and drawbacks. Because of the nature of the preconcentration step applied in this method, the major type of interference in adsorptive stripping measurements is the presence of other surface-active species in the sample solution. In this case, competitive adsorption usually occurs which leads to a decrease in the measured current or (at very high surfactants concentrations) to significant suppression of the signal. As a result of the diminished sensitivity, the difficulties of determining

surfactants in mixtures and interference problems are certainly among the main drawbacks affecting the development of AdSV as a perfect and universal analytical technique. The presence of organic surfactants that adsorb on the mercury surface and inhibit the analytical signal is not the only type of interference. Beside, its competition for surface sites, the surfactant may also yield a stripping peak (redox or tensammetric). In many practical situations, a large response associated with an interfering constituent may mask almost completely the AdSV peak of interest. Additional types of interference may occur in trace metal measurements by the metal-chelate approach, which are affected by co-existing metal ions that form reducible and adsorbable chelates with the ligand of interest. These can interfere via an overlapping response and/or competition for adsorption sites.

Nonetheless, in most cases, these interferences can be minimised or even eliminated if adequate attention is paid to certain key operations. Surfactant interferences can be reduced by employing shorter accumulation times, however, this approach is not suitable in the measurement of ultra-trace amounts of analyte. The inhibitive effect of accompanying substances can also be suppressed in some cases by proper choice of the preconcentration potential²⁴. For severe interfering situations, the interference effect of present substances on the analytical response of the analyte can be eliminated by applying a separatory technique to isolate the analyte of interest from unwanted co-adsorbing interferents. More recently a combination of AdSV and several separation techniques have been proposed for improving the selectivity and sensitivity of adsorption stripping measurements. Among these separation methods are ion-exchange, gel chromatography, TLC and HPLC. Alternatively, it is possible to perform the separation step in situ, at the electrode surface using a pre-selective polymeric coating such as cellulose acetate. In addition, chemical treatment (e.g. chemical ashing) of the sample and/or the use of UV irradiation, ozonation, γ -irradiation of the sample, prior to the determination to destroy and remove the trace interfering organic compounds, may also be useful in various situations.

1.5.6 Practical applications of AdSV

The AdSV method is known to be useful for many analytes that cannot be accumulated electrolytically. These advantages led to ways of finding a wide range of

analytical applications, which cannot be performed by conventional stripping methods. Many organic and inorganic species of clinical, pharmaceutical, industrial, and environmental interest have a strong tendency to be adsorbed onto an electrode surface and thus analysed by AdSV. The application of adsorptive stripping measurement can be basically divided into two main categories: organic molecules characterised by surface-activity or metal ions which form poorly soluble and adsorbable complexes with various chelating reagents (see Tables 1.1 and 1.2).

Analysis of biological and clinical materials: In recent years the analysis of biological materials has become (along with analysis of metal ions) one of the main fields of AdSV applications. This method has been applied for measuring trace levels of compounds of biological and clinical significance such as adenine and purine^{24,25}, riboflavin²⁶, folic acid²⁷, codeine and atropine²⁸, vitamin K²⁹ and vitamin B-12³⁰. Whereas early adsorptive stripping investigations were focused at low molecular weight compounds, recent activity has shifted to the measurements of macromolecules of biological significance. AdSV has been applied for the measurements of human deoxyribonucleic acids (DNA) and its cytosine, guanine and adenine residues³¹⁻³³. Various body proteins such as human serum albumin³⁴, trypsin and insulin³⁵, sex hormones³⁵ and growth hormone³⁶ have also been analysed by this approach.

Analysis of pharmaceutical drugs: There are numerous papers dealing with applications of voltammetric techniques to the determination of pharmaceutical compounds in body fluids³⁷. Adsorptive stripping measurements have been employed to the determination of several pharmaceutical drugs such as diazepam and nitrazepam^{38,39}, anti-tumor agent adriamycin⁴⁰, anti-cancer agent 5-fluorouracil⁴¹, anti-ulcer drug cometidine⁴², cardiovascular drug digoxin⁴³, anti-inflammatory drug indomethacin⁴⁴, anti-hypertensive drug doxazosin⁴⁵, tricyclic antidepressant drugs⁴⁶, penicillin and cephalosporin antibiotics⁴⁷ and anti-bacterial drug nitrofurantoin⁴⁸.

Analysis of pesticides: Adsorptive stripping procedures for measuring environmentally important compounds such as pesticides have been developed, trichlorobiphenyl and nitro or triazine-group-containing pesticides in waste and natural waters can be determined by AdSV technique with a detection limit of $5 \times 10^{-9} \text{ M}^{49}$.

This strategy has been applied to the determination of DDT⁵⁰, nitropesticides⁵¹ and pesticide chlorpyrifos⁵², as well as thiourea and thiourea derivatives in cattle feed and its direct analysis in urine⁵³.

Analysis of water: This technique has found a wide application in the determination of organic and inorganic compounds in natural waters⁵⁴, sea water⁵⁵, waste water⁵⁶, drinking water⁵⁷, sewage⁵⁸, etc. The analysed substances can be ionic, molecular and surface active species or solid and colloidal particles capable of adsorbing onto the electrode surface. Monitoring of pollution with surface-active pollutants such as petroleum⁵⁹, surfactants⁶⁰, detergents⁶¹, crude oil and oil products⁶² is carried out by AdSV. This method may be useful for determination of humic and fulvic acid⁶³. Numerous heavy metal ions are monitored via AdSV method⁶⁴. Several pesticides such as trichlorobiphenyl or nitro-containing pesticides in natural water were also determined⁴⁹.

Analysis of metal ions: AdSV technique has also been applied successfully to the determination of a wide variety of inorganic cations of very low concentrations. Because AdSV methods are becoming widely available for determination of many metals, they are expected to play a major role in future speciation investigations. In these applications the metal ions are generally complexed with surface-active complexing agents such as dimethylglyoxime (DMG)⁶⁵, catechol⁶⁶, oxine⁶⁷, tropolone⁶⁸, Di-o-Hydroxyazo dyes⁶⁹ and bipyridine⁷⁰. With relatively short preconcentration time, very low detection limits in the 10^{-10} to 10^{-11} mol l⁻¹ range have been reported. Adsorptive collection of metals as their surface-active complexes has been shown to be extremely useful for ultratrace measurements of metal such as aluminum⁷¹, copper⁷², iron⁷³, molybdenum⁷⁴, zinc⁷⁵, nickel⁷⁶, lead⁷⁷, vanadium⁷⁸, and selenium⁷⁹.

Analysis of dyes and food colouring matter: AdSV has been used for the determination of trace amount of several synthetic dyes and food colouring matters (colour additives). Fogg *et al.* reported effective adsorptive stripping measurements for 16 food colours in tablets and cosmetics⁸⁰. Furthermore, food additive azo dyes⁸¹, food dye colourant Tartrazine⁸², Sunset yellow (E-100)⁸³ and quinoline yellow

(E-104)⁸⁴ were also determined. Determination of a wide variety of synthetic dyes including Solochrome Violet RS⁸⁵, Mordant red⁸⁶, Mordant Blue⁸⁷, Xylenol orange⁸⁸ as well as, the monitoring of the hydrolysis and methanolysis products⁸⁹ of several reactive dyes were carried out by AdSV. However, Fogg has recently reviewed the utilisation of stripping voltammetric techniques for the determination and monitoring of environmentally important dyes^{90,91}.

Indirect analysis: A number of substances that cannot be reduced or oxidized electrochemically can be determined after derivatization with a suitable substance or by introduction of a reducible group such as nitroso, nitro, etc⁹². An example of derivative formation is the determination of estrone and estradiol after nitrosation⁹³, determination of aromatic amines after diazotization and coupling with 1-naphthol to form an azo dye⁹⁴. After diazotization histidine and tyrosine can be determined⁹⁵. Similar determination of nitrite at $\mu\text{g l}^{-1}$ levels is also achieved^{96,97}.

Finally, to facilitate broader applications of AdSV, the use of modern separation methods (GC, HPLC, electrophoresis) and complexing agents are required. However, it may be assumed that the importance and application range of the AdSV technique will grow, especially in connection with the growing importance of environmental pollution control, as well as biological and medical studies.

Table 1.1: Determination of organic compounds by the AdSV method^{2,9,15,22,35,97}.

Analyte	Sample	Electrode	Supporting Electrolyte	Detection limits
Vitamin K	Urine & blood	HMDE	Acetate 0.05M (pH6) + 60% methanol	1×10^{-9} M
Thiourea	Cattle feed, soil	HMDE	0.1M NaClO ₄	2×10^{-11} M
Folic acid	Natural water, snow	HMDE	Britton-Robinson buffer	5×10^{-6} M
Petroleum components	Natural & sea water	HMDE	Phosphate buffer	3×10^{-5} M
Riboflavin	Blood	HMDE	10^{-3} M NaOH	2.5×10^{-11} M
Sex hormones	Blood	HMDE	5×10^{-3} M NaOH	2×10^{-10} M
Bilirubin	Body fluid	HMDE	Acetate buffer	5×10^{-10} M
Mitomycin C	Blood plasma	HMDE	Phosphate buffer pH9	2×10^{-9} M
Ascorbic acid	-	CPE	Acetate buffer	2×10^{-7} M
Dopamine	Body fluid	Pt	Methanol	5×10^{-8} M
Digoxin	Body fluid	HMDE	5×10^{-3} M NaOH	2×10^{-10} M
Purines	Natural & sea water	HMDE	0.1M LiClO ₄	4×10^{-9} M
Codeine	Blood	HMDE	NaOH	1×10^{-8} M
Ametopterin	Blood	HMDE	0.01M Phosphate buffer (pH7)	2×10^{-8} M
Paracetamol	Urine & blood	GCE	Acetate buffer in 10% methanol	1.2×10^{-8} M
Guanine	Body fluid	HMDE	1M H ₃ PO ₃ +0.4M NaOH (pH8.5)	2×10^{-8} M
Sunset yellow	Refreshing drink	HMDE	0.5M NH ₄ Cl/NH ₃	5×10^{-9} M
Quinoline yellow	Refreshing drink	HMDE	0.01M HCl	1×10^{-9} M
Remazol.golden yellow	-	HMDE	Acetate buffer (pH4.5)	5×10^{-9} M
Azo sulfine drugs	Urine	HMDE	Acetate buffer (pH3.5)	5×10^{-8} M
Tartazine dye	Soft drink	HMDE	NH ₄ Cl/NH ₃	1×10^{-9} M

Table 1.2: Determination of trace metals by AdSV method^{3,9,16,22}

Metal	Complexing agent	Support electrolyte	Detection limits
Fe	Catechol	PIPES (pH6.8)	6×10^{-10} M
Mn	Black T	PIPES (pH12)	6×10^{-10} M
Pd	Dimethylglyoxime	$\text{NH}_4\text{Cl}/\text{NH}_3$ (pH12)	2×10^{-10} M
Pt	Formazone	Sulfuric acid	1×10^{-12} M
Al	Solochrome Violet RS	Acetate buffer (pH4.5)	5×10^{-9} M
Ni	Dimethylglyoxime	$\text{NH}_4\text{Cl}/\text{NH}_3$ (pH9.2)	1×10^{-10} M
Co	Nioxime	HEPES buffer	6×10^{-12} M
Cu	Tropolone	Borate buffer	3×10^{-10} M
Mo	Oxine	HCl (pH2.6)	1×10^{-10} M
I	Copper	Acetate buffer	3×10^{-9} M
Sn	Tropolone	Acetate buffer	2×10^{-10} M
Ga	Solochrome Violet RS	Acetate buffer (pH4.8)	1×10^{-9} M
Se	Copper	$(\text{NH}_4)_2\text{SO}_4$ (pH4.5)	3×10^{-9} M
Zn	Ammonium Pyrrolidinedithiocarbamate	BES (pH7.3)	3×10^{-11} M
Cr	Diethylenetriamine Pentaacetic acid	Sodium acetate	4×10^{-10} M
V	Catechol	PIPES (pH9)	1×10^{-10} M
Th	Mordant blue 9	Acetate buffer (pH6.5)	4×10^{-10} M
La	Cresolphthalexon	$\text{NH}_4\text{Cl}/\text{NH}_3$ (pH9.4)	2×10^{-10} M
Ce	o-cresophthalexone	NAC/ NH_4AC (pH9.4)	1.7×10^{-9} M
In	Oxine	$\text{NH}_4\text{Cl}/\text{NH}_3$ (pH4)	1.5×10^{-10} M
Tb	Cupferron	$\text{NH}_3/\text{NH}_4\text{Cl}$	4.4×10^{-9} M
Te	Copper	$(\text{NH}_4)_2\text{SO}_4$ (pH4.5)	1×10^{-8} M
U	Mordant blue 9	Acetate buffer (pH6.5)	2×10^{-10} M

PIPES : piperazine-N,N'-bis-2-ethanesulphonic acid.

HEPES : N-hydroxyethylpiperazine-N'-2-ethanesulphonic acid.

BES : N,N-bis (2-hydroxyethyl) -2- amino- ethanesulphonic acid.

REFERENCES

1. Wang, J., "Instrumentation for Stripping Analysis". In: *Analytical Instrumentation Handbook*, Ewing, G., (Ed.), Marcel Dekker, Inc., New York, 1990.
2. Kalvoda, R., and Kopanica M., "Adsorptive Stripping Voltammetry in Trace Analysis", *Pure Appl., Chem.*, (1987), **61**, 97.
3. Wang, J., *Analytical Electrochemistry*, VCH Publishers, Inc., New York, 1994.
4. Dewald, H.D., "Stripping Analysis" In: *Modern Techniques in Electroanalysis*, Winefordner, J.D. (Ed.), John Wiley & Sons, Inc., New York, 1996.
5. Plambeck, J.A., *Electroanalytical Chemistry: Basic Principles and Applications*, John Wiley & Sons, New York, 1982.
6. Bond, A.M., *Modern Polarographic Methods in Analytical Chemistry*, Marcel Dekker, New York, 1980.
7. Vydra, F., Stulik, K., and Eva, J., *Electrochemical Stripping Analysis*, Ellis Horwood Limited, New York, 1976.
8. Bard, A.J., and Faulkner, L.R., *Electrochemical Methods: Fundamentals and Applications*, John Wiley & Sons, New York, 1980.
9. Wang, J., *Stripping Analysis: Principles, Instrumentation and Applications*, VCH, Publishers, Inc., Florida, 1985.
10. Fogg, A.G., *Anal. Proc.*, (1995), **32**, 433.
11. Brainina, K.Z., *Stripping Voltammetry in Chemical Analysis*, John Wiley & Sons, New York, 1974.
12. Kissinger, P.T. and Heineman, W.R. (Ed.), *Laboratory Techniques in Electroanalytical Chemistry*, Marcel Dekker, Inc., New York, 1996.
13. Kolthoff, F.M., and Elving, P., (Ed.), *Treatise on Analytical Chemistry, Section D-2, Electrical methods of Analysis*, Interscience Publishers, New York, 1965.
14. Fogg, A.G., *Anal. Proc.*, (1994), **31**, 313.
15. Kalvoda, R., "AdSV in Trace Analysis" In: *Comtemporary Electroanalytical Chemistry*, Ivaska, A., Lewenstama, A., and Sara, R., (Ed.), Plenum Press, New York, 1990.
16. Wang, J., "Voltammetry After Nonelectrolytic Preconcentration" In: *Electroanalytical Chemistry*, Vol. 16, (Ed.), Bard, A.J., Marcel Dekker, New York, 1989.

17. Smyth, W.F., "Adsorptive Stripping Voltammetry of Selected Molecules" In: *Electrochemistry Sensors and Analysis*, Smyth, M.R., and Vos, J.G., (Ed.), Elsevier, Amsterdam, 1986.
18. Economou, A. and Fielden, P.R, *Trac-Trends Anal. Chem.*, (1997), **16**, 286.
19. Stulik, K. and Pacakova, V., "Chemically Modified Electrodes for Potentiometry and Voltammetry" In: *Instrumentation in Analytical Chemistry*, Zyka, J. (Ed.), Ellis Horwood Limited, New York, 1994.
20. Kalvoda, R., "Adsorptive Stripping Voltammetry" In: *Instrumentation in Analytical Chemistry II*, Zuka, J., (Ed.), Ellis Horwood, New York, 1996.
21. Galus, Z., (Ed.), *Fundamentals of Electrochemical Analysis*, Ellis Horwood, New York, 1994.
22. Brainina, K.H., and Neyman, E., *Electroanalytical Stripping Methods*, John Wiley & Sons, New York, 1993.
23. Wang, J., Czae, M., Lu, J. and Vuki, M., *Microchem. J.*, (1999), **62**, 121.
24. Kalvoda, R., "Tensammetry in Combination With Adsorptive Accumulation" In: *Electrochemical Detectors Fundamental Aspects and Analytical Applications*., Ryan, T.H., (Ed.), Plenum Press, New York, 1984.
25. Alvarez, J.L.M., Calzon, L.A.G., and Fonseca, J.M.L., *J. Electroanal. Chem.*, (1998), **457**, 53.
26. Economou, A., and Fielden, P.R., *Electroanalysis*, (1995), **7**, 447.
27. Szczepaniak, W., and Ren, M., *Electroanalysis*, (1994), **6**, 505.
28. Palecek, E., and Postbieglova, I., *J. Electroanal. Chem.*, (1986), **214**, 359.
29. Palecek, E., and Hung, M.A., *Anal. Biochem.*, (1983), **132**, 236.
30. Sawamoto, H., *Bunseki Kagaku*, (1994), **43**, 347.
31. Wang, J., Grant, D.H., Ozsoz, M., Cai, X.H., Tian, B.M., and Fernandes, J.R., *Anal. Chim. Acta*, (1997), **349**, 77.
32. Jin, W.R., Wei, H.Y., and Zhao, X., *Anal. Chim. Acta*, (1997), **347**, 269.
33. Jelen, F., Tomschik, M., and Palecek, E., *J. Electroanal. Chem.*, (1997), **423**, 141.
34. Flores, J.R., Marin, C., Gonzalez, E., Pariente, F., and Lorenzo, E., *Electroanalysis*, (1991), **3**, 405
35. Wang, J., *Electroanalytical Techniques in Clinical Chemistry and Laboratory Medicine*, VCH Publishers, Inc., New York, 1988.
36. Hernandez, P., Paton, F., and Hernandez, L., *Electroanalysis*, (1997), **9**, 1372.

37. Kalvoda, R., *Anal. Chim. Acta*, (1984), **162**, 197.
38. Chaney, E.N., and Baldwin, R.P., *Anal. Chem.*, (1982), **54**, 2556.
39. Vire, J.C., Kauffmann, J.M., and Patriarche, G.J., *J. Pharm. Biomed. Anal.*, (1989), **7**, 1323.
40. Webber, A., Shah, M., and Osteryoung, J., *Anal. Chim. Acta*, (1983), **154**, 105.
41. Khodari, M., Ghandour, M., and Taha, A.M., *Talanta*, (1997), **44**, 305.
42. Wang, J., Mohmoud, J.S., Faries, P.A.M., *Analyst*, (1985), **110**, 855.
43. Wang, J., Tuzh, P., Lin, M.S., and Tapia, T., *Talanta*, (1986), **33**, 707.
44. Ali, A.M.M., *J. Pharm. Biomed. Anal.*, (1999), **18**, 1005.
45. DeBetono, S.F., Moredo, J.M., Arranz, A., and Arranz, J.F., *Anal. Chim. Acta*, (1996), **329**, 25.
46. Benadikjova, H., and Kalvoda, R., *Anal. Lett.*, (1984), **17**, 1519.
47. Jin, L.T., Ning, B., Ye, J.N., and Fang, Y.Z., *Mikrochim. Acta*, (1991), **1**, 115.
48. Khodari, M., Mansour, H., Eldin, H.S., and Mersal, G., *Anal. Lett.*, (1998), **31**, 251.
49. Lam, N.K., and Kopanica, M., *Anal. Chim. Acta*, (1984), **161**, 315.
50. Li, C., James, B.D., and Madee, R.J., *Electroanalysis*, (1990), **2**, 63.
51. Kotoucek, M., and Opravilova, M., *Anal. Chim. Acta*, (1996), **329**, 73.
52. Elshahawi, M.S., and Kamal, M.M., *Fresenius J. Anal. Chem.*, (1998), **362**, 344.
53. Zutic, V., Cosovic, B., and Kozara, Z., *J. Electroanal. Chem.*, (1977), **78**, 113.
54. Adeloju, S.B., and Hadjichari, A., *Anal. Sci.*, (1999), **15**, 95.
55. Scarano, G., and Morelli, E., *Anal. Chim. Acta*, (1994), **296**, 277.
56. Giroussi, S.T., Voulgaropoulos, A.N., and Stravroulias, S., *Chemica Anal.*, (1996), **41**, 489.
57. Meyer, A., and Henze, G., *Fresenius J. Anal. Chem.*, (1994), **350**, 150.
58. Flora, C.J., and Nieboer, E., *Anal. Chem.*, (1980), **52**, 1013.
59. Kozarac, Z., Zutic, V., and Cosovic, B., *Tenside Peterg.*, (1976), **13**, 260.
60. Hattori, T., Kato, M., Tanaka, S., and Hara, M., *Electroanalysis*, (1997), **9**, 722.

61. Raspor, B., Nurnberg, H., Valenta, P., and Branica, M., *Mar. Chem.*, (1984), **15**, 231.
62. Kovac, M., Kalvoda, R., Novonty, L., and Berka, A., *Electroanalysis*, (1992), **4**,
63. Batley, G.E., and Florence, T.M., *J. Electroanal. Chem.*, (1974), **55**, 23.
64. Van den Berg, C.M.G., *Analyst*, (1989), **114**, 1527.
65. Sanlloriente, S., Ortiz, M.C., Arcos, M.J., and Lopez, P., J., *Electroanalysis*, (1996), **8**, 285.
66. Limson, J., and Nyokong, T., *Anal. Chim. Acta*, (1997), **344**, 87.
67. Wang, J., and Zadeil, J., *Anal. Chim. Acta*, (1987), **182**, 147.
68. Xue, H.B., and Sunda, W.G., *Enviro. Scie. Tech.*, (1997), **31**, 1902.
69. Wang, J., Farias, P.M., and Mohmould, J.S., *Anal. Chim. Acta*, (1985), **172**, 57.
70. Gao, Z.Q. and Siow, K.S., *Talanta*, (1996), **43**, 255.
71. Stryjewska, E. Rubel, S., Sadowska, J., and Karpiuk, M., *Chemia Anal.*, (1993), **38**, 175.
72. Shams, E., *Anal. Lett.*, (2000), **33**, 465.
73. Gawrys, M. and Golimowski, K., *Electroanalysis*, (1999), **11**, 1318.
74. Fraga, I.C.S., Farias, P.A.M. and Ohara, A.K., *Fresenius J. Anal. Chem.*, (2000), **366**, 307.
75. Hernandezbrito, J.J., Perezpena, J., Geladocaballero, M.D., and Colladosanchez, C., *Anal. Chim. Acta*, (1993), **284**, 405.
76. Sanlloriente, S., Ortiz, M.C., Arcos, M.J., *Analyst*, (1998), **123**, 513.
77. Yokoi, K., Yamaguchi, A., Mizumachi, M., and Koide, T., *Anal. Chim. Acta*, (1995), **316**, 363.
78. Vega, M., Van den Berg, C.M.G., *Anal. Chim. Acta*, (1994), **293**, 19.
79. Van den Berg, C.M.G., and Khan, S.H., *Anal. Chim. Acta*, (1990), **231**, 221.
80. Fogg, A.G., and Bhanot, D., *Analyst*, (1981), **106**, 883.
81. Castrillejo, Y., Pardo, R., Barrado, E., and Batanero, P.S., *Electroanalysis*, (1990), **2**, 553.
82. Nevado, J.J., Flores, J., and Villasenor Llerena, M.J., *Talanta*, (1997), **44**, 467.
83. Nevado, J.J., Flores, J., and Villasenor Llerena, M.J., *Quimica Anali TICA*, (1997), **16**, 51.

84. Xu, Gang, O'Dea, J.J. and Osteryoung, J.G., *Dyes and Pigments*, (1996), **30**, 201.
85. Downard, A.J., Powel, H.K.J., and Xu, S.H., *Anal. Chim. Acta*, (1992), **262**, 339.
86. Zhou, J., and Neeb, R., *Fresenius J. Anal. Chem.*, (1994), **221**, 269.
87. Wang, J., and Zadeii, J.M., *Analyst*, (1986), **188**, 187.
88. Abdelh amid, R.; Elsagher, H.M., and Rabia, M.K., *Can. J. Chem.-Rev.*, (1997), **75**, 162.
89. Fogg, A.G. and Zanoni, M.V.B., *Port. Electrochim. Acta*, **14**, (1996), 229.
90. Fogg, A.G., *Port. Electrochim. Acta*, **16**, (1998), 5.
91. Zima, J., Barek, J., Moreira, J.C., Meejstic, V. and Fogg, A.G., *Crit. Rev. Anal. Chem.*, **29**, (1999), 125.
92. Kalvoda, R., *Fresenius J. Anal. Chem.*, (1994), **349**, 565.
93. Hu, S.S., He, Q., and Zhao, Z.F., *Analyst*, (1992), **117**, 181.
94. Fogg, A.G., and Lewis, J.M., *Analyst*, (1986), **111**, 1443.
95. Moreira, J.C., and Fogg, A.G., *Analyst*, (1991), **116**, 249.
96. Fogg, A.G., and Alonso, R.M., *Analyst*, (1988), **113**, 1337.
97. Smyth, W.F., *Voltammetric Determination of Molecules of Biological Significance*, John Wiley & sons, New York, 1992.

INTRODUCTION TO REACTIVE DYES

2.1 Introduction

Reactive dyes are one of the most recent classes of synthetic dyes and they are so called "reactive" because of the readiness with which they interact with certain substrates (e.g. cellulose), under appropriate conditions¹. The most important distinguishing characteristic of reactive dyes is that they form covalent bonds with the substrate that is to be coloured. They are attached to cellulose or wool (e.g. in textile fibres) by means of forming a covalent bond between a carbon atom of the dye molecule and an oxygen, nitrogen or sulfur atom of -OH, NH₂, -SH group respectively, present on the fibres, protein fibres and polyamide substrates to be dyed². In fact, dyes of this group depend for their chemical reactivity upon the presence of one or more reactive chlorine atoms or a vinylsulfone group. This bond formation between the functional group and the substrate results in high wet-fastness properties, thus, these dyes differ fundamentally from other types that owe their wet-fastness to physical adsorption or mechanical retention.

Numerous reactive dyes are commercially available, they have been developed for both wool and polyamide, but the major success has been in the application to cotton, thus, the term "reactive dye" normally refers to a dye applicable to cotton. It is clear from the number of published patents relating to reactive dyes that this field is regarded as being of the highest importance by the dye-maker and dye-user. Much work is also being done on the kinetics and physical chemistry of dyeing and printing processes in which reactive dyes are involved.

2.2 History of Reactive Dyes

Prior to the mid-nineteenth century virtually all colorants originated from animal, vegetable or mineral sources. The economic limitations of these dyes became increasingly apparent in the late eighteenth century as the industrial revolution took hold in Europe and by the 1850's, the textile industry was ripe for the introduction of cheaper synthetic dyes with a greater reliability of supply. This major goal was achieved by the development of the manufacture of synthetic dyes from coal tar. The idea of establishment of a covalent bond between dye and substrate (e.g. cellulose) which is the basis of reactive dyes, had been perceived for many years. It was in 1884, when Bottiger³ discovered the azo dye, congo red. However, the first recorded chemical combination of a dye with cellulose was achieved in 1895 by Cross and Bevan. Several other attempts from about 1906 were subsequently made to achieve the aim of attaching dyes to cellulose by means of covalent bond.

The first reactive dye C.I. Acid Orange 30, was introduced in 1932 by Forben for dyeing wool. During the 1930's fast dyeing on wool was produced using dyes containing chloroacetyl amino and β -chloroethylsulfamoyl groups. It was not realised at that time that the high wet-fastness of these dyes was due to the reaction between the labile chlorine atom and the amino groups in wool. In 1953, Hoechst introduced the Remalan range (dyes containing vinylsulfone and β -sulfatoethylsulfone substituents), and two years later Ciba marketed the Cibalan range of dyes for wool, both of which had only limited success owing to the low rate of the dyes on the fibre. The attempt that followed led to the development which resulted in the introduction of the first range of reactive dyes for cellulose, marketed by ICI in 1956 as the Procion M Dyes⁴. The initial members of this range were all highly reactive dichlorotriazinyl derivatives capable of reaction with cellulose under cold-dyeing conditions. They were quickly followed by the less active monochlorotriazinyl dyes (Procion H range) requiring hot-dyeing conditions. The success of the Procion dyes led rapidly to many of the major dyestuff manufacturers introducing ranges of reactive dye for cotton and wool on a variety of reactive systems.

The development of reactive dyes has continued to be rapid and world demand for such materials reached ca. 97,000t in 1990. Reactive dyes thus constitute the largest of the textile dye classes on a monetary basis, accounting for 17% of the textile dye market by volume.

2.3 Classification of Dyes

In general, dyes can be grouped in accordance with two different principles:

- a) Chemical structure (chemical classification) such as azo, anthraquinone, triphenodioxazine, xanthene formazan dyes etc.
- b) Dyeing methods and areas of application (colouristic classification) such as acid, basic, direct, mordant, disperse, vat and sulfur dyes⁵.

However, neither system of classification is satisfactory by itself, as a result, there are several ways to classify dyes. For example, they may be classified by type of substrate, such as dyes for nylon, dyes for cotton, dyes for polyester and so on. Dyes may also be classified by their method of application to the substrate, such a classification would include direct dyes, reactive dyes, vat dyes, disperse dyes and several more types. Dyes can also be classified either as natural or synthetic dyes, and as organic or inorganic dyes. When they are classified according to their areas of application, they may be textile dyeing, leather, fur, plastics and polymers dyeing, printing, paints, surface coating, and in paper manufacture. However, the most appropriate system for the classification of dyes is by chemical structure, or rather, upon their chromophoric system or systems⁶.

In fact, reactive dyes are often classified according to the number of reactive systems they contain, leading to the term mono-anchor, double-anchor, and multiple-anchor dyes (those with three or more reactive groups). On the other hand, the reactive systems may be divided into two main groups:

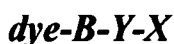
I) Systems involving nucleophilic substitutions, in which the mobile reactive group X is replaced by an attacking base. The mono-chlorotriazine and di-chlorotriazine dyes are

representative examples of such a group. This group accounts for 50% of all reactive dyes used in commerce.

II) Systems involving nucleophilic addition occurs across a polarised double bond. The Remazol dyes, which employ the vinylsulfone group, is an example of this system⁷.

2.4 Structure of Reactive Dyes

The reactive dye molecule may be regarded as a combination of the following units:



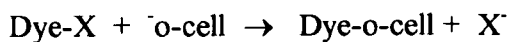
Where *dye* is the chromophoric system, which determines the colour of the dye. Commonly used chromogens include azo, metallised-azo, anthraquinone, phthalocyanine, and metal-complex formazan derivatives, however, virtually every conceivable chromophore can be used in the synthesis of reactive dyes.

- *B* is a bridging atom or group, although this in many cases is part of the chromophore system, it usually consists of an amino group but sometimes -SO₂ or NHCO- groups. The nature of the bridging group, between the chromophore and the reactive group, not only affects the shade, strength and affinity of the dye, but also can significantly affect its reactivity and stability of the dye-fibre bond.

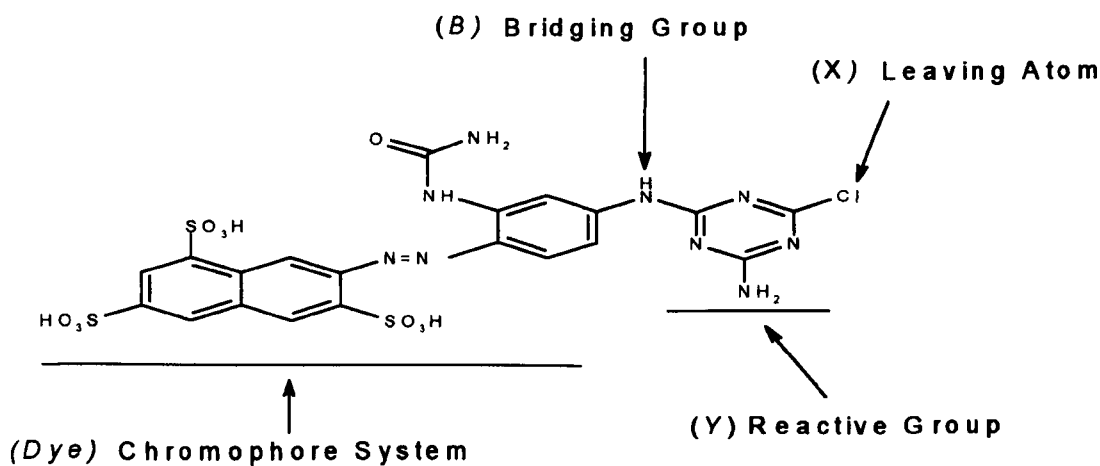
- *Y* is the reactive system, which is the group that binds the dye to its substrate via a stable covalent bond. The activity of the reactive group depends to a large extent upon the nature of Y. The reactivity increases in the series Cl < SO₂CH₃ < F. Generally, the reactive system used in commercially available reactive dyes can be classified into two groups: reactive systems based on nucleophilic substitution and reactive systems based on nucleophilic addition.

- *X* is the leaving group, which is the group that reacts with the fibre. In principle, a reactive dye should contain a leaving group *X* that can undergo nucleophilic displacement

by a hydroxyl group or amino group of cellulose (Cell-OH) in the presence of aqueous alkaline solution:



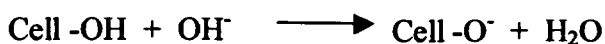
In principle, practically any desired chromophoric system can be combined with reactive groups to produce reactive dyes. The properties of the resulting dye, however, are affected by both of these groups. Proper combination is, therefore, needed to obtain dyes with good qualities such as high tinctorial strength, good solubility, good fastness properties and economy. Finally, the characteristic structural features of a Reactive Yellow 84, which acts as a representative example for reactive dyes are shown schematically as follows:



2.5 Mechanism of Cellulosic Fibre Dyeing (Textile Dyeing)

The idea of joining dye molecules to fibres via covalent linkages has attracted much attention over the years, because fibres coloured in this way are expected to possess good wash-fastness. When these dyes were first introduced, some work was carried out to establish the fact that a covalent bond was formed between the fibre and the dye⁸. Stamm, Zollinger and co-workers have endeavoured to obtain experimental evidence of the formation of a covalent link and to demonstrate its position in the D-glucose unit of cellulose⁴. A covalent bond between a dye molecule and a fibre can only be established if the fibre which is to be dyed contains suitable groups which can be substituted. Among the suitable groups are -OH, -SH and -NH₂. Such groups are present mainly in cellulosic and protein fibres, which are formed from natural polymers⁹.

The process of dyeing cellulose requires the presence of a base (e.g. Na₂CO₃ or NaOH) together with an electrolyte usually NaCl or Na₂SO₄, which increases the fixation yield (which normally varies from 60% to 90%). The dyeing of cellulosic fibres with reactive dyes normally is limited to the alkaline pH range as the -OH group of cellulose does not dissociate in acidic media. Chemically speaking, under strongly aqueous alkaline conditions, the hydroxyl groups in the cellulose molecules (cell-OH) are partially ionised and dissociated (cell-O⁻), thus, producing a high negative charge on the fibre and in addition, breaking down interchain hydrogen bonding. The resulting anionic group on the fibre can act as nucleophilic reagents and react much faster with the reactive groups of the dye:

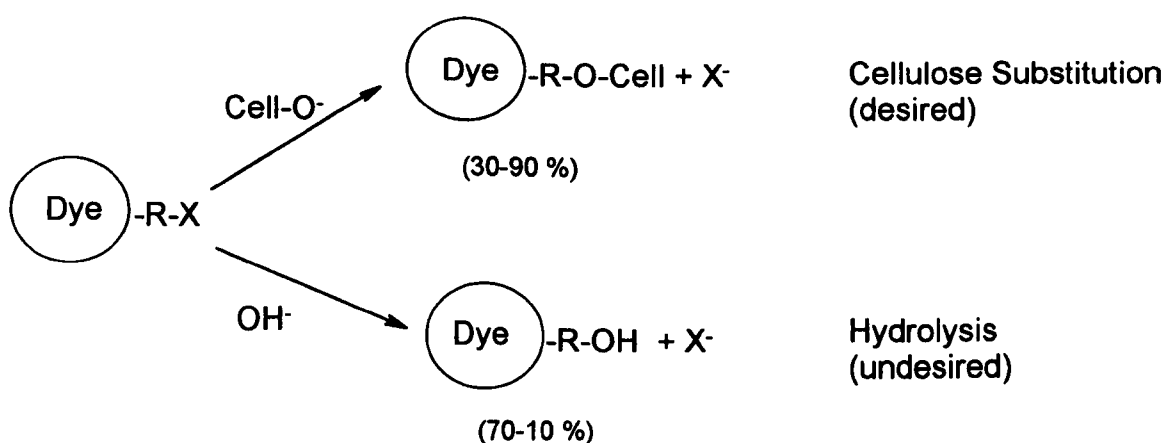


2.6 The Problem of Hydrolysis of Reactive Dyes

The fundamental problems associated with reactive dyeing arise from the reaction of the electrophilic group of the reactive dye with water (hydrolysis), it competes with the fixation reaction. The hydrolysed dye cannot react with the fibre. In other words, when dyeing cellulosic fibre for example, with reactive dyes in alkaline medium, the cell-O⁻ group is not the only reaction partner. Reactions are also possible with the OH group of water, which implies that the reactive dyeing of cellulosic fibre is always accompanied by a partial hydrolysis of the dye being used.

However, it has been shown that the dissociation constant for cellulose is higher than that of water, thus cell-O⁻ reacts faster than OH⁻ with the reactive group of the dyestuff. Owing to the competition between the fixation reaction and hydrolysis reaction, a high rate of fixation to hydrolysis is therefore an important requisite for high fixation. The level of fixation of the dyes varies enormously from 30% to 90%, and consequently considerable effort is still being directed towards achieving approximately 100% fixation¹⁰.

The process of hydrolysis can be illustrated as follows:



2.7 Types of Reactive Dyes

2.7.1 Azo reactive dyes

The azo dyes and pigments form the largest group of all synthetic colorants, and they play a prominent part in almost every type of application. These dyes are by far the most important class, accounting for over 50% of all commercial dyes.

Structure: The chromophoric system consists essentially of the azo group (-N=N-) in association with one or more aromatic system. There may be more than one azo group present in the dye molecule and thus one speaks of monoazo, diazo, triazo and polyazo dyes according to whether there are one, two, three, or more rarely four azo groups present in the dye molecule⁴. The azo group is usually attached to two aromatic residues, they exist in the more stable trans form rather than the cis form. However, the azo groups are mainly bound to benzene or naphthalene rings, but in some cases they are also attached to aromatic heterocycles or aliphatic groups.

Synthesis: Azo dyes are made almost exclusively by the diazation of a primary aromatic amine to give a diazo or diazonium salt, a reaction of fundamental importance to the dye industry. The diazo compound is then coupled with a second substance, usually a phenol, a ketone or an aromatic amine.

Properties: The range of hues covered by this group is very wide and can include yellows, a great number of reds and oranges, navy blues, violets and blacks. Colours such as brown, olive and green, which are difficult to obtain in self-shade dyes can be produced by mixtures of dyes⁶.

Examples: A representative examples for azo dyes are Reactive Red 141, Basic Yellow 25, Direct Blue 14, Acid Orange 7, Remazol Black B, Mordant Orange 1, Disperse Red 1, Remazol Red F3B, Direct Red 28 and Acid Orange GG.

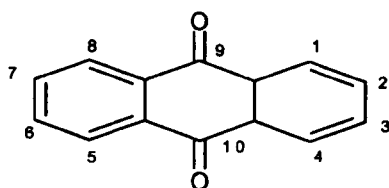
Formazan dyes: Formazan dyes bear a formal resemblance to azo dyes, since they contain an azo group but have sufficient structural dissimilarities to be considered as a separate class of dyes. The most important formazan dyes are the metal complex,

particularly copper complexes, of tetradentate formazan. They are used as reactive dyes for cotton, producing red to greenish-blue shades.

2.7.2 Anthraquinone reactive dyes

Anthraquinone-based dyes are the second most important class of reactive dye types, they are also one of the oldest types of dyes. The principle reason why anthraquinone dyes are less widely used commercially than azo dyes is simply that they are less cost effective. Two factors are responsible for this: the inherently lower tinctorial strength of these dyes relative to azo dyes; the second factor is the reduced versatility in the synthesis of anthraquinone dyes, since, in contrast to azo dyes synthesis, the substituents generally have to be introduced into a preformed anthraquinone nucleus¹⁰.

Structure: These dyes are based on 9,10 anthraquinone, which is essentially colourless. To produce commercially useful dyes powerful electron donor groups such as amino or hydroxyl are introduced into one or more of the four alpha positions (1,4,5 and 8). To maximise the properties, primary and secondary amino groups and hydroxyl groups are employed. These ensure the maximum degree of π -orbital overlap, enhanced by intermolecular H-bonding. Anthraquinone derivatives that have -OH or NH₂ groups generally exhibit better resistance to sublimation, better solubility and better affinity for textile substrates.



Synthesis: There are many methods of synthesis in anthraquinone chemistry. These dyes are prepared by the stepwise introduction of substituents into the preformed anthraquinone skeleton. This highlights two very important points. First, the degree of freedom for producing a variety of different structures is restricted. Second, the

availability of only eight substitution centres imposes a further restriction on synthetic flexibility.

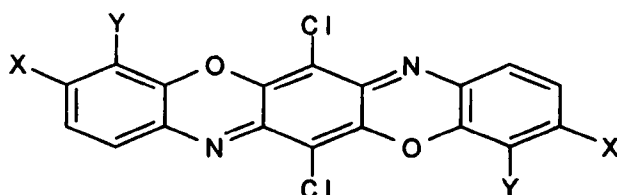
Properties: Anthraquinone-based dyes are significant because of their brilliance, good light fastness, and chromophore stability under both acidic and basic conditions. By variation of substituent, bluish violet to bluish green colours with the bright reddish to mid-blues can be achieved. However, these attributes are offset by their major disadvantage; they are not cost effective because they are both expensive and tinctorially weak.

Examples: Various anthraquinone dyes such as Cibacron Blue F3G-A, Remazol Brilliant Blue R, Pigment Violet 2, Disperse Red 15, Disperse Blue 180, Disperse Violet 1, and Acid Blue 62 have been used successfully.

2.7.3 Triphenodioxazine reactive dyes

Dyes derived from the triphenodioxazine ring system have been commercially available since 1928. The triphenodioxazine chromophore was tested in almost every class of dyes, but its only major commercial application was as a direct dye and pigment. Only recently has it been introduced into reactive dyes. However, the commercial success of these products has stimulated considerable research activity and in recent times, these dyes have owned approximately 10% of the blue reactive dye market. Currently, research efforts tend to concentrate in this area, and further new products are anticipated⁶.

Structure: The basic structure of these dyes is based on the unsubstituted triphenodioxazine (which is of no importance as a colorant).



By varying the substituents on the original parent substance, particularly in the position para to the amino groups, its colour can be modified. Red to red-violet shades result when X= OH or OR, and blue colours when X= NH₂ or NHR' are present.

Synthesis: Synthesis of the parent molecule of triphenodioxazine has been significantly improved. The most important industrial process for synthesising these dyes involves reaction of two equivalents of an aromatic amine with 2,3,5,6-tetrachloro 1,4 benzoquinone and subsequent oxidative closure of the ring.

Properties: These dyes can offer bright hues, strong tinctorial strength, brilliance, and high light-fastness. By variation of substituent, they give rise to red, red-violet, blue and greenish-blue colours.

Examples: C.I. Reactive Blue 163 is dichlorotriazinyl dye with a greenish-blue colour. Other triphenodioxazine dyes include a monochlorotriazinyl derivate (C.I. Reactive Blue 198), a phosphonic acid derivate (C.I. Reactive Blue 172), and, more recently, a fluorotriazine derivative (C.I. Reactive Blue 204) has become available.

2.7.4 Phthalocyanine reactive dyes

Phthalocyanine reactive dyes are a relatively new class of dye discovered earlier this century. Since then they have become important, particularly as pigments. These dyes are used for bright turquoise hues, which cannot be achieved using other dyes. The most important reactive phthalocyanine dyes contain copper or nickel as their central atom, they are substituted with sulfonic acid and also with reactive groups joined via sulfonamide bridges.

Structure: The chromophore of dyes of the phthalocyanine series of ring systems is a cyclic system of conjugated double bonds with 18 π -electrons⁵. They bear a close structural relationship to the natural pigments such as the porphyrins, in fact these dyes are derivatives of tetrazaporphin, and in common with porphyrins these form meta complexes. Transition metals especially copper, form the most stable complexes, other less important derivatives include Zn, Fe, Co, Cd, and Mg complexes.

Synthesis: The synthesis of the most important phthalocyanine derivatives usually succeeds with simple starting materials without isolation of intermediate products. Technical processes start from phthalic acid from which, with or without the addition of urea, phthalamide is formed. Substituted phthalocyanines are obtained either by direct substitution in an existing molecule or by synthesis with substituted starting materials.

Properties: The major commercial impact of these dyes is based on the combination of groups of properties as their beautiful bright blue to green shades, their high tinctorial strength, remarkable chemical stability and finally their excellent fastness to light¹⁰.

Examples: The first commercial products were Monastral Fast Blue B, and Monastral Fast Blue G (C.I. Pigment Blue 18). These dyes can also be used in the form of vat dyes. An interesting commercial dye Indanthren Brilliant Blue 4G (C.I. vat Blue 29, Cobalt (III)- phthalocyanine monosulphonic acid) is another example of these reactive dyes.

2.8 Environmental and Health Hazards Associated with Dye Industrial Effluents

Recent estimates indicate that approximately 12-15% of the synthetic textile dyes used each year are lost to waste streams during the manufacturing and processing operations¹¹, and that 20% of these losses will enter the environment through effluents from waste water treatment facilities. The consequential problems that arise for disposal of these amounts of pollutants in the environment around industrial areas are not only that associated with the coloured streams resulting from effluent from dyehouses which are a major concern to the public and authorities, but also the problems related to the health issues, the effect on ecological balance, and hazards to aquatic life by the residual dyes in plant effluents from dye production or application. However, possible environmental damage does not depend solely on the quantity released, but also on the ecotoxicological properties of the individual products and their environmental transport characteristics.

Chemical carcinogens are of increasing concern to the dye industry. Major dye manufacturers have recognised the need for additional information concerning toxicological, ecological, and analytical problems common to synthetic dyes. A few aromatic amines used as dye intermediate have been classified by governmental agencies as cancer suspect agents. For example, the International Agency for Research on Cancer has evaluated the carcinogenicity of 44 individual organic colorants and benzidine-based dyes. The largest chemical group of dyes, the azo dye, has undoubtedly attracted the most attention with regard to carcinogenicity. In fact, a number of azo dyes have exhibited genotoxic or ecotoxic properties¹². The available data are consistent with the conclusion that an azo dye, which on reductive cleavage of one or more azo groups will form carcinogenic aromatic amines, is a carcinogen. It is estimated that about 150 azo dyes currently in commerce would form, on reductive cleavage of azo groups, an aromatic amine that is generally acknowledged to be an animal carcinogen. On the other hand, a greater number of dyes are skin and/or eye irritant. Moreover, sensitisation effects (both skin and respiratory sensitisation) associated with some dyes also have acute effects and warrant separate consideration.

2.9 Dyehouse Effluent Removal Treatment

Many governments and industries have placed a high priority on reducing or minimising hazardous chemical waste (e.g. textile wastewater) by limiting the amount of pollutants produced, i.e. reducing the production of pollutants at their source rather than controlling them at the end of the manufacturing process such as waste treatment facilities. However, after the fixation process, the remaining unreacted reactive dyes and their hydrolysis forms have to be washed out of the fabric. Under modern legislation the residual dye must be removed from the effluent before discharge, particularly in the case of some reactive dyes which have a long half-life in near neutral solution, thus, they have higher probability to react with proteins, etc., in the ecosystem.

The removal treatment technologies used for the removing of the unreacted and unhydrolysed synthetic dyes include the use of activated charcoal (Adsorption technology) of various origins and qualities. This method seems particularly suitable for Acid, Basic and Reactive dyes. Ion-exchange resins have been used for the elimination of anionic and cationic dyestuffs. Other processes including the use of nanofiltration and reverse osmosis membranes (Membrane technology) are effective in separating large dye molecules from the effluent. Of the chemical processes used for colour removal, ozone destruction treatment techniques have achieved the largest practical importance. Other methods are based on using either ultra-violet radiation or catalysis (ozone or chlorine) for removing colour from effluent by cleaving bonds in the dye molecule to produce uncoloured species. Although these and other more advanced technological methods such as biofilters, improved inorganic adsorbers and electrochemical treatment are used to remove colour from textile coloration effluents, however, it is possible that a portion of the reactive form of the dyes may escape the treatment process and enter the waste stream.

2.10 Economic Importance of Reactive Dyes

The size of the synthetic reactive dye industry can be conveniently seen from the figures given in Table 2.1, which shows the annual production for reactive dyes in the United States, compared to total dye production over the period 1960 to 1976. The rapid growth of reactive dyes clearly observed from the dramatic increase of production of these dyes from 0.2%, to 1.4% of the total synthetic dyes production, during the given period. Moreover, this remarkable growth can clearly be observed during a particular period between 1960 and 1965, where the production of these dyes increased by a factor of 545%. However, the estimated total world reactive dye production in 1990 was nearly 97,000 tons, thus, reactive dyes accounts for nearly 17% of the textile dye market by volume. In addition, reactive dyes have increased continuously in number since their

inception in 1956. Currently, there are a total of 697 reactive dyes listed in the Colour Index.

Table 2.1: Annual production of reactive dyes¹³

YEAR	PRODUCTION, t	% OF TOTAL
1960	130	0.2
1965	720	0.8
1970	1,010	1.0
1971	1,680	1.5
1976	1,590	1.4

In addition, Table 2.2 illustrates the most recent breakdown according to dyeing chemical constitution class related to the reactive dyestuff industry. These figures indicate the position of Anthraquinone and Azo dyes in synthetic organic dyestuff industry, since these two approximately account for 78 % of the reactive dye market share world-wide.

Table 2.2: Breakdown of reactive dyes according to chemical class¹⁴

CHEMICAL CLASS	PRODUCTION (thousand metric tonnes)
Anthraquinone	24.99
Azo	32.26
Azoic	3.16
Methine	0.95
Phthalocyanine	1.06
Sulphur	8.07
Triarylmethane	3.29

REFERENCES

1. Gurr, E., *Synthetic Dyes*, Academic Press, London, 1971.
2. Zollinger H., *Colour Chemistry*, VCH, Weinheim (Germany), 1987.
3. Robinson, S., *A History of Printed Textiles*, Studio Vista, London, 1969.
4. Abrahart, E.N., *Dyes and Their Intermediates*, Edward Arnold, London, 1977.
5. Rys, P., and Zollinger, H., *Fundamentals of The Chemistry And Application of Dyes*, John Wiley and Sons Ltd., London, 1972.
6. David, R.W., and Geoffrey, H., *The Chemistry and Application of Dyes*, Plenum Press, New York, 1994.
7. *The Theory of Coloration of Textile, Reactive Dye-Fiber system*, The Dyes Company Publication Trust, 1975.
8. Peters, R.H., *Textile Chemistry*, Vol III: *The Physical Chemistry Of Dyeing*, Elsevier Scientific Publishing Company, Oxford, 1975.
9. Venkataraman, K., (Ed.), *The Chemistry of Synthetic Dyes, Vol. VI: Reactive Dyes*, Academic Press, New York, 1972.
10. Gordon, P.F., and Gregory, P., *Organic Chemistry In Colour*, Springer-Verlag, Berlin, 1983.
11. Clarke, E., and Anliker, R., *Organic Dyes and Pigments*. In *Handbook of Environmental Chemistry*, Springer, Berlin, 1980.
12. Anonymous, *IARC Monographs on Carcinogenic Risk of Chemicals To Man*, Vol. 8, International Agency For Research on Cancer, Lyon, 1974.
13. *Synthetic Organic Chemicals - U.S. Production and Sales, 1960-1976*, U.S. Government Printing Office, Washington, D.C., 1971-1977.
14. *U.S. Tariff Commission : Synthetic Organic Chemicals. U.S. Production and Sales Of Dyes*, 1968. U.S. Government Printing Office, Washington, 1968.

ANALYSIS OF REACTIVE DYES

3.1 Introduction

There is a significant need for analytical methods for monitoring synthetic dyes and particularly reactive dyes which form a major part of the dye market, since it is estimated that about 15% of the total world production of colorants is lost in the synthesis and processing of dyes, and during textile dyeing and washing. Moreover, quantitative analysis of dyes is required for quality control in the dyeing industry and to control the dye concentration in commercial products in the process of manufacture. Therefore, a wide variety of analytical methods and techniques were introduced to monitor and determine trace concentration of reactive dyes, their intermediates and hydrolysis products in the environment around industrial areas. In general, the analytical methods used for identification of the type and structure as well as the analysis and evaluation of dyestuffs and colorants can be classified into three main categories: spectroscopic methods, separation techniques and electroanalytical methods. More comprehensive information and descriptions of the separation and analysis of reactive dyes can be found elsewhere¹⁻⁵.

3.2 Spectroscopic Methods

3.2.1 Visible Spectroscopy

It is among the most important and most commonly used technique for quantitative analysis of reactive dye concentration. Visible spectroscopy can also be used for dye identification by the fingerprint method. Quantitative analysis is accomplished

by transmittance spectrophotometry of reactive dye solutions or by reflective spectrophotometry of dyed textiles. Such analyses are currently performed by most dye manufacturers and textile mills.

3.2.2 UV Fluorescence

Fluorescence phenomena can sometimes prove useful in the analysis of dye compounds. Fluorescence dyes and compounds which do not absorb visible light but emit fluorescence light, have replaced conventional dyes for some staining techniques in the past two decades. This is due to the fact that fluorescence methods provide far greater sensitivity and an enhanced signal to noise ratio.

3.2.3 Infrared Spectroscopy

IR spectroscopy can be enormously useful in the analysis of reactive dyes, however, this technique is not only very useful in identification of reactive dyes by the so-called fingerprint method (comparison with dyes of known structure), but also to gain insight into the structural details of unknown reactive dyes (especially when using a combination of this method with NMR and MS techniques). The spectra are compared with spectra of known dyes or analysed on the basis of group frequency correlation.

3.2.4 Nuclear Magnetic Resonance Spectroscopy

This technique is particularly useful in the structural elucidation of dyes, as well as configurational analysis. In addition, specialised versions of NMR such as ^{13}C NMR are also employed for the direct observation of carbon skeletons and carbon-containing functional groups that have no attached protons. Analyses of some dyes by NMR, however, present some difficulties because they are insufficiently soluble in NMR compatible solvents. Also, occasionally only a limited amount of sample is available.

3.2.5 Mass Spectroscopy

The most useful mass spectral technique for identification of reactive dyes is high resolution MS. Modern high-resolution MS spectrometers are capable of measuring mass-to-charge ratio (m/c) with a practical accuracy of 10 ppm. The identification of the unknown reactive dyes by the MS method is accomplished by pattern recognition methods or by matching against a reference library or file of MS patterns (fingerprint).

3.3 Separation Techniques

3.3.1 Paper and Thin-layer chromatography

Both of these techniques are separation methods useful for dye identification. The dyes are extracted from fibres with suitable solvents, or dissolved if in powder form, and applied to chromatographic paper strips or plates which are then developed in a tank with suitable eluent. Not only is it possible in this way to separate reactive dye mixes into their components, but reactive dye identification is feasible based on comparisons with known dyes. In such cases, it is generally necessary to compare the dyes in at least two different eluent systems. For semi-quantitative or quantitative analysis, the separated dyes can be measured with a reflectance densitometer.

3.3.2 HPLC and GLC

High pressure liquid chromatography (HPLC) with UV/visible detection is used to monitor reactive dyes and their reaction products. In addition to its success for separation and accuracy in quantitative analysis of dyes, this method is generally faster and more convenient than thin layer chromatography, however, it requires considerably more expensive equipment. UV and visible spectroscopic methods are used for detection

and for quantitative purposes, therefore, in some situations the detection limits is not adequate.

Although Gas Liquid Chromatography (GLC) is generally rapid and convenient for obtaining qualitative and/or quantitative analysis for many classes of organic compounds, there are very few dyes or related compounds that can be separated and identified by this technique. The reason for the unpopularity in this field is due to the vast majority of dyes not being volatile enough to elute through the GLC column, and not thermally or chemically stable at the temperature necessary for elution.

3.3.3 Electrophoresis

Both the reversed-polarity mode of capillary electrophoresis and paper electrophoresis are used for rapid determination of the purity, separation, and determination of reactive textile dyes. These methods are valuable aids in the constitutional analysis of reactive dyes and in the study of their colouristic properties. Electrophoresis separation methods are based on the differential mobility of charged molecules or particles (e.g. dyes) in an electric field. The reactive dyes are spotted on the chromatographic paper, which is saturated with a suitable buffer. The most frequently employed is the low-voltage method with horizontally placed paper. Methods have been developed for the analysis of various synthetic textile dyes using Capillary Zone Electrophoresis (CZE). The anionic dyes have an electrophoretic mobility towards the anode, opposite to the electroosmotic flow, and, hence, have long migration times compared with cations and neutral species, therefore the method can be used as a basis for a subsequent separation process.

3.4 Electroanalytical Determination of Reactive Dyes

Although spectrophotometric analysis is usually considered to be the most commonly used method for the determination and studying of reactive dyes, it cannot

distinguish between the reactive dye and the unreactive hydrolysed dye or intermediate forms. Furthermore it can hardly afford a satisfactory result from a system where mixtures of more than one dye normally give overlapping absorption spectra, as well as, the inadequate detection limits in some situations. Such difficulties and limitations indicate the advantages of applying electroanalytical methods for overcoming such difficulties. Therefore, the electroanalytical techniques in some cases could be directly applied to any dye solution for the simultaneous determination of reactive dyes without further separation of them from the basic matrices, with remarkable sensitivity and extremely low detection limits when utilising advanced stripping voltammetric techniques.

Numerous types of synthetic dyes and their intermediates or reaction products can be studied by various electroanalytical techniques. The reactive dyes can be determined directly by electroanalytical measurements since they contain a reducible group such as the azo and anthraquinone group. Thus, reactive dyes classified as electroactive species that can easily be determined by a voltammetric method (or any other technique) by reducing the reducible groups (chromophore systems) at the working electrode. Others, however, can be indirectly analysed as they form stable and reducible complexes with electropositive metal ions including Cu, Ni, Al, Mg, Ga, and Cr.

3.4.1 Amperometric titration

Although there is no particular example for the analysis of reactive dyes by this technique (and some of the next electroanalytical techniques) there are, however, several examples for determination of the synthetic dyes in general by such a technique, which can be easily adapted and applied for analysis of reactive dyes since they contain similar electroactive properties. More comprehensive information and descriptions can be found in reference [2].

Amperometric titrations of the synthetic dyes have been studied by means of DP polarography. The end points for the titration curves of acid dyes with a standard crystal

violet solution and basic dyes with a sodium tetraphenylborate solution were easily determined by a simple graphical method². These amperometric titration curves were reproducible within a range of 3% for ten titrations. An amperometric titration between the surfactant (Manoxol OT) and Methylene Blue dye has been proposed by Buchanan and Griffith⁶. However, it was found that sufficient time for complete reaction and settling of the precipitate should be allowed before polarographic analysis. Saikine et al. has studied amperometric titration of some monoazo dyes with cobalt and nickel salt⁷. In addition, C.I. Basic Green 4 has been determined in its chromatic form in drinking and river water using HPLC with amperometric detection at a carbon fiber electrode⁸. The limit of detection of the technique was 0.07 mg l^{-1} and the linear range extended from $0.07\text{-}10 \text{ mg l}^{-1}$. This technique was found to be reproducible with a mean relative standard deviation of 5.4 and 3.6 % at the 0.25 and 5 mg l^{-1} levels, respectively.

3.4.2 Potentiometric titration

Potentiometric determination of dyes has been reported using ion-selective electrodes responsive to dyes. PVC and liquid state natural rubber membrane ion-selective electrodes have been developed for the determination of acid and basic dyes². Reasonable good shapes of titration curves were obtained from those titrations, which indicate their applicability to the assay of dye samples. The potentiometric determination of azo dyes with Mohr's salt in a glycerol medium has reported by Nikolaev and colleagues⁷. Direct, azo, and sulfato dyes could be analysed by the introduction of potentiometric titration with sodium nitrite in an excess of benzidine⁹. The potentiometric titrations of acid dyes with crystal violet solution and basic dyes with sodium tetraphenylborate using PVC membrane electrodes produced satisfactory results with a big potential jump in the end point area. Moreover, the reactive chlorothiazine dyes have been determined potentiometrically by direct titration of the water-soluble anthraquinone derivatives with vanadium sulfate¹⁰.

Fifteen azo dyes containing a hydroxy group, phenol, 1-naphthanol and 2-naphthanol were titrated potentiometrically with tetrabutylammonium hydroxide (TBAH) at room temperature. Potentiometric titration curves of these compounds in acetonitrile with TBAH propan-2-ol-methanol are similar to those of weak acids obtained in aqueous media with strong bases¹¹. The thermodynamic aspects of the self-association of three monoazo dyes, Acid Red 88, Acid Orange 7 and Acid Orange 8 in aqueous solution have been studied by means of a potentiometric method. An ion-selective membrane electrode, selective to a dye anion, has been constructed¹². Finally, Vytras and colleagues¹³ reported the use of simple coated-wire electrodes for monitoring the Potentiometric titration of seven metal-complex dyes with chromium (III). High potential breaks were observed on the titration curves, with well-defined end-points corresponding to a titration dye-titrant stoichiometric ratio of 1:3; the reproducibility of the results obtained in assaying the dye samples was very satisfactory.

3.4.3 Coulometric titration

The synthetic dyes Orange 11, Tartrazine, P-aminoazobenzene, Amaranth, and Methyl Violet have been analysed coulometrically with electrolytically generated ions¹⁴. Peng *et al.*¹⁵ reported the electrochemical reduction of four azo dyes in acid media investigated by a constant potential coulometric method. Furthermore, Makoto described the coulometric titration of dyestuffs with electrolytically generated dithionite and milligram amounts of dye were titrated with an average error of 0.5 %¹⁶.

3.4.4 Conductivity

The state of aggregation of C.I. Reactive Orange in an aqueous medium was studied by electrical conductivity techniques as a function of dye concentration. A marked decrease in the equivalent conductance of the dye solution of a concentration higher than 0.149 mM, as well as the decrease of viscosity of the dye solution when

increasing temperature from 5 to 55°C indicates the formation of dye aggregates¹⁷. Nine organic dyes were studied by measuring their electrical conductivity¹⁸. The degree of Dye/Surfactant interaction between direct or acid dye and nonylphenolethoxylates has been investigated by a simple and accessible method based on conductivity measurement¹⁹.

3.4.5 Polarography

The applicability of polarography and voltammetry is growing in dye analysis. In general, polarography may be superior in convenience to other electroanalytical techniques, particularly in situations where several dyes have to be determined in each sample. Furthermore it has remarkable advantages of sensitivity, selectivity, and reliability.

Procion Blue MX-R (PB) and Cibacron Blue 3GA (CB) anthraquinone-based chlorotriazine reactive dyes have been studied by direct current and differential pulse polarographic techniques. Fogg and Zanoni²⁰ reported that for both dyes reduction peaks are observed: for the two-electron reversible reduction of the anthraquinone moiety, followed by one (CB) and two (PB) reduction processes associated with the reduction of the mono- and dichlorotriazine groups, respectively. These latter processes appear to involve the reductive elimination of the chlorine atoms. Only the anthraquinone reduction process is observed when the dyes are hydrolysed. A simultaneous determination of the two studied dyes would be difficult owing to the similar peak potentials of CB and PB. In alkaline solution the reduction process is complicated by adsorption and kinetic effects. Thus, acidic solutions ($\text{pH} < 6$) are preferred for analytical purposes such as monitoring of reactive dyes in dyeing procedures or in effluents. However, determination of dyes is also possible in alkaline solution, which would be more convenient for monitoring dyes during nucleophilic reactions.

The polarographic reduction of five triazinyl azo dyes differing only in their potentially reactive groups (e.g. Cl, NH_2 , OCH_3 ...etc.), using a hanging mercury drop

electrode have been investigated by Fogg and colleagues²¹. They studied the effect of changing the leaving group on the polarographic and voltammetric behaviour of the dye. In addition, they established the mechanism of the reduction process and determined the optimum conditions for the determination of their trace amounts. The azo reduction process is present for all the test dyes and hydrolysis or methanolysis products. Two of the dyes, -Cl and -SCH₂CH₂OH derivatives exhibit another process at more negative potentials, which is shown to be due to 2e⁻ reduction of the leaving group/triazine bond followed immediately by a 2e⁻ reduction of C=N bond in the triazine ring. Finally, their hydrolysis and methanolysis could be monitored by observing the loss of the corresponding peak. In addition, two further types of triazinyl reactive dyes with different leaving groups (4-carboxypyridyl, and 1,4-diazabicyclo[2,2,2]octane(DACO)) and the dye base have been studied by DC and DP polarography²². Peaks corresponding to the reduction of azo and the reactive group were clearly observed in DP and DC polarograms. A further peak was observed for the 4-carboxypyridyl dye; this was shown to be due to free 4-carboxypyridine impurity. The peak, due to the reduction of the reactive groups, was absent when the dyes were hydrolysed. The hydrolysis of the 4-carboxypyridine reactive dye can be monitored by the decrease of the reactive peak. However, it also can be followed by the increase in the peak at more negative potential due to the formation of the free 4-carboxypyridine.

The voltammetric determination by DC voltammetry using a glassy carbon electrode of four reactive dyes (two of which contain the monoazo and the other two contain the mono anthraquinone group) have been investigated²³. The reduction peaks for the azo or anthraquinone group and for the reactive groups (e.g. Cl, F) were observed. The peak due to the reduction of the reactive group was observed at more negative potentials except for one anthraquinone dye. For one azo dye a shift of about 130 mV for the azo signal between the reactive dye and its hydrolysis product was observed. Sahn suggested that this discrimination is probably due to further hydrolysis of the chromophoric group; a benzamide function is cleaved and an amine function is formed.

The amine function, being a strong electron donating group thus shifts the reduction potential of the azo group towards more negative values.

The polarographic and voltammetric reduction of the azo dye 4-nitro-3'-tert-butyl-2'-hydroazobenzene in B-R buffer with the pH range between 3 and 12 at room temperature has been investigated in aqueous-ethanol solutions of ratio 1:1. Two straight lines were obtained from the E_p -pH plots for the compound²⁴. Diffusion controlled reduction behaviour was observed in the acidic and alkaline media but the products were different.

3.4.6 Cyclic Voltammetry

Bogdanovskaya *et al.*²⁵ applied the cyclic voltammetric technique to study the adsorption and electrochemical behaviour of the azo dye, Reactive Brilliant Red 65 at the pyrolytic graphite electrode. Adsorption was found to depend on the sign and size of potential and acidity of the medium. The reversibility and the cyclic voltammetric behaviour at the HMDE of two anthraquinone-based chlorotriazine reactive dyes (Procion Blue MX-R and Cibacron Blue 3GA) have been observed²⁰. Typical cyclic voltammograms reflect the reversibility of the first electrode process (the reduction of the anthraquinone group) at different scan rates for PB and CB in acetate buffer and Britton-Robinson buffer. However, in B-R buffer the anodic peak (IA) is decreased and another anodic peak (IIA) is obtained at a less negative potential. This behaviour occurs over the full pH range investigated. At low scan rates only one cathodic peak and one anodic peak (IA) are seen in both voltammograms. In addition, a more detailed cyclic voltammetric study was also carried out in order to obtain more information about the nature of the electrode processes and to observe any differences in the reduction of the dyes at stationary electrodes.

Ali²⁶ discussed using cyclic voltammetry for studying the cathodic reduction behaviour of azo dye sulfa drug at the HMDE in different supporting electrolytes, at different pH values, range from 1 to 11 and at different ionic strength. The two related

compounds for the sodium salt of azo dye sulfa drug have been also studied at 0.1M acetic acid-sodium acetate buffer. Furthermore, the electrochemical reduction of four azo dyes was studied by the cyclic voltammetry method¹⁵. All of the azo groups of the studied dyes were irreversible one-step and four-electron reduction at $\text{pH} < 2$.

3.4.7 Adsorptive Stripping Voltammetry

Franklin Smyth and co-workers²⁷ have studied and compared the behaviour of six reactive dyes in both adsorptive stripping voltammetric (AdSV) and reversed-polarity Capillary Electrophoresis. They also compared the correlation coefficient of the calibration graphs, limits of detection, and selectivity for both techniques in the analysis of textile reactive dyes. Only four of the six starting dyes (Remazol Yellow RNL, Remazol Navy Blue GG, Remazol Black B, Remazol Red RB, Cibacron Red C-2G, and Cibacron Orange CG) could be separated in the reversed-polarity mode of CE, whereas AdSV was shown to be very sensitive for monitoring the individual six dyes. Although AdSV has a particularly low limit of detection, it lacks the selectivity to deal with a complex mixture, hence the dyes with similar reduction potentials give a single peak when all six dyes are analysed in a single run. The AdSV voltammogram of a mixture of all six reactive dyes following accumulation at 0.0 V shows three separate peaks. The first peak at -245 mV is due to the reduction of Remazol Blue GG, Yellow RNL, and Black B; the second peak at -341 mV is associated with the reduction of Remazol Red RB, and Cibacron Red C-2G, and the final peak at -476 mV is related to Cibacron Orange CG.

Fogg and Yusoff have discussed the cathodic stripping voltammetry using the hanging mercury drop electrode of copper-complexed vinyl sulfone reactive dyes (Reactive Violet 4²⁸ and Reactive Violet 5²⁹). Two peaks were observed for both dyes in Britton-Robinson buffer; these are the complexed copper reduction peak and the azo reduction peak. However, because of this latter azo reduction peak the original Reactive

Violet dye and its hydrolysis product are sufficiently well separated. This allows the hydrolysis reaction of the reactive dye to be monitored effectively. For both dyes at intermediate pH values (pH 6) the azo reduction peak is preceded by a complexed-copper reduction peak, which aids the identification of the dyes. In pH 6 EDTA buffer the copper peak is absent while the azo peaks of Reactive Violet dye and its hydrolysis product is resolved. This unusual use of EDTA as pH buffer facilitates the determination of mixtures of the dyes and its hydrolysis products.

Khdier³⁰ studied the electrochemical reduction and determination of two reactive dyes (Reactive Orange 23 and Reactive Black) by the technique of differential pulse adsorptive stripping voltammetric using a HMDE. She also studied the hydrolysis reaction of the two dyes and the effect of adding tetraphenyl phosphonium chloride (TPPC), Triphenyl n-butylphosphonium bromide (Tpn-bPb) and Sorbitol on the AdSV behaviour of the two reactive dyes. The result obtained showed that both reactive dyes adsorbed onto the HMDE surface, for the Reactive Orange 23 it gives two well-defined peaks at -0.63 V and -0.79 V. However, by adding (TPPC) the two waves shifted to more negative potentials, but the second wave was depressed and became ill-defined. TPN-bPb produced similar effects on the Reactive Orange dye, whereas Sorbitol and Glycerol have a very slight effect on the reactive dye. However, the first wave of Reactive Black is shifted 0.12 V to a more positive potential by adding TPPC, while the second peak is not affected. TPN-bPb has the same effect on Reactive Black.

Pre-concentration and quantitative determination of Reactive Red 41 and Reactive Red 96 have been investigated by cathodic stripping voltammetry (CSV) technique³¹. The azo reduction peak in CSV voltammogram of 2,3-dichloroquinoxaline Reactive Red 41, and those of its hydrolysis product are sufficiently separated for the hydrolysis of Reactive Red 41 to be followed using the height of these peaks. In the case of 1,4-dichlorophthalazine reactive dye, Reactive Red 96, the azo peaks of the reactive and hydrolysis dyes are too close to be used to monitor the hydrolysis reaction, but peaks associated with reduction of 1,1-dichlorophthalazine group are present which could be used to monitor the hydrolysis of Reactive Red 96. For both dyes, if a sufficient amount

of copper is present, the hydrolysis process can be monitored by the increase in the peak due to the reduction of the complexed copper in the hydrolysed product.

Cathodic stripping voltammetry with adsorptive accumulation has been employed successfully for the analysis of two types of anthraquinone-based dye and their hydrolysis, methanolysis, and reaction products at the nanomolar level³²⁻³⁴. The differential-pulse cathodic stripping voltammetry (DPCSV) of the two reactive dyes after accumulation at the HMDE, gives rise to a large well-defined peak around -1.1 V which is attributed to the reduction of the chlorotriazine moiety, while only a small differential-pulse voltammetric signal of about -0.7 V is observed for the reduction of the anthraquinone moiety; the peak is slightly larger for Procion Blue. These peaks are even smaller in acidic solution. The lack of a DPCSV signal for the first reduction process of anthraquinone-based dyes illustrated a general theory that adsorbed species that are reduced reversibly to an adsorbed product do not give a differential-pulse signal. In addition, it was found that in an alkaline medium (as in pH 10 carbonate buffer), the anthraquinone-based dyes, PB MX-R and CB 3GA, and their hydrolysis products can be discriminated without the need for prior separation, this can be achieved by observing the loss of chlorotriazine peak or the appearance of anthraquinone peak signals. The progress of hydrolysis process was studied by carrying out stripping voltammetry at various times during a 1 hour hydrolysis and observing the gradual decrease in height of the chlorotriazine reduction peak and the corresponding increase in the height of the anthraquinone reduction peak. Clearly, the replacement of the reactive chlorine group on the dye by hydroxyl removes the ability to reduce the triazine moiety.

Triazine-based azo dyes with different reactive groups were analysed by adsorptive stripping voltammetric at the HMDE²¹. The reduction process of the azo group was used for the monitoring of the dyes to a remarkable detection limit. The accumulation potential has only a negligible effect on peak height of all the reactive dyes with different reactive groups. Under these conditions the peak heights increased with accumulation time nearly up to 15 minutes. By a suitable choice of accumulation time linear calibration dependence can be obtained within the range 1×10^{-10} - 2×10^{-8} mol l⁻¹.

With an accumulation time of 5 minutes limits of detection around $2 \times 10^{-8} \text{ mol l}^{-1}$ can be obtained. In addition, two further triazine-based azo dyes (4-carboxypyridyl and 1,4-diazobicyclo[2,2,2] octane (DABCO)) were studied by CSV technique^{22,35}, together with the information on their hydrolysis products. In the case of the 4-carboxypyridyl reactive dye it has been shown that its hydrolysis form can be monitored by observing the decrease in the peak height of the reactive group and by observing the increase in the height of the peak due to one of the hydrolysis products, 4-carboxypyridine. The hydrolysis of the DABCO dye could be monitored by following the decrease in the second and third peaks of the dye, which are eliminated on hydrolysis.

The electrochemical reduction of vinylsulfone azo reactive dye Remazol Brilliant Orange 3R at a hanging mercury drop electrode was studied by AdSV³⁶. This reactive dye showed only a voltammetric peak for the reduction of azo group. No peak was observed for the reduction of the sulfatoethylsulfone or vinylsulfone reactive groups. The reduction of a pre-protonated azo group involved a two-electron process, giving a hydrazo derivative in acidic solution. In alkaline solution the reduction process occurred at a more negative potential with the formation of an unstable hydrazo compound which decomposed via HN-NH bond cleavage and loss of a sulfato group.

Finally, Fogg and colleagues have studied other reactive dyes such as Reactive Orange 4, Reactive Orange 13³⁷ and Reactive Green 19³⁸ which are still under preparation for publication.

REFERENCES

1. Venkataraman, K., (Ed.), *The Analytical Chemistry of Synthetic Dyes*, John Wiley & Sons Inc., New York, 1977.
2. Yoo Kwang-Sik, *Electroanalytical Studies of Dyes*, A Ph.D. Thesis, Loughborough University, 1979.
3. Venkataraman, K., (Ed.), *The Chemistry Of Synthetic Dyes*, Vol. VI: Academic Press, New York, 1972.
4. Macek, K., (Ed.), *Pharmaceutical Applications of Thin Layer and Paper Chromatography*, Elsevier, 1972.
5. Pearson, D., *The Chemical Analysis of Foods*, Churchill Livingstone, Edinburgh, 1976.
6. Buchanan, G.S., and Griffith, J.C., *J. Electroanal. Chem.*, (1963), **5**, 204.
7. Saikine, M.K., Nikolaev, G.N., Tsekhanskil, R.S., and Gorbunova, K.A., *Fiz-Khim, Izuch, Nerogan Sedin*, (1977), **5**, 84.
8. Sagar, K., Smyth, M.R., Wilson, J.G., and McLaugh, K., *J. Chrom.*, (1994), **659**, 329.
9. Krasovitskiy, B.M., Ostrovskaya, B.J., and Pereyaslova, P.G., *Zhur. Anal. Kim.*, (1956), **11**, 216.
10. Lyande, Y.V., Savenkova, V.V., and Cherkasski, A.A., *Zab-Lab*, (1975), **41**, 1966.
11. Serin, S., and Kurtoglu, M., *Analyst*, (1994), **119**, 2213.
12. Simoncic, B., Span, J., and Vesnaver, G., *Dyes and Pigments*, (1994), **26**, 257.
13. Vytras, K., Novak, F., Kalous, J., and Macounova, H., *Dyes and Pigments*, (1993), **23**, 205.
14. Parsons, J.S., and Seaman, W., *Anal. Chem.*, (1955), **27**, 210.
15. Peng, X.J., Yang, J.Z., and Wang, J.T., *Dyes and Pigments*, (1992), **20**, 73.
16. Makoto, M., *Talanta*, (1958), **1**, 110.
17. Elfassm, M.M., Sallam, H.B., Elsabghagh, I.A., and Mahmoud, A.A., *Polish J. Chem.*, (1993), **67**, 285.
18. Ivanova, C., and Peneva, V., *Lect. Notes Phys.*, (1977), **65**, 647.
19. Jocic, D., *Textile Res. J.*, (1995), **65**, 409.

20. Fogg, A.G., and Zanoni, M.V.B., *Anal. Chim. Acta.*, (1995), **315**, 41.
21. Barek, J., Fogg, A.G., and Moreira, J.C., *Anal. Chim. Acta.*, (1996), 320, 31.
22. Fogg, A.G., Zanoni, M.V.B., Yusoff, A.R.H., Ahmad, R., Barek, J., and Zima, J., *Anal. Chim. Acta*, (1998), **362**, 235.
23. Sahn, U., Kinttel, D., and Scholmeyer, E., *Fresenius J. Anal. Chem.*, (1990), **338**, 824.
24. Menek, N., and Cakir, O., *Turkish Chem.*, (1995), **19**, 135.
25. Bogdanovskaya, V.A., *Soviet Electrochem.*, (1991), **27**, 1020.
26. Ali, A., *Anal. Lett.*, (1993), **26**, 1635.
27. Oxspring, D.A., Smyth, W.F., and Marchant, R., *Analyst*, (1995), **120**, 995.
28. Fogg, A.G., Yusoff, A. Rahim and Ahmad, R., *Malaysian J. Anal. Sci.*, **3**, (1997), 157.
29. Fogg, A.G., Yusoff, A. Rahim and Ahmad, R., *Talanta*, (1997), **44**, 125.
30. Kdhier, W., *Voltammetric Identification of Dyes Using Surfactants*, A Master of Philosophy Thesis, Loughborough University, 1989.
31. Yusoff, A.R.H.M., Fogg, A.G., and Ahmad, R., *Talanta*, (1998), **47**, 797.
32. Fogg, A.G., and Zanoni, M.V., *Anal. Proc.*, (1994), **31**, 173.
33. Zanoni, M.V., and Fogg, A.G., *Anal. Proc.*, (1994), **21**, 217.
34. Zanoni, M.V.B., Fogg, A.G., Barek, J., and Zima, J., *Anal. Chim. Acta*, (1997), **349**, 101.
35. Yusoff, A.R.H.M., *Cathodic Stripping Voltammetric Studies on Sulfonamides and Reactive Dyes*, A Ph.D. Thesis, Loughborough University, 1996.
36. Zanoni, M.V.B., Carneiro, P.A., Furlan, M., Duarte, E.S., Guaratini, C.C.I. and Fogg, A.G., *Anal. Chim. Acta*, **385**, (1999) 385.
37. Zima, J., Barek, J. Moreira, J.C., Mejstic, V. and Fogg, A.G., in press.
38. Guaratini, C.C.I., Fogg, A.G. and Zanoni, M.V.B., prepared for publication.

EXPERIMENTAL

4.1 Apparatus

Adsorptive stripping and cyclic voltammetric measurements were carried out using a Metrohm E612 voltammetric scanner and E611 voltammetric detector (Metrohm, Herisau, Switzerland) with Houston Instruments 2000 X-Y recorder, a Metrohm 663 VA Multimode Electrode stand (MME) was used in the hanging mercury drop electrode (HMDE) mode. The three electrode system was completed by means of a platinum auxiliary electrode and an Ag/AgCl (3M KCl) reference electrode. In addition, Metrohm 646 VA voltammetric processor coupled with a Metrohm 647 VA stand was also used for obtaining adsorptive stripping voltammetric measurements.

The working electrode: The working electrode is the characteristic multi-mode electrode (MME) in which three types of mercury electrodes are combined into a single design: Hanging mercury drop electrode (HMDE), dropping mercury electrode (DME) and static mercury drop electrode (SMDE).

Reference electrode: The Ag/AgCl reference electrode is in many respects the most satisfactory of all reference electrodes and certainly the simplest. It consists of a silver/silver chloride wire in 3 M potassium chloride solution.

Auxiliary electrode: The third functional electrode is the auxiliary electrode, which is made of an inert material like platinum or of glassy carbon. This electrode is the current carrying electrode in the three-electrode system. It is placed directly opposite the reference electrode.

For differential pulse voltammetry at the HMDE, a scan rate of 5 mVs^{-1} and pulse amplitude of 50 mV with a pulse interval of 1 s were used. The medium stirring speed was used during accumulation with mercury drop size of 0.4 mm^2 . Usually reactive dyes were monitored over the voltage range from 0.0 to -1.3 V. pH measurements were made using an Orion pH

meter, previously calibrated. All glassware, voltammetric cell and electrode systems were cleaned prior to determination and washed three times with de-ionised water. De-ionised water was produced by a Maxima ultra pure water system.

4.2 Reagents

(a) Reactive Dyes (samples)

All chemicals and samples used were of the highest purity available and were used without further purification. Zeneca Specialties (Manchester, UK) kindly provided sample of Reactive Blue -19. Fluorotriazine and chlorotriazine reactive dyes were generously supplied by BASF PLC (Manchester, UK). Table 4.1 lists the reactive dyes used in these studies together with their chemical structures, molecular formula and molecular weight. Stock solutions of each dye of concentration $1 \times 10^{-2} \text{ mol l}^{-1}$ in de-ionised water were prepared by dissolving an accurately weighed amount of pure substance. Solutions with lower concentration were prepared daily by diluting the stock solutions with de-ionised water. For obtaining a standard solution of the intermediate form Reactive Blue 19-Vinyl Sulfone (RB 19-VS), a solution of $1 \times 10^{-3} \text{ mol l}^{-1}$ of the original dye was stirred at pH = 11 at room temperature for one hour. The pH was adjusted to pH 7 by the addition of 0.1 M HCl. In order to obtain solutions of fully hydrolysed dye of Reactive Blue 19 (RB 19-OH), or fluorotriazine-based and chlorotriazine-based azo reactive dyes, solutions of original reactive dyes in sodium carbonate at pH 10 were heated for at least one hour or alternatively $1 \times 10^{-3} \text{ mol l}^{-1}$ solution of dye solution were refluxed at pH 11 for 3-4 hours.

(b) Supporting electrolytes

The buffer solutions used in all experiments were prepared using analytical-grade materials (Analar grade) as following: hydrochloric acid (Fisons chemical ltd.), sodium hydroxide (BDH), boric acid (Fisons), glacial acetic acid (Fisons), orthophosphoric acid (BDH), sodium acetate (Fisons), sodium hydrogen carbonate (Fisons), and disodium carbonate (Fisher scientific).

Britton-Robinson buffer (pH ~ 2; 0.04 M in each constituent) was prepared by dissolving 2.47 gm of boric acid in 500 ml of distilled water containing 2.3 ml of glacial acetic then adding

2.7 ml of orthophosphoric acid and diluting to 1 L with distilled water. The desired pH of the buffer was adjusted with 4 M sodium hydroxide solution. A 0.02 M acetate buffer was prepared from both acetic acid and sodium acetate. The carbonate buffer was 0.1 M in both sodium hydrogen carbonate and disodium carbonate.

(c) Surfactants

The non-ionic surfactant Triton X-100 (stock solution: 200 mg l⁻¹) was obtained from Sigma (Dorset, UK). The anionic surfactant Aerosol OT (1 mV⁻¹) and Gelatine (0.5 mV⁻¹) were purchased from BDH (Poole, England). Glycerol (200 mg l⁻¹) and Sorbitol (2 mV⁻¹) both were supplied by Aldrich (Gillingham, England). Tetraphenyl phosphonium chloride (TPPC) cationic surfactant (1×10^{-2} M) was obtained from Janssen chimica (Geel, Belgium). Finally, BDH (Poole, UK) supplied the complexing agent EDTA (1×10^{-4} M).

(d) Metal ion solutions

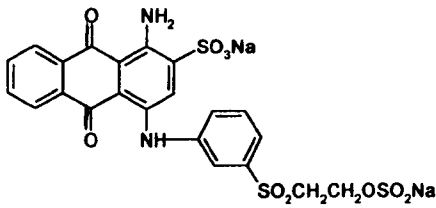
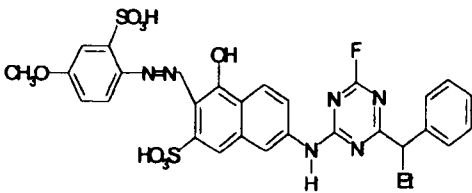
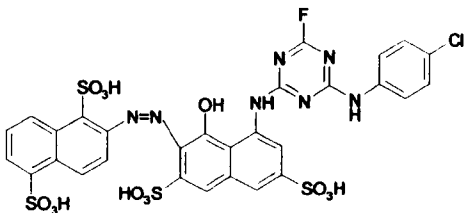
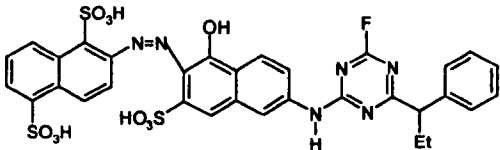
Standard solutions of metal ions: Zinc (II), Copper (II), Cobalt (II), Lead (II), Tin (II), Iron (II), Indium (III), Titanium (IV), Selenium (IV), Silicon (II), Gold (I), Lithium (I), Sodium (I), Magnesium (II), and Barium (II) were prepared by diluting Fisons spectral atomic absorption standard solutions.

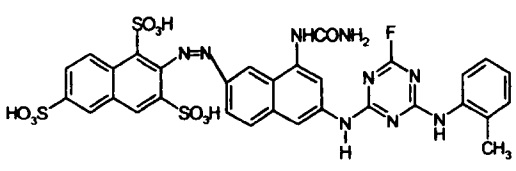
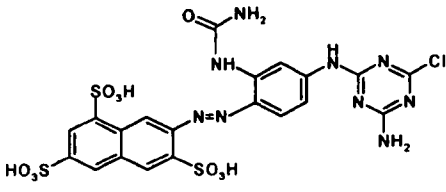
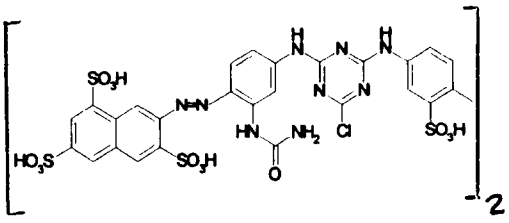
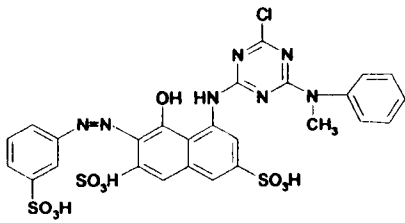
4.3 Working Procedure

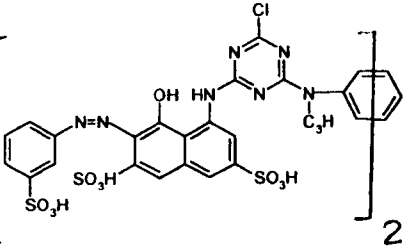
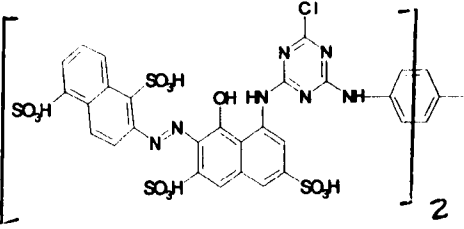
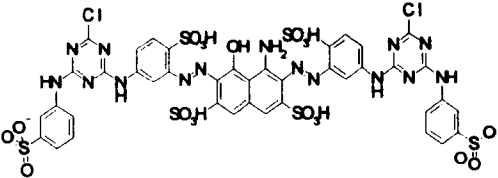
The general procedure adopted for obtaining adsorptive stripping voltammograms were as follows. A 20 ml aliquot of an appropriate buffer was placed in a clean dry voltammetric cell and the required stock solution of the test substance was added. Solutions were deoxygenated by bubbling with nitrogen for 5 min initially, while the solution was stirred at medium stirring speed. Adsorptive accumulation was carried out whilst stirring the solution. An accumulation potential at 0.0 V was applied to the working electrode for 2 min (unless otherwise stated). At the end of the accumulation period in stirred solution, the stirrer was stopped and after 20 s had

elapsed and the solution had become quiescent, cathodic scans were carried out over the voltage range 0.0 to -1.3 V. Cyclic voltammetry was carried out immediately after forming a new HMDE. A new hanging mercury drop was formed after removing oxygen and after recording of the curves. All measurements were obtained at room temperature.

Table 4.1: Molecular structures of the studied Reactive Dyes.

	NAME	STRUCTURE	MF	MW
1	Reactive Blue 19		$C_{22}H_{16}O_{10}N_2S_3Na_2$	610
2	Fluorotriazine Dye 1		$C_{29}H_{25}O_8N_6S_2F$	682
3	Fluorotriazine Dye 2		$C_{29}H_{19}O_{13}N_7S_4FCl$	856
4	Fluorotriazine Dye 3		$C_{32}H_{24}O_{10}N_6S_3F$	781

5	Fluorotriazine Dye 4		$C_{31}H_{21}O_{10}N_9S_3F$	794
6	Reactive Yellow 84		$C_{20}H_{16}O_{10}N_9S_3Cl$	674
7	Reactive Orange 12		$C_{52}H_{38}O_{26}N_{18}S_8Cl_2$	1656
8	Reactive Red 24		$C_{26}H_{20}O_{10}N_7S_3Cl$	721

9	Reactive Red 120		$C_{46}H_{32}O_{20}N_{14}S_6Cl_2$	1362
10	Reactive Red 141		$C_{52}H_{34}O_{26}N_{14}S_8Cl_2$	1596
11	Reactive Blue 171		$C_{40}H_{27}O_{19}N_{15}S_6Cl_2$	1283

DIFFERENTIAL PULSE ADSORPTIVE STRIPPING VOLTAMMETRIC DETERMINATION OF REACTIVE BLUE 19 AT THE HMDE

5.1 Introduction

Approximately, there are 40 types of reactive groups that have been listed for commercial dyes. They were being widely used in dyeing cellulose, cotton, wool and silk. Of these, the highest volumes of commercial products are those containing the 2-sulfatoethylsulfone moiety. Anthraquinone-based Reactive Blue 19 (Remazol Brilliant Blue R special) is considered as a representative of this type of reactive dyes. Currently, C.I. Reactive Blue 19 is one of the highest volume reactive dyes on the market¹. In the dye bath, the original RB-19 dye undergoes facile conversion to the intermediate reactive form, the vinylsulfone (RB 19-VS) by treatment with base. The dye-fibre adduct is formed in a subsequent reaction by Michael-Type 1,4-nucleophilic addition. Competing with this reaction is nucleophilic addition of the hydroxide ion to the vinylsulfone group to give the 2-hydroxy ethyl sulfone (RB 19-OH) form². This competitive reaction is the reason for the relatively low fixation rates. The chemical formation of the hydrolysed and intermediate forms is represented in Fig. 5.1.

For the majority of vinylsulfone reactive dyes, the degree of fixation ranges from 75% to 80% on cotton, which means that 20-25% of this reactive dye enters the waste stream of the textile mill. These compounds can be transported from municipal sewers to rivers and ground waters because of their high water solubility. Such figures emphasise

the concern associated with RB 19-VS because it has been shown to be resistant to treatment, 25% of the RB 19-VS passed through a municipal wastewater treatment plant without degradation. However, the concern over RB 19-VS is heightened because of the electrophilic nature of the vinyl sulfones, which may lead to possible ecotoxicity and mutagenicity effects. In addition, reactive dyes have been shown potentially to have a long half-life in near neutral solution in the environment. In addition, it can react with proteins in the ecosystem and it also exhibits strong DNA binding properties. Therefore, the environmental problem and health risks associated with this reactive dye calls for analytical control of effluents before discharge and the development of analytical methods capable of monitoring this reactive dye and its products in dyeing and dyeing simulation reactions.

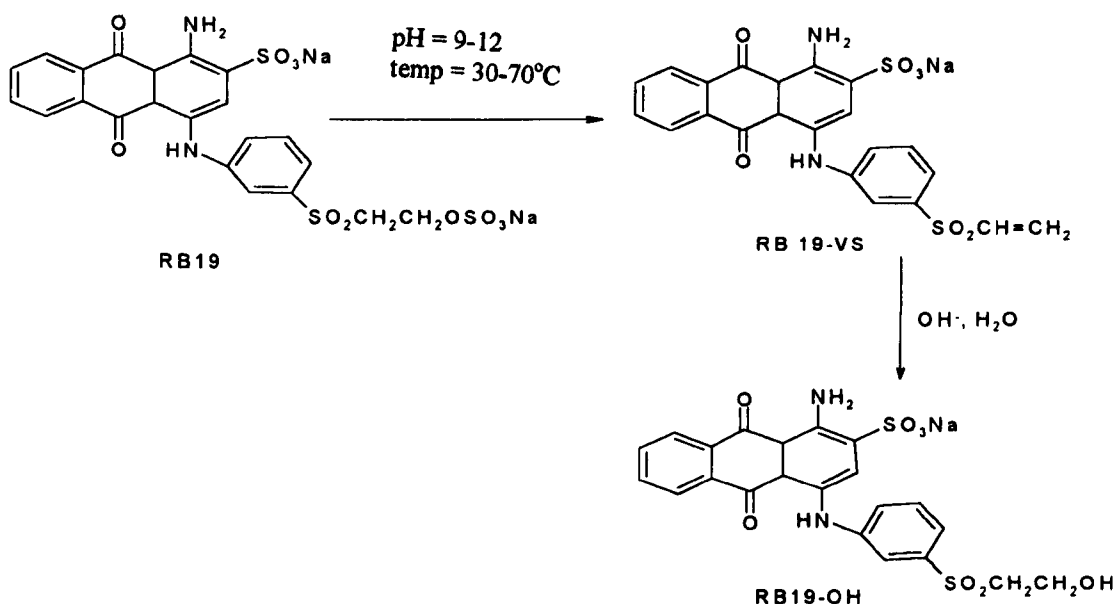


Figure 5.1: Reaction pathway of the formation of RB 19-VS and its reaction with hydroxide ion (hydrolysis).

Camp and Sturrock³ developed an analytical procedure using a swept-potential electrochemical detector and HPLC for the separation and identification of hydroxy (RB 19-OH) and vinyl sulfone (RB 19-VS) derivatives of RB-19 in textile wastewater. They

reported RB 19-VS and RB 19-OH in textile effluent at concentration of 760 and 80 $\mu\text{g l}^{-1}$, respectively. They obtained extra information from the three dimensional data which permits easier and more accurate identification. However, the hydrolysis kinetics of RB-19 vinylsulfone over a pH range of 4-11 and temperature range of 25-85°C were studied by liquid chromatographic analysis². The estimated half-life for RB 19-VS in natural waters at 25°C was 46 years.

Fogg and colleagues studied similar anthraquinone-based dyes to RB-19. Both Procion Blue MX-R and Cibacron Blue 3GA dyes were studied by DC, DP polarography, cyclic voltammetry⁴ and cathodic stripping voltammetry⁵. Furthermore, the stripping voltammetric behaviour of two anthraquinone-based dyes Alizarin Red S and Ostacetate Blue P3R which in the basic molecular structure are similar to Reactive Blue RB-19, were studied by AdSV. Square wave voltammetric studies, involving AdSV methodology of Alizarin Red S indicates the reversible and fast reduction of its anthraquinone moiety⁶. The sensitivity of the determination of this dye can be improved if current sampling is made earlier after the pulse application. However, the AdSV behaviour of anthraquinone dye Ostacetate Blue P3R in a mixed water-ethanol (1:9) medium and optimal conditions were investigated⁷. Five minutes accumulation in unstirred solution allows determination of this anthraquinone-based dye in the 0.02-1 $\mu\text{mol l}^{-1}$ concentration range. Reactive Blue-19, its reactive form (RB 19-VS) and its hydrolysed form (RB 19-OH) were examined by using liquid secondary ion mass spectrometry/tandem mass spectrometry in the negative-ion mode under low-energy collision conditions⁸. Structurally, characteristic fragment ions were obtained which provided information about which form of the reactive group was present in the structure. Therefore, the true reactive form of the dye (RB 19-VS) can be distinguished from its unreactive parent form and its hydrolysed form. Moreover, possible pathways for the formation of product ions were also proposed in these studies. However, this vinylsulfone-based anthraquinone reactive dye was also studied by employing electron paramagnetic resonance (EPR) techniques⁹ and small angle X-ray scattering method¹⁰.

5.2 Aim of the Study

To date, few adsorptive stripping voltammetric studies have been carried out for the determination of reactive dyes, and no specifically devoted studies for the analysis of RB-19 at the HMDE using differential pulse adsorptive stripping voltammetry (DP AdSV) in different supporting electrolytes have been reported. However, there is only one paper⁶ in the literature, very briefly mentioning the voltammetric behaviour of RB19. Nonetheless, no specific informations (e.g. E_p , i_p) are given in that article.

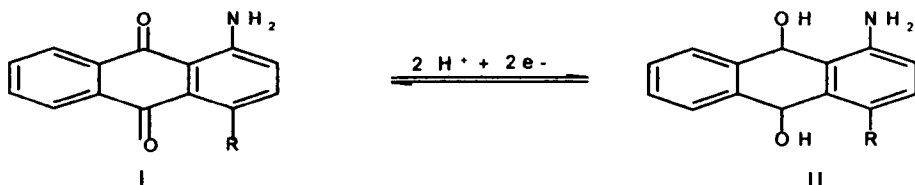
It is interesting to see if the cathodic reduction process of the anthraquinone group in this sulfatoethylsulfone-based anthraquinone reactive dye was as fast as that for anthraquinone chlorotriazine dyes (Procion Blue MX-R and Cibacron Blue 3GA) previously studied. Hence, the aim of this present work is to investigate the electroanalytical behaviour of RB-19 reactive dye by AdSV at a HMDE. Another objective of this study is to investigate whether this new reactive group vinylsulfone gives any electroanalytical signal and hence, studying the related intermediate active and hydrolysed forms. Furthermore, the basic study was carried out to illustrate the optimum conditions required for the determination of the trace amounts of this reactive dye and its reaction products.

5.3 Mechanism of the Electrochemical Reduction of the Anthraquinone Group

Anthraquinones, particularly the 9,10-compounds, are of great importance in chemistry, mainly in connection with production of dyestuffs and pharmaceuticals. Because of the pronounced oxidation-reduction properties of anthraquinones, several electrochemical methods are convenient for their determination. In general, the quinone/hydroquinone system is among the most detailed studied systems in organic polarography¹¹. The electrochemical reduction behaviour of these compounds has been

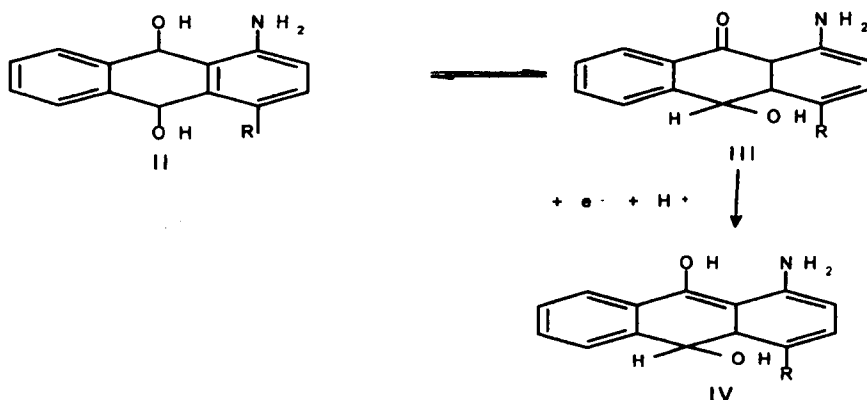
studied extensively and has attracted a lot of attention¹²⁻¹⁶. In addition, in the extensive literature dealing with electrochemistry of anthraquinones, there are several reports providing data for the electrochemical reduction of several anthraquinone derivatives in various media^{17,18}. Despite this considerable progress in the study of the anthraquinone moiety, the literature shows different interpretations of the electrochemical behaviour of compounds having an anthraquinone functional group especially in alkaline media. For instance, the appearance of an extra anthraquinone analytical signal at pH >7 can be related to the cathodic reduction of the anthrone derivative (tautomerised with 1-aminohydroquinone) or alternatively to the further reduction for the stable semiquinone intermediate products (AQH) to form anthrohydroquinone (AQH₂) compounds. Another possible explanation might be associated with the change of the ability of forming hydrogen bonds between amino and carbonyl groups of the anthraquinone moiety and thus stabilise the quinoid form¹⁹. The shortage of protons in alkaline media may cause the amino group to alter the reduction mechanism, the protonation equilibrium producing other electroactive forms which gives rise to the extra reduction peaks in the voltammograms⁴.

In general, in protic aqueous solutions, the electrochemical reduction of the anthraquinone moiety in anthraquinone-based reactive dyes exhibited either one or two electrochemical steps depending on the pH value of the supporting electrolyte. For instance, in acidic and neutral Britton-Robinson buffer, a single peak attributed to the reversible reduction of 1-aminoanthraquinone (I) to 1-aminoanthrahydroquinone (II) was observed, in a direct two-electron, two-proton process^{20,21} (see Scheme 1). The peak current for this electrochemical wave varies with the pH in the 2-8 range, with a negative shift in its peak potential as expected for electrochemical process in which hydrogen ions were consumed. However, the absence of protons for pH values higher than 10 resulted in the expected independence of E_p on pH.



Scheme 1

However, in alkaline media (e.g. carbonate buffer pH 10) 1-aminoanthrahydroquinone (II) undergoes tautomeric rearrangement and is transformed into the corresponding product anthrone (III). This latter compound is reducible at a more negative potential²². The occurrence of the second AdSV signal is probably associated with the cathodic reduction of the anthrone product as can be seen from Scheme 2.



Scheme 2

5.4 The Differential Pulse-AdSV and Linear Sweep-AdSV Behaviour of RB-19

The electrochemical behaviour of RB-19 has been investigated in this work at the HMDE using various supporting electrolytes at different pH values. The molecular structure of this reactive dye is given in Fig 5.2. This reactive dye yielded a well-

developed defferential pulse-AdSV peak in Britton-Robinson buffer at pH 4.5. A typical adsorptive stripping voltammogram for $5 \times 10^{-7} \text{ mol l}^{-1}$ RB-19 in B-R buffer is shown in Fig 5.3. The obtained AdSV peak is due to the cathodic reduction of the anthraquinone moiety of the dye, and its electrochemical peak potential (E_p) is at -0.41 V with 19 nA peak current. The linear sweep-AdSV behaviour of RB-19 in pH 4.5 B-R buffer was also investigated (Fig. 5.4). The voltammogram shows one analytical peak corresponding to the anthraquinone functional group at E_p potential of -0.44 V ($i_p = 13.4 \text{ nA}$).

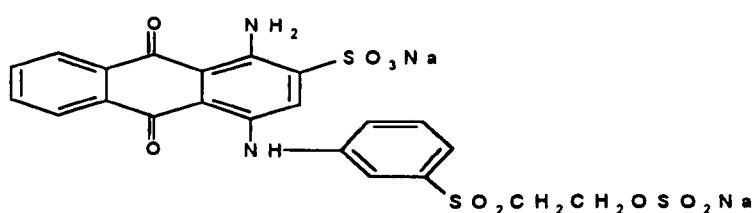


Figure 5.2: Molecular structure of Reactive Blue 19.

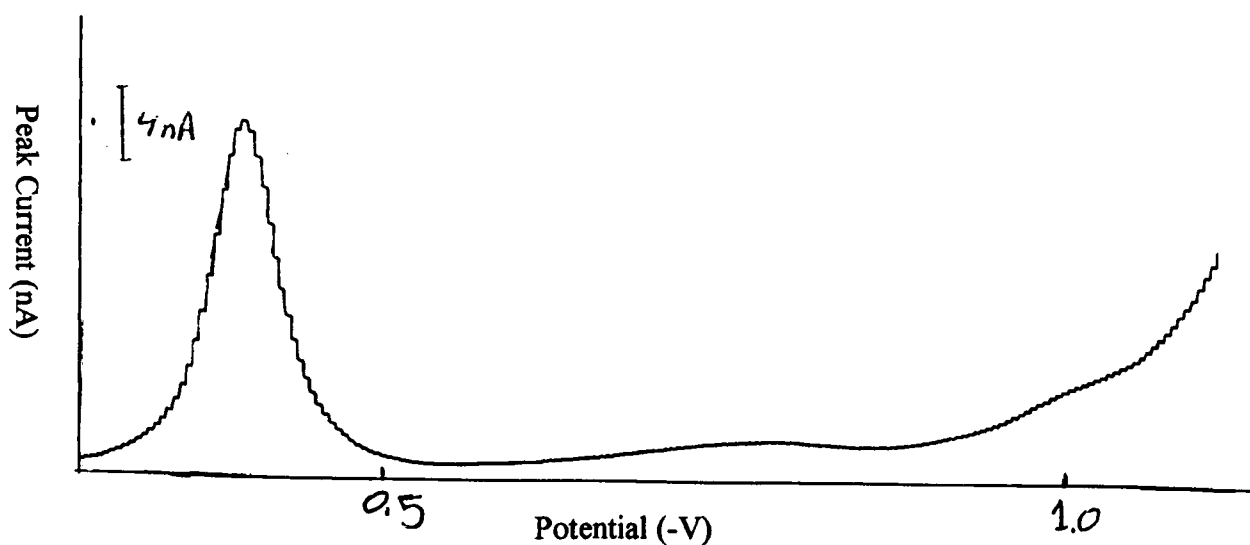


Figure 5.3: Differential-pulse adsorptive stripping voltammogram for $5 \times 10^{-7} \text{ M}$ Reactive Blue 19 in pH 4.5 Britton-Robinson buffer. Accumulation time: 2 min, accumulation potential: 0.0 V and scan rate: 5 mV s^{-1} .

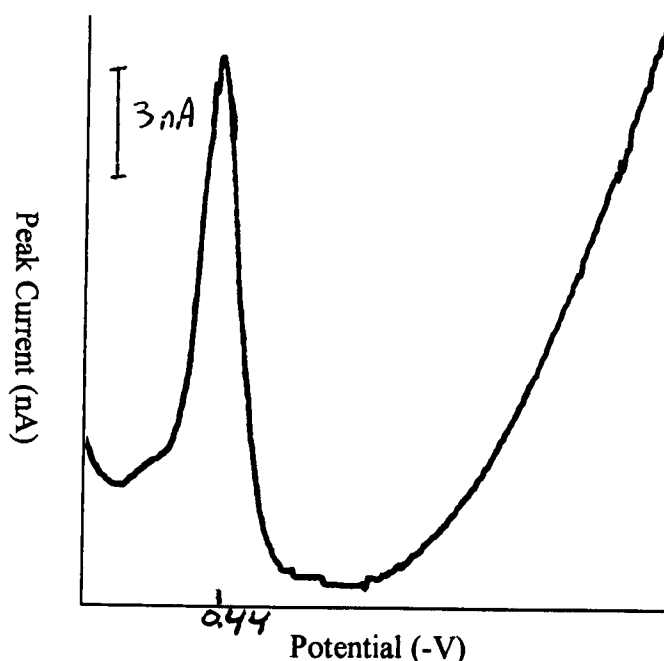


Figure 5.4: Linear sweep adsorptive stripping voltammogram for 5×10^{-7} M RB-19 in pH 4.5 B-R buffer. Scan rate: 5 mV s^{-1} , accumulation time: 2 min and accumulation potential: 0.0 V.

DP-AdSV voltammograms for $5 \times 10^{-7} \text{ mol l}^{-1}$ RB-19 in acetate buffer at pH 5 shows a weak stripping voltammetric signal obtained at $E_p = -0.48 \text{ V}$ with 2.8 nA peak current (see Fig. 5.5). This AdSV peak was due to the cathodic reduction process of the anthraquinone group. At the same experimental conditions, the linear sweep-AdSV voltammogram of RB-19 illustrates a well-defined analytical peak due to reduction of anthraquinone group at -0.5 V. The linear sweep-AdSV behaviour of this reactive dye in acetate buffer (pH 5) is given in Fig 5.6. From the comparisons of differential pulse-AdSV and linear sweep-AdSV response of the investigated reactive dyes, a further evidence and example illustrating Komorsk-Lovric and Lovric theory was obtained. This theory has indicated that, for a very fast and reversible reduction of an adsorbed specie, which yields an adsorbed product, reduction of the adsorbed specie occurs immediately the pulse is applied, and that no faradaic current remains when the current is monitored near the end of pulse application. Therefore, a very small or no signal should be obtained when employing differential pulse or square wave techniques²³. The absence (or the

vestige of the signal in this case) of the DP stripping peak of anthraquinone group in acetate buffer indicates that the reduction process of the anthraquinone moiety of the adsorbed dye is being very fast and reversible giving an adsorbed product according to the above theory. However, the presence of boric acid in the supporting buffer used in the AdSV of reactive dyes caused the differential pulse stripping peak associated with reduction of the anthraquinone group to appear and enhance. As mentioned previously, when Britton-Robinson buffer (which contains boric acid) is used a well-developed peak was obtained. Similar outcomes were also observed when acetate buffer to which boric acid was added, was used. This behaviour is believed to be caused by the slowing down of reduction of the adsorbed dye owing to the presence of borate. Boric acid is known to complex the aminoanthraquinone group of the reactive dyes^{5,24,25}, therefore, it seems to have an overall slowing effect on the rate of the electron transfer at the electrode (i.e. alters the current-time profile for the reduction of the adsorbed reactive dye).

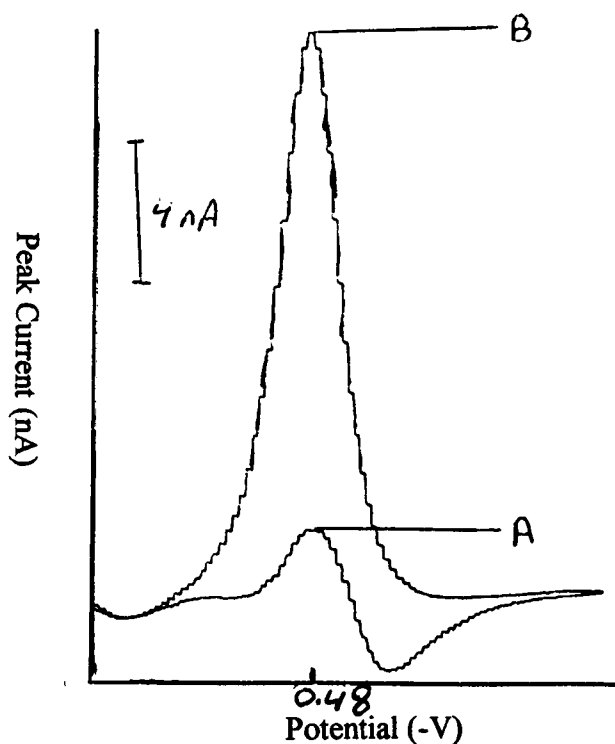


Figure 5.5: Differential pulse adsorptive stripping voltammogram of $5 \times 10^{-7} \text{M}$ RB-19 in pH 5 acetate buffer (A), and with addition of boric acid (B). $T_{\text{acc}} = 2 \text{ min}$, $E_{\text{acc}} = 0.0 \text{ V}$ and scan rate = 5 mV s^{-1} .

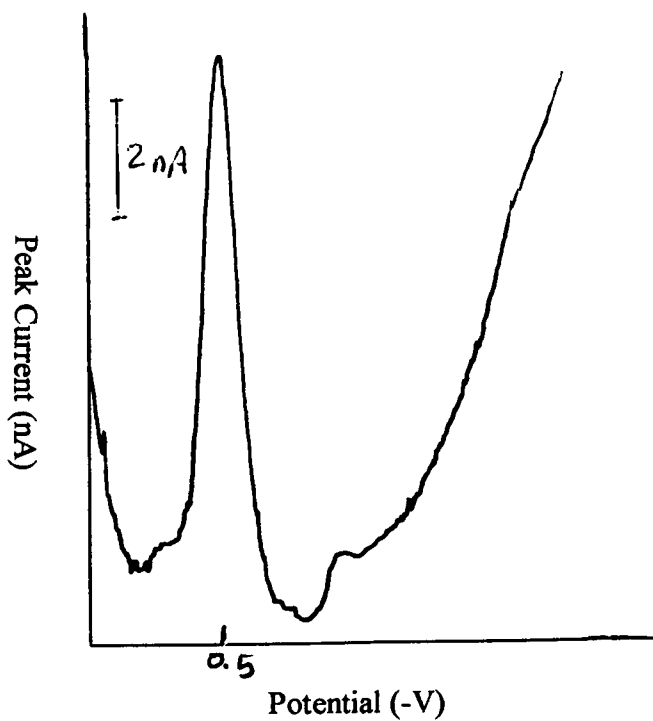


Figure 5.6: Linear sweep adsorptive stripping voltammogram for $5 \times 10^{-7} \text{ M}$ Reactive Blue19 in pH 5 acetate buffer. $T_{\text{acc}} = 2 \text{ min}$, $E_{\text{acc}} = 0.0 \text{ V}$ and scan rate = 5 mV s^{-1} .

Similar observations and results were recorded when studying DP-AdSV for $5 \times 10^{-7} \text{ mol l}^{-1}$ RB-19 in pH 10 carbonate buffer. The reactive dye exhibited two stripping signals corresponding to the reduction of anthraquinone moiety and anthrone derivative at -0.73 V and -1.1 V , respectively (Fig. 5.7). As a result of the high value of pH of carbonate buffer, the reduction of anthraquinone to anthrahydroquinone becomes more difficult, thus the AdSV peak potentials were shifted to more negative values. However, when adding boric acid to the sample solution the peak height of anthraquinone signal increased sharply (nearly twice the initial signal) as a result of the anthraquinone-borate complex formation.

However, Fogg and colleagues had reported similar electrochemical behaviour of the lack and absence of differential pulse cathodic stripping voltammetric signal at the HMDE for the reduction process of anthraquinone-based reactive dyes^{5,26}. They observed

that the differential pulse signal associated with the reduction of the anthraquinone moiety was not obtained when acetate or carbonate buffers were used, and at low pH values of B-R buffer. But at higher pH values of B-R buffer or when adding boric acid to acetate solution the DP signal was present and its size seen to increase with increasing accumulation time.

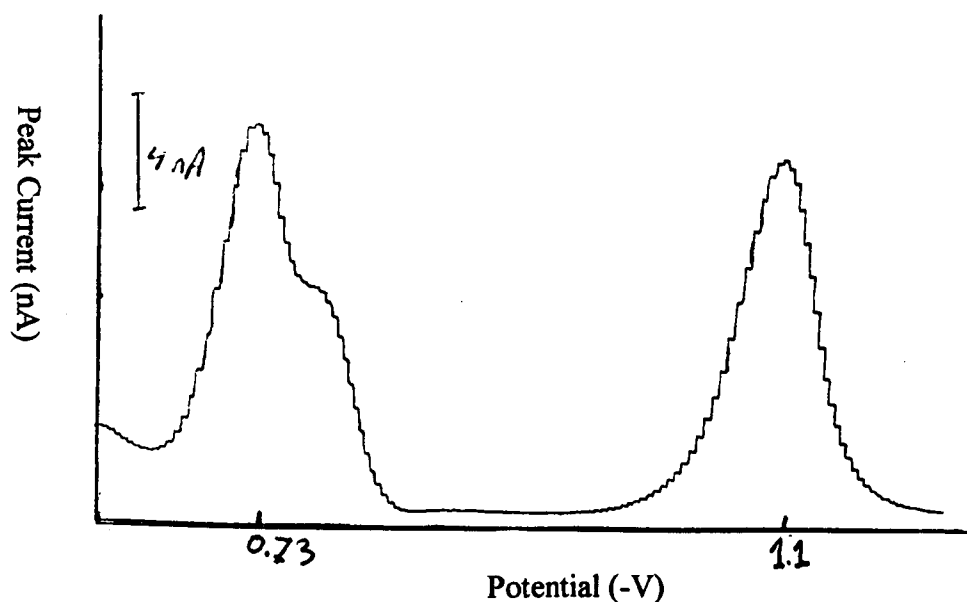


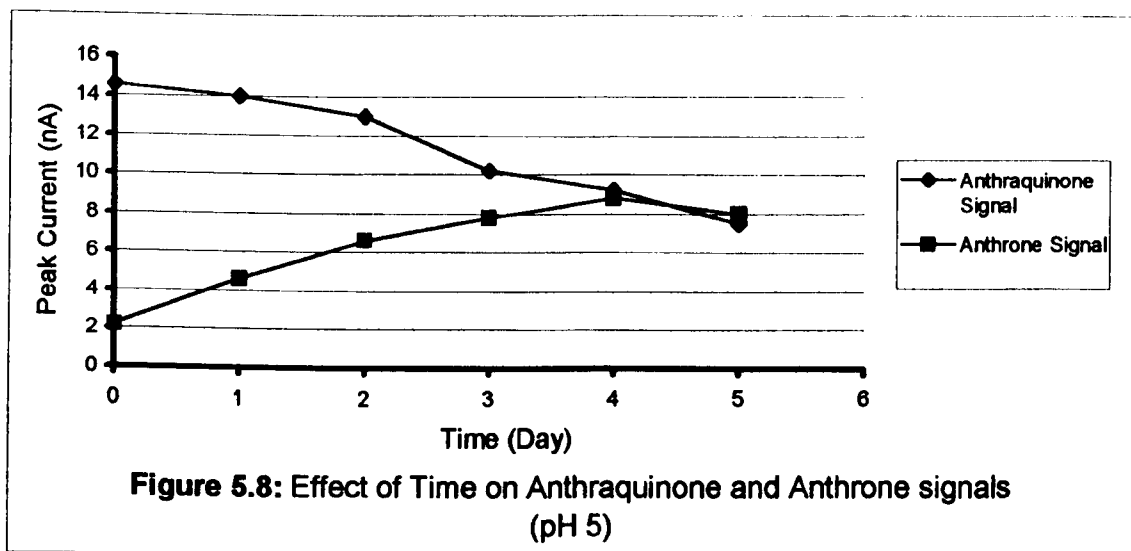
Figure 5.7: Adsorptive stripping voltammogram for 5×10^{-7} M Reactive Blue 19 in pH 10 carbonate buffer. Accumulation time: 2 min, accumulation potential: 0.0 V and scan rate 5 mV s^{-1} .

The reduction of Anthrone derivative: in alkaline solution (e.g. $\text{pH} > 8$) 1-aminoanthrahydroquinone undergoes tautomeric rearrangement and transforms into the corresponding anthrone compound. This product is reducible at a more negative potential. Hence, the stripping voltammogram of RB-19 exhibits a further AdSV peak at -1.1 V ($i_p = 13 \text{ nA}$) associated with the cathodic reduction of the anthrone derivative. It is obvious from Fig. 5.7 that the electrochemical determination of the studied reactive dye is possible via the direct monitoring of the adsorptive stripping response of the

electrochemical reduction of the anthrone product. The appearance of this second AdSV peak at more negative potential in alkaline solution is practically enough to permit direct analysis of RB-19 in spite of the use of the anthraquinone electroanalytical signal.

The published studies of the two anthraquinone-based reactive dyes (Procion Blue MX-R and Cibacron Blue 3GA)^{4,5} omitted the observation of the anthrone AdSV signal probably owing to the presence of the chlorotriazine reduction wave, which masks and covers this extra adsorptive stripping peak. However, when these chlorotriazine-based anthraquinone reactive dyes were hydrolysed, the reactive group peak was partially loosed. As a result, the monitoring of these reactive dyes in basic medium (pH 10 B-R buffer) indicates the existence and occurrence of the anthrone electrochemical signal. In addition, the voltammograms of the intermediate reactive form, the vinylsulfone (RB 19-VS) and the hydrolysed RB-19 (RB 19-OH) in alkaline solutions exhibited the second AdSV peak related to the anthrone reduction process.

However, at higher pH values (e.g. pH>8), the equilibrium between 1-aminoanthrahydroquinone and anthrone tautomer was attained almost instantaneously, thus, two electroanalytical signals of nearly equal peak height for the reduction of anthraquinone and anthrone groups were observed. In contrast the rate of equilibrium for the previous tautomerization at lower pH value (e.g. pH 5) decreased dramatically. In fact, typical tautomerization of anthrone via 1-aminoanthrahydroquinone at pH 5 required several days. It was observed that the anthraquinone group is not stable at pH 5 and its peak current decreased slightly with increasing time to a lower value with simultaneous appearance of a new cathodic wave at a less negative potential. This new cathodic wave increased in height at approximately the same rate as the decrease of the parent wave, however, the total current (parent wave + new wave) remains approximately at the original height of the initial wave as can be seen from Fig. 5.8. This electroanalytical behaviour is typical for tautomerism of anthraquinone to the corresponding reduced derivative^{15,19,24}.



Sulfone reactive group: The RB-19 molecule has, in addition to the anthraquinone group, sulfone and sulfonate reactive groups both of which are not electroactive in aqueous solutions. Actually, for all the used supporting electrolytes, no electrochemical peak was observed for the sulfatoethylsulfone or vinylsulfone reactive groups (see Fig. 5.3). Such outcomes and observations confirmed the electro-inactive property of this anchoring system. Similar observations were reported for other vinylsulfone-based reactive dyes such as Remazol Brilliant Orange 3R²⁷ and Reactive Violet 5²⁸. However, the sulfone reactive group can only be electro-reduced in aprotic media and the wave obtained is not recommended for trace analytical purposes²⁹.

5.5 Cyclic Voltammetric Studies of RB-19

Cyclic voltammetric scans of 1×10^{-4} mol l⁻¹ RB-19 in pH 4.5 B-R buffer show a reversible reduction process for the anthraquinone group. Figure 5.9 illustrates a typical cyclic voltammogram at the HMDE of the reactive dye over the full potential range. As can be seen from the cyclic voltammogram, the presence of a pair of well-defined cathodic peak (IIC) and anodic peak (IIA) indicates that the reduction of the

anthraquinone wave is considered a reversible process. The peak potential separation is about 64 mV. However, the peak height of anodic peak is less than the peak height of cathodic peak, which suggests that the oxidation process is less reversible than the reduction step. The cyclic voltammogram of RB-19 at $1 \times 10^{-4} \text{ mol l}^{-1}$ concentration level exhibits a pre-peak (IC) which appears only as a shoulder at a less negative potential than the anthraquinone peak (IIC). This shoulder is presumably due to the diffusion process occurring at a relatively higher dye concentration level ($1 \times 10^{-4} \text{ mol l}^{-1}$) from the bulk of the solution to the hanging drop electrode. At lower concentration ($1 \times 10^{-7} \text{ mol l}^{-1}$) this shoulder was totally eliminated. However, In B-R buffer the anodic peak (IIA) is decreased and another anodic peak is obtained at a less negative potential (Peak IA) due to chemical reaction following the charge transfer. Nonetheless, at low scan rates (e.g. 10 mV s^{-1}) only IIC and IIA are seen in both voltammograms (Fig. 5.10). However, when the scan rate is increased, the increase in the height of peaks IIA and IIC is much greater than the corresponding increase in the height of peaks IA and IC, respectively.

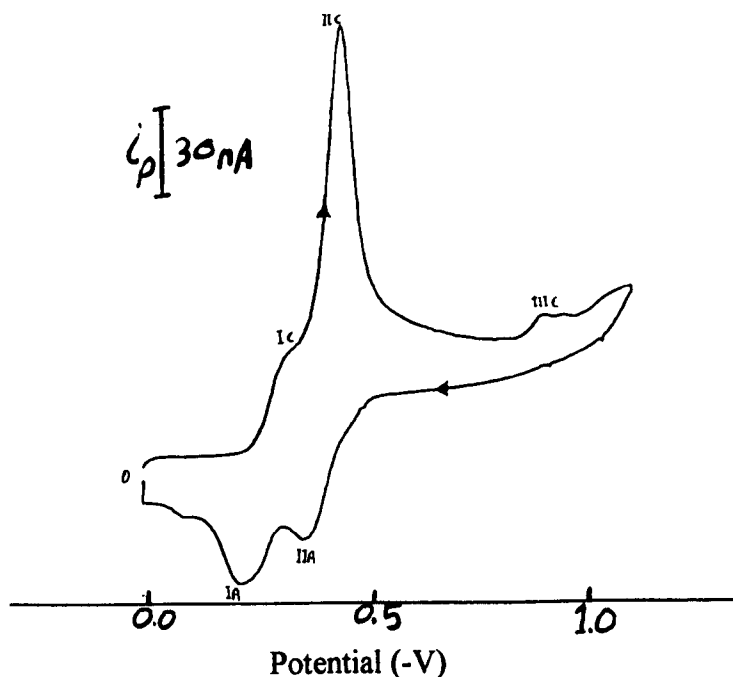


Figure 5.9: Cyclic voltammogram of $1 \times 10^{-4} \text{ M}$ RB-19 in pH 4.5 B-R buffer, scan rate 5 mV s^{-1} .

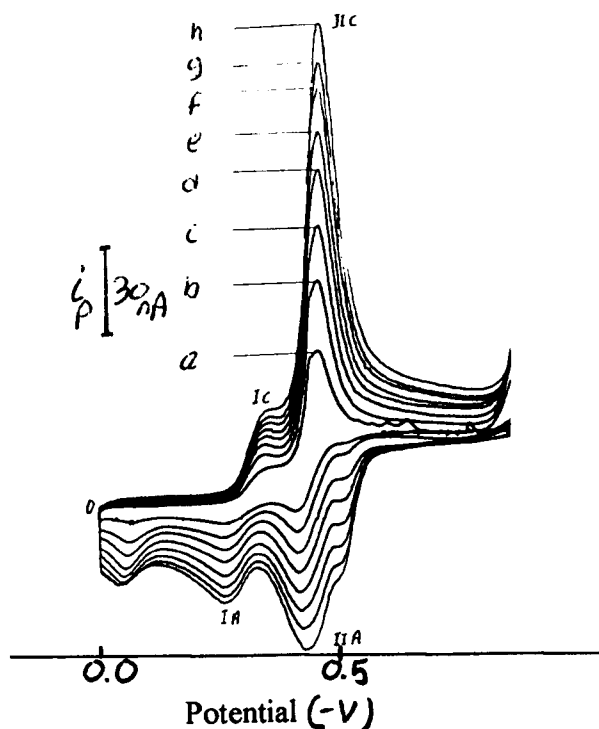


Figure 5.10: Cyclic voltammogram of anthraquinone group (1×10^{-4} M RB-19 in pH 5 acetate buffer) at different scan rates: a, 10; b, 20; c, 30; d, 40; e, 50; f, 60; g, 70; h, 80 mV s^{-1} .

This cyclic voltammetric behaviour is in good agreement with that reported for the cyclic voltammetric characteristic of the two anthraquinone-based reactive dyes Procion Blue MX-R and Cibacron Blue 3GA³⁰ in pH 4.5 B-R buffer.

On the other hand, at high pH values of B-R buffer or in carbonate buffer, the absence of an anodic peak (i.e. lack of oxidation wave) coupled with the cathodic peak (IIC) related to the electrochemical reduction of anthrone product indicates the irreversibility of the second reduction process. This agrees with similar work on 1-amino-9,10-anthraquinone derivatives in weakly alkaline media²¹. At high pH values, such as in carbonate buffer, a more complicated voltammogram was observed (see Fig. 5.11). It can be seen from the RB-19 cyclic voltammogram obtained in pH 10 carbonate buffer that the first reduction peak (IC) was followed by a new smaller cathodic peak (IIC) at a more negative potential. A new small anodic peak (IIA) is coupled with this new peak. The presence of the new post-cathodic peak (IIC) or pre-anodic (IIA) peak is

probably associated with the adsorption of a new compound formed in alkaline solutions. Some authors suggested that in an alkaline medium (e.g. pH 10 carbonate buffer), tautomerization of aminoquinones may have occurred¹⁹. This would lead to the formation of a quinoneimine structure. Both species might exist at equilibrium in solution giving two voltammetric waves. However, in basic solutions, the shortage of protons may also cause the substituent amino group to alter the reduction mechanism, the protonation equilibrium producing other electroactive forms which give rise to the post-peak (IIC) in the cyclic voltammogram. The electrodensity of the quinone function is increased by the electron-donating character of the unprotonated amino substituent and consequently the reduction of the quinone will become more difficult which results in the negative shift in the reduction potential of the new product^{5,19}. In addition, the presence of the post-cathodic peak (IVC) succeeding the AdSV peak (IIIC) associated with the cathodic reduction of anthrone product is probably due to the adsorption of the possible surface-active reactant yielded from the reduction of anthrone product.

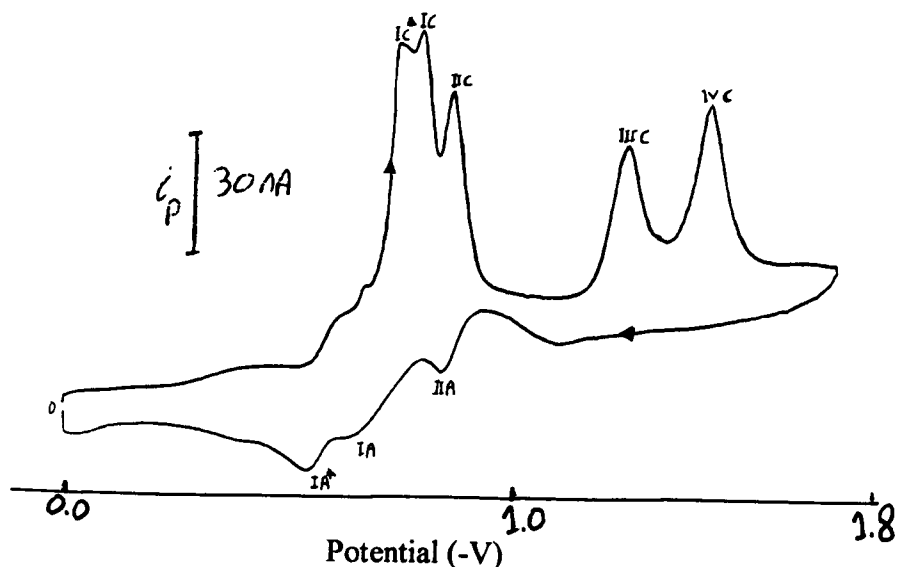
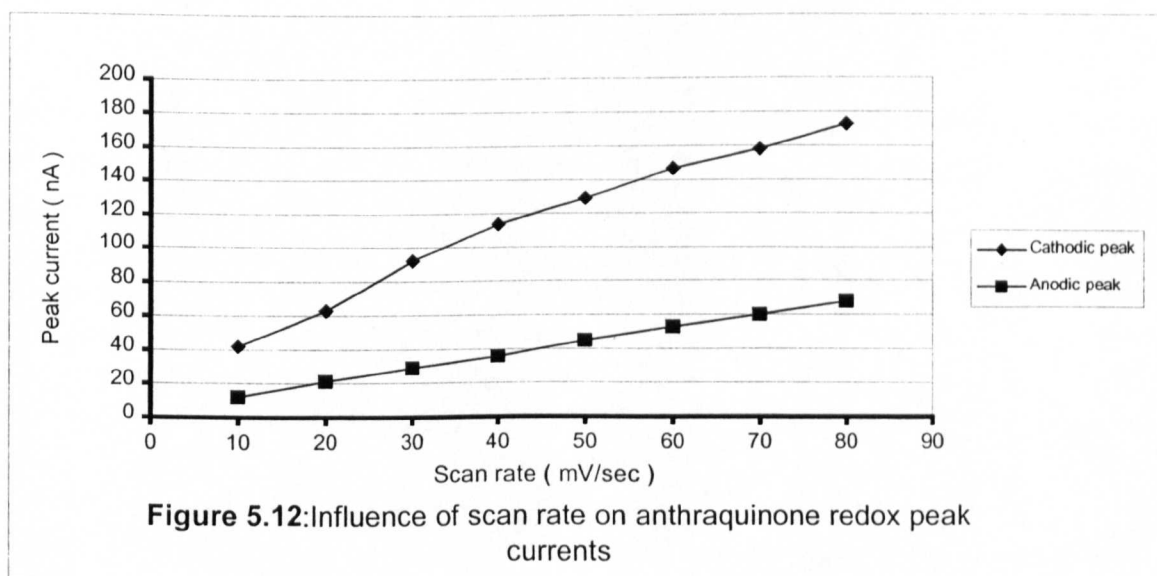


Figure 5.11: Cyclic voltammogram of 1×10^{-4} M RB-19 in pH 10 carbonate buffer, scan rate 50 mV s^{-1} .

A more detailed cyclic voltammetric study was carried out in order to obtain more information about the nature of the redox reactions of the reactive dye at the electrode surface. The influence of scan rate on the anthraquinone reduction peak is illustrated in Fig. 5.10. The heights of the anodic and cathodic peaks are plotted as a function of the scan rate in Fig 5.12. The peak height of the reduction current increases linearly with the scan rate. The cathodic peak potential slightly shifted in the negative direction when the scan rates become faster. These differences in peak potentials with scan rates reflect an increasing degree of irreversibility at higher scan rates. Moreover, the ratio of the anodic-to-cathodic peak heights ($i_p \text{ IA} / i_p \text{ IC}$) is smaller than unity and increase with scan rate from 0.3 ($\nu=10 \text{ mVs}^{-1}$) up to 0.4 ($\nu=80 \text{ mVs}^{-1}$), which indicates that the diffusion process is predominating and weak adsorption of the reactant is occurring³⁰. However, when reversing the scanning potential of the electrode to the positive-going potential immediately after the reduction of the first anthraquinone reversible wave, the height of the anodic peak dramatically increased to nearly more than four times its original height when the full potential range was used.



Further enhancement in the limiting current was observed when multi-cyclic sweeps ($\nu=50 \text{ mVs}^{-1}$) mode were applied. A gradual growth of the cathodic and anodic peak currents was observed, indicating progressive adsorptive accumulation of the analyte at the HMDE during the multi-cyclic operation (see Fig. 5.13).

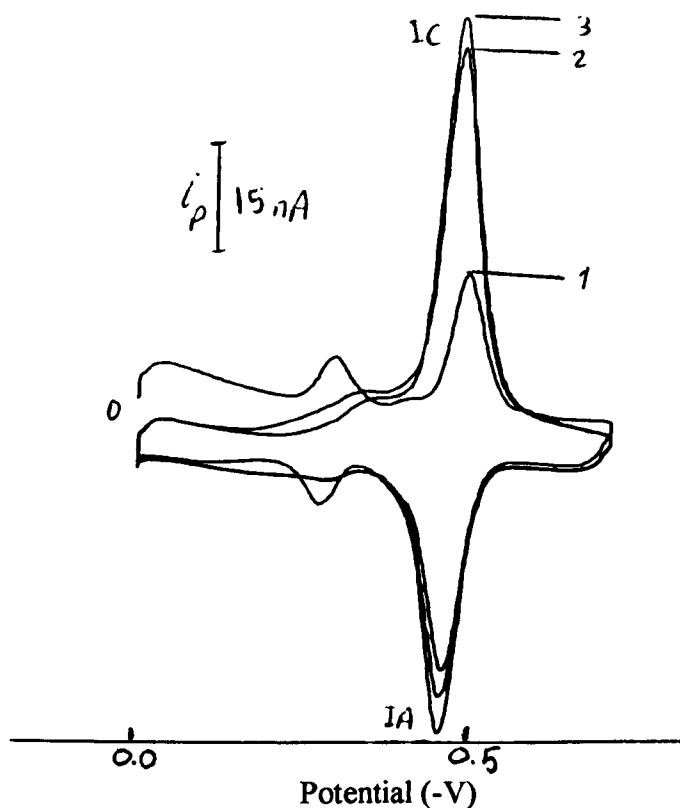


Figure 5.13: Multi-cyclic voltammogram of anthraquinone group of RB-19 in pH 5 acetate buffer, scan rate 50 mV s^{-1} .

5.6 Optimum Experimental Conditions

The necessary conditions for the adsorptive accumulation of the reactive dye under investigation was studied using the HMDE as a working electrode for the differential pulse mode recording of the stripping voltammetric curve in the whole accessible potential range. The optimal supporting electrolyte, optimal pH, the optimal

and potential of the analyte, as well as all the necessary instrumental parameters were established in these studies.

5.6.1 Effect of accumulation time

Preconcentration of RB-19 on the surface of the HMDE is the essential condition for highly sensitive determinations. The amount of adsorbed reactive dye depends on the accumulation potential used and on the intensity of stirring. It also depends on the length of time over which adsorption is allowed to proceed. The longer the duration of the accumulation time, the more RB-19 is adsorbed and the larger the peak current. The duration of the accumulation is limited by complete coverage of the electrode surface.

The reduction current of 5×10^{-7} mol l⁻¹ RB-19 solution was measured as a function of accumulation time (t_{acc}) in B-R buffer (pH 4.5) as can be seen from Fig 5.14. In this diluted solution, the relationship $i_p = f(t_{acc})$ is almost linear. The rectilinear relationship is observed up to 5 min and then becomes curved owing to the saturation of the hanging mercury drop by the analyte. For subsequent experiments an accumulation time of 2 min was selected as an optimum t_{acc} because it provided high peak current with adequate practical time.

5.6.2 Effect of accumulation potential

Generally, the adsorption process at the electrode/solution interface depends on the electrode potential. The optimum E_{acc} value can be found by measuring the dependence of the peak height of the analytical signal on preconcentration potential while gradually changing E_{acc} from an original value (e.g. 0.0 V) towards more negative or positive values. The cathodic stripping peak height was therefore measured versus the accumulation potential E_{acc} . Stirred collection was carried out for 2 min at each selected potential. The effect of the accumulation potential on stripping peak current was examined over the +0.1 to -0.4 V range (Fig. 5.15). When the accumulation potential is more positive than the reduction peak potential ($E_p = -0.4$ V) of RB-19, the peak current remain nearly constant (with exception of the 0.0 V value), whereas it decreases sharply

when E_{acc} is near to E_p (it is totally eliminated at -0.6 V E_{acc} value). An accumulation potential of 0.0 V was selected as optimum E_{acc} as it provided the highest peak current. The variation of preconcentration potential did not produce significant shifts in E_p value.

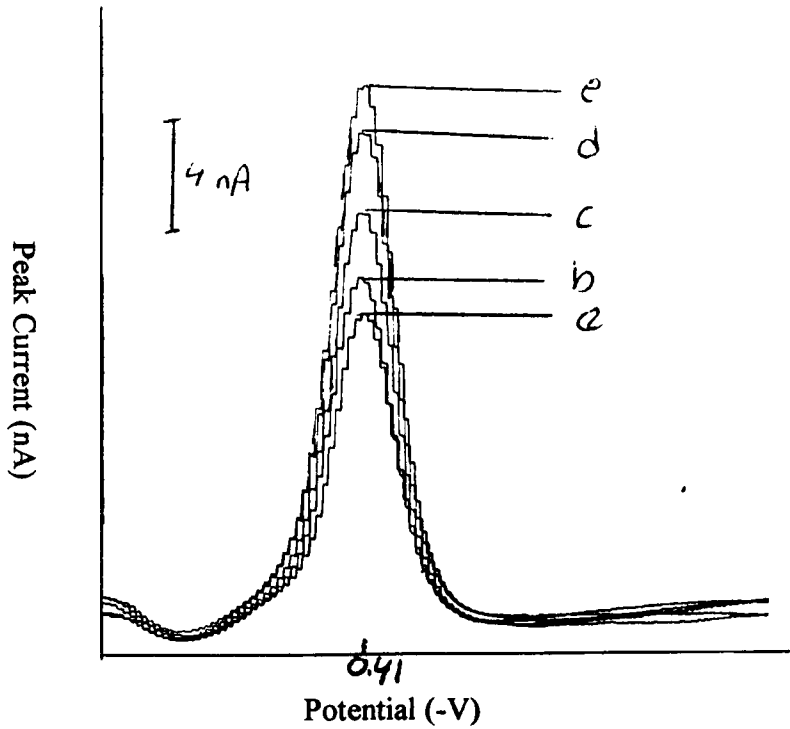


Figure 5.14: Effect of accumulation time on anthraquinone reduction process in pH 4.5 B-R buffer. Accumulation time: a=30, b=60, c=90, d=120 and e=150 s.

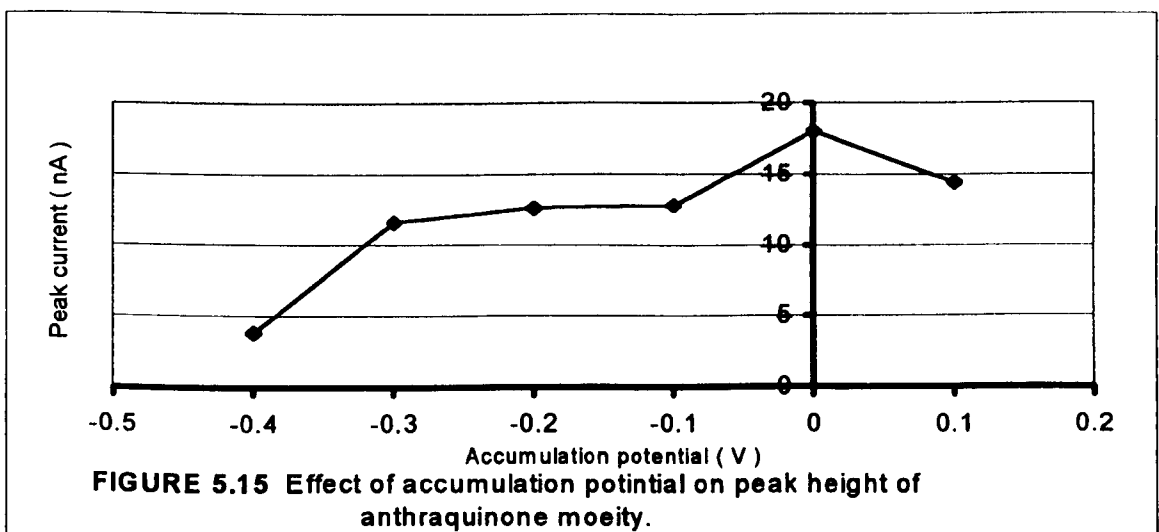
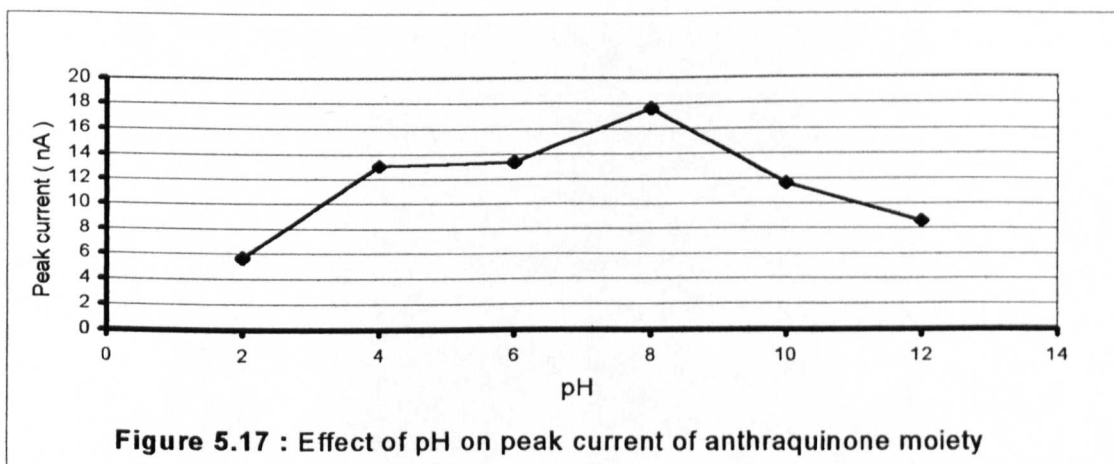
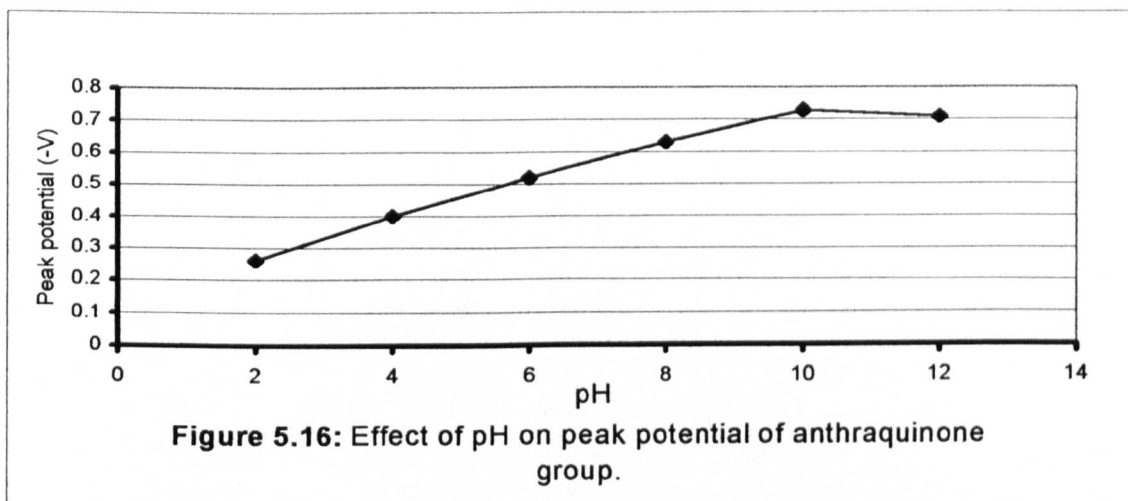


FIGURE 5.15 Effect of accumulation potential on peak height of anthraquinone moiety.

5.6.3 Effect of pH

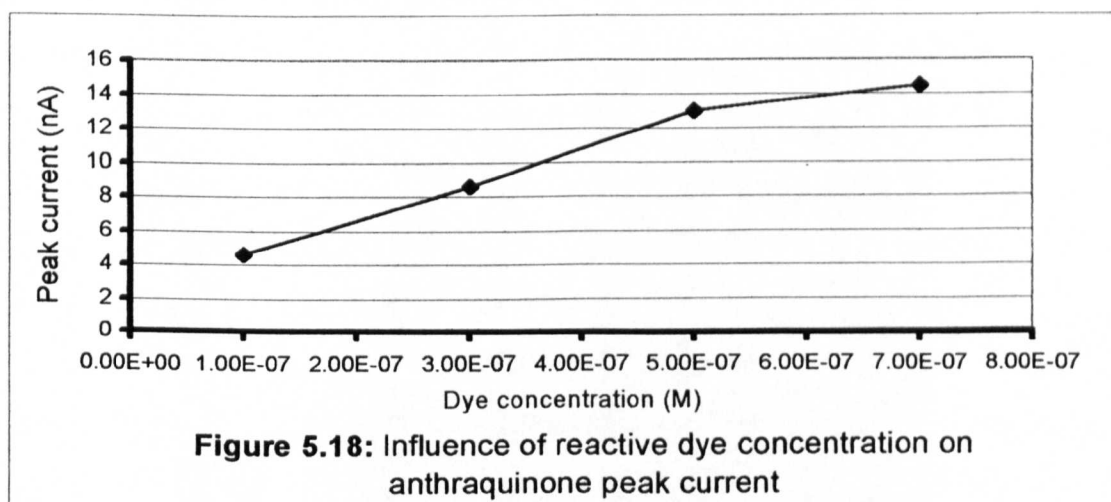
The acidity of the supporting buffer is one of the most important factors which influences the reduction process, because, both peak height and peak position of anthraquinone are pH dependent. Furthermore, in some cases, it controls the stability of the analyte or its complexes and hence can be used to minimise the effect of interferences. The effect of pH on the differential pulse adsorptive stripping voltammograms of RB-19 (5×10^{-7} mol l⁻¹) in B-R buffer with 2 min accumulation time at 0.0 V is shown in Fig 5.16 and Fig 5.17. The analysed reactive dye was shown to be adsorbed and to give stripping voltammetric peaks over the pH range 2-12. The peak potential of the adsorptive stripping signal was shifted to more negative values when the pH increased, which indicates that E_p was pH dependent (as expected for a reaction in which hydrogen ions take part in the electrochemical process). The plots of E_p versus pH (Fig. 5.16) showed a linear relationship between pH 2 and pH 10 with a slope of 50 mV pH⁻¹ unit. However, an inflection point can be observed at pH 10 where the reduction of RB-19 becomes independent of pH. These experimental observations are in a good agreement with the suggested electrode mechanism for the reduction of the anthraquinone moiety (see section 5.3). Furthermore, at pH > 8 the anthraquinone reduction peak splits into two peaks, which probably relates to the adsorption of a new compound formed due to the tautomerization and formation of quinoneimine structure (refer to section 5.4).

The influence of the solution pH value on the peak height obtained for RB-19 was examined. The optimum pH value for the reactive dye determination seems to lie in the 4-10 pH range (Fig. 5.17). At pH 8 the peak current reached its maximum value, thus it would be convenient to monitor the dye during the dyeing process (which usually occurs in alkaline media). Nevertheless, for practical analysis, the optimum pH values over 4-7 were chosen because the reduction peak showed relatively high sensitivity and with a simple uncomplicated voltammogram and to avoid the splitting in the anthraquinone AdSV peak which occurred at higher pH values.



5.6.4 Effect of reactive dye concentration

The effect of varying the RB-19 concentration on the peak current of the reduction of the anthraquinone group was also investigated by adsorptive stripping voltammetry. The peak height of the reactive dye was measured as a function of RB-19 concentration; it was found (Fig. 5.18) that it increases almost linearly in the concentration range from 1×10^{-7} to 5×10^{-7} mol l⁻¹. Hence, the RB-19 3×10^{-7} concentration was selected as optimal dye concentration for further studies.

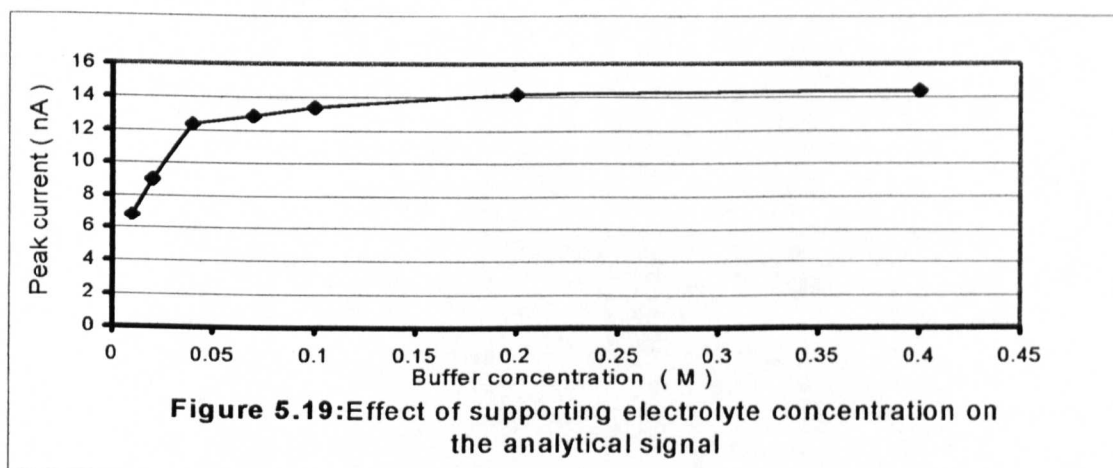


5.6.5 Effect of supporting electrolyte and boric acid concentrations

Varying the concentration of the supporting electrolyte (pH 4.5 B-R buffer) can influence the adsorption process. The effect of the electrolyte concentration on the adsorptive stripping response of RB-19 was evaluated and is illustrated in Fig 5.19. When the buffer concentration was increased from 0.01 to 0.04 mol l⁻¹, the analytical response also increased remarkably. The peak height increases gradually beyond this electrolyte concentration level, until it becomes constant at 0.2 mol l⁻¹. Hence, 0.04 mol l⁻¹ buffer concentration was selected as optimal because it provided the largest peak

current in the linear range. On the other hand, a noticeable shift by 25 mV in the positive direction was observed when increasing the buffer concentration from 0.01 to 0.04 mol l⁻¹. However, the peak potential remains relatively constant after 0.06 mol l⁻¹ concentration.

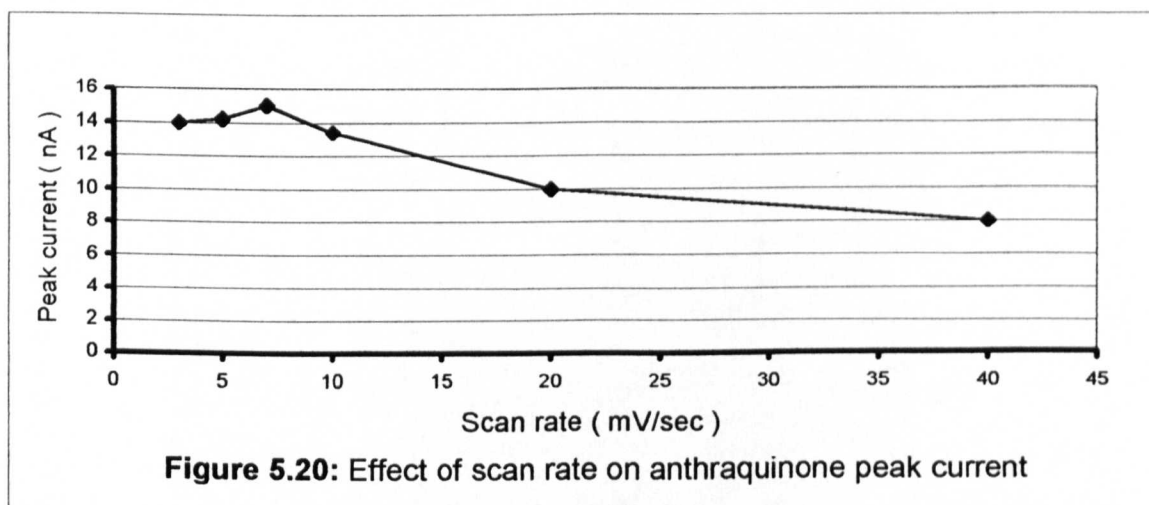
It was recently reported (section 5.4) that the presence of boric acid in the supporting buffer used in the AdSV analysis of reactive dyes caused the differential pulse stripping voltammetric peak associated with the reduction of anthraquinone group to appear and enhance. Consequently, the peak current of the anthraquinone group of RB-19 was investigated as a function of boric acid concentration. The observed peak height was found to be directly proportional to the boric acid concentration up to the 0.08 mol l⁻¹ level.



5.6.6 Effect of scan rate

The effect of scan rate (Fig. 5.20) on the adsorptive stripping current of 5×10^{-7} mol l⁻¹ RB-19 in pH 4.5 B-R buffer was examined over the 3-40 mV s⁻¹ range. When the potential was scanned at increasing rates from 3 to 7 mVs⁻¹, a proportional relationship was observed between the peak intensity and the scan rate, which indicated that the redox reduction process being examined occurs in the adsorbed state (i.e. the reduction process is controlled by the adsorption of the reactive dye on the surface of the working

electrode)³¹. When the scan rate became higher than 9 mV s^{-1} the peak height declined gradually from 14 nA at 9 mV s^{-1} to 8 nA at 40 mV s^{-1} . The half-width ($W_{1/2}$) of the analytical signal of anthraquinone group in this scan rate range increased when the scan rate approached higher values. When the scan rate increment was tested, the increase of this parameter produced an increase in the peak current; but also a great distortion in this signal was observed at high scan rates, resulting in very poor and broad AdSV peak shape. It was concluded that an intermediate value of 5 mV s^{-1} was most appropriate for the best the electrochemical signal with adequate practical time. Thus, it was selected for subsequent work.



5.6.7 Effect of convection rate

Other instrumental parameters and experimental conditions that can affect the adsorptive stripping response of RB-19 are stirring rate and the surface area of the working electrode. The effect of the stirring rate on the peak current was tested. Increased stirring rate (position 0 to 6 speed on the voltammetric stand) provided, as expected, an increase in the peak current and did not affect the value of E_p (Table 5.1).

Stirring speed 2 (approximately $1400 \text{ rev min}^{-1}$) was chosen as an optimum value, which provided adequate preconcentration effect without saturating the HMDE.

Table 5.1: Influence of stirring rate on i_p and E_p for RB-19 response

Stirring Speed Position	0	2	4	6
Peak Current (nA)	9.4	12.2	15.4	16.4
Peak Potential (-V)	0.42	0.42	0.42	0.42

5.6.8 Effect of working electrode area

The influence of the surface area of the Hg-drop working electrode (large, medium, small) on the anthraquinone reduction current was also evaluated. In this study, the increase in area yielded a linear enhancement in the peak response (Table 5.2) and did not affect the value of the peak potential. The large size (approximately 0.29 mm^2) was considered as optimum because it provided the highest intensity. For $5 \times 10^{-7} \text{ mol l}^{-1}$ RB-19 solution the peak current went up with a slope of 74.3 nA mm^{-2} in the range of 0.15 to 0.29 mm^2 Hg-drop area.

Table 5.2: Influence of Hg-drop size on i_p of RB-19

Hg-drop area (mm^2)	0.15	0.22	0.29
Peak current (nA)	13.0	18.6	23.4

5.7 Analytical Application

Once the most ideal and suitable chemical conditions and instrumental parameters for the adsorptive stripping determination of RB-19 were established (Table 5.3), voltammograms at various conditions for RB-19 were recorded to investigate several analytical applications such as linearity range, detection limits, reproducibility and stability.

Table 5.3: Optimum conditions for the analysis of RB-19 by the AdSV technique

Parameter	Variation range	Optimum value
B-R buffer conc.	0.01-0.4 mol l ⁻¹	0.04 mol l ⁻¹
pH	2-12	4-7
T _{acc}	0 - 6 min	2 min
E _{acc}	+0.1 - (-0.4) V	0.0 V
Scan rate	3 - 40 mV s ⁻¹	5 mV s ⁻¹
Stirring rate	0 - 2100 rev min ⁻¹	1400 rev min ⁻¹
Electrode area	0.15 - 0.29 mm ²	0.29 mm ²

5.7.1 Calibration graph

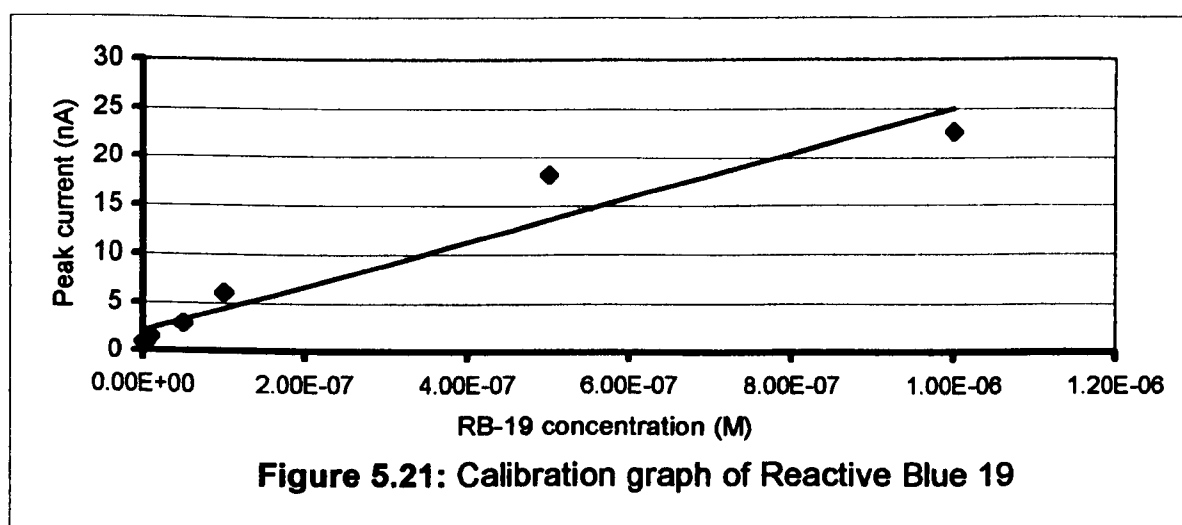
Quantitative evaluation is based on the dependence of the adsorptive stripping peak current on the concentration of the analyte (reactive dye). This dependence of the analytical response on the reactive dye was measured in the concentration range from 1×10^{-9} to 1×10^{-6} mol l⁻¹. The calibration graph was obtained when successive additions of the standard dye solution were added to a B-R buffer solution (pH 4.5). Figure 5.21

shows the calibration curve obtained for the AdSV of RB-19. The signals were shown to be rectilinear up to a concentration of at least $5 \times 10^{-7} \text{ mol l}^{-1}$ of the reactive dye. Least-squares analysis of the linear range of the calibration plot yielded the following results:

Slope of the linear range $X = 0.034 \text{ A mol}^{-1}$, Intercept, $Y = 1.3 \text{ nA}$, Correlation coefficient $r = 0.995$. The regression equation of the calibration line can have the form:

$$i_p(\text{A}) = 1.3 \times 10^{-9} + 0.034 C (\text{mol l}^{-1}) \quad r = 0.995 \quad n=6$$

Obviously, the linear conditions only exist for low surface coverage, so deviations from linearity are expected at higher reactive dye concentrations (which were observed at $1 \times 10^{-6} \text{ mol l}^{-1}$ concentration level) and/or when using longer accumulation times.



5.7.2 Detection limits

The effective preconcentration during the adsorption process of RB-19 makes it possible to achieve very low detection limits. The detection limit, defined as three times the signal-to-noise ratio ($S/N = 3$) reached in the optimum conditions for monitoring RB-19 was $5 \times 10^{-9} \text{ mol l}^{-1}$ ($T_{\text{acc}} = 2 \text{ min}$). However, when applying longer accumulation

time (e.g. 7 min) a detection limit less than 1×10^{-10} mol l⁻¹ can be achieved. This latter detection limits is more sensitive than the detection limits obtained by other analytical techniques currently available for the analysis of RB-19 by liquid chromatography^{2,3}, and liquid secondary ion mass spectrometry⁸.

5.7.3 Reproducibility

The high sensitivity of AdSV is accompanied by good reproducibility of the obtained results. This can be attributed to the reproducible area and self-cleaning control provided by the stripping voltammetric stand (i.e. the use of new drop of reproducible area in each run); as well as the stability of the reactive dye. Under the previously optimised conditions, the reproducibility of the measured analytical signal was checked from eight successive measurements of 5×10^{-7} mol l⁻¹ of RB-19 solutions. A relative standard deviation of 3.4% was calculated in such conditions.

5.7.4 Stability

Under optimum conditions, the stability of a 5×10^{-7} mol l⁻¹ of RB-19 solution was investigated. The solution of this reactive dye seemed to be stable for a period of four hours at least, which was more than enough to carry out all the experimental measurements for the reduction of anthraquinone moiety by AdSV technique.

5.8 Measurements of the Hydrolysed Reactive Dye

Hydrolysis of the vinylsulfone functional group ($-\text{SO}_2\text{CH}=\text{CH}_2$) before fixation is one of the fundamental problems and main competitive reaction associated with reactive

dye technology, because the hydrolysed dye (RB 19-OH) will not fix and has no additional affinity for the fibre. For the majority of vinylsulfone reactive dyes, the degree of fixation ranges from 75% to 90% on cotton. The possible discrimination between the original dye (RB-19) and its hydrolysed form (RB 19-OH) as well as the intermediate form (RB 19-vinylsulfone) was investigated by the AdSV technique. For obtaining a standard solution of RB 19-VS, a solution of 1×10^{-3} mol l⁻¹ of the original dye was stirred at pH 11. In order to obtain solutions of fully hydrolysed dye, a solution of original dye in sodium carbonate at pH 10 was heated for at least one hour or alternatively by refluxing at 1×10^{-3} mol l⁻¹ solution of RB-19 at pH 11 for three hours.

The adsorptive stripping voltammograms of both the hydrolysed dyes and the vinylsulfone dye, at various supporting electrolytes, were compared with the voltammogram of the original dye. No significant changes in the peak shape or potentials of the anthraquinone reduction process were observed. However, marked variations in the peak current for these different forms (RB 19, RB 19-VS and RB 19-OH) were recorded (Table 5.4). Consequently, these variations in the peak height of the anthraquinone functional group (or anthrone peak in carbonate buffer) can be used to some extent for the distinguishing between the RB-19 derivatives and its hydrolysis products. Nonetheless, the full discrimination between these different forms of the reactive dye directly without any pre-treatment procedures (e.g. chromatographic separation) is inadequate when applying the AdSV technique as an analytical method. The limitation of this developed electroanalytical method for the measurement of the hydrolysed or intermediate products is due to the lack and absence of the AdSV signal for the sulfone anchoring system associated with the hydrolysis process for this particular reactive dye. Similar results and conclusions were obtained for the reaction of the analysed reactive dye with other hydroxy substances (e.g. methanolysis process).

Nevertheless, the AdSV technique has been used with great success for the monitoring and distinguishing between the original reactive dyes and their hydrolysis products for various reactive dyes such as Reactive Red 41³², Reactive Orange 23³³ Procion Blue MX-R, Cibecron Blue 3GA⁵ and several triazine-based azodyes³⁴.

However, an alternative electroanalytical approach, which can secure a desirable discrimination between the RB-19 and its hydrolysis/methanolysis and/or structurally similar anthraquinone-based reactive dyes, can be accomplished by applying different square wave frequencies. It is possible that by employing such strategy at a selected SW frequencies, the stripping voltammetric peak potential shifts for these various forms is different enough to ensure reasonable differentiation between these different compounds and forms. Such anticipations and expectations are based on view of observations reported recently, which indicates that by applying the mentioned electrochemical procedure, analytical discrimination between two substances with very similar reduction potentials can be achieved^{35,36}. However, because this strategy is usually required different reversibilities between the two analytes to be monitored simultaneously and due to the lack of the appropriate electrochemical instrumentation, similar experiments can not be carried out at this stage.

In contrast, other analytical approaches using liquid secondary ion mass spectrometry⁸ or high pressure liquid chromatography (HPLC)³ coupled with a swept-potential electrochemical detector were successfully used for simultaneous monitoring and identification of the hydroxy and vinylsulfone derivative of RB-19 dye.

Table 5.4: Influence of hydrolysis process on the E_p and i_p for RB-19

Electrolyte	Derivative	Anthraquinone Peak		Anthrone Peak	
		E_p (-V)	i_p (nA)	E_p (-V)	i_p (nA)
B-R buffer	RB-19	0.42	11.6	-	-
	RB 19-VS	0.43	8.2	-	-
	RB 19-OH	0.43	6.8	-	-
Acetate buffer	RB-19	0.46	2.8	-	-
	RB 19-OH	0.43	4.6	-	-
Carbonate buffer	RB-19	0.73	12.0	1.1	15.6
	RB 19-OH	0.73	8.0	1.1	13.0

5.9 Conclusions

Adsorptive stripping voltammetry (AdSV) can be used effectively to analyse the anthraquinone-based reactive dyes. The results given here demonstrate clearly the applicability of the developed procedure for the determination of Reactive Blue-19 dye at nanomolar levels. Proposed electrode reduction mechanisms for both anthraquinone and anthrone systems were suggested and discussed. Voltammetric studies of the reactive dye exhibited either one or two cathodic reduction processes depending on the pH value of the supporting buffer. This investigated reactive dye can be determined directly via monitoring the stripping voltammetric waves of anthraquinone and/or anthrone groups. However, the vinylsulfone reactive system shows no electrochemical activity. The DP adsorptive stripping voltammetry at the HMDE and cyclic voltammetric studies shows a very similar electrochemical behaviour of RB-19 to the behaviour and results obtained for structurally similar anthraquinone-based reactive dyes. The cyclic voltammetric study confirmed the reversibility of the two-electron, two-proton redox reaction for the anthraquinone moiety, whereas, the redox process related to the anthrone product appeared to be an irreversible process, as no current was observed in the reverse scan. The influence of various experimental conditions and instrumental parameters on the determination of this reactive dye was discussed in detail. The calibration graph was linear in the 1×10^{-9} - 5×10^{-7} mol l⁻¹ range with a detection limit of 5×10^{-9} mol l⁻¹. Finally, owing to the nature of the reactive anchoring group in RB-19, the distinguishing between the original dye and its hydrolysed form is limited when using the AdSV technique.

REFERENCES

1. Weber, E.J., Sturrock, P.E., and Camp, S.R., *Reactive Dyes in Aquatic Environment: A Case Study of Reactive Blue 19*, Environmental Protection Agency, US (August 1990).
2. Weber, E.J., and Stickney, V.C., *Wat. Res.*, (1993), **27**, 63.
3. Camp, S.R., and Sturrock, P.E., *Wat. Res.*, (1990), **24**, 1275.
4. Fogg, A.G. and Zaroni, M.V.B., *Anal. Chim. Acta*, (1995), **315**, 41.
5. Zaroni, M.V.B., Fogg, A.G., Barek, J., and Zima, J., *Anal. Chim. Acta*, (1997), **349**, 101.
6. Almeida, P.J., Rodrigues, J.A., Barros, A.A. and Fogg, A.G., *Anal. Chim. Acta*, (1999), **385**, 287.
7. Barek, J., Beranova, J. Fogg, A.G., Mejstrik, V. Moreira, J.C. and Zima, J. *Anal. Chim. Acta*, (1997), **356**, 231.
8. Richardson, S.D., Thurston, A.D., McGuire, J.M., and Weber, E.J., *Org. Mass Spectrom.*, (1993), **28**, 619.
9. Camage, R.S.K., McQuillan, A.J., and Peake, B.M., *J. Chem. Soc. Farada Trans.*, (1991), **87**, 365.
10. Shimode, M., Mimura, M., Urakawa, H., Yamanaka, S., and Kajiwara, K., Sen – I. Gakkarshi, (1996), **52**, 301.
11. Chambers, J.Q., in *The Chemistry of Quinoid Compounds*, part II, Patai, S. (Ed), Wiley, NewYork, 1974.
12. Qureshi, G.A., Svehla, G., and Leonard, M.A., *Analyst*, (1979), **104**, 1241.
13. Gill, R., and Stonehill, H.I., *J. Chem. Soc.*, (1952), 1845.
14. Gill, R., and Stonehill, H.I., *J. Chem. Soc.*, (1952), 1857.
15. Anderson, J.C., and Broadbent, A.D., *Can. J. Chem.*, (1986), **64**, 127.
16. Furman, N.N., and Stone, K.G., *J. Am. Chem. Soc.*, (1948), **70**, 3055.

17. Revenge, J., Rodrique, F., and Rijero, J., *J. Electrochem. Soc.*, (1994), **141**, 330.
18. Dournaghi-Azar, M.H., and Golabi, S.M., *Talanta*, (1988), **35**, 959.
19. Driedergen, R.J., Hartigh, J.D., Holthouis, J.J.M., Hulshoff, A., Oort, V.W.J., Kelder, P.S.J., Verboom, W., Reinhoudt, D.N., Bos, M. and Van der Linden, W.F., *Anal. Chim. Acta*, (1990), **233**, 251.
20. Comminellis, C.H. and Plattner, E., *J. App. Electrochem.*, (1985), **15**, 771.
21. Reddy, G.S., Reddy, S.J. and Reddy, C.R., *Indian Chem. Soc.*, (1992), **69**, 737.
22. Broadbent, A.D. and Sommermann, E.F., *J. Chem. Soc. (B)*, (1968), 519.
23. Komorsky-Lovric, and Lovric, M.Z., *Anal. Chem.*, (1989), **335**, 289.
24. Broadbent, A.D., Donald Hewson, W., McDonald, H.A., and Melanson, R.J., *Can. J. Chem. Soc.*, (1977), **55**, 2946.
25. Nemodruk, A.A. and Karalova, Z.K., *Analytical Chemistry of Boron*, Ann Arbor-Humphrey science publishers, London, 1969.
26. Fogg, A.G., and Zanoni, M.V.B., *Anal. Proc.*, (1994), **31**, 173.
27. Zanoni, M.V.B., Carneiro, P.A., Furtan, M., Duarte, E.S., Guaratini, C.C.I., Fogg, A.G., *Anal. Chim. Acta*, (1999), **385**, 385.
28. Fogg, A.G., Yusoff, A. Rahim and Ahmad, R., *Talanta*, (1997), **44**, 125.
29. Smyth, W.F., *Voltammetric Determination of Molecules of Biological Significance*, John Wiley & sons, New York, 1992
30. Zanoni, M.V.B., Fogg, A.G., Barek, J. and Zima, J., *Anal. Chim. Acta*, (1995), **315**, 41.
31. Wopschall, R.H. and Shain, I., *Anal. Chem.*, (1967), **39**, 1514.
32. Yusoff, A.R.H.M., Fogg, A.G., and Ahmad, R., *Talanta*, (1998), **47**, 797.
33. Kdhier, W., *Voltammetric Identification of Dyes Using Surfactants*, A Master Of Philosophy Thesis, Loughborough University, 1989.
34. Yusoff, A.R.H.M., *Cathodic Stripping Voltammetric Studies on Sulfonamides and Reactive Dyes*, A Ph.D. Thesis, Loughborough University, 1996.

-
35. Barros, A.A., Rodrigues, J.A., Almeida, P.J., Rodrigues, P.G. and Fogg, A.G., *Anal. Chim. Acta*, (1999), **385**, 315.
 36. Almeida, P.J., Rodrigues, J.A., Barros, A.A., and Fogg, A.G., *Anal. Chim. Acta*, (1998), **332**, 1.

ADSORPTIVE STRIPPING VOLTAMMETRY OF REACTIVE BLUE 19 IN THE PRESENCE OF SURFACTANTS

6.1 Introduction

In previous studies reported in chapter five, the analysis of anthraquinone-based Reactive Blue 19 dye by AdSV at the HMDE has been investigated. However, the direct monitoring process of this reactive dye in natural or polluted waters (i.e. real sample) can be a complicated task owing to the occurrence of severe interference caused by the competitive adsorption of electro-active, as well as electro-inactive compounds. The determination of reactive dye molecules in natural waters is governed by the presence of surface-active materials in the sample. Surfactants compete with the analyte for adsorption sites on the electrode surface, resulting in decreased peak heights, lower sensitivity and narrower linear ranges¹. In extreme cases the stripping response may even be completely suppressed. Surface-active substances such as surfactants are known to adsorb at the electrode/solution interface and this can modify the behaviour of the electroactive species, hence, changes in the rate and kinetics of the electrode process (e.g. reducing the rate of electrode reaction) and/or changes in the thermodynamic properties of the system in the interfacial region are to be expected². As a result, a shift of the half-wave potential, splitting of the analytical peak, decrease of limiting current and other phenomena, have been observed³. In addition, if the surfactant is an electroactive

substance, it can produce adsorptive stripping peaks during the stripping step that may overlap with the analyte peaks⁴. On the other hand, the presence of surfactants may also result in an enhancement for the height of the voltammetric signal². In such cases, the thermodynamic properties of the system in the interfacial region are affected and the coadsorption process has an acceleration and catalytic influence on the electrode reaction. However, several approaches have been used to alleviate and overcome the surfactant coadsorption problem in AdSV^{5,6}. A proper choice of accumulation potential or the use of short accumulation times can minimise modest suppressions of the adsorptive stripping peaks. Calibration curves or standard addition experiments, also correct for such modest effects. More severe peak depressions usually require a time-consuming separatory technique (e.g. HPLC or molecular exclusion chromatography) to isolate the analyte from co-adsorbing interferents. Finally, the addition of fumed silica to sample solutions, or applying ultraviolet (UV) irradiation, can be used for the elimination of many of the surfactant problems characterising some AdSV measurements.

In recent years, the effect of surfactants on AdSV of various synthetic dyes and colouring matters has been receiving considerable attention. In a recent publication, the influence of the addition of Triton X-100 on the AdSV behaviour of two anthraquinone-based reactive dyes (Procion Blue MX-R and Cibacron Blue 3GA) was reported^{7,8}. The addition of surfactants has an effect that seems to be more complex than a simple competition for adsorption sites. In the presence of Triton X-100, the rate of the electrochemical process slowed down, a fact that would explain the increase of the voltammetric signal for larger current sampling times⁸. However, Fogg and colleagues studied the effect of various surfactants on the differential-pulse voltammetric determination and identification of synthetic colouring matters in drugs and cosmetics^{9,10}, synthetic food colouring matters^{3,11}, and two reactive dyes (Reactive Orange 23 and Reactive Black)¹². In addition, the influence of the surfactant tetraphenyl phosphonium chloride (TPPC) on the voltammetric signal of the azo colouring matter Azorubine¹³ and Carmoisine¹⁴ was recently reported. In general, similar inhibition actions caused by several surfactants were observed in most of these reported studies.

6.2 Aim of the Study

The aim of this present work was to investigate the influence of various surfactants on the AdSV response in order to evaluate the possibilities and limitations of the application of differential pulse adsorptive stripping voltammetry in monitoring the concentration of Reactive Blue 19 at ng l^{-1} levels in the presence of competitive interferences. Thus, the optimal experimental conditions that can lead to minimise the inhibitory and suppression effects of these surfactants have to be defined and controlled.

This study was also aimed at improving the knowledge of the possible effect of surfactants on the stripping voltammetric peak potential for this reactive dye. Such possible shifts in peak potential may allow direct determination of the studied Reactive Blue 19 dye in the presence of its hydrolysis products or other anthraquinone-based reactive dyes reduced at similar stripping voltammetric potentials. This procedure is known as "selective damping" or electrochemical masking of the interfering substance with a surface-active species.

6.3 Effect of Various Surfactants on the Anthraquinone Reduction Process

The influence of several surfactants on the AdSV behaviour of RB-19 was investigated under identical conditions i.e. by performing the accumulation stage for 2 min at a preconcentration potential of 0.0 V in pH 4.5 Britton-Robinson buffer. The concentration of the studied reactive dye was $5 \times 10^{-7} \text{ mol l}^{-1}$ and the concentration of surfactants was varied within an appropriate range for each surfactant. The results obtained were expressed as dependence of the relative peak heights i_p/i_o (where i_p is the peak height of the reactive dye in the presence of surfactant, and i_o is that in the absence of surfactant) on the concentration of surfactants.

6.3.1 Effect of Glycerol

The competitive adsorption of Glycerol has practically no influence on the shape and potential position of the analytical signal of the reduction of the anthraquinone moiety. A typical DPAdSV signal of $5 \times 10^{-7} \text{ mol l}^{-1}$ of RB-19 in the presence of varying concentration of Glycerol surfactant is given in Fig. 6.1. The addition of a very low concentration (6 mg l^{-1}) of Glycerol caused a decrease in the peak current of RB-19, by about 12 % of the original signal. A continuous decline in the anthraquinone peak current was observed when varying the surfactant concentration within the range 6-60 mg l^{-1} (see Fig. 6.2). Such electrochemical behaviour can be explained by the competitive co-adsorption of surfactants that have a strong adsorptive ability on the surface of the hanging mercury drop electrode. This inhibiting effect of Glycerol surfactant is probably related to the possible decrease in the electrode process rate constant for the reduction of the anthraquinone moiety due to changes in the rate of charge and mass transfer^{15,16}.

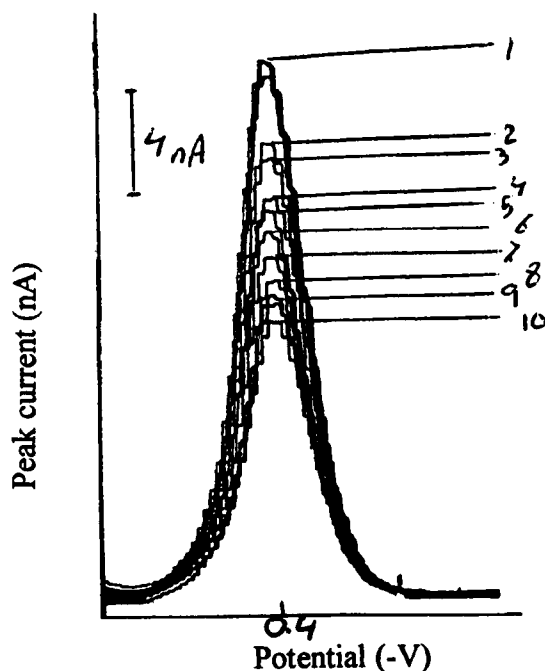
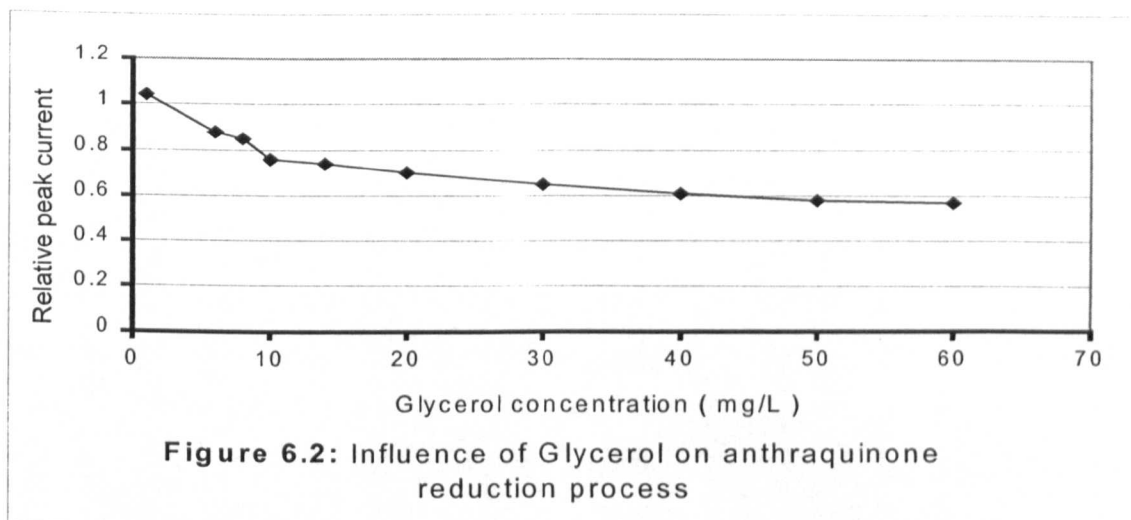
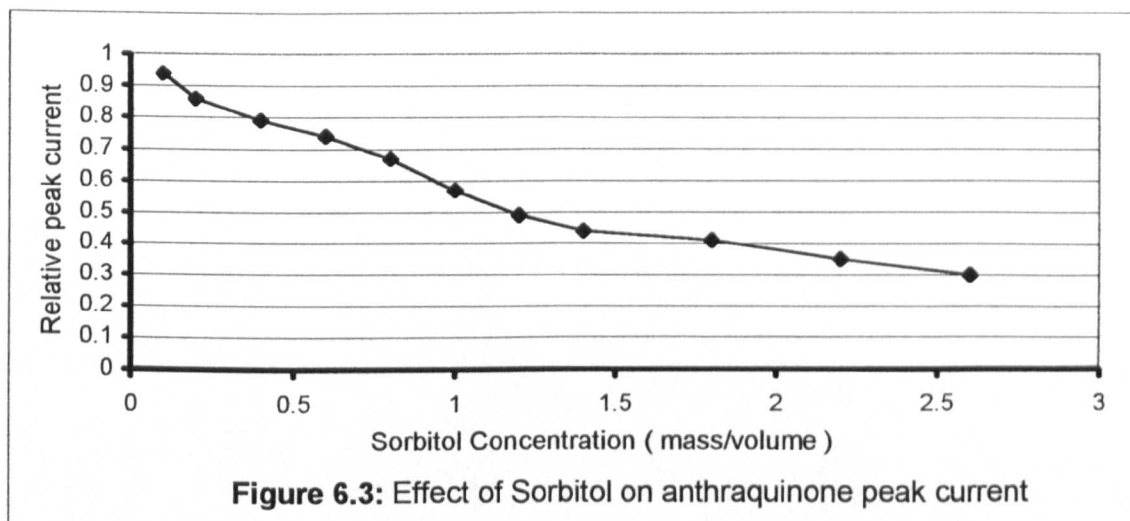


Figure 6.1: Influence of the presence of Glycerol on DPAdSV signal of Reactive Blue 19. Surfactant concentrations: 1:2, 2:6, 3:8, 4:10, 5:14, 6:20, 7:30, 8:40, 9:50, 10:60 mg l^{-1} .



6.3.2 Effect of Sorbitol

Figure 6.3 illustrates the influence of the competitive adsorption of Sorbitol surfactant on the analytical response of $5 \times 10^{-7} \text{ mol l}^{-1}$ RB-19. A gradual decrease in peak current when increasing the concentration of Sorbitol was recorded. In comparison with Glycerol a relatively higher concentration ($0.1 \text{ mass Volume}^{-1}$) of this surface-active reagent was required to start affecting the anthraquinone peak current, whereas trace amounts as low as 4 mg l^{-1} concentration of Glycerol was sufficient to produce similar inhibition effect. The suppression of the measured anthraquinone peak current is possibly caused by the working electrode surface blockage due to adsorption of the Sorbitol surfactant. In contrast, Sorbitol has practically no influence on the adsorptive stripping peak shape and potential. The degree of RB-19 damping within the range of concentration of surfactant under investigation does not exceed 30% of the original signal.

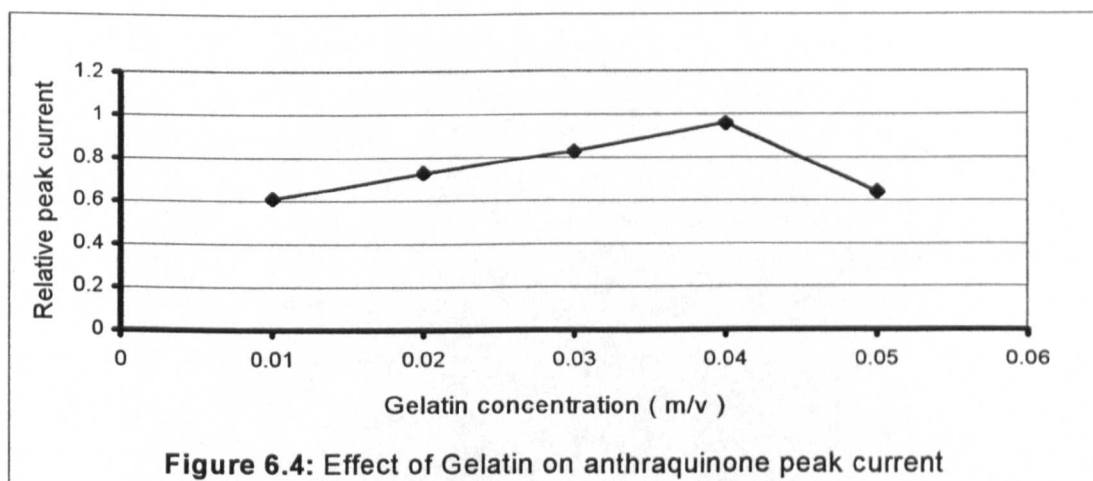


6.3.3 Effect of Gelatine

The dependence of peak height of Reactive Blue 19 on the concentration of Gelatine in a narrow concentration range of surfactant ($0.01\text{-}0.05\text{ mass Volume}^{-1}$) is given in Fig. 6.4. In contrast to the results obtained with Glycerol and Sorbitol surfactants, the addition of Gelatine leads to an increase in the analytical response when increasing the Gelatine concentration. However, this enhancement is dominant in the surface-active concentration range from 0.01 to $0.04\text{ mass volume}^{-1}$, then starts to decrease when the concentration of the presence surfactant exceeds the $0.04\text{ mass volume}^{-1}$ level. Moreover, the introduction of Gelatine surfactant has less effect on the peak potential of RB-19 stripping voltammetric peak. A 28 mV shift in peak potential to the negative direction was observed. However, the literature described similar results for the enhancement of peak current of several synthetic dyes by the presence of Gelatine^{9,10}. After the addition of Gelatine two competing effects were observed; the retarding effect due to the surface layer of Gelatine blocking the electrode reaction and the catalytic effect of the Gelatine in promoting the protonation of the reactive dye prior to reaction and

hence catalysing the overall electrode reaction⁹. Clearly, The Gelatine concentration determines which of these two effects (inhibition or catalyst effect) predominates.

However, at this stage it is difficult to suggest precise reasons for this unexpected effect of Gelatine on increasing the sensitivity of Reactive Blue 19 analysis. Nonetheless, this peak current enhancement might be attributed to the different kinetic characteristics of the surface redox reaction of this reactive dye adsorbed on the mercury electrode that initially covered by the co-adsorbed surface-active molecules.



6.3.4 Influence of surfactant charge

The influence of the distribution of the electrical charge on the molecule of surfactant on the adsorptive stripping voltammetric behaviour of the reactive dye was examined on the well-defined electrochemically reversible wave of anthraquinone reduction process at pH 4.5 B-R buffer. Three categories of surfactant which have different electrical charge on the molecule were studied: a cationic surfactant in which the hydrophobic portion of the compound is attached to a residual positive charge (Tetraphenyl phosphonium chloride); an anionic surfactant in which the hydrophobic

portion of the molecule is attached to the residual negative charge (Aerosol OT), and a non-ionic surfactant in which there is no residual electrical charge (Triton X-100).

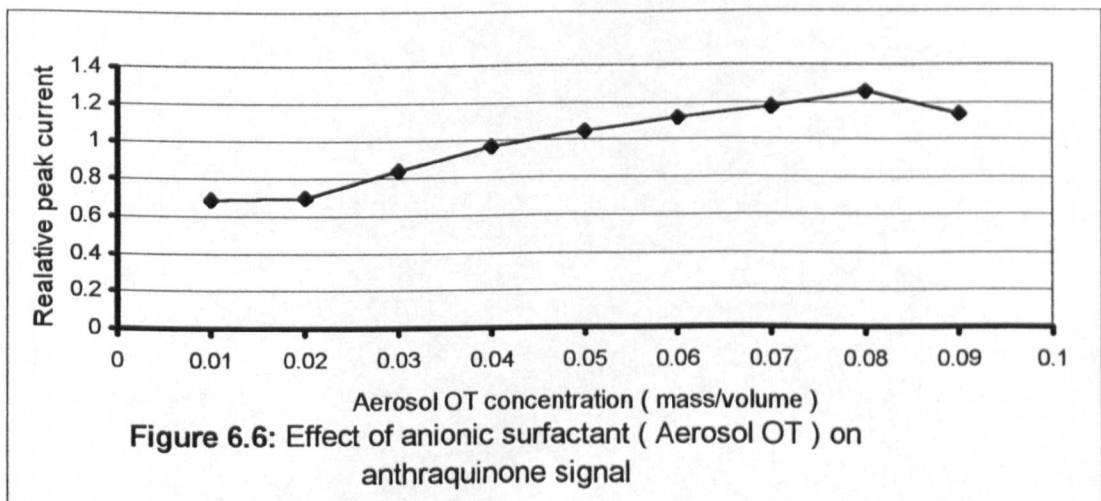
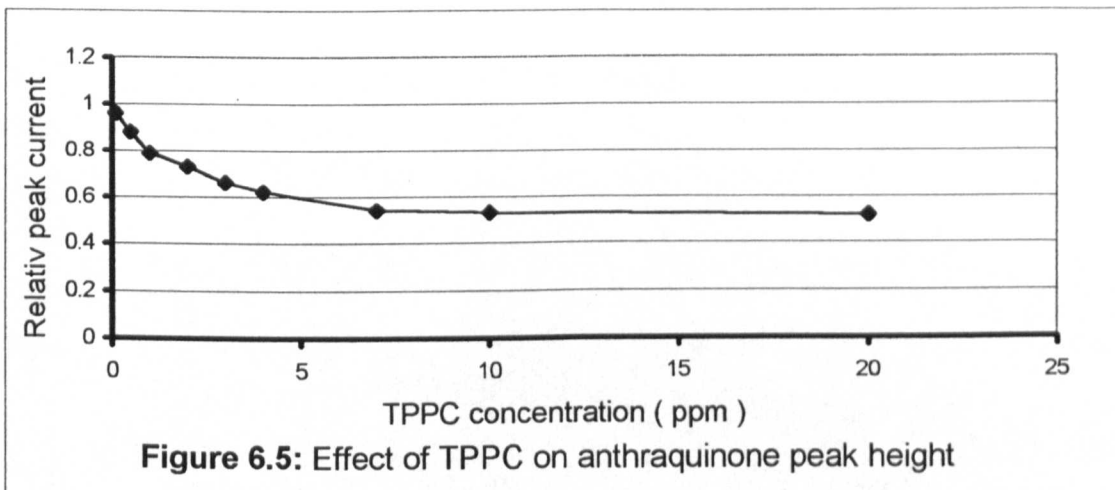
6.3.4.1 Effect of cationic surfactant (TPPC)

Tetraphenyl phosphonium chloride (TPPC) has a noticeable effect on the DP AdSV response of anthraquinone-based RB-19. Although no significant effect on the adsorptive stripping peak potential was observed, a marked reduction on the peak current with the continuous addition of the cationic surfactant was recorded. The effect of variation of the surfactant concentration on peak current was evaluated over the range 0.1-20 $\mu\text{g ml}^{-1}$ TPPC. Results presented in Fig. 6.5 evidently show that, the presence of a very low quantity of the cationic surfactant (20 $\mu\text{g ml}^{-1}$) was sufficient to reduce the peak height to half its initial value. The co-adsorption action of TPPC, probably caused changes in the structure of the double layer, which was reflected in changes in the electrochemical reaction, taking place there and its rate constant.

6.3.4.2 Effect of anionic surfactant (Aerosol OT)

The influence of the Aerosol OT anionic surfactant on the AdSV behaviour of RB-19 was complex. As can be seen from Fig. 6.6, the anthraquinone analytical signal decreased sharply to nearly less than two-thirds its original value after the addition of 0.01 mass volume⁻¹ Aerosol OT. However, after this initial retardation effect on the electrode reaction, a catalytic and acceleration impact was observed with increasing concentration of the anionic surfactant. This enhancement effect was predominant within the concentration range 0.02-0.08 mass Volume⁻¹ (Fig. 6.6). Nevertheless, a new inhibition action was observed beyond 0.09 mass Volume⁻¹ level. On the other hand, when increasing anionic surfactant concentration from 0.01 to 0.09 mass volume⁻¹, a very slight (14 mV) change in the positive direction of peak potential was recorded.

Although the influence of these surfactants is not fully understood at this preliminary stage, such electrochemical behaviour might be explained by assuming that



after the introduction of the anionic surfactant, its molecules compete with the analyte for the surface-adsorption sites, hence, leading to the initial depression of the adsorption stripping peak of interest. However, by introducing further additions of the Aerosol OT, it is possible that the negatively charged adsorbed layers of the anionic surfactant can be attached by electrostatic forces to the reactive dye molecules. As a result of this collecting and accumulating effect, the monitored electroanalytical response is enhanced and increased.

In contrast, on the basis of such a scenario one can explain why the presence of a very low concentration of the TPPC cationic surfactant can lead to a marked and profound inhibition effect for the cathodic reduction process of the anthraquinone group. In this case, the reactive dye molecules have to cross through the positively charged adsorbed layers of the cationic surfactant.

6.3.4.3 Effect of non-ionic surfactant (Triton X-100)

Triton X-100 is a surface-active substance very often used in the study of the inhibition phenomena because of its great effect on various electrode processes. Its important role is described in many published papers^{15,17,18}. The influence of Triton X-100 on the peak shape and peak position of the adsorptive stripping peak of RB-19 is not significant (Fig. 6.7). The decrease in the peak current of Reactive Blue 19 as a function of the concentration of Triton X-100 was investigated. As may be observed in Fig. 6.8 a dramatic decline in the peak height was obtained when increasing the non-ionic surfactant concentration from 0.1 to 1 mg l⁻¹. However, the reduction of peak height remains approximately constant beyond the 1 mg l⁻¹ level. The decrease in the peak height of RB-19 does not exceed 40%. The severe effect of Triton X-100 on RB-19 response is probably due to the non-potential-dependent π -electron interaction between the several aromatic (phenyl) rings in its molecule and the mercury surface^{6,19}. In consequence of the addition of Triton X-100 surfactant, its molecules move to the electrode surface already covered with the reactive dye molecules. At high concentrations of Triton X-100

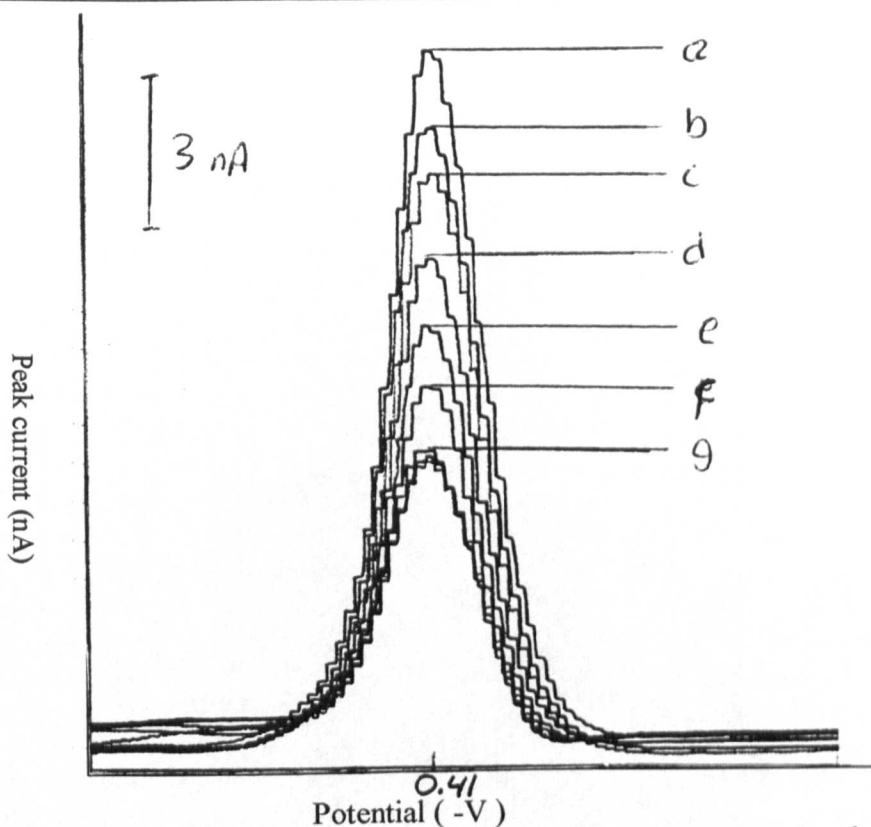


Figure 6.7: Effect of Triton X-100 on peak height of anthraquinone functional group. Surfactant concentrations: a:0, b:0.1, c:0.2, d:0.4, e:0.6, f:0.8, g: 1.0 mg l⁻¹.

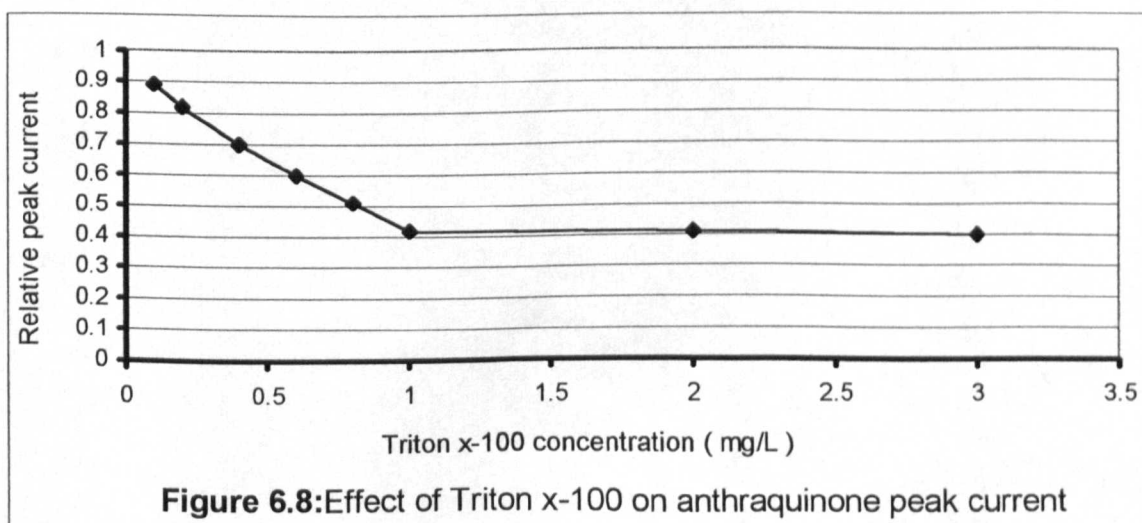


Figure 6.8:Effect of Triton x-100 on anthraquinone peak current

most of the RB-19 molecules could be removed from the working electrode surface. Hence, a marked suppression for the analytical response is anticipated.

In conclusion, Triton X-100 is a strongly adsorbable surfactant that adsorbed at the mercury electrode and affects the electrochemical process at the electrode/electrolyte interface. However, owing to its non-ionic nature it has a moderate action on the anthraquinone cathodic reduction response compared to the severe inhibition action observed with the TPPC cationic surfactant and the catalytic action recorded with Aerosol OT anionic surfactant. Accordingly, the type and overall charge of the applied surfactants have a noticeable and significant influence on the electrochemical signal of interest. This seems to indicate that a cationic surfactant has a greater inhibiting action than the anionic surfactants.

6.4 Influence of Experimental Conditions

In studies of the influence of surfactants on the adsorptive stripping peaks of reactive dyes, a significant role can be also played by other experimental conditions such as pH, supporting electrolyte, accumulation time, preconcentration potential ... etc. As a consequence, the optimal experimental conditions that can ensure the possible minimum suppression effect can be defined. In order to evaluate the contribution of such parameters with surfactant actions, Triton X-100 was chosen as a “model surfactant”. Besides its intermediate influence, the choice of Triton X-100 was justified by the fact that this surfactant is frequently used in the study of the inhibition phenomena for various substances at different working electrodes.

6.4.1 Effect of pH

The effect of pH over a wide range (2-12) with a combination of the addition of four different Triton X-100 concentrations (0.2, 0.5, 0.8, and 1.2 mg l⁻¹) on the adsorptive

stripping process was examined on the anthraquinone well-defined electrochemical wave of $5 \times 10^{-7} \text{ mol l}^{-1}$ Reactive Blue 19. A summary of such effects is given in Table 6.1. In general, the relative peak current value increased with the increase of pH value right up to pH 12. As can be noticed from the previous Table, the anthraquinone electrochemical signals in the presence of low surfactant concentration and at high acidic aqueous solutions (pH 2-4) were sharply decreased. As expected, it suppressed further when the Triton X-100 surfactant concentration was increased. For instance, less than one third (29%) of the original analytical signal was recorded when 1.2 mg l^{-1} Triton X-100 was present in pH 2 B-R supporting electrolyte solution. However, a significant recovery for the analytical response (average 68%) was observed between pH 6 and pH 10. Further improvement and enhancement for the analytical signal was observed at pH 12. In fact, The peak current recovery reached 160% after the addition of 0.8 mg l^{-1} Triton X-100.

Table 6.1: Effect of pH on AdSV signal in the presence of Triton X-100 surfactant.

Triton X-100 (mg l ⁻¹)	pH					
	2	4	6	8	10	12
0.2	0.52 *	0.65	0.73	0.72	0.77	1.17
0.5	0.34	0.45	0.60	0.70	0.74	1.35
0.8	0.31	0.38	0.58	0.71	0.73	1.6
1.2	0.29	0.38	0.56	0.68	1.0	1.13

* Relative peak current.

The results obtained in these experiments can be understood in view of the suggestions made by some authors¹⁷ that most of the functional groups of surfactant molecules (Triton X-100 in this case) are deprotonated at higher pH and thus are negatively charged. Hence, electrostatic forces can attach the reactive dye molecules to the adsorbed layer of the surfactant at the electrode surface. Accordingly, the

accumulation and collection effect on the Reactive Blue 19 compound causes an enhancement in the electrochemical reduction signal of the anthraquinone moiety. On the basis of the previous observations, alkaline solutions (pH 8-10) can be selected as optimum to reduce the surfactant co-adsorption problem in AdSV analysis of this reactive dye in a real test sample.

On the other hand, the addition of Triton X-100 at higher pH values was shown to cause the peak potential of the anthraquinone system to be shifted 51 mV and 90 mV in the positive direction at pH 10 and pH 12, respectively. The dependence of peak potential on the concentration of Triton X-100 in the concentration range over 0.2-1.2 mg l⁻¹ is illustrated in Table 6.2. The recorded shift in the adsorptive stripping peak potential to less negative value with the addition of surfactant at higher pH, may confirm the deprotonation of the functional groups of Triton X-100 at higher pH, thus reducing the effect of pH on the electrochemical reduction of the anthraquinone group. This latter assumption seems to be valid from observing that the cathodic reduction process becomes less difficult to achieve. However, the effect of Triton X-100 on the peak potential at pH values less than 10 is not significant. Despite the occurrence of such considerable potential peak shifts at higher pH, the discrimination of this reactive dye from its hydrolysis products and/or structurally similar anthraquinone-based reactive dyes via the selective damping method was not possible owing to their similar stripping voltammetric potentials. After all, the cathodic reduction for all these various forms resulted in one overlapped electrochemical signal.

Finally, the second analytical peak related to the anthrone cathodic reduction process was totally suppressed after the addition of the non-ionic surfactant at pH >8.

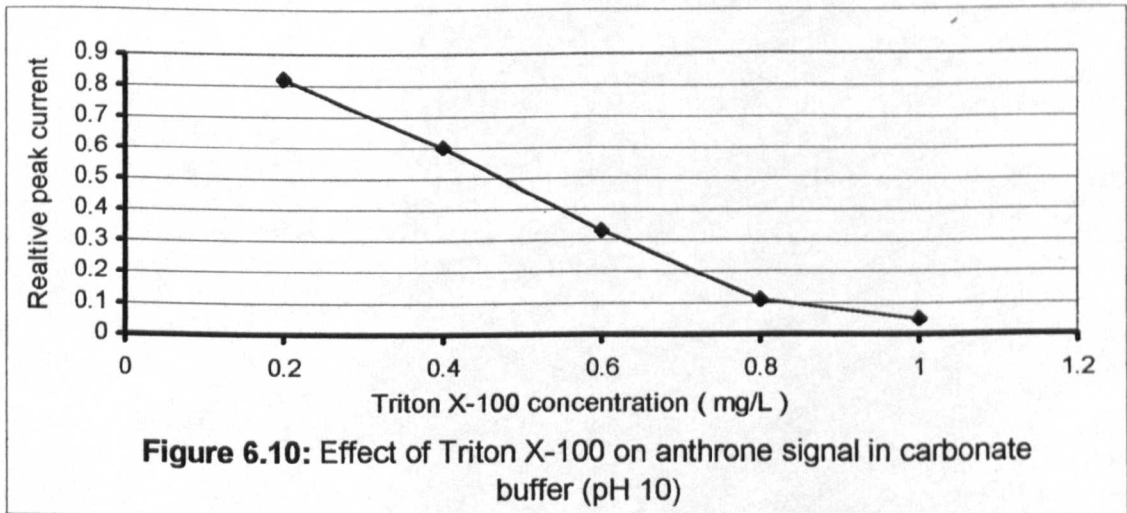
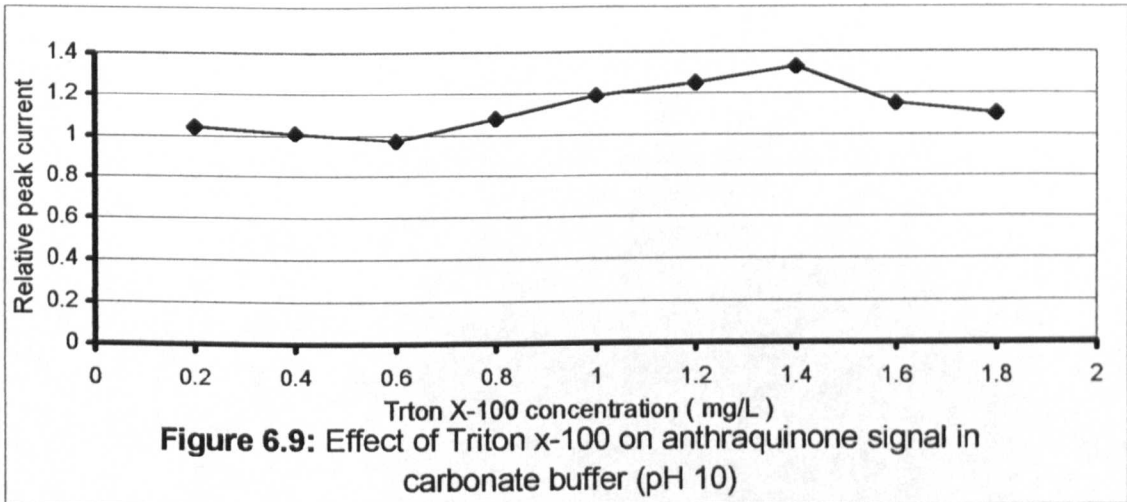
Table 6.2: Influence of surfactant on anthraquinone peak potential at different pH values

Triton X-100 (mg l ⁻¹)	0	0.2	0.5	0.8	1.2
Peak potential (pH 10) -V	0.736	0.732	0.697	0.693	0.685
Peak potential (pH 12) -V	0.827	0.784	0.748	0.741	0.737

6.4.2 Effect of supporting electrolytes

All the previous measurements were obtained by employing Britton-Robinson buffer (pH 4.5) as a supporting electrolyte, however, several other supporting electrolytes can be used. The behaviour of the anthraquinone reduction process in the presence of Triton X-100 at several concentrations when using carbonate buffer as a supporting electrolyte is given in Fig. 6.9. In general, the addition of the surfactant has a catalytic effect on the anthraquinone reduction process. The reactive dye electrochemical response was relatively constant when the concentration of surfactant was less than 0.6 mg l^{-1} . However, it increases linearly with the continuous introduction of Triton X-100 till it reached its highest value (133%) at 1.4 mg l^{-1} . However, the inhibition action is predominated at a very high Triton X-100 concentration ($>1.4 \text{ mg l}^{-1}$). It appears that this electrochemical behaviour is very similar to that previously reported for Britton-Robinson supporting electrolyte at a higher pH. Therefore, an analogous explanation can be used to describe the obtained results (refer to section 6.4.1). Meanwhile, a significant shift of 60 mV in the less negative direction for the AdSV peak potential was reported when the surfactant concentration was varied over $0.2\text{-}1.8 \text{ mg l}^{-1}$ concentration range.

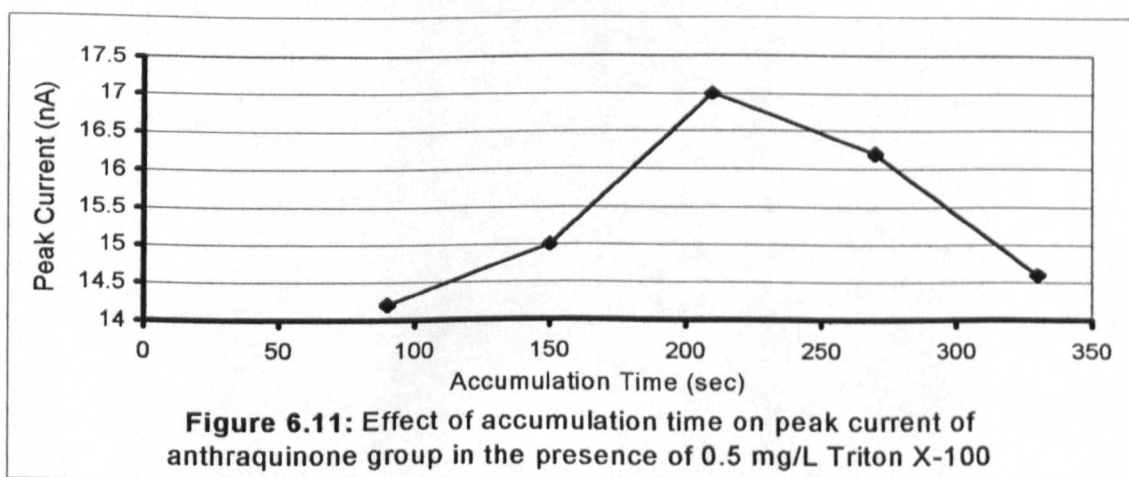
In contrast, the second analytical signal associated with the cathodic reduction of the anthrone product was gradually decreased with the addition of Triton X-100 till it was totally eliminated at a surfactant concentration of 1.0 mg l^{-1} (see Fig. 6.10). The elimination of the second electroanalytical wave by the addition of Triton X-100, can be used to overcome the AdSV limitation arises from the overlapping problem between this signal and other popular and important electroactive systems (e.g. chlorotriazine reactive group) which reduce at a similar voltammetric potential to that recorded for anthrone. Consequently, simultaneous analysis of this reactive dye with chlorotriazine-based reactive dyes (for instance) in mixtures, via the anthraquinone and the resolved and recovered chlorotriazine response can be achieved at higher pH solution and after the addition of the surfactant.



Furthermore, the influence of using acetate buffer as a supporting electrolyte on the electrochemical behaviour of 5×10^{-7} mol l^{-1} Reactive Blue 19 in the presence of Triton X-100 was also evaluated. Similar results and outcomes to that observed for Britton-Robinson and carbonate buffers were obtained. Apart from the solution pH value, the influence of the kind of supporting electrolyte used did not affect the electrochemical signal considerably.

6.4.3 Effect of T_{acc} and E_{acc} in the presence of surfactant

Figure 6.11 illustrates the effect of accumulation time (T_{acc}) on the reactive dye peak current in the presence of $0.5 \text{ mg } l^{-1}$ Triton X-100 at pH 4.5 B-R buffer. The analytical signal of anthraquinone group gradually increased with increasing the duration period in the range 90-210 sec. However, it significantly decreased when longer accumulation times were used. This is probably due to the serious competitive coadsorption action of the surfactant molecules for the adsorption sites on the working electrode surface, when applying longer preconcentration times.



By contrast, in the absence of surfactant a constant response at higher T_{acc} has been reported (see section 5.6.1) rather than this inhibition effect caused by the surfactant. As a result, applying short accumulation times (e.g. $T_{acc} = 120$ sec) could be a proper choice to overcome the modest interference problem related to the presence of surface-active surfactants in the test samples. This conclusion is in a good agreement with the recommendations reported by several researchers in the literature^{20,21} to reduce the influence of surfactants on the adsorptive stripping response of interest.

The AdSV behaviour of the anthraquinone signal in the presence of different Triton X-100 concentrations (0.2, 0.4 and 0.8 mg l⁻¹) at various accumulation potentials (E_{acc}) is summarised in Table 6.3. As can be extracted from the given results, the relative peak current ratio (i_p/i_o) reaches its maximum value (hence, indicating less surfactant action) at -0.3 V accumulation potential. This weak co-adsorption action of surfactant on the negatively charged mercury electrode surface at $E_{acc} = -0.3$ V, presumably arises from the repulsion phenomenon between the negative electrode and the partially deprotonated surfactant molecules in addition to the attraction between the dye molecules and the electrode. Anyway, -0.3 V accumulation potential was adopted as optimal to alleviate and reduce the surfactant inhibitory effect. Finally, the combination of either accumulation potential or accumulation time with the addition of Triton X-100 has no significant effect on the peak position at the investigated experimental conditions.

Table 6.3: Effect of accumulation potential on anthraquinone AdSV signal in the presence of Triton X-100.

Triton X-100 (mg l ⁻¹)	Accumulation Potential (E_{acc})						
	-0.3	-0.2	-0.1	0.0	+0.1	+0.2	+0.3
0.2	0.73 *	0.55	0.63	0.63	0.53	0.56	0.55
0.4	0.53	0.40	0.43	0.41	0.37	0.42	0.43
0.8	0.46	0.36	0.42	0.37	0.43	0.42	0.45

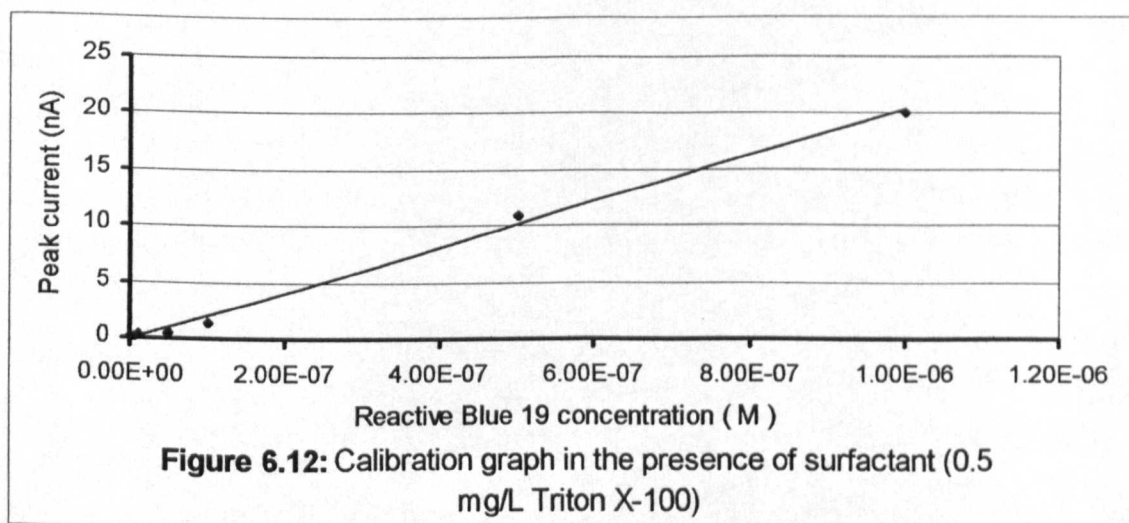
* Relative peak current.

6.5 Analytical Application

Figure 6.12 illustrates the effect of the addition of Triton X-100 surfactant (0.5 mg l⁻¹) on the resulting calibration curve for the adsorptive stripping measurements of Reactive Blue 19. The calibration plot has been estimated over the reactive dye concentration range between 1×10⁻⁹ mol l⁻¹ and 1×10⁻⁶ mol l⁻¹. The calculated correlation coefficient was 0.998 and the corresponding regression line can be represented by:

$$Y (A) = 0.02 X (\text{mol l}^{-1}) - 0.07 \times 10^{-9} \quad r = 0.998 \quad n = 6$$

This calibration line approximately passes through the origin, it was found not to be totally identical with the calibration line for Reactive Blue 19 without Triton X-100 in the sample (refer to section 5.7.1). The addition of relatively low concentration of Triton X-100 (0.5 mg l⁻¹) to the test sample seems to improve and extend the linear range. However, the detection limit of the proposed method is poorer ($\approx 6 \times 10^{-8}$ mol l⁻¹) than that available with conventional adsorptive stripping methods because of the surfactant coadsorption problem.



Finally, the effect of applying the optimum experimental conditions required for minimising the inhibition action of surfactants on the anthraquinone AdSV peak of

interest was evaluated. The electrochemical signal of $1 \times 10^{-8} \text{ mol l}^{-1}$ Reactive Blue 19 was reduced to only 22 % of its original response due to the addition of 0.5 mg l^{-1} Triton X-100. Nonetheless, a 65 % and 44 % recovery of the stripping voltammetric peak current were observed when adjusting the pH of the buffer solution to 8 and accumulation potential to -0.3 V, respectively.

6.6 Conclusions

Relatively simple electrochemical methods have been used to follow the influence of different surfactants on the anthraquinone reduction process. Some conclusions regarding reactive dye determination therefore can be drawn. This study has demonstrated that the presence of surfactants in the analysed sample can lead to a co-adsorption problem for the AdSV application. Generally, in the most studied cases the presence of surfactant has an inhibition influence on the analytical response such as the cases of Glycerol, Sorbitol, TPPC and Triton X-100. However, the addition of these surfactants shows no practically significant effect on the shape and peak potential of the anthraquinone AdSV signal. However, there are some exceptions to this conclusion. For instant, the presence of Gelatine, Aerosol OT and Triton X-100 (in carbonate buffer or at higher pH in B-R buffer) has a catalytic action and enhances the electroanalytical response. A probable explanation for such AdSV behaviour was also proposed. Moreover, comprehensive studies of the contribution of several experimental parameters on the anthraquinone reduction process in the presence of surfactant were also carried out. Consequently, recommended optimum experimental conditions such as short accumulation time, proper choice of preconcentration potential and higher pH buffer solution, were suggested to ensure minimum surfactants co-adsorption limitation in AdSV analysis of this anthraquinone-based reactive dye.

REFERENCES

1. Wang, J. "*Voltammetry After Nonelectrolytic Preconcentration* in: *Electroanalytical Chemistry*, Bard, A.J., (Ed.), Vol. 16, Marcel Dekker, New York, 1989.
2. Harman, A.R., and Baranski, A.S., *Anal Chem.*, (1991), **63**, 1158.
3. Fogg, A.G., and Bhanot, D. *Analyst*, (1980), **105**, 234.
4. Wang, J. *Am. Lab.*, (1985), May, 41.
5. Wang, J., and Kubiak, W., *J. Electroanal. Chem.*, (1989), **258**, 41.
6. Economou, A., and Fielden, P.R., *Analyst*, (1993), **118**, 1399.
7. Almieda, P.J., Rodrigues, J.A., Barros, A.A. and Fogg, A.G., *Anal. Chim. Acta*, (1999), **385**, 287.
8. Fogg, A.G., Almeida, P.J., Rodrigues, J.A., and Barros, A., *Electrochem. Soc. Proc.*, (1997), **19**, 324.
9. Barros, A.A., Cabral, J., and Fogg, A.G., *Analyst*, (1988), **113**, 853.
10. Fogg, A.G., Barros, A.A., and Cabral, J., *Analyst*, (1986), **111**, 831.
11. Fogg, A.G., and Bhanot, D., *Analyst*, (1987), **112**, 1319.
12. Kdhier, W., *Voltammetric Identification of Dyes Using Surfactants*, A Master Of Philosophy Thesis, Loughborough University, 1989.
13. Barros, A.A., Rodrigues, J.A., Almieda, P.J., Rodrigues, P.G. and Fogg, A.G., *Anal. Chim. Acta*, (1999), **385**, 315.
14. Barros, A.A., and Rodrigues, J.A., *Portug. Electrochim. Acta*, (1996), **14**, 233.
15. Kozarac, Z., Nikolic, S., Ruzic, I. and Cosovic, B., *J. Electroanal. Chem.*, (1982), **137**, 279.
16. Opydo, J., *Talanta*, (1992), **39**, 229.
17. Plavsic, M., and Cosovic, B., *Anal. Chim. Acta*, (1994), **284**, 539.
18. Szymanski, A., and Lukaszewski, Z., *Anal. Chim. Acta*, (1992), **260**, 25.
19. Damaskin, B.B., Petril, O.A., and Batrakov, V.V., *Adsorption of Organic Compounds on Electrodes*, Plenum Press New York, 1971.

-
20. Wang, J., Luo, D.B. and Farias, P.A.M., *J. Electroanal. Chem.*, (1985), **185**, 61.
 21. Kalvoda, R., *Anal. Chim. Acta*, (1984), **162**, 197.

DETERMINATION OF FLUOROTRIAZINE-BASED AZO REACTIVE DYES BY AdSV AT THE HMDE

7.1 Introduction

In chapter five, the AdSV behaviour of the first type of reactive dyes based on the anthraquinone chemical structure was investigated. However, azo dyes are considered as one of the largest group of organic dyes. It was estimated that there are more than three thousand azo dyes currently in use all over the world¹ and azo dyes constitute more than 35% of the global production of all dyes. Hence, the fate of these synthesised dyes as environmental pollutants through discharge of plant effluents is inevitable. Accordingly, their control and monitoring require a suitable analytical procedure for the sensitive determination of trace amounts of these compounds.

Owing to the importance of the azo-based reactive dyes in analytical chemistry, the electrochemical properties of a further representative examples of these widely used reactive dyes were studied using stripping voltammetric methods that have already been found useful for the determination of a variety of structurally similar reactive dyes. Triazine-based azo dyes have attracted considerable recent interest as reactive dyes. In fact, the electrochemical behaviour and properties of several synthetic dyes containing a chromogen azo group and/or a halo-triazine anchoring reactive group have been investigated over the years²⁻⁶.

7.2 Aim of the Study

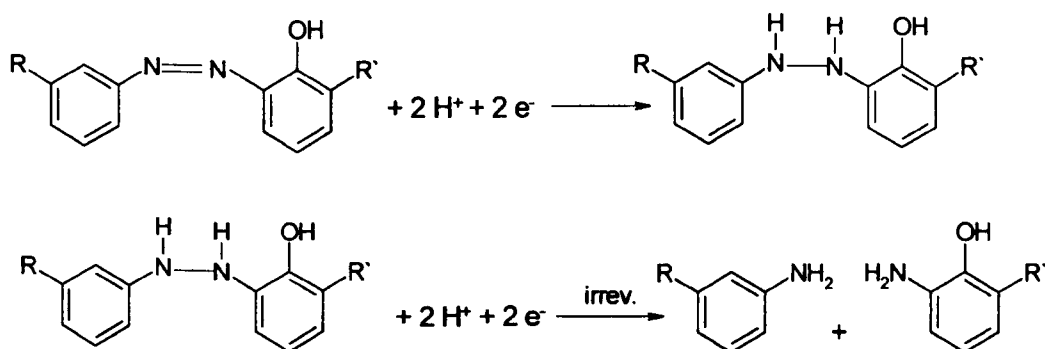
Although several triazine-based azo reactive dyes with different reactive and leaving groups including -Cl, -OCH₃, -NH₂, -SCH₂CH₂OH and -C₅H₄NCOOH have been studied by the AdSV technique^{7,8}, no study has been extended to azo dyes with a fluorotriazine reactive group. Hence, the present study was devoted to evaluate the

applicability of the AdSV method for studying the electroanalytical behaviour and finding the optimum experimental condition for the determination of the ultra-trace amounts of these fluorotriazine-based azo reactive dyes and their hydrolysis products. A full comparison with the stripping voltammetric behaviour of the previously studied chlorotriazine-based azo dyes is also reported. This present work illustrates the analytical advantages of the developed procedure for differentiating between the tested reactive dyes, thus, carrying out a simultaneous analysis of these dyes in mixtures. Finally, the mechanisms of azo and fluorotriazine electrochemical reductions on the HMDE has also been discussed.

7.3 The Electrode Reduction Processes of Azo and Fluorotriazine Functional Groups

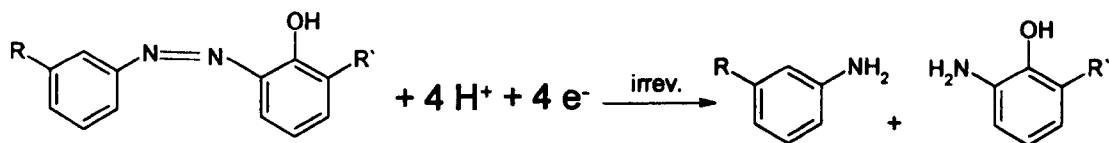
7.3.1 Azo group

The electrochemical behaviour of a variety of azo compounds and dyes has been studied extensively^{1,9-12}. The numbers of electrons involved in the reduction of azo dyes depends on the pH of the electrolyte buffer and its constituents as well as the substituents on the electrochemical active moiety. It is known that reduction of azo compounds containing strong electron-donating groups such as the ortho-hydroxy group (which is the case with these tested fluorotriazine-based azo reactive dyes) at the surface of a mercury electrode is accompanied by cleavage of the $-N=N-$ bond and formation of the corresponding amines⁹. Otherwise, the reduction of the azo group will only proceed to the hydroazo derivatives via a two-electron reduction process. However, in neutral or alkaline media, a two-step reduction mechanism has been proposed for these azo-based reactive dyes. The first step is likely to be a two-electron, two-proton, reduction process resulting in the formation of a hydrazo form. This newly formed hydrazo derivative then undergoes irreversible reductive cleavage to give the corresponding aromatic amines (see Scheme 1). Nevertheless, only one electrochemical wave is observed because the reaction of the intermediate form is fast enough to transfer hydrazo derivative to related amines products, hence, leading to an overall four-electron, four proton irreversible reduction. The consumption of four-electrons in this proposed mechanism was confirmed coulometrically^{13,14}.



Scheme 1

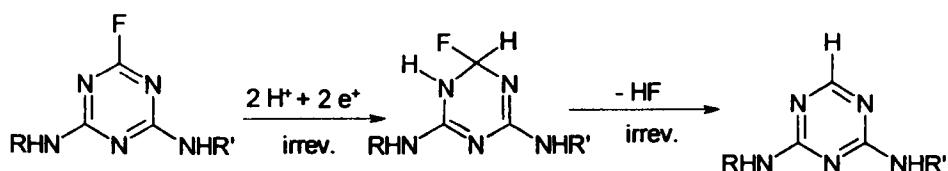
In contrast, in acidic media the overall process of the reduction of $-\text{N}=\text{N}-$ functional group occurs in one single irreversible reduction step (Scheme 2). 4-e^- and 4-H^+ are consumed and exchanged in this latter electrochemical reduction process.



Scheme 2

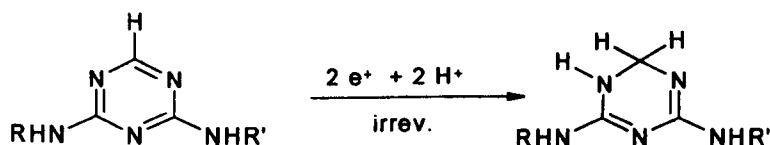
7.3.2 Fluorotriazine group

The electrochemical reduction process of halo-triazine anchoring group has gained considerable attention and has been studied frequently^{3,4,7,15-17}. Based on the previously reported studies on the chlorotriazine group, the mechanism of the electrochemical reduction of the fluorotriazine group proceeds in a similar way to that proposed for chlorotriazine reactive group. The following mechanism can be suggested for the electrochemical elimination of fluorine atoms. At low pH values, a two electron irreversible reduction of one double-bond of the triazine ring is taking place, resulting in formation of an energetically unstable intermediate form which is stabilised by the release of a HF molecule. The coulometric studies confirm that this irreversible process was involved in the consumption of two-electron and two-proton per molecule¹⁷. The mechanism of fluorotriazine reduction process is briefly represented in Scheme 3.



Scheme 3

However, at high pH values this first stage can be reduced further by immediate two-electron and two-proton reduction of a C=N bond in the triazine ring (see Scheme 4). This reduction process yields one rather drawn-out wave, which becomes confirmed by the observation of a second voltammetric wave that is not well separated and partly overlapped with the first fluorotriazine wave.



Scheme 4

7.4 The AdSV Behaviour of the Studied Azo-Based Reactive Dyes

Preliminary studies for these fluorotriazine-based azo reactive dyes indicate that they were adsorbed effectively onto the HMDE and they can be monitored by AdSV after scanning from 0.0 V in the negative direction. All the four synthesised reactive dyes gave two stripping voltammetric reduction waves, which could be used in the electroanalytical determinations. When applying the HMDE as a working electrode all these fluorotriazine reactive dyes in 0.02 mol l^{-1} Britton-Robinson buffer (pH 8) exhibited a reproducible well-defined first wave, which is thought to have resulted from the cathodic reduction of the azo group. The peak potential for the azo electrochemical signal for these azo reactive dyes in pH 8 B-R buffer, differs significantly owing to the variation in the chemical structure of the studied azo reactive dyes. The peak potentials of azo group usually lie between -0.49 and -0.70 V (vs. Ag/AgCl reference electrode). The tested fluorotriazine reactive dyes also exhibited a further small, broad and ill-developed peak at more negative potential (e.g.

-1.1V), which probably corresponds to the reduction of the fluorotriazine reactive group. A representative adsorptive stripping voltammogram obtained for 5×10^{-7} mol l⁻¹ fluorotriazine-based azo reactive dye 1 at pH 8 in Britton-Robinson buffer is shown in Fig. 7.1. The cathodic step attributed to the reduction of the azo group is observed at -0.68 V ($i_p = 16.6$ nA), whereas, the cathodic reduction of the fluorotriazine reactive group is obtained at -1.07 V ($i_p = 2.1$ nA). However, fluorotriazine reactive dye 2 yielded a further electroanalytical signal at -0.95 V ($i_p=1.74$ nA), which is believed to be due to the reductive elimination of the active chlorine atom on the aromatic ring (see Fig. 7.2).

In addition, the irreversibility of azo group reduction process was confirmed by cyclic voltammetric measurements at a scan rate of 50 mV s^{-1} of a fluorotriazine-based azo reactive dye solutions in B-R buffer (pH 8). No anodic peak was observed on any of the measured cyclic voltammograms. These results are in good agreement with observations obtained for other azo compounds. Similarly, these cyclic voltammograms show only the cathodic peak associated with the fluorotriazine reduction process. No reoxidation peak corresponding to this reduction process was observed when the reverse sweep was applied.

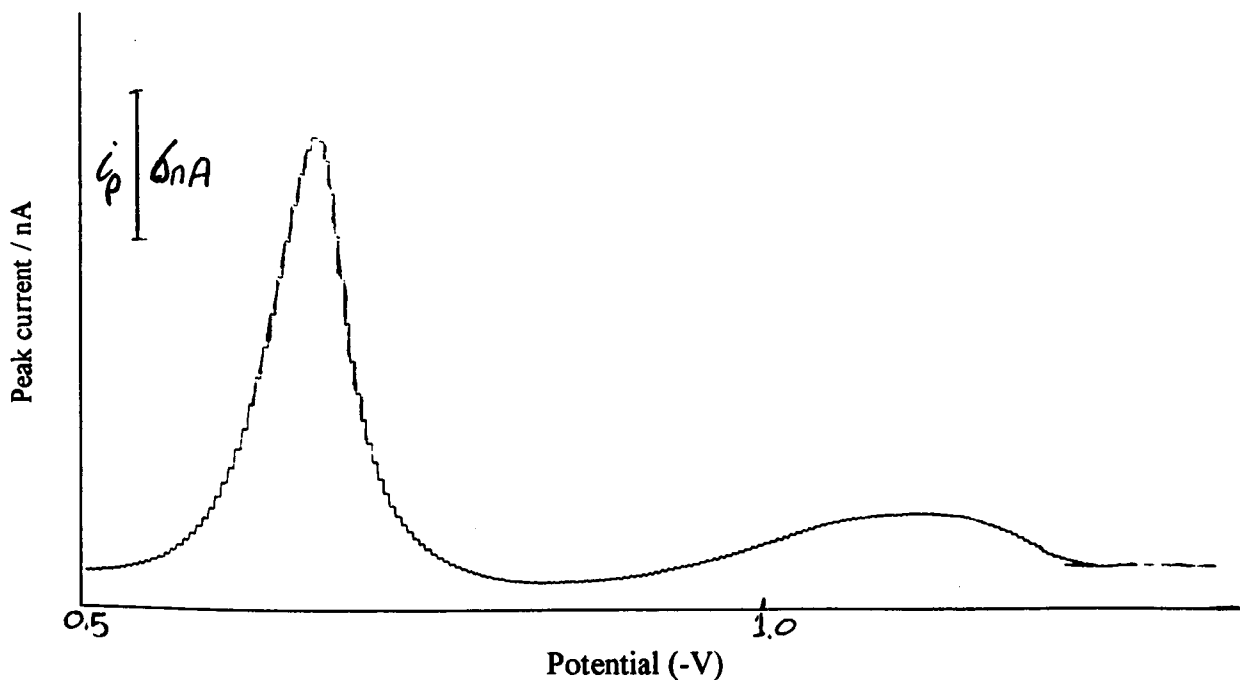


Figure 7.1: Typical AdSV voltammogram obtained for 5×10^{-7} M fluorotriazine-based azo reactive dye 1 following a 2 min accumulation time at 0.0 V in pH 8 Britton-Robinson buffer. Scan rate 5 mV s^{-1}

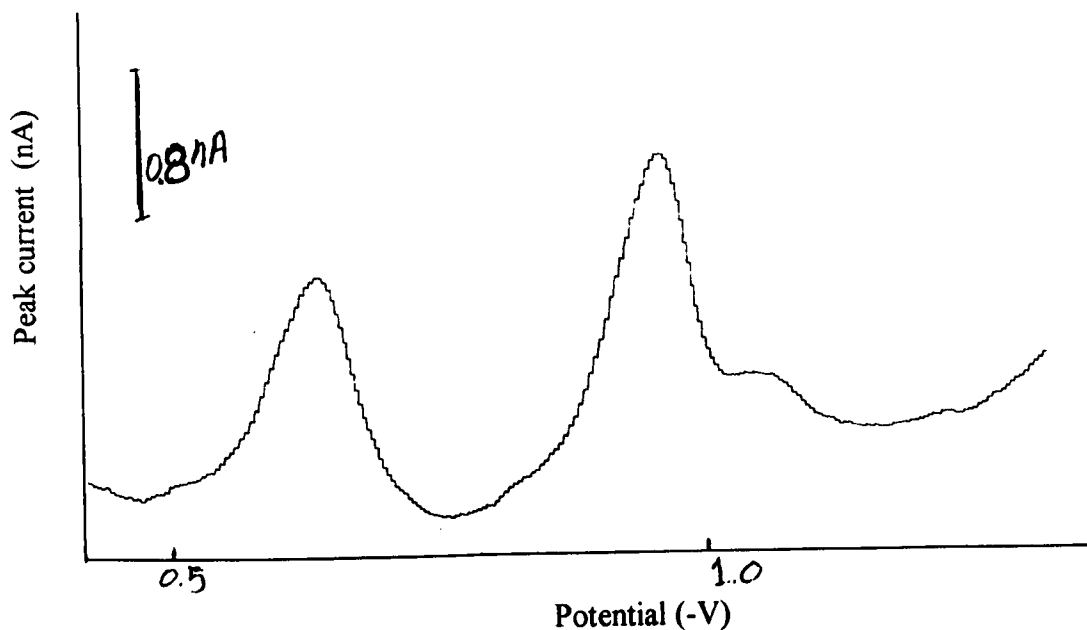


Figure 7.2: Adsorptive stripping voltammogram for 1×10^{-7} M fluorotriazine-based azo dye 2 in Britton-Robinson solution (pH 8). Accumulation time: 2 min, accumulation potential: 0.0 V and scan rate: 5 mV s^{-1} .

7.5 Parameters Affecting the Adsorptive Stripping Response

7.5.1 Effect of pH

The adsorbed molecules of fluorotriazine-based azo reactive dyes exhibited two AdSV peaks, which are mainly pH dependent. It is found that, generally in acidic media, the height of the first peak (azo group) decreased while that of the second peak (fluorotriazine) slightly increased with increasing pH. However, at high pH values the height of the first peak increased while that of the second peak decreased and almost disappeared at $\text{pH} > 11$. Meanwhile, the peak potential (E_p) of the azo wave showed a shift towards negative potentials with increasing pH as illustrated in Fig. 7.3. This revealed that proton ions were consumed in the reduction process and indicating prior protonation in the region of the azo group, leading to a decrease in the electron density on the electroactive functional group, hence, facilitating the electron transfer during the voltammetric reduction. As a result, the tested compound is more readily reducible in

acid medium^{7,18}. The E_p -pH plots of this reduction wave for the analysed azo reactive dyes 1, 2 and 3 were found to consist of two straight line segments with slopes of 86-107 mV/pH at low pH values (pH 2-8) and 38 mV/pH at higher pH values (pH >8). The breaks occurred on the E_p versus pH plots at pH 8 are probably indicate a different number of protons participating in the reduction process in acidic and alkaline regions⁶. However, fluorotriazine dye 4 shows only one single straight line with a slope of 62 mV/pH over the studied pH range. Unlike the rest of the tested fluorotriazine reactive dyes in this study, the molecular structure of fluorotriazine reactive dye 4 has no *o*-hydroxy electron-donating group. In view of the electrode reduction mechanism proposed in section 7.2.1, the voltammetric reduction process of azo group of azo reactive dye 4 in alkaline media will possibly only proceed to the hydrazo derivative form. The cleavage of the -N=N- bond and the formation of the corresponding amines only occurs for azo compounds that have an electron-releasing group such as the *o*-hydroxy group.

The influence of the solution pH value on the peak current of the azo group was examined and is summarised in Table 7.1. In general, for the studied azo reactive dyes 1,2 and 3, the peak current decreased with increasing of pH values in the acidic range. However, the azo peak current reached its maximum value at higher pH values. The peak current of azo reactive dye 4 fluctuated considerably due the pH variation, it increased dramatically over the pH range 2-4 and decreased thereafter and eventually reached its excessive maximum value ($i_p = 36.6$ nA) at pH 12. On the other hand, when measuring the peak current of the fluorotriazine reactive system as a function of pH value, a successive decreasing in the peak height was observed at high pH values. This electrochemical behaviour can be attributed either to the hydrolysis reaction of the triazine reactive group, or to the fact that only the protonated form of triazine molecules is reduced in the useful potential range^{4,17}.

For analytical purposes, the optimum pH value for the determination of these fluorotriazine-based azo reactive dyes seems to lie in the 8-10 pH range. Although the second electrochemical wave associated with the fluorotriazine reactive group can also be used for the analytical determination of the tested reactive dyes to some degree, only the azo group reduction process, which yielded a well-developed and defined sharp peak, was selected for further investigations for obtaining the optimum experimental conditions for the analysis of these dyes of interest. Moreover, the second cathodic wave was difficult to evaluate because it was close to the potential of

decomposition of the supporting electrolyte, in addition to being an ill-developed and broad small AdSV peak. Table 7.1 summarises the AdSV behaviour of the four fluorotriazine dyes at pH 2-12.

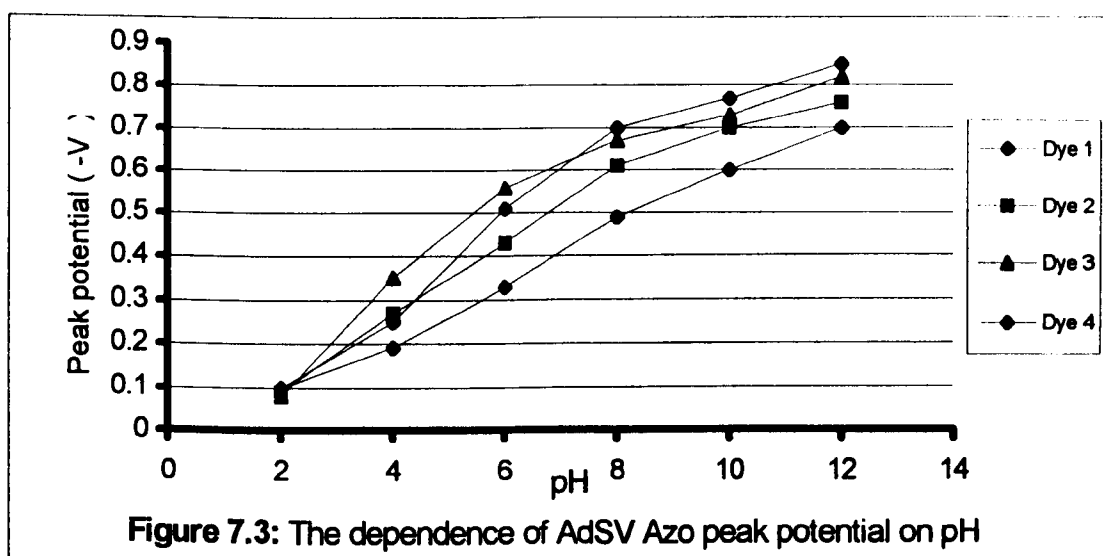


Table 7.1: Effect of pH on the AdSV behaviour of azo group of the studied fluorotriazine reactive dyes.

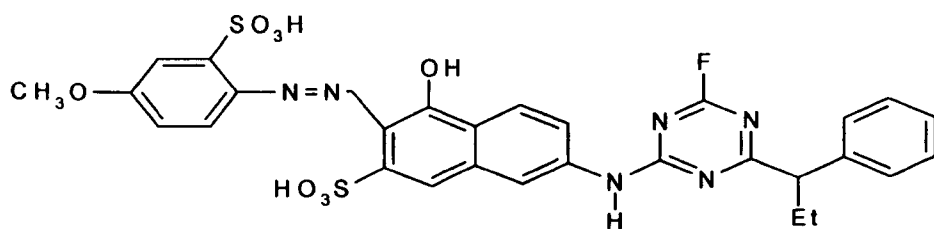
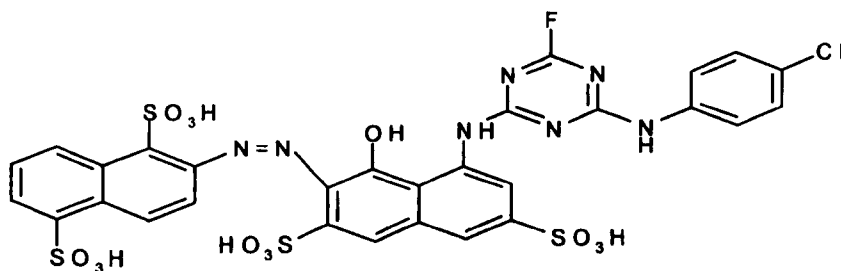
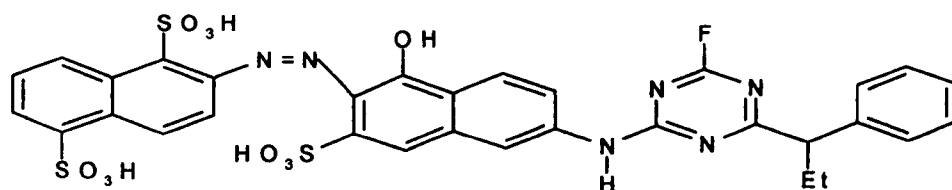
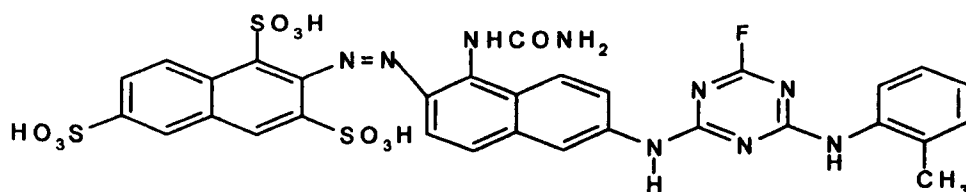
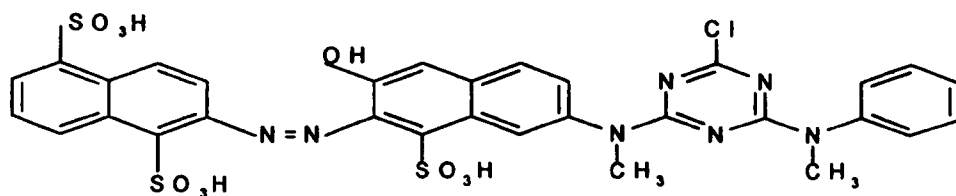
pH	Dye 1		Dye 2		Dye 3		Dye 4	
	E _p (-V)	i _p (nA)	E _p (-V)	i _p (nA)	E _p (-V)	i _p (nA)	E _p (-V)	i _p (nA)
pH 2	0.1	7	0.09	6	0.08	7.6	0.1	2.8
pH 4	0.19	8.8	0.27	5.8	0.35	2.6	0.19	27.6
pH 6	0.53	1.8	0.43	7	0.56	5.2	0.3	19.6
pH 8	0.7	16.6	0.61	7.4	0.67	17.7	0.49	10
pH 10	0.77	19.6	0.7	12.6	0.73	12.4	0.6	9.6
pH 12	0.85	13.3	0.76	15.2	0.82	17.2	0.7	36.6

7.5.2 Effect of dye molecular structure

The half wave potentials and peak currents of the azo group of the tested reactive dyes revealed dissimilarity between these reactive dyes. At pH 8 the peak potentials decreased in the following order: dye 1, dye 3 < dye 2 < dye 4. This variation of peak potential with different substituents near to the azo group indicates that the electrochemical environment around the electroactive centre of the molecules is dissimilar, thus, each azo reactive dye behaves voltammetrically in a different manner to the other azo reactive dyes.

The structure of fluorotriazine-based azo reactive dye 1 reveals that the aromatic ring on the dye molecule has an electron-releasing methoxy group substituent on the meta position to the azo functional group (see Fig. 7.4). This electron-donating group increases the electron density on the azo group. The resultant increasing of electron density make the reduction of azo functional group more difficult to achieve, therefore, the stripping voltammetric peak potential for fluorotriazine-based azo reactive dye 1 occurs at more negative potential value (-0.7 V). Whereas, for the fluorotriazine-based azo reactive dye 4 the replacement of the hydroxy group on the aromatic ring by the less electron-donating NHCONH₂ group leads to a less increase of the electron density on the nearby azo functional group on the ortho position. The substitution of this less electron-releasing group facilitates the reduction process of the azo group by improve the electron transfer and acceptance, hence, the electrochemical cathodic peak occurs at a less negative potential (-0.49 V). However, the molecular structure of fluorotriazine-based azo reactive dye 2 has a electron-donating group -OH which have a moderate electron releasing property between the methoxy and NHCONH₂ groups. Hence, leading to an intermediate electrochemical environment around the azo group compared to azo reactive dye 1 and dye 4. As a result, an intermediate peak potential value of -0.6 V for the reduction of the azo group of dye 2 was observed.

In addition, a comparison between the stripping voltammetric behaviour of the fluorotriazine-based azo reactive dye 2 and the recently studied chlorotriazine-based azo reactive dye⁷ was carried out. Both halo-triazine based reactive azo dyes have nearly similar molecular structure. The azo peak potential of the chlorotriazine-based azo reactive dye measured by differential pulse voltammetry at the hanging mercury drop electrode (HMDE) in pH 8 B-R buffer was -0.62 V which is very similar to

*Dye 1**Dye 2**Dye 3**Dye 4***I) Fluorotriazine-based azo dyes****II) Chlorotriazine-based azo dye.****Figure 7.4:** Molecular structures of the analysed reactive dyes

the peak potential value obtained for the fluorotriazine-based azo reactive dye 2 measured at the same experimental conditions ($E_p = -0.61$ V).

Finally, the reduction of the fluorotriazine functional group for all four analysed fluorotriazine-based azo reactive dyes occurred in the region of -1.1 V. As can be seen from the molecular structures shown in Fig. 7.4 for the studied fluorotriazine reactive dyes, the electrochemical environments around the reactive triazine groups is approximately similar and the different substituent on the azo functional groups are too far and remote from this reactive group to generate any noticeable influence on its AdSV reduction process. In contrast, the reduction of the chlorotriazine reactive group occurred at a more negative potential (e.g. $E_p = -1.2$ V) which indicates that the elimination of chlorine atom from the triazine ring is more difficult than that of the fluorine atom.

7.5.3 Effect of accumulation time

The dependence of the AdSV voltammogram of the reactive dyes under investigation on the accumulation time (T_{acc}) was followed at 5×10^{-7} mol l⁻¹ fluorotriazine-based azo reactive dyes at pH 8 Britton-Robinson buffer. The accumulated amount on the electrode surface depends on the length of time over which the adsorption is allowed to proceed. Figure 7.5 shows the influence of this parameter on the peak current of the azo group. For most of the tested fluorotriazine reactive dyes, a proportional relationship is observed up to 3 minutes at this concentration. However, above this time the peak current remained nearly constant due to the saturation of the HMDE by the adsorbate. The potential of the first cathodic reduction peak remained constant in all these experiments. The accumulation time of 2 minutes is found to be adequate for all subsequent work. Figure 7.6 shows the AdSV behaviour of the representative analysed fluorotriazine-based azo reactive dye 3 under various preconcentration times.

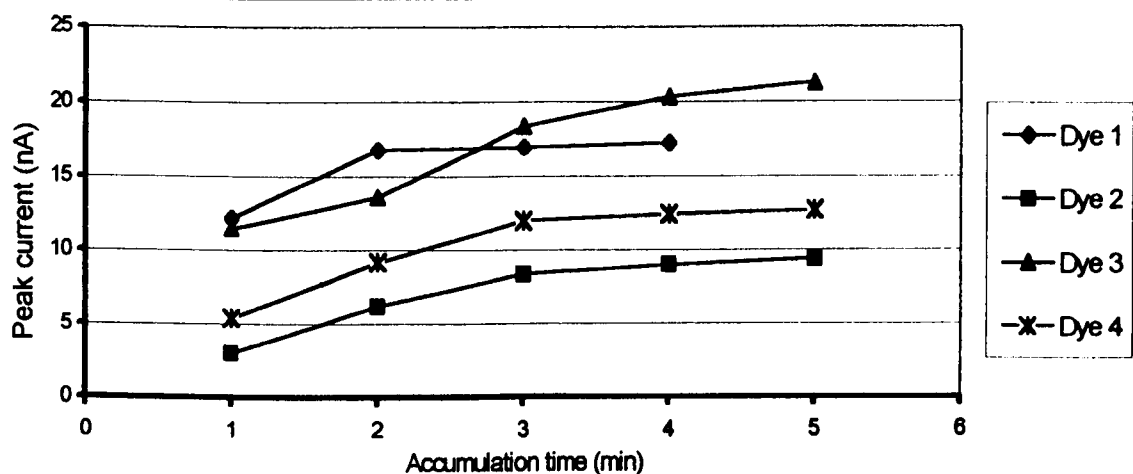


Figure 7.5: Effect of variation accumulation time on Azo group peak current

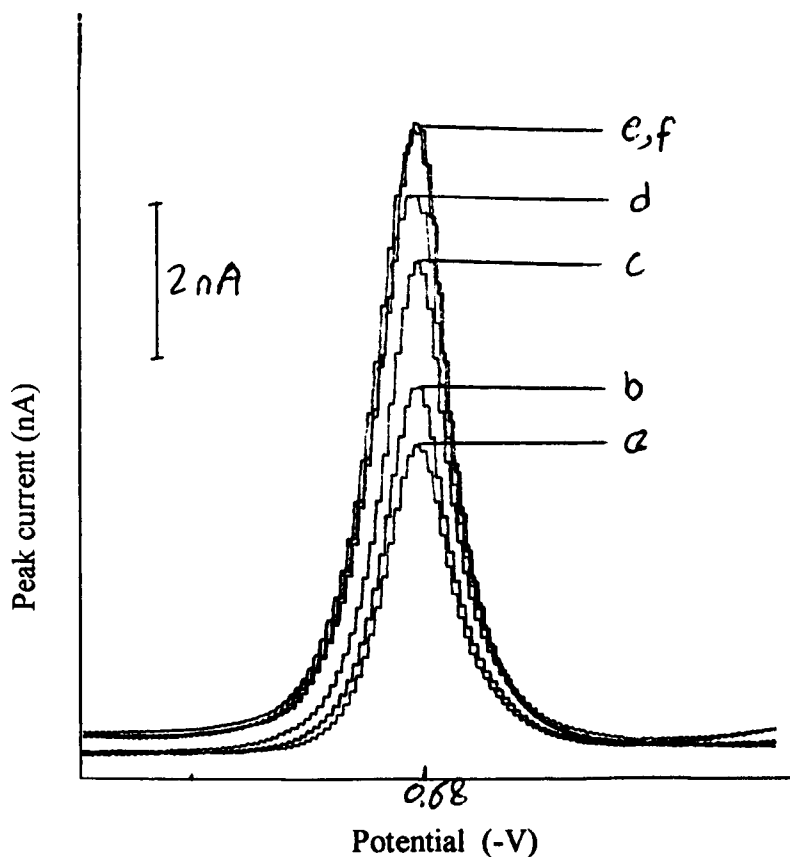


Figure 7.6: The influence of accumulation time on the peak height of azo group of the representative fluorotriazine-based azo reactive dye 3 (5×10^{-7} M). Accumulation potential: 0.0 V, Scan rate: 5 mV s^{-1} . Accumulation time: a, 1; b, 2; c, 3; d, 4; e, 5; f, 6 min.

7.5.4 Effect of accumulation potential

The influence of the accumulation potential (E_{acc}) on the peak current of the azo group over the potential range from -0.2 V to +0.2 V and after 2 minutes preconcentration period in pH 8 Britton-Robinson buffer solution was evaluated. As can be observed from Table 7.2, the effect of accumulation potential on the azo group stripping voltammetric current was negligible. The optimum accumulation potential was chosen to be 0.0 V, this value was therefore used for all forthcoming analytical measurements.

Table 7.2:Effect of accumulation potential on Azo group peak current.

DYE	ACCUMULATION POTENTIAL				
	- 0.2 V	- 0.1 V	0.0 V	+ 0.1 V	+0.2 V
Dye 1	18.7 nA	18.8 nA	18.4 nA	18.8 nA	19 nA
Dye 2	7.5 nA	7.4 nA	7.4 nA	7.6 nA	7.7 nA
Dye 3	18 nA	17.4 nA	17.7 nA	17.7 nA	17.8 nA
Dye 4	10 nA	9.8 nA	9.8 nA	10.1 nA	10.1 nA

7.5.5 Effect of supporting electrolyte constituent

The choice of a suitable medium is important for the determination of these reactive dyes. In general, AdSV voltammograms of 5×10^{-7} mol l⁻¹ for all the fluorotriazine-based azo reactive dyes in acetate buffer (pH 5) and carbonate buffer (pH 10) showed very similar electrochemical behaviour related to the voltammetric reduction of the azo functional group in Britton-Robinson buffer at the corresponding pH values. On the other hand, the reduction process of the second cathodic wave attributed to the fluorotriazine reactive group indicates a significant influence of buffer composition on the AdSV characteristic of fluorotriazine dyes. The reduction process of the fluorotriazine group was not observable in acetate buffer. Meanwhile, the stripping voltammetric behaviour of this group was identical in both Britton-Robinson buffer and carbonate buffer. Table 7.3 summarises the AdSV properties of the four fluorotriazine-based azo reactive dyes in different supporting electrolytes.

Table 7.3: Effect of supporting electrolyte constituent on fluorotriazine-based azo reactive dyes AdSV behaviour.

DYE	Buffer	Azo peak		Fluorotriazine peak	
		E_p (-V)	i_p (nA)	E_p (-V)	i_p (nA)
Dye 1	B-R Buffer	0.68	3.9	1.06	2.4
	Acetate	0.26	4.2	-	-
	Carbonate	0.77	4.0	1.05	0.55
Dye 3	B-R Buffer	0.67	3.2	1.06	1.96
	Acetate	0.40	2.8	-	-
	Carbonate	0.75	4.9	1.04	0.50
Dye 4	B-R Buffer	0.47	1.7	1.07	2.7
	Acetate	0.26	4.1	-	-
	Carbonate	0.60	6.8	0.84	0.40

7.3-A

DYE	Buffer	Azo peak		Chloro peak		Fluorotriazine peak	
		E_p (-V)	i_p (nA)	E_p (-V)	i_p (nA)	E_p (-V)	i_p (nA)
Dye 2	B-R	0.61	1.24	0.95	1.74	1.10	0.42
	Acetate	0.32	6.20	-	-	-	-
	Carbonate	0.72	4.50	0.94	1.20	1.20	0.20

7.3-B

7.5.6 Effect of reactive dye concentrations

The effect of fluorotriazine reactive dye concentrations on the current of the main azo reduction process was investigated. Analysis of the azo wave was carried out over the dye concentration range $1 \times 10^{-7} \text{ mol l}^{-1} - 9 \times 10^{-7} \text{ mol l}^{-1}$. The variation in peak height with the continuous addition of the tested fluorotriazine-based azo reactive dye is shown in Fig. 7.7 for the representative fluorotriazine reactive dye 3. In general, the linear correlation was obtained only in the range of $1 \times 10^{-7} - 5 \times 10^{-7} \text{ mol l}^{-1}$ dyes. At reactive dye concentrations higher than $5 \times 10^{-7} \text{ mol l}^{-1}$ the peak current starts to level off (see Fig. 7.8) owing to the saturation of the surface of the working electrode. Consequently, determination of such high concentration is possible only by using the calibration plot method after previous dilution of the sample solution. A $1 \times 10^{-7} \text{ mol l}^{-1}$ fluorotriazine-based azo reactive dye concentration was selected as optimum for all further investigations.

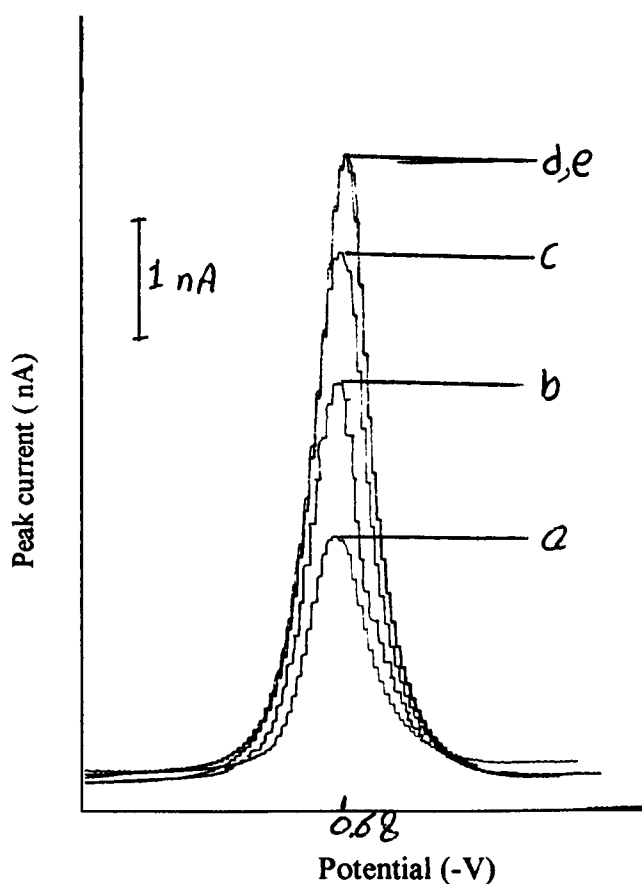
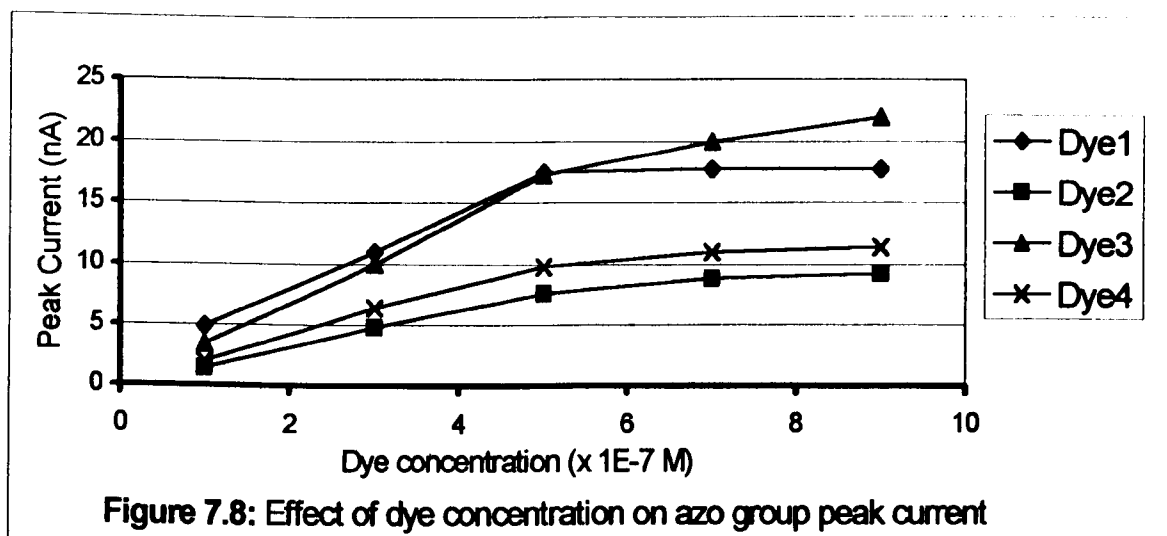


Figure 7.7: The dependence of peak height on the fluorotriazine-based azo reactive dye 3 concentration. $T_{\text{acc}} = 2 \text{ min}$, $E_{\text{acc}} = 0.0 \text{ V}$, Scan rate = 5 mV s^{-1} . Reactive dye concentration: a, 1×10^{-7} ; b, 3×10^{-7} ; c, 5×10^{-7} ; d, 7×10^{-7} ; e, $9 \times 10^{-7} \text{ M}$.



7.6 Analytical Application

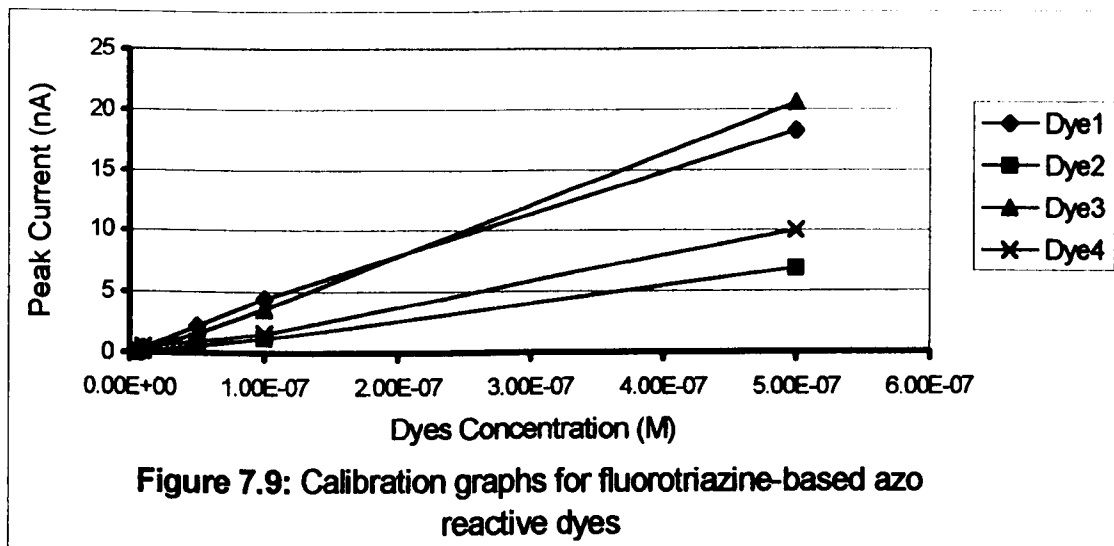
Based on the results obtained from the previous sections, the following optimal conditions for the determination of the fluorotriazine-based azo reactive dyes are recommended for optimal work: medium, pH 8 Britton-Robinson buffer; accumulation potential, 0.0 V; accumulation time 2 minutes and dye concentration, $1 \times 10^{-7} \text{ mol l}^{-1}$.

7.6.1 Calibration graph

Under the optimum conditions a very good linear correlation was obtained between the azo functional group peak current and fluorotriazine-based azo reactive dye concentrations in the range of 5×10^{-9} - $5 \times 10^{-7} \text{ mol l}^{-1}$. Figure 7.9 shows the calibration plots obtained when successive additions of the individual standard dye solution were added to the Britton-Robinson buffer solution. The least-square treatment of the calibration graph of the representative fluorotriazine-based azo reactive dye 1 yields a slope of 0.036 A mol^{-1} , an intercept of 0.25 nA and a

correlation coefficient of 0.999. Thus, the regression equation of the calibration line has the form:

$$i_p (\text{A}) = 0.25 \times 10^{-9} + 0.036 C (\text{mol l}^{-1}) \quad r = 0.999 \quad n = 6$$



7.6.2 Detection limits

The lowest concentration of fluorotriazine-based azo reactive dyes 1, 2, 3, and 4 detected is 3.5×10^{-9} , 4.6×10^{-9} , 3.7×10^{-9} and 4.9×10^{-9} mol l⁻¹, respectively at an accumulation time of 2 minutes. These detection limits were estimated based on the signal-to-noise characteristic (S/N=3) of the response of 1×10^{-7} mol l⁻¹ reactive dye. The sensitivity of the method (calculated from the slope of the linear regression) with the characteristics of the calibration straight-line (slope and intercept), correlation coefficient, detection limit and relative standard deviation (%RSD) for each fluorotriazine-based azo reactive dye are given in Table 7.4.

7.6.3 Reproducibility and stability

The high sensitivity of adsorptive voltammetry is accompanied by good reproducibility. The reproducibility of the AdSV technique for the determination of the fluorotriazine azo reactive dyes was evaluated from 8 repeated measurements of the AdSV azo peak height of 1×10^{-7} mol l⁻¹ solutions of the four reactive dyes of

interest. Very low relative standard deviation values of 1.2%, 1.5%, 1.2% and 1.6%, respectively, were found. The stability of 1×10^{-7} mol Γ^{-1} fluorotriazine-based azo reactive dyes solutions was tested; it seemed to be stable for a period of two hours at least.

Table 7.4: Parameters of calibration curves for AdSV determination of fluorotriazine-based azo reactive dyes.

	Concentration Range (mol Γ^{-1})	Slope (A mol $^{-1}$)	Intercept (nA)	Correlation Coefficient	Detection Limits (mol Γ^{-1})	Sensitivity (A/mol Γ^{-1})	%RSD
Dye 1	5×10^{-9} - 1×10^{-6}	0.036	0.25	0.999	3.5×10^{-9}	0.036	1.17
Dye 2	5×10^{-9} - 1×10^{-6}	0.014	-0.08	0.999	4.6×10^{-9}	0.014	1.53
Dye 3	5×10^{-9} - 1×10^{-6}	0.042	-0.32	0.999	3.7×10^{-9}	0.042	1.23
Dye 4	5×10^{-9} - 1×10^{-6}	0.020	0.01	0.998	4.9×10^{-9}	0.020	1.64

7.7 Hydrolysis Studies

The alkaline hydrolysis of the reactive fluorotriazine group of the studied reactive dyes was investigated using adsorptive stripping voltammetry. The preliminary studies on the hydrolysis reaction of fluorotriazine reactive dyes was carried out in both carbonate buffer (pH 10) and 0.1 mol Γ^{-1} NaOH solution heated for more than one hour at 80°C. The effect of the hydrolysis process on the similar substituted-triazine reactive groups, namely chlorotriazine group has been recently reported^{7,19,20}. For instance, the determination of the hydrolysed chlorotriazine-based azo reactive dye⁷ was monitored by observing the loss of the peak corresponding to the reactive group. In fact, the chlorotriazine peak height decreased continually with the length of the heating time and the peak was completely eliminated after only 60 minutes of heating. This is evidence that the triazinyl reactive functional group is substituted by a hydroxyl group due to the hydrolysis reaction and the resulting derivative is electroinactive in the potential range studied.

Since the reactivity of the substituted triazine functional group is increased in the order $F > Cl$ substituents, it was theoretically expected that the fluorotriazine reactive group would be hydrolysed more readily than the chlorotriazine reactive group. However, when comparing the AdSV voltammogram of the hydrolysed dyes with the AdSV voltammogram of the original reactive dyes, only slight changes in the peak current or peak potential of the fluorotriazine reactive group were observed in going from the initial dyes to the attempted hydrolysed form. However, when applying a longer heating time (e.g. 5 hours), the appearance of the formed fluorotriazine wave was easily observed. Under these mentioned hard hydrolysis conditions, a decrease was observed in the peak height of fluorotriazine-based azo reactive dyes 1, 2, 3, and 4 cathodic wave by only 33%, 22%, 20% and 18%, respectively, from the original recognised peak heights. Moreover, the replacement of the active fluorine atom on the triazine ring by other alkoxide groups such as methanol was attempted. Unlike the methanolysis process of the chlorotriazine group which occurred at room temperature and in the presence of low methanol concentration (ca. 1.2% v/v), the attempted methanolysis process of the fluorotriazine reactive group led to virtually no impact on the fluorotriazine reactive peak. However, increasing the methanol concentration to 5% v/v level and heating the buffer solution for 3 hours yields a decline in the reactive group peak height of fluorotriazine-based azo reactive dye 1, 2, 3 and 4 by 39%, 37%, 4% and 20% of the initial peak heights, respectively.

However, despite the various experimental investigations and attempts to identify and hence illuminate the reason for such very slow hydrolysis reaction for these fluorotriazine-based azo reactive dyes, the cause of this odd and theoretically unexpected electrochemical behaviour of the hydrolysed fluorotriazine reactive group is not fully understood at this stage. Nevertheless, a possible explanation for why the hydrolysis of the fluorotriazine group yields little change on the peak current is on the assumption that the original fluorotriazine reactive dye samples themselves are changed and already hydrolysed, or alternatively, the hydrolysis rate of the fluorotriazine reactive group is very fast, hence the diminishing of the electroanalytical signal associated to the reduction of the fluorotriazine reactive group occurred instantly at room temperature after the addition of the reactive dyes to the buffer solution. Therefore, the observed stripping voltammetric peak at potential -1.07 V should not be attributed to the elimination of the fluorine atom from the triazine ring but rather due to the further reduction process of one double bond $C=N$ in

the triazine ring (refer to section 7.3.2). In fact, it should be recalled that the investigated AdSV behaviour of fluorotriazine reactive system in this study only yielded a broad and ill-developed electrochemical peak compared with the well-defined AdSV peak obtained for chlorotriazine reactive dyes, hence, the attempted hydrolysis reaction may not affect its peak current considerably. However, other analytical approaches such as UV spectroscopy were briefly used to monitor the progress of the hydrolysis process. Nonetheless, the preliminary studies and comparisons between the original and hydrolysed fluorotriazine reactive dyes UV spectra were not promising i.e. no significant variations were observed between the UV spectra of the original reactive and that for the attempted hydrolysed form.

7.8 Simultaneous Analysis of Fluorotriazine Dyes in Mixtures

To study the applicability of the proposed procedure for performing simultaneous determination, sample solutions containing all the four tested fluorotriazine-based azo reactive dyes were analysed. Figure 7.10 displays an adsorptive stripping voltammogram of fluorotriazine-based azo reactive dyes 1, 2, 3, and 4 mixture measured after 2 minutes pre-concentration period at 0.0 V in pH 8 Britton-Robinson buffer. The separation in the peak potential between the cathodic wave due to the reduction of azo group of fluorotriazine dye 4 at $E_p = -0.48$ V and cathodic wave due to the reduction of azo group of fluorotriazine dye 1 at $E_p = -0.68$ V, is virtually enough to allow efficient simultaneous determination of these two reactive dyes. However, fluorotriazine dye 2 can be easily monitored in a mixture from its unique electrochemical signal at -0.93 V corresponding to the reductive elimination of chlorine atom on the aromatic ring. On the other hand, no significant variations in the voltammograms of fluorotriazine dye 1 and dye 3 were observed in this supporting electrolyte solution i.e. both analysed dyes act as a single dye, thus, they can be accounted as one single reactive dye.

However, discrimination between fluorotriazine dye 1 and dye 3 can be achieved when using acetate buffer as supporting electrolyte. The separation in the peak potentials in this case can be as much as 150 mV. It can be concluded that it is possible to carry out multi-compounds analysis by the AdSV method for the fluorotriazine-based azo reactive dyes 2, 4 and dye 1 or dye 3.

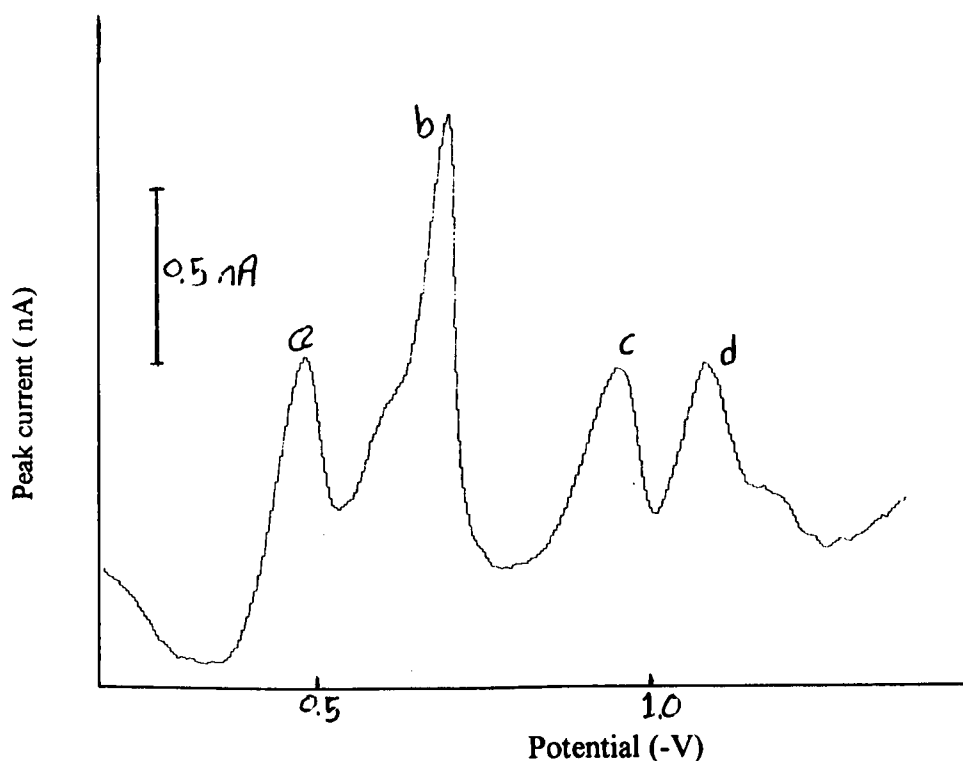


Figure 7.10: Simultaneous analysis of a mixture of 1×10^{-7} M fluorotriazine-based azo reactive dyes in B-R buffer: a, azo peak (dye 4); b, azo peak (dye 1); c, chloro peak (dye 2); d, fluorotriazine peak. $T_{\text{acc}}=2$ min, $E_{\text{acc}}=0.0$ V and scan rate= 5 mV s^{-1} .

A proper choice of the experimental conditions is required to assure that the simultaneous determination of each individual dye in a mixture is not badly affected by the presence of the other co-existing reactive dyes. For the sake of simplicity, only fluorotriazine reactive dye 1 and dye 4, which have a good peak potential separation ($\Delta E_p = 0.2$ V) of azo reduction wave, were studied. The AdSV azo peak currents of fluorotriazine dye 1 and dye 4 was measured as a function of the pH in Britton-Robinson buffer solutions. The results were demonstrated as the effect of pH values in the range of 2-12 on the peak potential separation ΔE_p . As can be seen from Table 7.5, the best peak separation was observed at pH 6 ($\Delta E_p = 0.26$ V). Nevertheless, at this pH value the azo group cathodic wave for reactive dye 1 was poorly developed. Hence, the selection of pH 8 as optimum value is once again more adequate. However, it was observed that at pH 4 the peak height of both fluorotriazine dye 1 and dye 4 were nearly equal for identical concentrations.

Table 7.5: Effect of pH on azo peak potential separation.

pH	pH 2	pH 4	pH 6	pH 8	pH 10	pH 12
Peak Potential Separation (V)	0.06	0.1	0.24	0.22	0.17	0.16

For significant analytical utility the developed procedure must exhibit simultaneous concentration dependence for the both analytes²¹. The concentration dependence of fluorotriazine dye 1 between 1×10^{-7} and 9×10^{-7} mol l⁻¹ in the presence of 1×10^{-7} mol l⁻¹ fluorotriazine dye 4 was evaluated. Linearity was obtained in the range 1×10^{-7} - 5×10^{-7} mol l⁻¹ and the least-squares analysis of the data yields slope of 0.028 A mol⁻¹ l, intercept of 3.6 nA and correlation coefficient of 0.96. In comparison, the electroanalytical signal relating to the azo group of fluorotriazine dye 4 decreased to approximately 10% of its original peak height due to the competition on the adsorption sites on the working electrode surface (HMDE). Similar experiments were carried out for fluorotriazine dye 4 over the concentration range 1×10^{-7} and 9×10^{-7} mol l⁻¹ in the presence of 1×10^{-7} mol l⁻¹ fluorotriazine dye 1. The calibration graph for fluorotriazine dye 4 was linear up to 5×10^{-7} mol l⁻¹ with a slope of 0.016 A mol⁻¹ l, intercept of 1.4 nA and correlation coefficient of 0.98. Unlike the peak height of fluorotriazine dye 4, which was considerably suppressed in the presence of a high quantity of fluorotriazine dye 1, it was observed that it is possible to monitor fluorotriazine dye 1 in the presence of up to 10 times as much fluorotriazine dye 4 as illustrated in Fig. 7.11. As anticipated, the influence of accumulation potential on the stripping voltammetric response of fluorotriazine dye 1 and dye 4 was negligible in agreement with the effect of this parameter on the electrochemical response of individual reactive dyes. However, the dependence of accumulation time on the azo group peak height of fluorotriazine dye 1 and dye 4 is shown in Fig. 7.12. Both peak heights increase linearly with increasing pre-concentration period. Thus, simultaneous measurements following short accumulation time (e.g. 2 min) will be convenient to avoid the saturation of the HMDE. Finally, similar results were observed when measuring the azo peak currents of both fluorotriazine reactive dyes as a function of varying the concentration of both reactive dye 1 and dye 4.

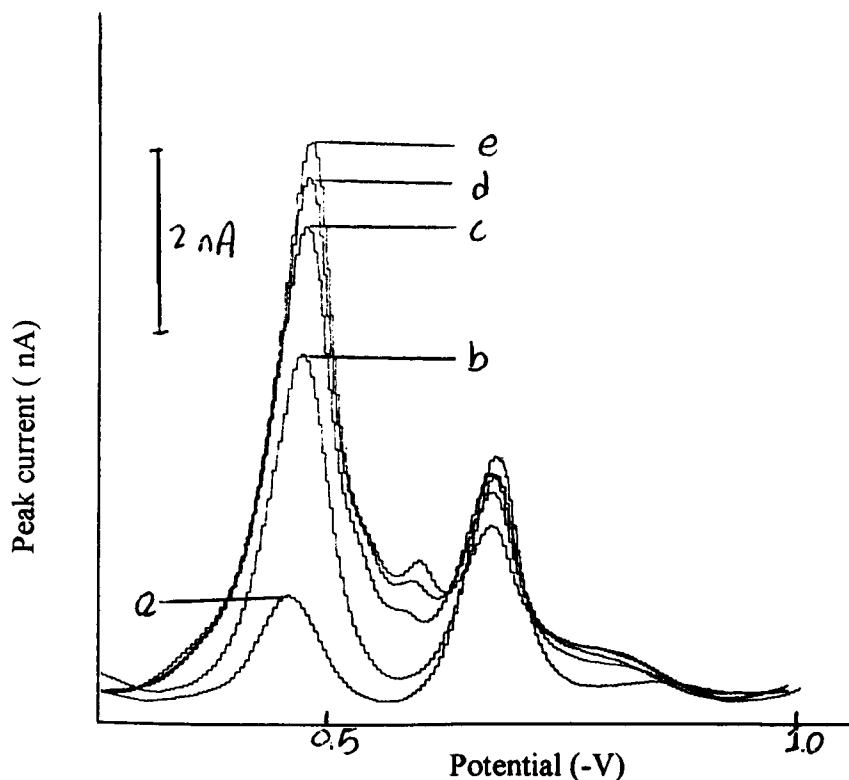


Figure 7.11: The dependence of the AdSV azo peak height on the concentration of fluorotriazine dye 4. Reactive dye 4 concentration: a, 1×10^{-7} ; b, 3×10^{-7} ; c, 5×10^{-7} ; d, 7×10^{-7} ; e, 9×10^{-7} M. T_{acc} : 2 min, E_{acc} : 0.0 V, scan rate: 5 mV s^{-1} and fluorotriazine dye 1 concentration: 1×10^{-7} M.

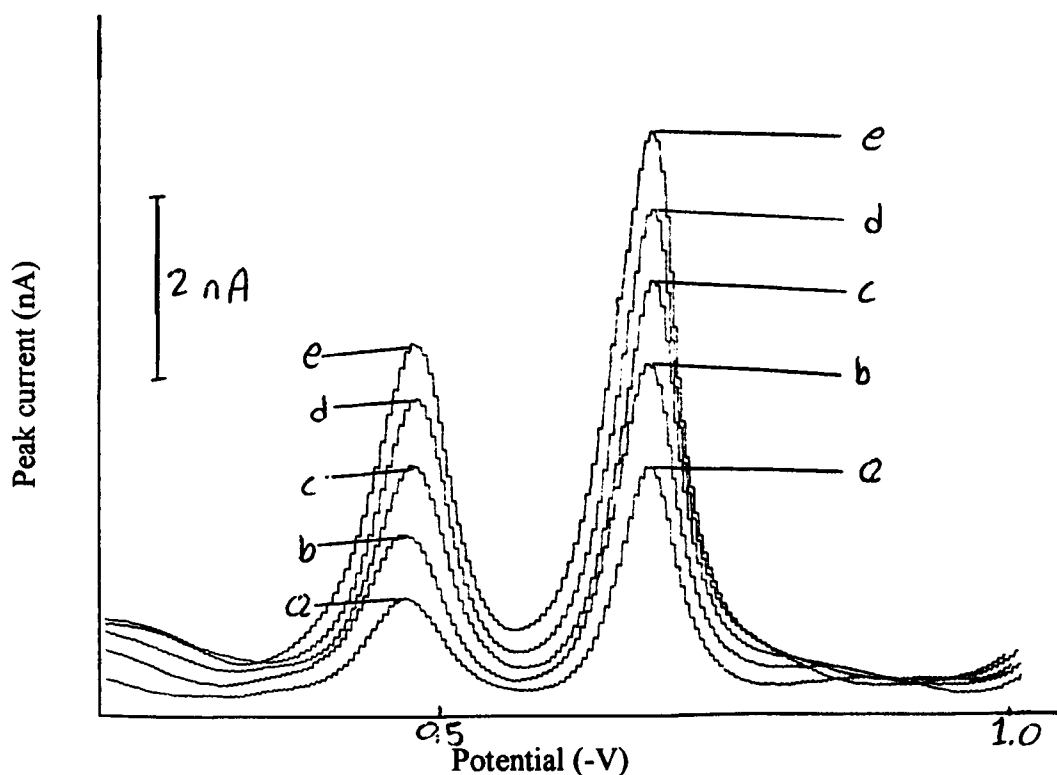


Figure 7.12: Effect of variation of accumulation time on the simultaneous analysis of fluorotriazine dye 1 and dye 4 in pH 8 B-R buffer. T_{acc} : a, 1; b, 2; c, 3; d, 4; e, 5 min, E_{acc} : 0.0 V, scan rate: 5 mV s^{-1} .

7.9 Conclusions

Fluorotriazine-based azo reactive dyes are adsorbed effectively onto the hanging mercury drop electrode, hence, an electroanalytical procedure was developed for the adsorptive stripping voltammetric determination of these reactive dyes in aqueous solutions. The observed reduction waves were due to the reduction of azo functional group and fluorotriazine reactive system. Mechanisms for their reduction processes at the HMDE were suggested. The optimum conditions for quantitative analysis of the fluorotriazine-based azo reactive dyes were also investigated in detail. These tested azo reactive dyes can be monitored by AdSV method down to the ng l^{-1} levels with satisfactory small relative standard deviations. However, the electrochemical discrimination between the original fluorotriazine-based azo reactive dyes and their hydrolysis or methanolysis products suffered from some limitations owing to the continuance of the fluorotriazine cathodic wave after the attempted hydrolysis or methanolysis processes. Finally, owing to the influence of the chemical structure of the tested reactive dyes on the azo moiety peak potential, the developed method was successfully applied to the simultaneous determination of the studied fluorotriazine reactive dyes in mixtures.

REFERENCES

1. Xu, G., O'Dea, J.J. and Osteryoung, J.G. *Dyes and Pigments*, (1996), **30**, 201.
2. Castrillejo, Y., Pardo, R., Barrado, E. and Batanero, P.S. *Electroanalysis*, (1990), **2**, 553.
3. Sahm, U., Knittel, D. and Schollmeyer, E., *Fresenius, J. Anal. Chem.*, (1990), **338**, 824.
4. Zanoni, M.V.B., Fogg, A.G., Barek, J. and Zima, J., *Anal. Chim. Acta*, (1995), **315**, 41.
5. Zanoni, M.V.B., Fogg, A.G., Barek, J. and Zima, J., *Anal. Chim. Acta*, (1997), **349**, 101.
6. Hart, J.P. and Smyth, W.F. *Analyst*, (1980), **105**, 1255.
7. Barek, J., Fogg, A.G., Moreira, J.C., Zanoni, M.V.B. and Zima, J., *Anal. Chim. Acta*, (1996), **320**, 31.
8. Fogg, A.G., Zanoni, M.V.B., Yusoff, A.R.H., Ahmad, R., Barek, J., and Zima, J., *Anal. Chim. Acta*, (1998), **362**, 235.
9. Florence, T.M. *Electroanal. Chem.* (1974), **52**, 115.
10. Gupta, P.N. and Raina, A., *J. Indian Chem. Soc.*, (1985), **62**, 363.
11. Peng, X. and Yang, J., *Dyes and Pigments*, (1992), **20**, 73.
12. Florence, T.M., *Aust. J. Chem.*, (1965), **18**, 609.
13. Barek, J. Balsiene, J., Tietzova, B. and Zima, J., *Collect. Czech. Chem. Commun.*, (1988), **53**, 921.
14. Barek, J. Ghosh, A. and Zima, J., *Collect. Czech. Chem. Commun.*, (1989), **54**, 1536.
15. Skopalova, J. and Kotoucek, M., *Fresenius J. Anal. Chem.*, (1995), **351**, 650.
16. Smith, D.L. and Elving, P.J., *J. Am. Chem. Soc.*, (1962), **84**, 2741.
17. Ignjatovic, L.M., Markovic, D.A., Veselinovic, D.S. and Besic, B.R., *Electroanalysis*, (1993), **5**, 529.
18. Barek, J., Balsiene, J., Berka, A., Hauserova, I. and Zima, J., *Collect. Czech. Chem. Commun.*, (1988), **53**, 19.
19. Bently, T.W., Ratcliff, J., Renfrew, A.H.M. and Taylor, J.A., *J. Chem. Soc. Perkin Trans. 2.*, (1996), **2377**.
20. Plust, S.J., Loehe, J.R., Feher, F.J., Benedict, J.H. and Herbrandson, H.F., *J. Org. Chem.*, (1981), **46**, 3661.
21. Wang, J., Lu, J., Wang, J., Luo, D. and Tian, B., *Anal. Chim. Acta*, (1997), **354**, 275.

CATALYTIC-AdSV DETERMINATION OF FLUOROTRIAZINE-BASED AZO REACTIVE DYES AT A HMDE IN THE PRESENCE OF NICKEL ION

8.1 Introduction

The use of the AdSV electrochemical technique for the analysis of the fluorotriazine-based azo reactive dyes has been demonstrated in chapter seven. In this chapter, the indirect analysis of these reactive dyes via their catalytic waves is investigated. The present study describes a catalytic-adsorptive stripping procedure for the measurement of low concentrations of fluorotriazine reactive dyes in the presence of nickel (II). The applied method relies on the effective interfacial accumulation of Ni (II)/Fluorotriazine dye complex on a HMDE and the catalytic reduction of the adsorbed complex. Usually, the dual adsorptive-catalytic amplification effect results in improving the sensitivity over the conventional adsorptive stripping procedure¹.

A series of reagents such as dihydroxy naphthalene², catechol³, cupferron⁴, nioxime⁵ and glutathione⁶ can form reducible complexes with several metal ions and catalyze the reduction of their complexes on a HMDE. The application of the catalytic effect for the analysis of several metal ions such as cobalt⁷, titanium⁸, molybdenum⁹, chromium¹⁰, iron¹¹ and platinum¹² was very successful. It has been reported that several thiol compounds such as cysteine¹³, glutathione¹⁴, and D-penicillamine¹⁵ and mordant red 74¹⁶ azo ligand gave cathodic stripping peaks which are due to the catalytic reduction of nickel ion. The complexed nickel is reduced with a lowered overpotential. Thus two electrochemical waves were obtained, the free (hydrated) nickel wave which reduced at ca. -1.0 V and complexed nickel wave reduced at -0.6 V (vs. Ag/AgCl electrode). This latter wave is catalytic because the catalyst substance (thiol or azo

ligand) released on reducing the complexed Ni(II) is free to complex further Ni (II) ions and to cause their reduction. Moreover, 2-mercaptobenzothiazole (MBT)⁷, trimercaptos-triazine (TMT)¹⁷ and 6-mercaptapurine-9-D-ribose (6-MPR)¹⁸ compounds catalysed the reduction of nickel ion and gave characteristic peaks with different overpotentials at -0.95 V, -0.73 V and -0.8 V, respectively.

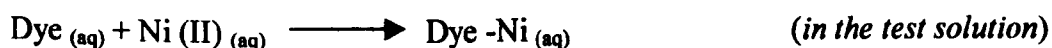
8.2 Aim of the Study

Stripping voltammetry has been used in conjunction with the catalytic nickel wave for determining suitable ligands, particularly thiols, in the presence of excess of nickel ion. However, apart from the study of Mordant Red 74¹⁶ azo ligand, no attempt has been made so far to use the catalytic nickel wave for monitoring any other synthesized dyes namely azo-based reactive dyes. Hence, it was the aim of this work to demonstrate the advantages of adsorptive stripping voltammetry connected with catalytic nickel reduction for enhancing the determination of these reactive dyes. Detailed optimization and characterization are also evaluated.

8.3 The Catalytic Reduction Mechanism

The electrode process associated with the catalytic reduction of fluorotriazine-based azo reactive dyes in the presence of nickel ion is assumed to be under the category of the EC mechanism. In this reaction mechanism, the electrochemical reaction process E (electrode reaction) is followed by a homogeneous chemical reaction C (solution reaction) which regenerates the reagent of the electrode reaction. In other words, in EC mechanism, the initial electroactive specie is regenerated by the homogeneous chemical reaction^{19,20}. A desirable peak current enhancement is gained as a consequence of this catalytic cycle. The catalytic mechanism can be summarized by the following reaction sequence:

Complex Formation Step: This initial step is based on the reaction of the catalyst/ligand (fluorotriazine-based azo reactive dye in this case) with the nickel (II) ion in the bulk solution to form the reducible Reactive Dye/Ni (II) complex. It is assumed that the Reactive Dye/Ni (II) complex involves chelation through the azo nitrogen, *o*-hydroxy and sulfate groups which act as co-ordination binding sites. This assumption is supported by the lack of the catalytic wave for fluorotriazine reactive dye 4, where the binding of Ni (II) by *o*-hydroxy site is not possible due to the replacement of this binding site by NHCONH₂ group.



Adsorption Step: After the formation of the Reactive Dye/Ni (II) complex in the bulk solution, it diffuses towards the working electrode surface where it is adsorbed and accumulated.



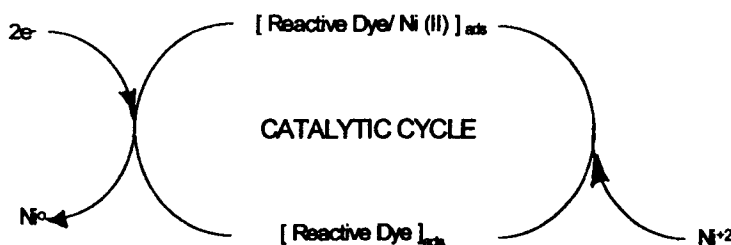
Electrochemical Reduction Step: During the cathodic scan, nickel ion in the adsorbed complex is reduced to the elemental state and amalgamated. Meanwhile, the reactive dye is released from the complex in this potential scan. These released ligand/catalyst molecules can subsequently enter the next step and bind other Ni (II) ions.



Chemical Reaction Step: After the electrochemical reduction process, the regenerated free reactive dye molecules can react with further nickel (II) ions, giving the reducible complex and closing the catalytic cycle. Owing to the high excess of nickel (II) ion in the test solution, the diffusion of metal ions to the diffusion layer and subsequent Reactive Dye/Ni (II) complex formation is ensured. Hence, the reducible ligand-metal ion complex is readily regenerated and repeated, which leads to the catalytic increase in the cathodic reduction current.



According to the above reaction steps, the general scheme for the catalytic process may be expressed and represented as:



8.4 Catalytic AdSV Characteristic of Fluorotriazine Dye-Ni (II) Complex

Preliminary experiments on AdSV of fluorotriazine-based reactive dyes are reported in the previous chapter. In the absence of the nickel ion, these reactive dyes were voltammetrically active via the cathodic reduction of their azo functional moiety and/or fluorotriazine reactive system. For instant, AdSV study of fluorotriazine-based dye 1 in Britton-Robinson buffer indicates the presence of a reduction peak at -0.26 V, when a potential scan is made from 0.0 V in the negative direction. The observed electrochemical peak was due to the cathodic reduction of the azo group in the analyzed dye. In contrast, Fig. 8.1 illustrates a typical stripping voltammogram for 1×10^{-7} mol l^{-1} fluorotriazine dye 1 in the presence of 1×10^{-4} mol l^{-1} nickel ion recorded following 2 min stirring at 0.0 V in a medium containing 0.04 M Britton-Robinson buffer solution (pH6). Addition of the nickel ion to the test solution, slightly shifted the potential of the azo group of the free reactive dye in the positive direction, and also noticeably suppressed its peak height. In fact, similar electrochemical behavior was reported for some thiol compounds and azo ligand in the presence of high excess of nickel ion¹³⁻¹⁶.

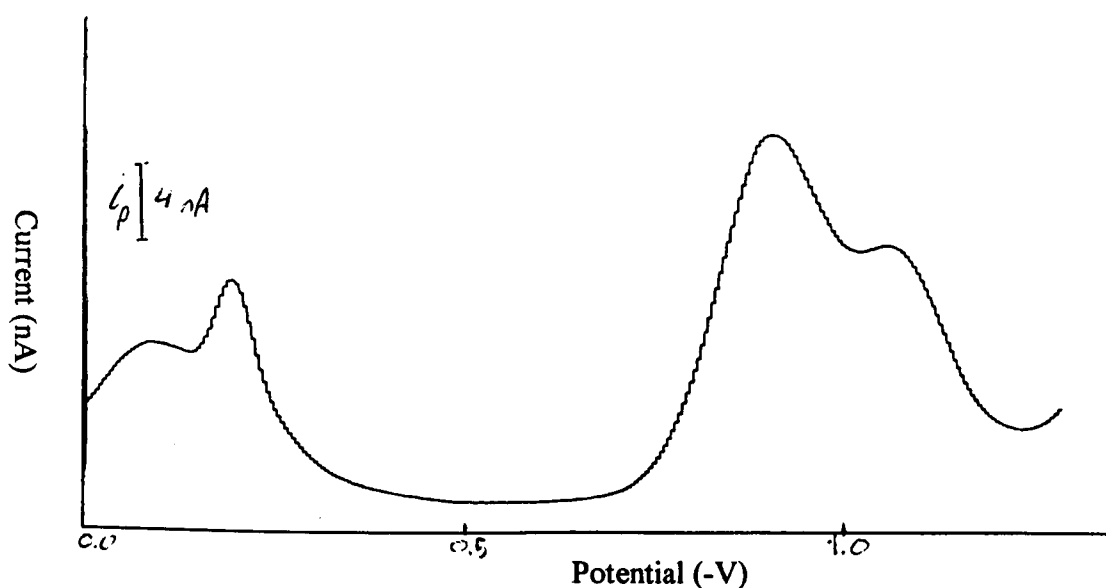


Figure 8.1: Catalytic-Adsorptive stripping voltammogram for 1×10^{-7} M fluorotriazine dye 1 in the presence of 1×10^{-4} M Ni (II) ion in pH 6 B-R buffer. Accumulation time: 2 min, accumulation potential: 0.0 V and scan rate: 5 mV s^{-1} .

However, the previous voltammogram displays a new well-defined catalytic-adsorptive stripping peak at -0.82 V ($i_p = 16.2 \text{ nA}$), which was presumed to involve the reduction of nickel (II) in the adsorbed complex. This observed peak lies in the potential range nearly characteristic for the reduction of nickel ion catalyzed by other catalytic agents (azo ligand)¹⁶. Furthermore, the presence of nickel ion in high concentration led to the appearance of a diffusion-controlled free nickel peak at -1.1 V ($i_p = 11 \text{ nA}$). The catalytic nickel peak is partly discrete from the diffusion-controlled free nickel peak due to the large overpotential for reduction of the hydrated ion (free Ni (II) ion), however, the addition of a complexing agent such as the azo ligand can reduce the overpotential, with the net result that the reduction occurs at a less negative potential.

In addition to the presence of the free azo, catalytic nickel and free nickel AdSV peaks, the stripping voltammogram of fluorotriazine-based azo dye in the presence of nickel ion in basic solutions ($\text{pH} > 8$, B-R buffer) exhibited an extra small electrochemical peak at -0.65 V which is probably associated with the Ni (II)-Reactive

dye complex peak. The adsorptive stripping voltammogram represented in Fig. 8.2 illustrates the appearance of the Ni (II)-Azo dye complex peak discrete from the free ligand peak and the catalytic nickel peak discrete from the free nickel peak. However, the free and complexed reactive dye peaks are very small relative to the catalytic nickel peak and the latter peak is well separated from the free nickel electrochemical peak. This variation in the peak height between azo peak and catalytic Reactive dye/ Ni (II) complex peak indicates the superiority and preference for monitoring these reactive dyes via the catalytic-AdSV procedure over the conventional direct measurement using the cathodic reduction of their azo group. This catalytic-AdSV behaviour is very similar to that reported for Mordant Red 74 azo ligand in the presence of nickel ion¹⁶.

Fluorotriazine dye 2 and 3 stripping voltammograms displayed similar catalytic nickel signals in the presence of Ni (II) ion owing to their ability to form a Reactive Dye/Ni (II) chelate complex. In contrast, fluorotriazine dye 4 lacks the ortho-hydroxy binding site which is involved in complex formation, hence, no catalytic nickel wave was observed for this reactive dye as can be seen from Fig. 8.3. In fact, the molecular structure of the ligand (reactive dye) may affect the catalytic activity through the applicability of reactive dye to form a chelating complex. This characteristic could be beneficial from the standpoint of selectivity. Consequently, these previous remarks and observations can be applied as a basis for a simultaneous analysis of a solution containing fluorotriazine dye 4 and any other fluorotriazine reactive dyes. Furthermore, this developed method may be used to enable a selective analysis of these fluorotriazine-based azo reactive dyes in the presence of other reactive dyes such as anthraquinone-based dyes (e.g. Reactive Blue 19) which can't undergo nickel complex formation.

Fluorotriazine-based azo reactive dye 1 will act as a representative model for the fluorotriazine-based reactive dyes in all the subsequent experimental investigation.

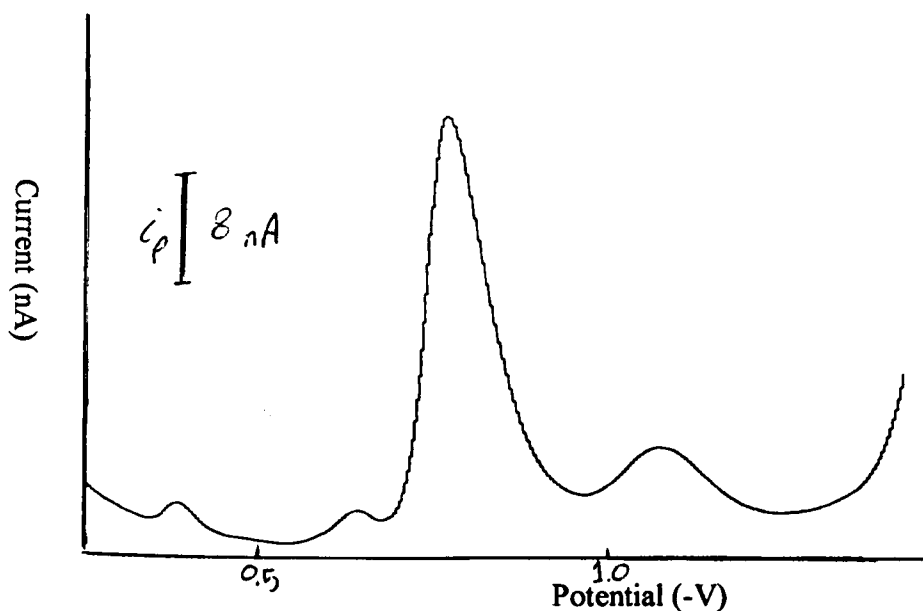


Figure 8.2: Catalytic-Adsorptive stripping voltammogram for fluorotriazine reactive dye 1 in pH 8 B-R buffer. T_{acc} : 2 min, E_{acc} : 0.0 V and scan rate: 5 mV s^{-1} .

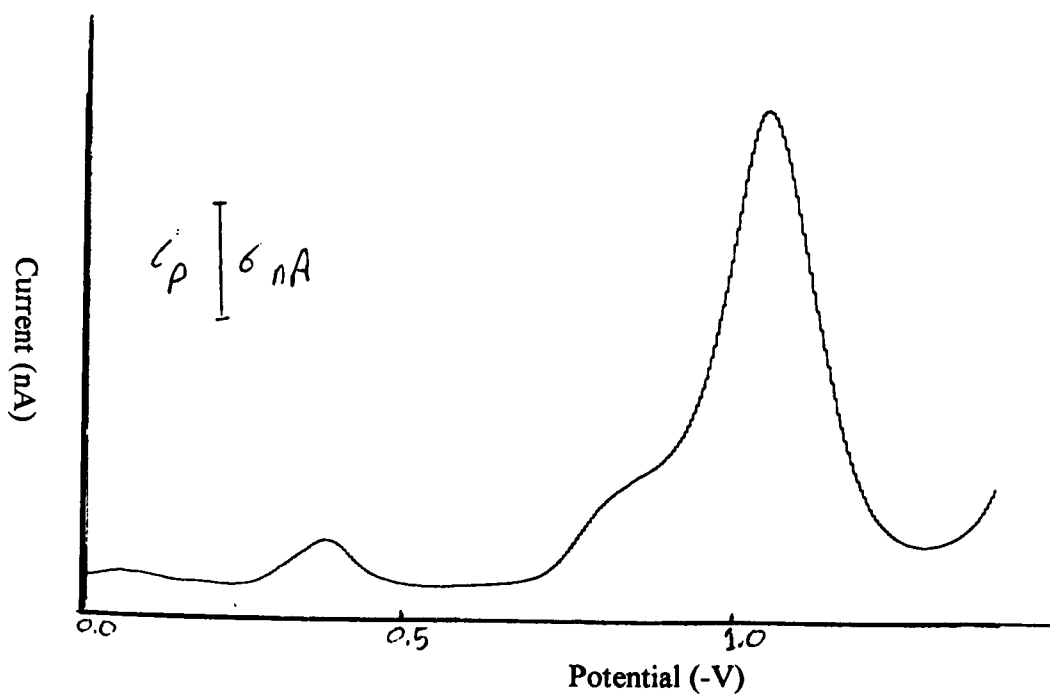
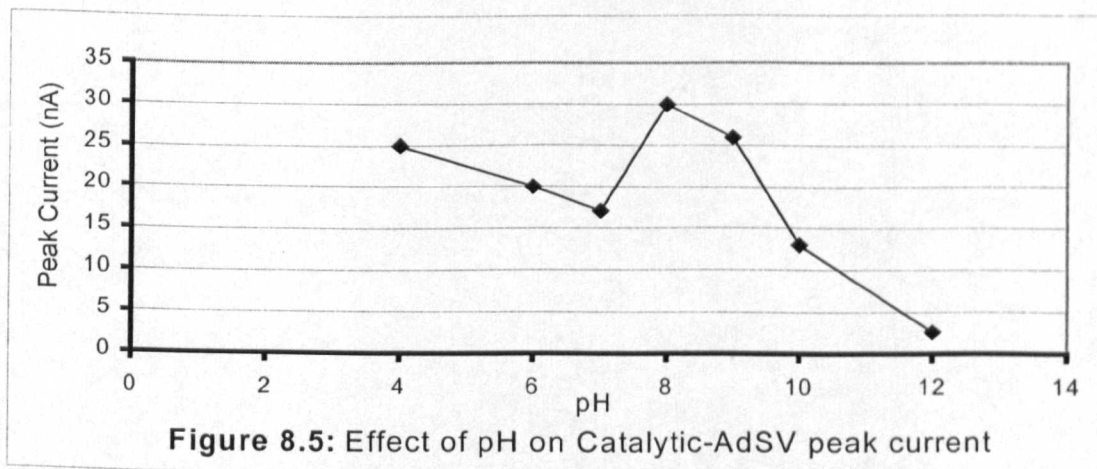
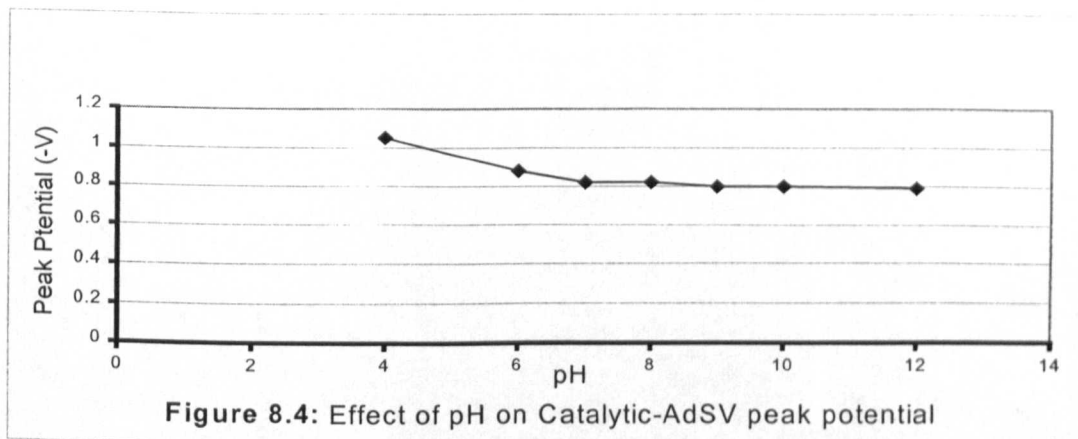


Figure 8.3: The absence of the Catalytic-AdSV response for fluorotriazine-based azo reactive dye 4 in the presence of Ni (II). B-R buffer (pH 6), T_{acc} : 2 min, E_{acc} : 0.0 V and scan rate: 5 mV s^{-1} .

8.5 Factors Affecting Catalytic-AdSV of Ni (II)-Dye Complex

8.5.1 Effect of pH

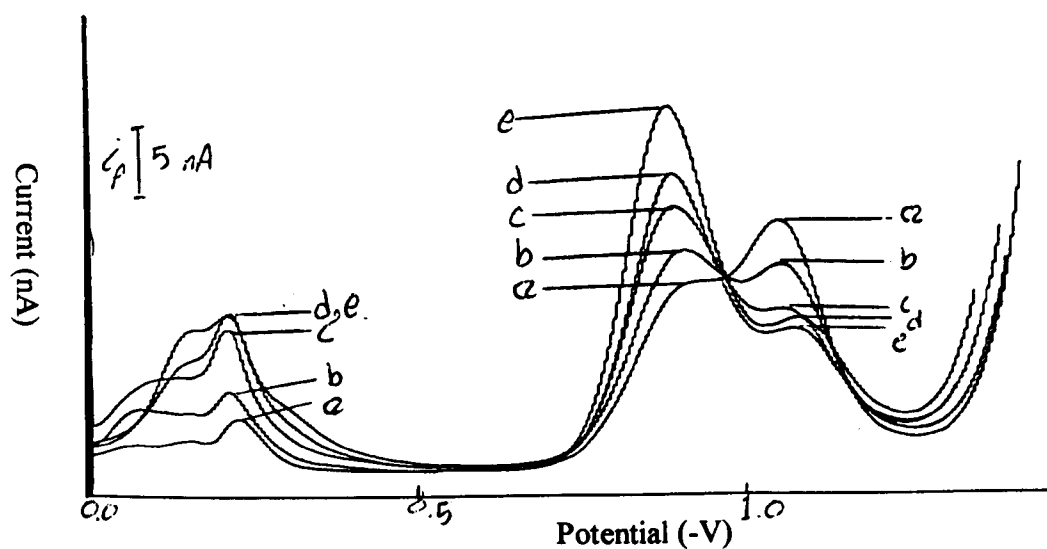
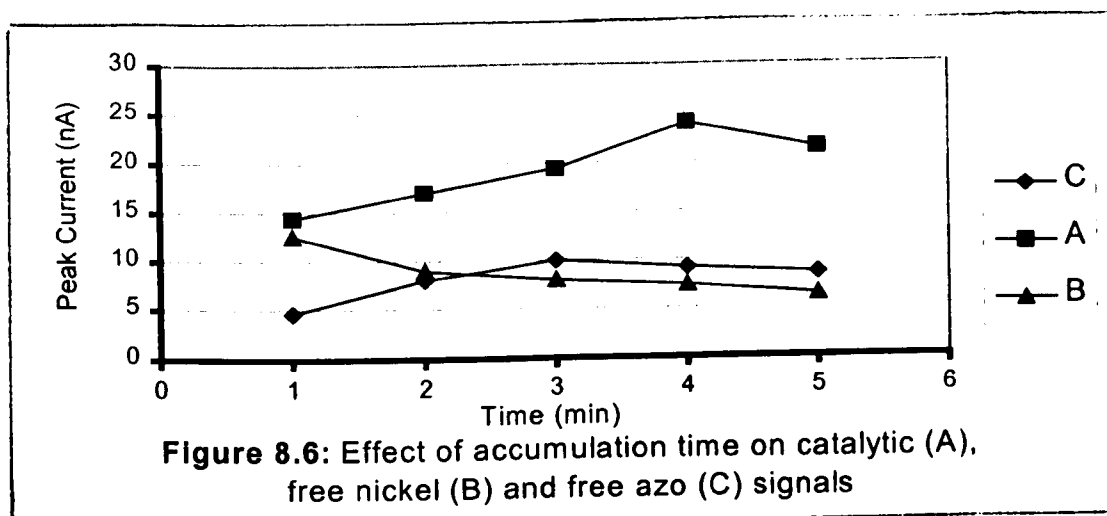
The pH of the solution has a significant effect on the response of both fluorotriazine reactive dye and its Ni (II) complex. The reduction of nickel ion catalyzed by the investigated dye is strongly dependent on pH owing to the competition between protons and Ni (II) for the binding sites in the complexing agent. Consequently, the influence of pH on the Reactive dye/Ni (II) system was investigated in Britton-Robinson buffer under conditions typical for catalytic stripping voltammetry, i.e. at low dye concentration and in the presence of a large excess of Ni (II)¹⁴. Figure 8.4 shows the effect of pH on the stripping voltammetric response. The peak potential shifted gradually in the positive direction from -1.05 V to -0.82 V over the pH range 4-8. However, the peak potential remained nearly constant at pH values higher than 8. The observed positive shift is probably due to the weak stability of the nickel-dye complex at higher pH values. On the other hand, the catalytic peak current decreased between pH 4 and pH 7, however, its maximum current was recorded at pH 8 (see Fig.8.5) and decreased thereafter due to competitive hydroxide formation (hydrolysis of Ni (II)). As a result, pH values between 6 and 8 are the most suitable for trace-level analysis. In fact, pH 8 was chosen for all subsequent work because it secures the maximum resolution between the catalytic and free nickel AdSV peaks along with the appreciable increase in the catalytic peak current.



8.5.2 Effect of accumulation conditions

The Ni (II)/Fluorotriazine dye complex is effectively accumulated in B-R buffer at a 0.0 V accumulation potential. Curves A, B and C in Fig.8.6 show the influence of preconcentration time on the catalytic (A), free nickel (B) and free azo (C) signals in pH 6 B-R buffer containing $1 \times 10^{-7} \text{ mol l}^{-1}$ fluorotriazine reactive dye and $1 \times 10^{-4} \text{ mol l}^{-1}$ Ni (II) collected at 0.0 V. According to the previous graph, variation of accumulation time (T_{acc}) indicates that the catalytic peak current increased linearly with T_{acc} at low accumulation time because the adsorbed complex is not saturated on the electrode surface. However, the catalytic response tends to deteriorate at longer accumulation time (more than 4 minutes). The decrease in the catalytic peak current at longer periods is possibly due to competitive adsorption of free nickel ions on HMDE. Similar influence of this parameter (T_{acc}) on the azo peak height of the free reactive dye was observed (refer to Fig 8.6). Meanwhile, when measuring the peak height of the free nickel ion as a function of the accumulation time, its AdSV peak height decreased with the accumulation time reflecting the competitive consumption of this metal ion during the Reactive dye/Ni (II) complex formation. The effect of preconcentration time on the free azo, catalytic and free nickel AdSV peak heights is presented in Fig.8.7. In contrast, the potentials of these AdSV peaks remained approximately constant for all these experiments. Obviously, a compromise between increase in sensitivity and speed is required in the optimum accumulation time, therefore, an accumulation time of 2 min was selected for subsequent work, combining adequate sensitivity with short analysis time and minimum interference by free Ni (II).

On the other hand, variation of accumulation potential (E_{acc}) was found to have a negligible effect on catalytic peak height under the same experimental conditions. An accumulation potential of 0.0 V was selected as an optimum value.



8.5.3 Effect of dye concentration

The concentration of fluorotriazine reactive dye has a profound effect on the catalytic peak height. Variation of dye concentration in the presence of $3 \times 10^{-5} \text{ mol l}^{-1}$ Ni(II) showed (see Fig. 8.8) that the peak current increased rapidly with the fluorotriazine dye concentration increasing from $1 \times 10^{-7} \text{ mol l}^{-1}$ to $6 \times 10^{-7} \text{ mol l}^{-1}$, however, then it starts to level off at higher concentrations as can be seen from Fig. 8.9. Meanwhile, the peak potential shifted slightly by 24 mV in the cathodic direction due to the variation of dye concentration. A $5 \times 10^{-7} \text{ mol l}^{-1}$ fluorotriazine dye concentration is suitable for further experimental studies.

8.5.4 Effect of nickel ion concentration

As expected, the catalytic wave resulting from the reduction of Ni (II) in the Nickel-Dye complex depends strongly on the metal ion concentration. The wave height at nickel concentrations in the range 1×10^{-5} - $2 \times 10^{-4} \text{ mol l}^{-1}$ has been measured. The concentration dependence is shown in Fig. 8.10 which displays the influence of successive addition of Ni (II) to $5 \times 10^{-7} \text{ mol l}^{-1}$ fluorotriazine reactive dye solution. The catalytic wave increased gradually with nickel concentration. In contrast, the peak potential was not affected by the variation of Ni (II) concentration. Therefore, to analyze ultra-trace amounts of these reactive dyes, the use of a range of higher Ni (II) concentration (e.g. $1 \times 10^{-4} \text{ mol l}^{-1}$) is more favorable. Nevertheless, nickel ion concentrations higher than 1 mM should be avoided in order to prevent strong interference from the free nickel peak produced by diffusion-controlled reduction⁶.

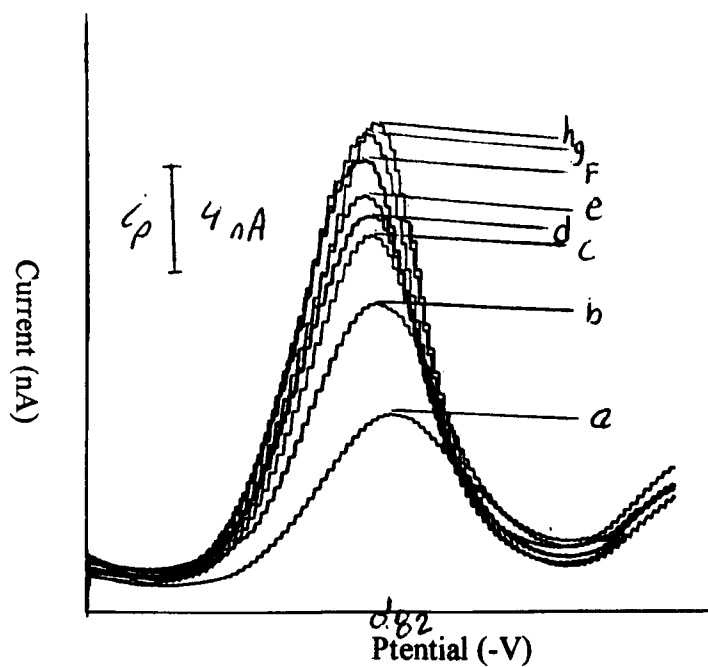
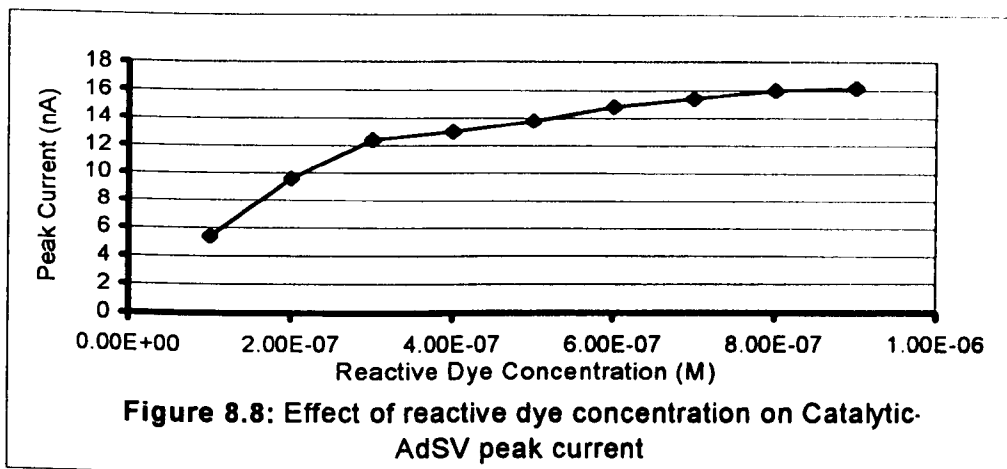
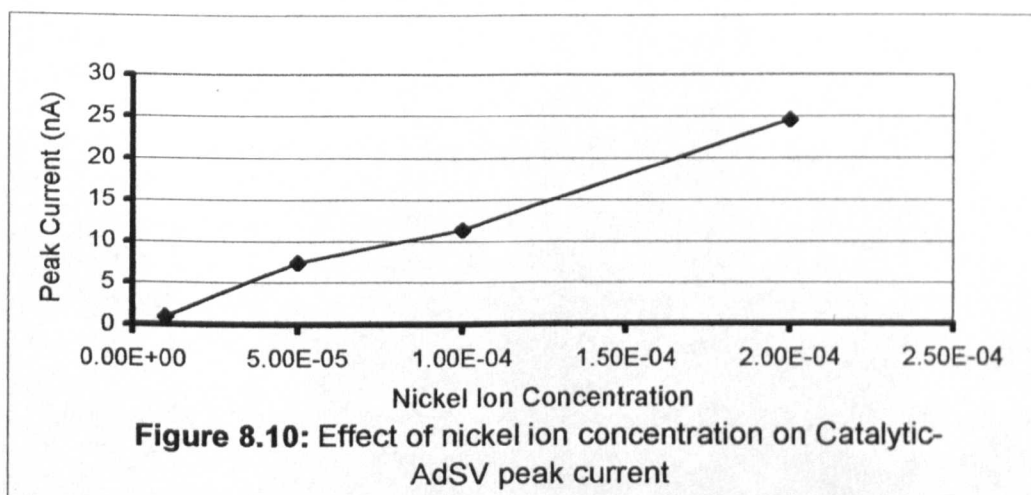


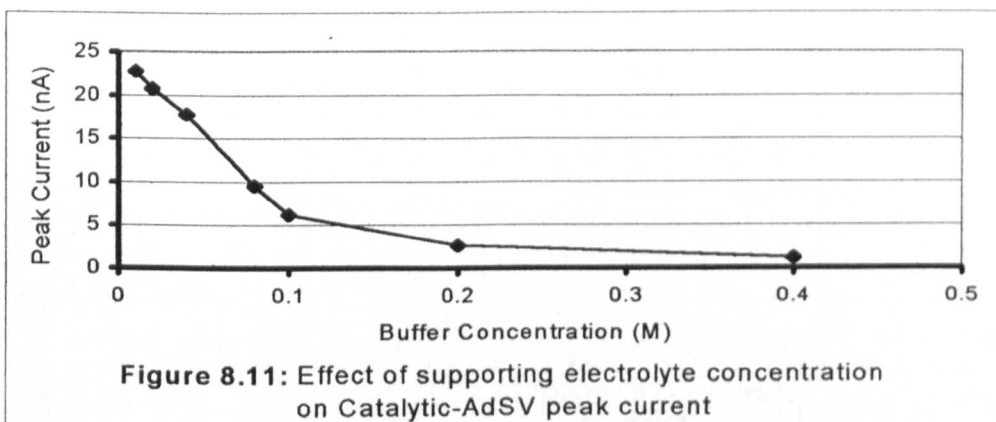
Figure 8.9: Effect of reactive dye concentration on Catalytic-AdSV peak height. pH 8 Britton-Robinson buffer. $T_{\text{BOC}} : 2 \text{ min}$, $E_{\text{BOC}}: 0.0 \text{ V}$, and scan rate: 5 mV s^{-1} . Reactive dye concentration: a: 1, b: 2, c: 3, b: 4, e: 5, f: 6, g: 7 and h: $8 \times 10^{-7} \text{ mol l}^{-1}$.



8.5.5 Effect of supporting electrolyte concentration and composition

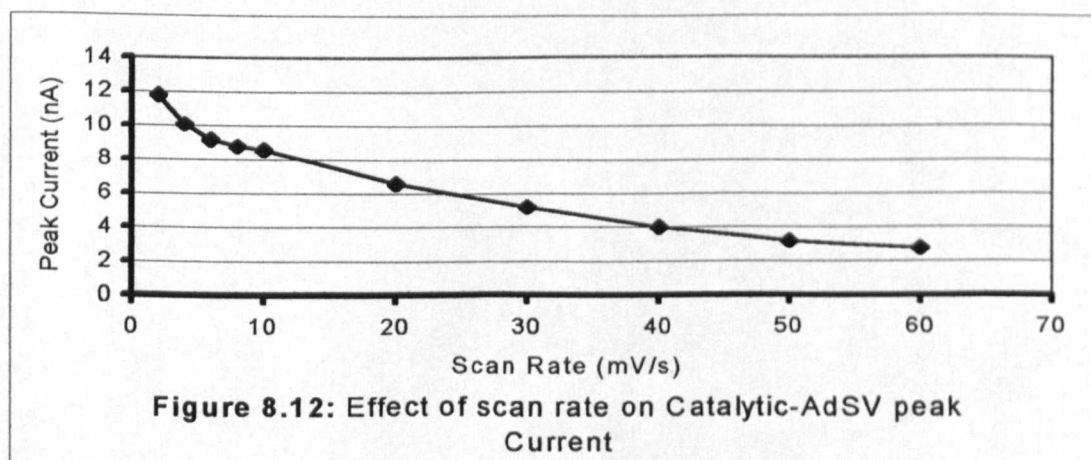
The concentration of Britton-Robinson buffer was varied under controlled conditions to investigate the influence of buffer concentration on the stripping response. The variation of the peak current as a function of electrolyte concentration, represented in Fig. 8.11 shows the gradual decline in peak current as buffer solution concentration increased from 0.01 mol l^{-1} to 0.4 mol l^{-1} . The peak current decreased almost 2-fold over that buffer concentration range. A 0.02 mol l^{-1} B-R buffer solution was selected for subsequent work because it gave the largest peak current.

Analogous catalytic-AdSV behavior of fluorotriazine-based azo reactive dye in the presence of excess nickel ion was observed when using acetate buffer (pH 5) as a supporting electrolyte, however, under this condition, the catalytic analytical peak was located about -0.88 V which means that the overlapping problem between the catalytic and the free nickel electrochemical peaks become worse.



8.5.6 Effect of scan rate

Variation of scan rate between 2 and 60 mV s^{-1} at constant ligand and metal ion concentrations caused the catalytic peak height to decrease gradually (see Fig. 8.12) suggesting slow kinetics of the catalytic process⁵ (i.e. the charge transfer becomes faster than the complex diffusion). The catalytic peak potential shifted to more negative potentials with increasing scan rate indicating the irreversible nature of the charge transfer⁵. A 5 mV s^{-1} scan rate was chosen as optimum for further investigations.



8.5.7 Effect of instrumental parameters

The catalytic peak current can be maximized by selecting a large surface area (large drop size). The relationship between the measured reduction current and the surface area of the drop was found to be linear for surface areas of 0.15-0.29 mm². For optimal sensitivity, a large drop size of the Hg-drop working electrode is favorable. Furthermore, the influence of stirring rate over the catalytic wave was investigated. An increase in the stirring rate yielded, as expected, an increase in the peak current and did not affect the value of peak potential (E_p).

8.6 Interference

The major sources of interference are likely to be from coexisting ions capable of forming complexes with the fluorotriazine dye or depositing at the mercury electrode. These may affect the catalytic response via an overlapping peak or may compete for adsorptive sites. Competition for the surface can be also caused by surfactants. Interference by diverse substances was investigated by adding appropriate amounts of interferences to 20 ml of solution containing 1×10^{-7} mol l⁻¹ Ni (II) and 5×10^{-7} mol l⁻¹ dye.

8.6.1 Interference by metal ions

Possible interferences from present metal ions were evaluated. Each metal ion was investigated at 1×10^{-6} mol l⁻¹ concentration for adsorption of its possible complex with the analyzed reactive dye. Addition of 1 μ M Zn(II), Fe(II), In(II), Ba (II), Sn (II), Se (II), Au(I), Si(II), Li(I) and Mg(II) caused no effect on the catalytic-AdSV response of nickel. However, Cu(II), Co(II) and Pb(II) metal ions compete with nickel for the ligand, causing a negative interference of 26%, 20% and 60% respectively. In contrast,

similar additions of Ti(IV) and Na(I) yielded 38% and 19% enhancements, respectively. Most of the metal ions tested above did not interfere at the 1×10^{-8} mol l⁻¹ level. Thus, the nickel ion may need not be isolated from these interfering trace-elements prior to its determination in real environmental samples.

8.6.2 Interference by surface-active surfactants

Surface-active materials occurring in natural waters could interfere by adsorbing competitively on the HMDE. The effects of various surfactants on Ni (II)/Reactive dye catalytic response were investigated for a 2 min preconcentration time at 0.0V. Several substances such as Triton X-100, Tetraphenyl Phosphonium Chloride (TPPC) and Aerosol OT were used as model compounds for surface-active surfactants. The catalytic wave was not affected by addition of 0.002 mg l⁻¹ of Triton X-100 (a non-ionic surfactant). Further additions up to 0.2 and 1 mg l⁻¹ resulted in 35% depression and total diminishing of the analytical response, respectively. The presence of 0.001 mass volume⁻¹ anionic surfactant Aerosol OT led the peak current to increase up to 70%. However, further additions of 0.002, 0.003 and 0.005 mV⁻¹ diminished the peak current by 10%, 33%, and completely, respectively. In contrast, the influence of the cationic surfactant TPPC on the catalytic wave was severe. Only 31 % of the initial catalytic peak current was observed after the addition of 1×10^{-5} mol l⁻¹ TPPC. Moreover, a 2×10^{-5} mol l⁻¹ TPPC concentration was found to be sufficient to cause total vanishing for the Ni (II)/ Reactive dye reduction peak.

8.6.3 Interference of complexing agent

The competitive effect of complexing agents on the nickel peak was modeled by addition of EDTA to a Britton-Robinson buffer (pH 6) containing 1×10^{-6} mol l⁻¹ Ni (II) and 1×10^{-7} mol l⁻¹ fluorotriazine reactive dye. There was virtually no effect for EDTA on the catalytic peak when the EDTA-to-Dye ratio was close to 1. However, a

marked gradual decline in the peak height was observed when further amounts of EDTA solution were added to the tested solution. The catalytic peak height diminished strongly at higher EDTA concentrations to about 80%, 52% and 43% of the original peak height in consequence of the presence of $5 \times 10^{-6} \text{ mol l}^{-1}$, $1 \times 10^{-5} \text{ mol l}^{-1}$ and $2 \times 10^{-5} \text{ mol l}^{-1}$ EDTA, respectively.

8.7 Analytical Application

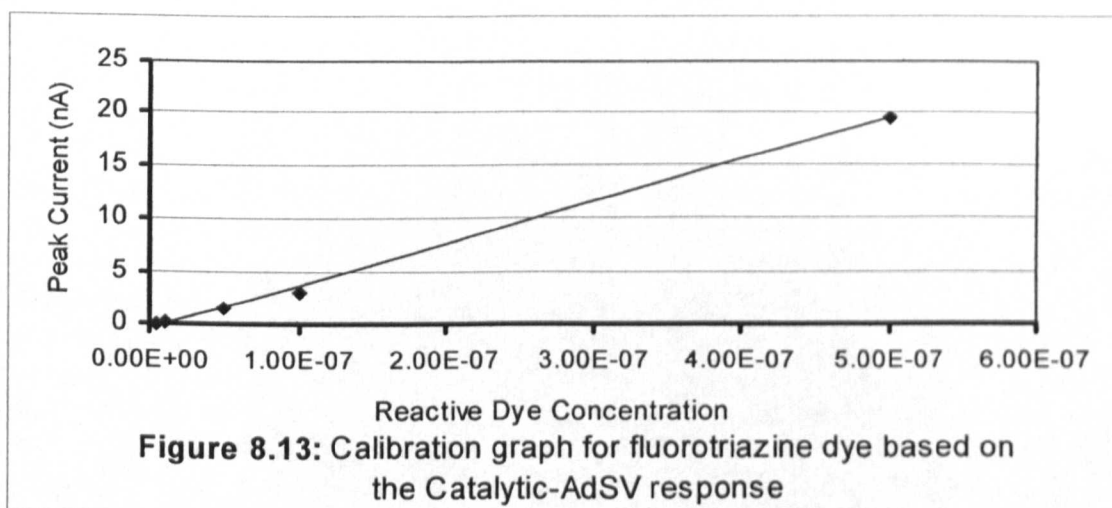
According to the comprehensive study presented above, the following media and optimized procedure can be used: $5 \times 10^{-7} \text{ mol l}^{-1}$ fluorotriazine dye, $1 \times 10^{-4} \text{ mol l}^{-1}$ nickel ion, 0.02 mol l^{-1} Britton-Robinson buffer (pH 8) accumulation time = 2 min, preconcentration potential = 0.0 V (vs. Ag/AgCl) and 5 mV s^{-1} scan rate.

8.7.1 Calibration graph

In order for the adsorptive preconcentration step to possess significant analytical utility, it must exhibit concentration dependence, which is both well characterized, and highly reproducible²¹. The linear calibration range for the optimized method was evaluated from the calibration plot of fluorotriazine reactive dye in B-R buffer containing $1 \times 10^{-4} \text{ mol l}^{-1}$ nickel ion. As can be seen from the calibration plot in Fig. 8.13, the catalytic peak current increased linearly with dye concentration over a very large concentration range (0.5 nM - 1 μM) when a 2 min preconcentration period was used. The parameters of the dye concentration-current straight line were calculated by the least-squares method. The regression equation of the calibration line has the form:

$$Y = 0.038X + 0.32 \qquad n = 6 \qquad r = 0.999$$

Where Y is the catalytic peak current in A, X is the concentration of fluorotriazine reactive dye in mol l^{-1} and 0.038 ($\text{A mol}^{-1}\text{l}$) and -0.32 (nA) are the values of the slope and the intercept, respectively. The correlation coefficient was 0.99.



8.7.2 Detection limit

The coupling of adsorptive and catalytic effects resulted in a quite low detection limit following short accumulation periods. For the fluorotriazine-based azo reactive dye 1 following the optimized procedure, the detection limit of $3.2 \times 10^{-9} \text{ mol l}^{-1}$ was estimated based on the signal-to-noise characteristic ($S/N = 3$) of the response of $1 \times 10^{-7} \text{ mol l}^{-1}$ reactive dye.

8.7.3 Reproducibility

The analytical precision of the method was verified from the reproducibility of 8 determinations of $1 \times 10^{-7} \text{ mol l}^{-1}$ fluorotriazine reactive dye in pH 8 Britton-Robinson buffer ($E_{\text{acc}} 0.0\text{V}$, $T_{\text{acc}} = 2 \text{ min}$). A relative standard division (%RSD) of 1.1 % was

obtained, which indicates reproducible accumulation of the metal-chelate complex on the mercury surface.

8.7.4 Stability

The stability of the catalytic response of $1 \times 10^{-7} \text{ mol l}^{-1}$ fluorotriazine reactive dye in the presence of $1 \times 10^{-4} \text{ mol l}^{-1}$ Ni (II) was evaluated under the optimized conditions, it seemed to be stable for a period of two hours at least.

8.8 Practical Applications

Owing to the unavailability of a real reactive dye samples that contains these fluorotriazine reactive dyes, the applicability of the developed method was demonstrated on the analysis of the metal ion (nickel) participating in the reactive dye complex formation. The proposed procedure was applied for the determination of trace levels of nickel ion in natural and environmental waters such as river water and tap water. Because of the inherent sensitivity of the method, the analyzed samples were diluted. The procedure for the preparation of sample was as follows: a known volume of the environmental sample (0.2ml) was added to 20 ml of Britton-Robinson buffer containing $1 \times 10^{-6} \text{ mol l}^{-1}$ fluorotriazine dye. The buffer solution was placed into the voltammetric cell and deoxygenated for 5 min. The Catalytic-AdSV response was measured after 3 min accumulation with stirring at 0.0V. The concentration of nickel in the analyzed samples evaluated by the standard additions methods (five successive additions) was $1.7 \times 10^{-8} \text{ mol l}^{-1}$ and $2.1 \times 10^{-8} \text{ mol l}^{-1}$ for river water and tap water, respectively. In general, these obtained results agree (to some degree) with previously reported results for the determination of nickel ion in similar environmental water samples by other methods of analysis²².

8.9 Conclusions

The present study demonstrated that the coupling of adsorptive accumulation with the catalytic action can constitute the basis for an effective means for the determination of ultra-trace levels of fluorotriazine reactive dye and/or Ni (II). Experimental parameters for the Catalytic-AdSV analysis of the reactive dye have been described and their conditions have been optimized. A few minutes of preconcentration are sufficient for the detection of the analyzed fluorotriazine-based azo reactive dye 1 at the 3×10^{-9} mol l⁻¹ level. Calibration plots show a linear response over the range 5×10^{-9} - 1×10^{-6} mol l⁻¹. The influence of co-existing interferences was also reported. The tested method has been successfully applied for direct determination of nickel ion in two environmental samples. In addition, a likely electrode mechanism was also proposed and discussed. The satisfactory results and small standard deviation obtained in the analysis of this reactive dye are an indication of the applicability of these methods for the analysis of other synthetic dyes which are applicable to undergo nickel chelate complex formation.

REFERENCES

1. Setidji, R., Wang, J. and Santana-Rios, G., *Talanta*, **40**, (1993), 845.
2. Li, H. and Smart, R.B., *Anal. Chim. Acta*, **333**, (1996), 131.
3. Vega, M. and Van den berg, C.M.G., *Anal. Chim. Acta*, **293** (1994), 19.
4. Baoxian, Y. and Shuxun, Y., *Talanta*, **41**, (1994), 537.
5. Vega, M. and Van den berg, C.M.G., *Anal. Chem.*, **69**, (1997), 874.
6. Banica, F.G., Fogg, A.G. and Moreira, J.C., *Talanta*, **42**, (1995), 227.
7. Fogg, A.G., Ismail, R., Ahmed, R. and Banica, F.G, *Talanta*, **44** (1997), 491.
8. Yokoi, K. and Van den Berg, C.M.G, *Anal. Chim. Acta*, **245**, (1991), 167.
9. Yokoi, K. and Van den Berg, C.M.G, *Anal. Chim. Acta*, **257**, (1992), 293.
10. Wang, J., Lu, J. and Olsen, K., *Analyst*, **117**, (1992), 1913.
11. Yokoi, K. and Van den Berg, C.M.G, *Electroanalysis*, **4**, (1992), 65.
12. Van den Berg, C.M.G. and Jacinto, G.S., *Anal. Chim. Acta*, **211**, (1988), 129.
13. Banica, A.G., Moreira, J.C. and Fogg, A.G., *Analyst*, **119**, (1994), 309.
14. Banica, A.G., Fogg, A.G. and Moreira, J.C., *Analyst*, **119**, (1994), 2343.
15. Ion, A., Banica, F.G.; Fogg, A.G. and Kozlowski, H., *Electroanalysis*, **8**, (1996), 40
16. Fogg, A.G., Ismail, R., Ahmed, R. Williams, S.L. and Zanoni, M.V.B., *Microchem. J.*, **57**, (1997), 110.
17. Fogg, A.G., Ismail, R., Yusoff, A.H.M, Ahmed, R. and Banica, F.G, *Talanta*, **44**, (1997), 497.
18. Ion, A., Banica, F.G. and Luca, C., *Electroanalysis*, **9**, (1997) 945.
19. Crow, D.R., *Principles and Application of Electrochemistry*, Blackie Academic and Professional, London, 1994.
20. Kissinger, P.T. and Heineman, W.R. (ed.), *Laboratory Techniques in Electroanalytical Chemistry*, Marcel Dekker, Inc., New York, 1996.
21. Greef, R., Peat, R., Peter, L.M., Pletcher, D. and Robinson J., *Instrumental methods in Electrochemistry*, Ellis Horwood, Chichester, 1990.
22. Lau, OW and Ho, SY, *Anal. Chim. Acta*, **117**, (1993), 151.

AdSV PROPERTIES OF DOUBLE ANCHOR-BASED BISAZO REACTIVE DYES AT THE HMDE

9.1 Introduction

All the investigated reactive dyes so far in this thesis have only one single chromogen functional group (either anthraquinone or azo groups). However, recently, a wide range of reactive dyes has been produced which are composed of more than one functional system. Some of these new class reactive dyes have a symmetrical molecular structure with two azo functional moieties and two chlorotriazine reactive groups. It was visually observed that these reactive dyes had darker colours compared to the other reactive dyes, which had similar molecular structure, but with a single azo functional group. Furthermore, these reactive dyes were theoretically expected to have a higher fixation rate with improved wash-fastness property, owing to the presence of double chlorotriazine anchoring systems. From an analytical point of view, it was considered interesting to evaluate and study the influence of doubling the existence of the functional systems on the electrochemical behaviour of these reactive dyes. The electrochemical behaviour and response of some synthesized bisazo dyes such as Direct Orange 31¹, Acid Red 150², Fast Sulfone Black-F³ and Direct Red 81⁴ and some genotoxic azodyes e.g. Congo Red⁵ and Trypan Blue⁶ have been studied and reported in the literature.

9.2 Aim of the Study

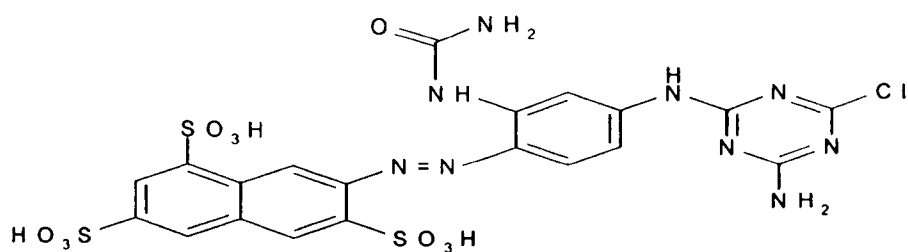
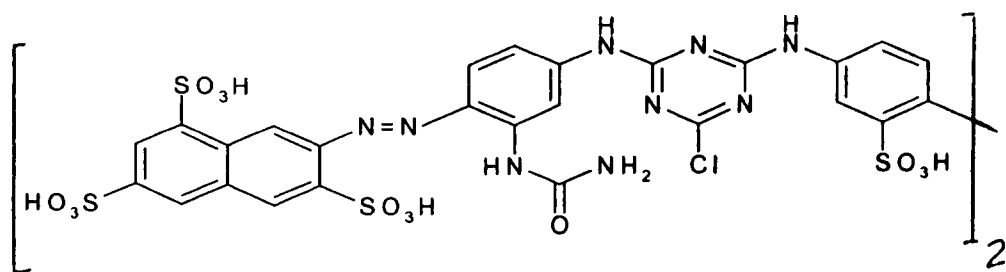
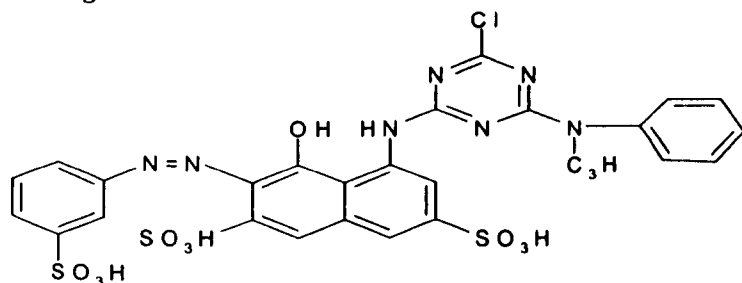
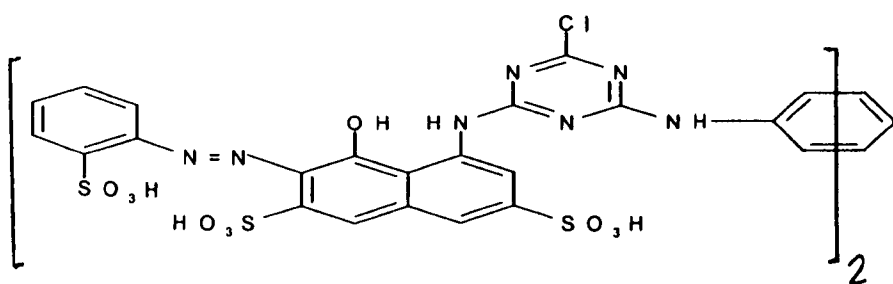
Although the electrochemical behaviour of numerous monoazo dyes have been the subject of several studies (see section 7.1), bisazo dyes in contrast, have attracted less attention, despite their importance role as a new class of azo industrial dyes. In fact, very little is known about bisazo dyes². In addition, no mention has been made in the current literature for the electrochemical properties of bisazo synthetic reactive

dyes that contain two reactive anchoring systems. Thus, this work was devoted to a detailed study of the AdSV behaviour of these double anchor-based bisazo reactive dyes at the HMDE in order to evaluate the influence of introducing a further functional chromogen group and anchoring system on the electrochemical behaviour and adsorption properties, as well as to determine the optimal conditions for the most sensitive determination of these reactive dyes. Moreover, the advantage of this present investigation is that it evaluates the effect of introducing a second functional and/or reactive group on the stripping voltammetric response, by carefully selecting and comparing two chlorotriazine-based azo reactive dyes. The molecule structure of one reactive dye is exactly twice that for the other reactive dye, i.e. the former dye has double functional (azo) and reactive (chlorotriazine) groups.

In this present work, the adsorptive stripping voltammetric behaviour of two reactive dye systems and arrangements of Reactive Orange 12–Reactive Yellow 84 and Reactive Red 120–Reactive Red 24 were studied as a representative model for these interesting and promising chlorotriazine-based bisazo reactive dyes.

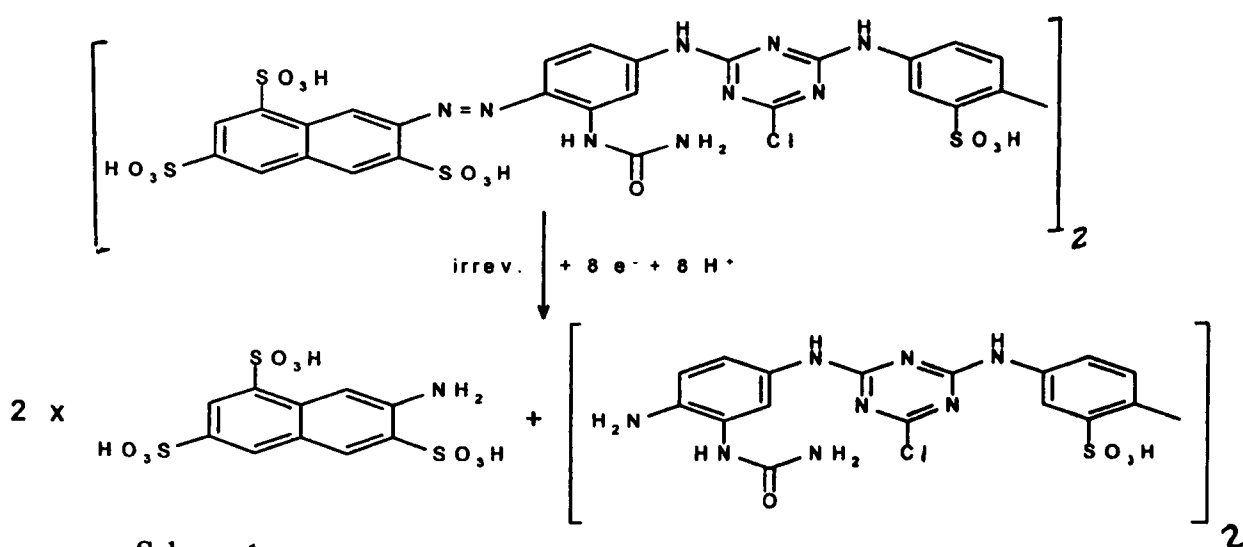
9.3 Preliminary Studies

Preliminary experiments were carried out to investigate whether the doubling of the functional and reactive systems had a significant effect on the electroanalytical characteristic at various experimental conditions. Both C.I. Reactive Orange 12 (Procion Yellow H-E4R) and C.I. Reactive Red 120 (Procion Red HE-3B) were composed of two azo moieties (see Fig. 9.1). These reactive dyes appear to adsorb on the hanging mercury drop electrode' surface in several supporting electrolyte solutions e.g. Britton-Robinson (pH 6), acetate (pH 4.5) and carbonate (pH 10) buffers. After adsorption accumulation at 0.0 V, two adsorptive stripping voltammetric peaks were produced following a scan in the negative direction. For 5×10^{-7} mol l⁻¹ of RO12 solution monitored by AdSV in pH 6 B-R buffer, two well-separated electrochemical waves were observed, as can be seen from Fig. 9.2. The first well-defined stripping voltammetric peak obtained at $E_p = -357$ mV (vs. Ag/AgCl) with 12.1 nA peak current is believed to be corresponding to the reduction of the two azo centres in the RO12 dye model. Since the chemical environment around each azo moiety in the dye molecule is identical (in addition to the symmetrical molecular structure for the

**Reactive Yellow 84****Reactive Orange 12****Reactive Red 24****Reactive Red 120****Figure 9.1:** The molecular structure of the studied chlorotriazine-based azo reactive dyes.

analysed reactive dye) the monitored azo groups act and behave as one large single adsorptive stripping signal. Accordingly, a significant enhancement in the AdSV peak current was achieved as a consequence of adding more azo functional group to the reactive dye molecular structure. Obviously, this is expected to lead to an improvement on the electroanalytical detection of these reactive dyes at ultra-trace levels by adsorptive stripping voltammetry.

Previous observations reported in the literature indicate that electrochemical reduction of a symmetrical bisazo dyes exhibited one single cathodic reduction wave related to the cathodic reduction of the two azo moieties^{4,5}. Whereas, asymmetrical bisazo dyes which have two azo moieties with different chemical environment around them, exhibited two separated well-defined electrochemical waves¹⁻⁴. However, based on the proposed electrode reduction mechanism given in section 7.3, it can be assumed that the symmetrical bisazo Reactive Orange 12 undergoes irreversible eight-electron, eight-proton electrochemical reduction process in Britton-Robinson buffer according to the Scheme 1:



In comparison, C.I. Reactive Yellow 84 (Procion Yellow P-3R), which has nearly half the molecular structure of RO12 and with only one single azo moiety, produced a typical electrochemical response similar to that obtained for RO12 dye, but with less azo peak current. In fact, it yielded a stripping voltammetric wave associated with the cathodic reduction of the azo group at $E_p = -353$ mV but with half the azo peak current recorded for RO12 (i.e. RY84 peak current = 6.2 nA). However, the second very well-defined adsorptive voltammetric signal was attributed to the cathodic

reduction of the chlorotriazine reactive group. The peak potential for this electrochemical signal was at -1.038 V and -1.039 V for RY84 and RO12, respectively. The presence of double chlorotriazine anchoring systems for RO12 caused a noticeable enhancement in the peak height of this electrochemical signal compared to that observed for RY84. For instance, when using B-R buffer (pH 6) as a supporting electrolyte, the peak current of chlorotriazine reactive group for RO12 was approximately twice that for RY84 (See Table 9.1). Moreover, the AdSV behaviour of the RO12–RY84 system in pH 4.5 acetate buffer was also evaluated. As can be noted from Table 9.1, only one cathodic reduction signal related to the electrochemical response for the azo functional group was obtained.

Similar results and observations were obtained for the RR120–RR24 system. The introducing of the second azo functional moiety to the molecular structure of RR120 caused a significant enhancement for the azo system stripping voltammetric peak current. For instance, 5×10^{-7} mol l⁻¹ RR120 solution in pH 10 carbonate buffer yielded a 42.3 nA cathodic peak current at $E_p = -750$ mV. The adsorptive stripping voltammetric response for 5×10^{-7} mol l⁻¹ RR120 in carbonate buffer after 2 minutes preconcentration period at 0.0 V accumulation potential is illustrated in Fig. 9.3. On the other hand, the cathodic reduction of azo group for 5×10^{-7} mol l⁻¹ monoazo Reactive Red 24 (Basilen Brilliant Red P-B) under the same experimental conditions produced an AdSV peak at $E_p = -720$ mV, yet with only 20.7 nA peak current. Beside the azo electrochemical peaks, another well-developed adsorptive stripping voltammetric peak attributed to the cathodic reduction of the chlorotriazine reactive group at peak potential ≈ -895 mV was observed. It is worthwhile to point out that the chlorotriazine reactive group of all these chlorotriazine-based azo reactive dyes yielded a well-defined and very large AdSV peaks compared to the poor and broad ill-developed peak shapes with weak peak currents for fluorotriazine reactive system of fluorotriazine-based azo reactive dyes studied in chapter 7. Table 9.1 summarises the effect of supporting buffer constituents on the AdSV properties for both RO12–RY84 and RR120–RR24 systems.

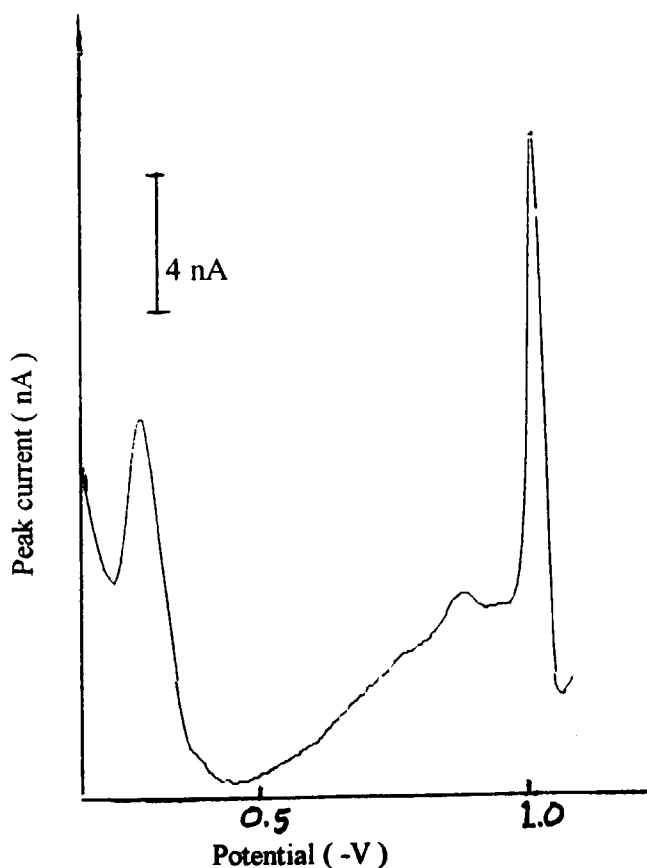


Figure 9.2: AdSV of 5×10^{-7} M of Reactive Orange 12 in pH 6 B-R buffer after 2 min accumulation time at $E_{acc} = 0.0$ V with 6 mV s^{-1} scan rate.

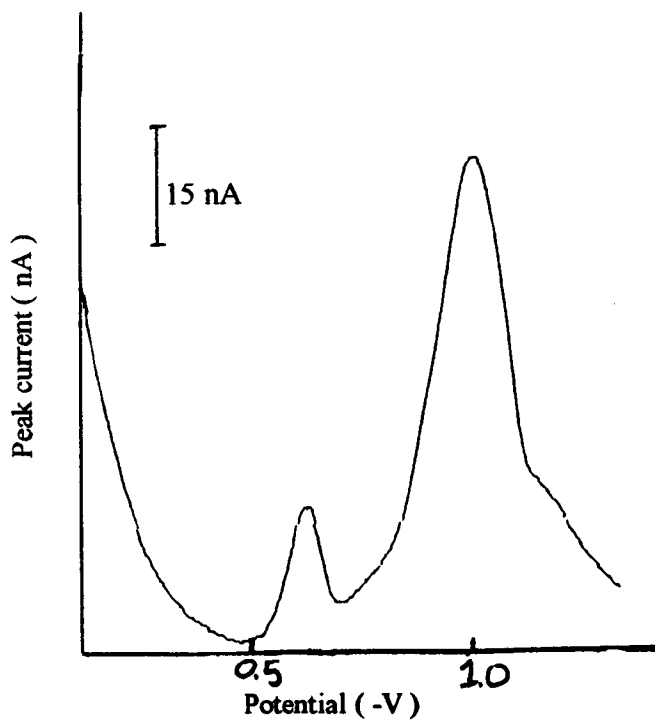


Figure 9.3: AdSV of 5×10^{-7} M of Reactive Red 120 in carbonate buffer (pH 10), accumulation time: 2 min, accumulation potential: 0.0 V, scan rate: 6 mV s^{-1} .

Table 9.1: Effect of supporting electrolyte constituent on the studied chlorotriazine-based azo reactive dyes' AdSV behaviour.

DYE	Buffer	Azo peak		Chlorotriazine peak	
		$E_p(-V)$	$i_p(nA)$	$E_p(-V)$	$i_p(nA)$
RO12	B-R Buffer	0.357	12.1	1.04	33.4
	Acetate	0.230	13.3	-	-
	Carbonate	0.603	20.2	1.08	9.2
RY84	B-R Buffer	0.353	6.2	1.04	15.3
	Acetate	0.270	4.3	-	-
	Carbonate	0.580	10.9	0.9	0.8
RR120	B-R Buffer	0.465	14.6	1.03	43
	Acetate	0.345	14.1	0.98	15.6
	Carbonate	0.750	42.3	0.9	85.9
RR24	B-R Buffer	0.479	12.7	1.03	27
	Acetate	0.353	10.9	1.03	8
	Carbonate	0.720	20.7	0.89	19.6

9.4 Optimum Conditions

9.4.1 Effect of pH

The effect of the variation of pH on the peak height and peak potential for the cathodic reduction of the azo peak signal was investigated. 1×10^{-7} mol l⁻¹ solution for all reactive dyes either bisazo or monoazo, was studied by AdSV in Britton-Robinson buffers of different pH values (2–12) after two minutes collection time at 0.0 V accumulation potential. The optimum pH for accumulating the RO12–RY84 system was found to be in the pH range 4–6. Generally, in basic medium (pH 7–11) virtually weak stripping voltammetric response was observed (see Fig. 9.4). The height of the azo peak decreased rapidly around pH 8, however, it showed a gradual increase beyond pH 10. In contrast, the stripping voltammetric peak current of the azo chromophore system for RR120–RR24 system reached its maximum values in pH 8–10. The behaviour of the peak current of these reactive dyes as a function of pH is represented in Fig. 9.5. In several of the studied pH values, the azo functional peak height for the bisazo reactive dyes (RO12 and RR120) was twice or more that for the monoazo reactive dyes (RY84 and RR24), respectively.

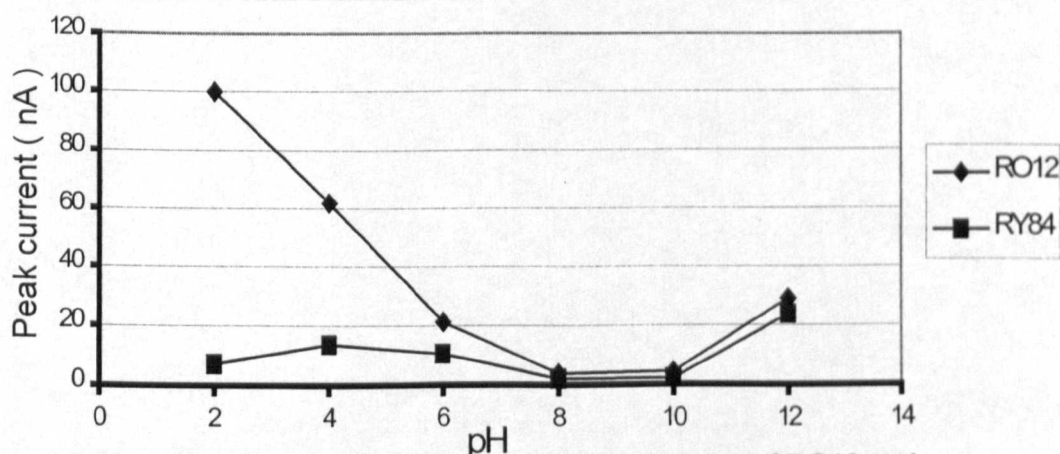


Figure 9.4: Effect of pH on peak current of azo group of RO12 and RY84

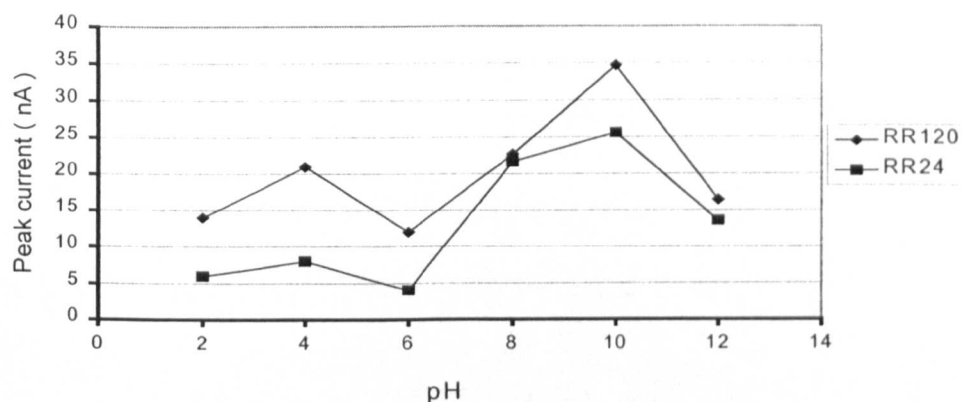


Figure 9.5: Effect of pH on peak current of azo group of RR120 and RR24

On the other hand, a gradual decrease in the peak current of chlorotriazine reactive group for RO12 – RY84 system when the pH value was increased from 2 to 12 was observed as can be extracted from Table 9.2. By contrast, in the case of RR120 – RR24, the influence of the variation of the sample solution pH value on the chlorotriazine peak was more complicated and fluctuated. However, the overall effect of increasing pH was a decrease in the chlorotriazine peak height.

The peak potential for the azo group was found to be dependent on the pH of the buffer solution. For all these reactive dyes a gradual shift to a more negative potential is observed for the azo wave potential with increasing pH from 2 to 12, showing consumption of hydrogen ions in the electrode reaction. A representation of the influence of pH on the peak potential for RO12–RY84 system is given in Fig. 9.6. The slopes of the E_p -pH linear plots for all these chlorotriazine-based azo reactive dyes were nearly equal. They were about 68, 63, 67 and 68 mV per pH unit (negative shift) for RY84, RO12, RR120 and RR24, respectively. However, as expected, no significant changes were perceived in the azo peak potential values when the reactive dyes molecular structure contain either single (monoazo) or double (bisazo) azo functional system.

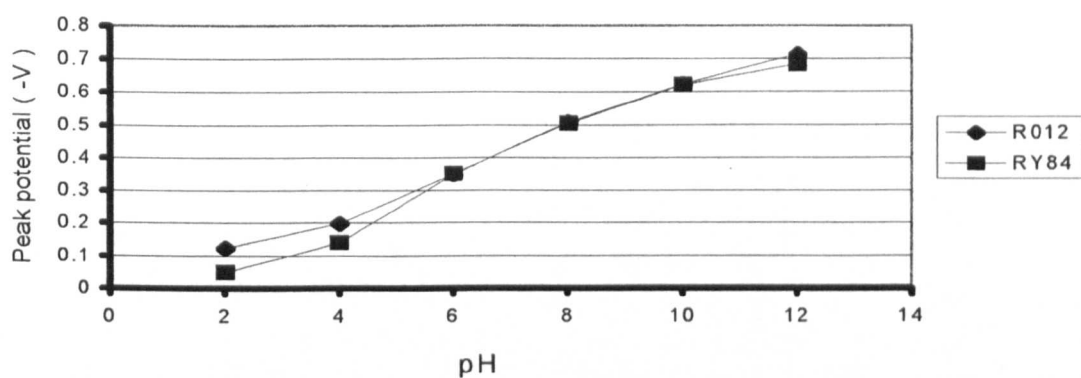


Figure 9.6: Effect of pH on peak potential of azo group of RO12 and RY84

Table 9.2: Effect of pH on the studied chlorotriazine-based azo reactive dyes' AdSV behaviour.

pH	RO12		RY84		RR120		RR24		
	E_p (-V)	i_p (nA)	E_p (-V)	i_p (nA)	E_p (-V)	i_p (nA)	E_p (-V)	i_p (nA)	
Azo Signal	pH 2	0.125	100	0.05	7	0.095	14	0.1	6
	pH 4	0.199	62	0.141	13.4	0.418	21	0.407	8
	pH 6	0.350	21.3	0.351	10.3	0.464	12	0.441	4
	pH 8	0.509	3.8	0.505	1.9	0.635	22.7	0.602	21.7
	pH 10	0.624	4.4	0.622	2.2	0.754	34.7	0.771	25.6
	pH 12	0.714	29.9	0.681	23.6	0.80	16.5	0.808	13.6
Chlorotriazine signal	pH 2	1.03	14	1.0	8.1	1.0	67	1.0	117
	pH 4	1.01	8.3	1.08	3.8	0.95	46	0.98	74.3
	pH 6	1.05	4.1	1.04	2.8	0.1	35	1.03	36.6
	pH 8	1.1	0.8	1.09	0.7	1.1	48	0.90	43.7
	pH 10	1.08	1.6	1.05	0.9	1.06	49.6	0.95	21.1
	pH 12	-	-	-	-	1.05	50.4	0.93	34.7

In brief, it is apparent that there is an analogy between the effect of pH on the AdSV response of RR120–RR24 system and that previously reported for the effect of the same parameter (pH) on the electrochemical behaviour of fluorotriazine-based azo reactive dyes 1, 2 and 3 (see section 7.5.1). In both cases, the azo functional moiety has an ortho-hydroxy electron-donating group. While the variation of pH caused similar results and outcomes on the adsorptive stripping voltammetric signals for both RO12–RY84 system and fluorotriazine-based azo reactive dye 4 (which are all have NHCONH₂ group rather than *o*-hydroxy group).

9.4.2 Effect of accumulation potential

In general, slight effects on the peak current of the azo moiety for RO12–RY84 was observed due to the variation of accumulation potential from 0.0 V to –0.5 V. Thus, the adsorptive accumulation of these reactive dyes RO12 and RY84 was shown to be nearly independent of preconcentration potential parameter; $E_{acc} = 0.0$ V was selected as an optimum value. However, the influence of this parameter on the AdSV azo group peak height for RR120–RR24 system is illustrated in Fig. 9.7. The azo peak current decreased sharply for accumulation potentials more positive than +0.1 V, however it increased slightly for accumulation potentials more negative than 0.0 V. Nevertheless, as accumulation potentials reached values more negatives than –0.4 V, the monitored peak current is substantially decreased. Therefore, the RR120–RR24 system has a wide range, 0.0 V to –0.4 V, which could be useful for accumulation of these reactive dyes. However, accumulation potential 0.0 V was chosen as an optimum potential.

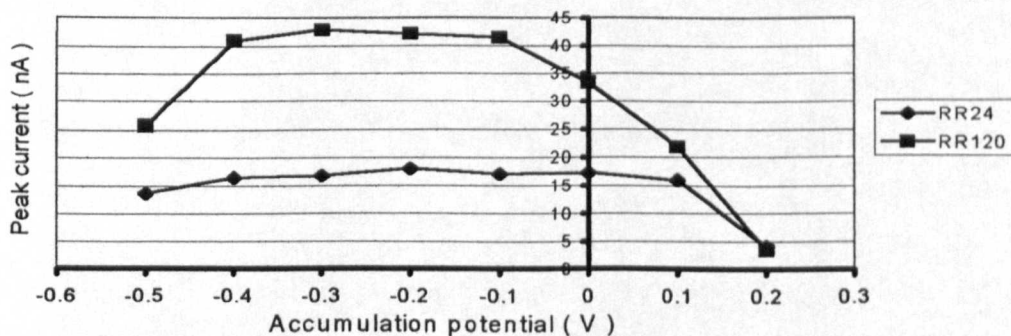


Figure 9.7: Effect of accumulation potential on peak height of azo group of RR24 and RR120

9.4.3 Effect of accumulation time

All these reactive dyes were found to adsorb strongly on the surface of the hanging mercury drop electrode (HMDE) in Britton-Robinson buffer. The peak height for the cathodic reduction of the azo functional group for these reactive dyes exhibits a proportional dependence on the duration of the accumulation time for lower dye concentration and/or shorter preconcentration times. Deviations from proportionality due to the saturation of the surface of the mercury drop occurred at relatively longer accumulation times of 180s and 210s for monoazo reactive dyes RY84 and RR24, respectively. In contrast, a rapid saturation of the surface of the working electrode is achieved after relatively shorter accumulation times of 120s and 150s for bisazo reactive dyes RO12, RR120, respectively. This indicates that reactive dyes, with bifunctional azo chromogen systems and double chlorotriazine reactive groups such as RO12 and RR120, had stronger adsorption properties on the HMDE. Consequently, their collection times, required for the full coverage of the mercury drop surface, is shorter. Furthermore, a slight shift in the negative direction for the azo signal peak potential was noticed when the accumulation period was continuously increased. Fig. 9.8 illustrates the effect of accumulation time T_{acc} for $5 \times 10^{-7} \text{ mol l}^{-1}$ reactive dye solution in B-R buffer at 0.0 V accumulation potential. A 120s and 60s time was adopted as the optimum accumulation time for monoazo reactive dyes (RY84 and RR24) and bisazo reactive dyes (RO12 and RR120), respectively.

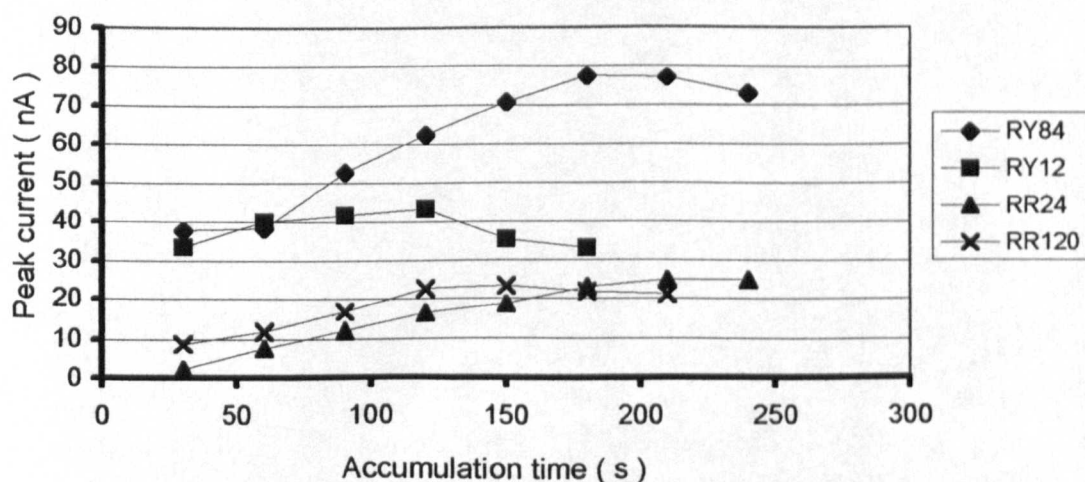
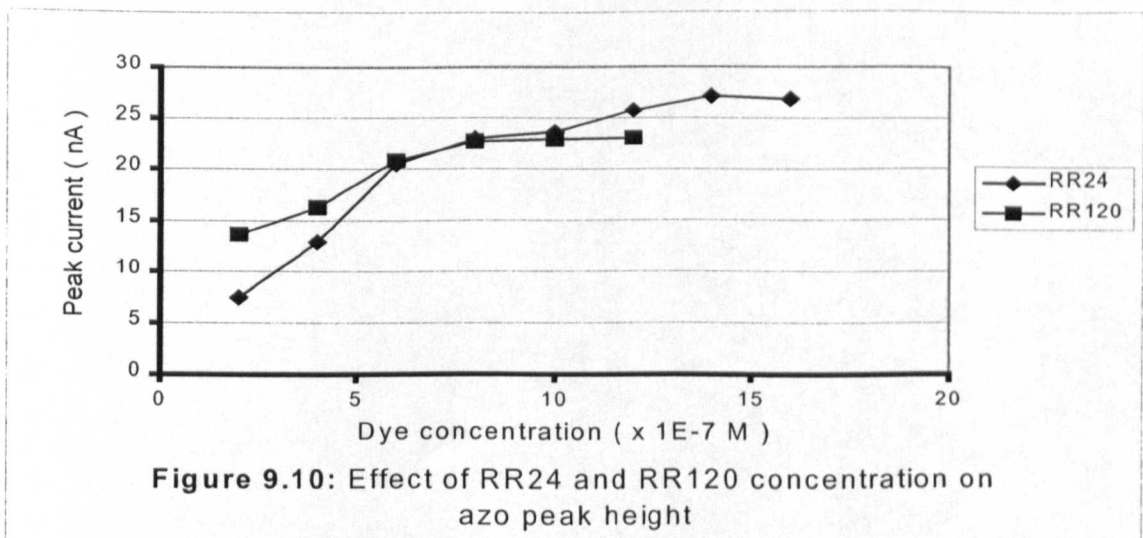
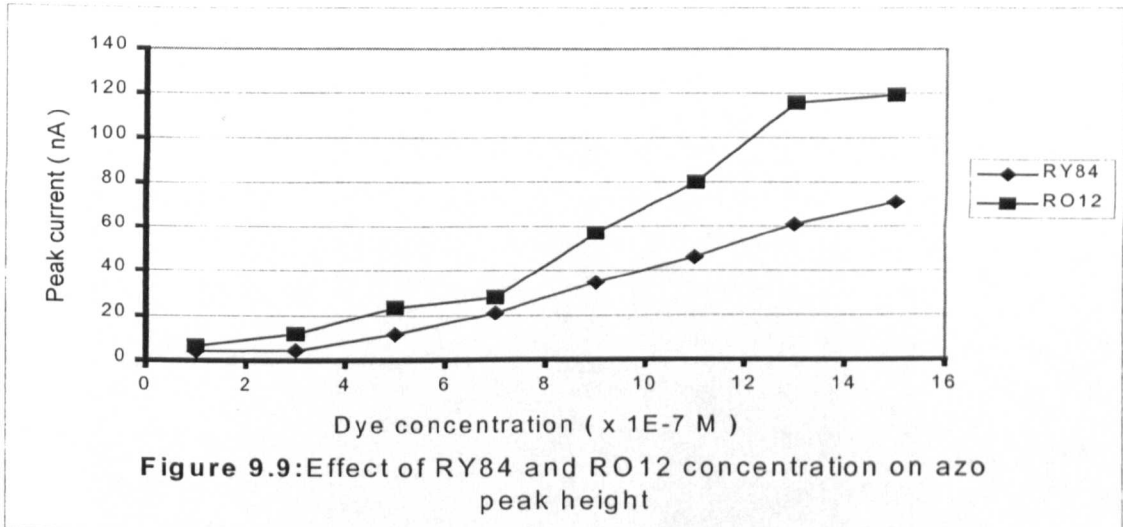


Figure 9.8: Effect of accumulation time on reactive dyes' azo peak current

9.4.4 Effect of reactive dye concentration

The adsorptive stripping voltammetric peak current of these reactive dyes increased as a function of their concentration. A similarity was found between the effect of accumulation time and reactive dye concentration on the azo group peak height i.e. a proportional relationship between the amount of the accumulated reactive dye and its quantity in the test solution. As can be seen from Fig. 9.9, the proportionality of the electrochemical response (monitored after 120s preconcentration time at 0.0 V accumulation potential in B-R buffer) with RO12 and RY84 concentration extends to 1.3×10^{-6} and $1.5 \times 10^{-6} \text{ mol l}^{-1}$, respectively. However, their peak potential exhibits a negative shift by 85 mV and 95mV, respectively, as the amount of the adsorbed reactive dye is increased as a function of its bulk concentration. However, if high concentration (more than $1.5 \times 10^{-6} \text{ mol l}^{-1}$) of RY84 was added gradually to the sample solution, the azo reduction peak of this reactive dye began to split with a second sharper peak appearing at a more negative potential. This is probably due to the complete formation (at a low concentration) of a monolayer of adsorbate. However, after the addition of more RY84 concentration, multilayers of adsorbate are formed and accumulated with different stripping voltammetric characteristics.

The dependence of azo peak current for the RR120-RR26 system on the concentration of the analysed reactive dye is shown in Fig. 9.10. A proportional relationship is observed for RR24 over $2 \times 10^{-7} \text{ mol l}^{-1}$ – $1.4 \times 10^{-6} \text{ mol l}^{-1}$, while for RR120 the proportional range is extending only to about $8 \times 10^{-7} \text{ mol l}^{-1}$. Beyond the linearity point, the peak current reached a plateau because of the saturation of the working electrode. However, the variation of these reactive dyes concentration has no significant effect on the peak potential for the azo group AdSV response. In brief, deviations from proportionality due to total coverage for the surface of the HMDE occurred at relatively diluted reactive dye concentrations for the analytes that had bifunctional azo and chlorotriazine groups such as RO12 and RR120.



9.4.5 Effect of scan rate

The cathodic peak currents of these reactive dyes were found to be directly proportional to the scan rate, particularly at low scan rate values, a phenomenon characterised for adsorbed material⁷. The effect of scan rate parameter on the azo functional group peak current and potential for RO12–RY84 system is summarised in Table 9.3. The peak height of the cathodic peak is linearly dependent on the scan rate up to 6 or 8 mV s^{-1} , thus indicating an adsorption phenomenon. However, a negative shift in the azo moiety peak potential by 22 mV and 24 mV for RY84 and RO12, respectively, was also observed with increasing scan rate which indicates a degree of irreversibility of the electrode process⁸. Similarly, for the RR120–RR 24 system, the azo peak current, obtained under constant experimental conditions, increased linearly with scan rate. For RR24, a negative shift in the cathodic peak potential from -591 mV to -650 mV was observed when the scan rate was changed from 2 to 12 mV s^{-1} . Equally, a cathodic shift by -64 mV was observed for RR120 under the same experimental conditions. However, apart from enhancing the stripping voltammetric peak current, it seems that the introducing of the double azo functional group in the reactive dye molecule has no significant influence when the scan rate experimental parameter was varied. In other words, the effect of the variation of scan rate on the azo peak height was nearly identical, regardless of whether the molecular structure of the investigated reactive dye was composed of a mono or bifunctional azo system.

Table 9.3: Effect of scan rate on the chlorotriazine reactive dyes' AdSV behaviour.

Scan Rate	RO12		RY84		RR120		RR24	
	E_p (-V)	i_p (nA)	E_p (-V)	i_p (nA)	E_p (-V)	i_p (nA)	E_p (-V)	i_p (nA)
2 mV s^{-1}	0.505	26.3	0.503	9.7	0.583	8	0.591	6.1
4 mV s^{-1}	0.512	33	0.509	18.5	0.613	15.7	0.614	10.3
6 mV s^{-1}	0.516	37.2	0.514	21	0.625	20.2	0.629	14.1
8 mV s^{-1}	0.522	41.9	0.520	21.6	0.630	24.6	0.639	20.3
10 mV s^{-1}	0.526	42.8	0.525	23.8	0.640	35	0.649	24.9
12 mV s^{-1}	0.529	44.2	0.525	25.8	0.647	40.3	0.650	32.3

9.5 Analytical Application

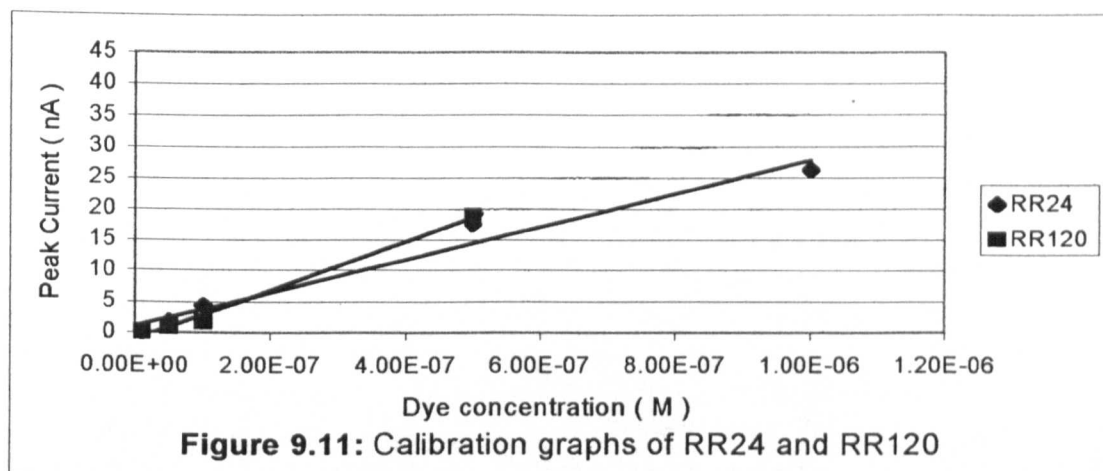
On the basis of the previously reported preliminary investigations, the applicability of the proposed AdSV procedure, as an analytical method for the determination of ultra-trace levels of these chlorotriazine-based azo reactive dyes, was evaluated.

9.5.1 Calibration graph

Calibration graphs over a relatively wide concentration range of the studied reactive dyes from 1×10^{-8} to 5×10^{-7} mol l⁻¹ for the bisazo reactive dyes RO12 and RR120 were obtained. In contrast, the calibration graphs for the reactive dyes that were composed of a single azo functional group, namely RY84 and RR24 can be extended further to a 1×10^{-6} mol l⁻¹ level before the saturation of the surface of HMDE. Figure 9.11 reflects the previous remarks and outcomes for the calibration graphs obtained from adsorptive stripping voltammograms for RR120 and RR24 reactive dyes recorded after an accumulation time of 120 s at 0.0 V preconcentration potential. The slopes of the linear region of the calibration plot for RR120–RR24 system calculated from the least-squared treatment of the calibration graph were 0.039 and 0.027 A/mol l⁻¹ for RR120 and RR24, respectively. The correlation coefficient for RR120 and RR24 reactive dyes were 0.996 and 0.99 with intercept values of -1.06 nA and 1.14 nA, respectively. As a result, the regression equations for the calibration lines for these reactive dyes had the form:

$$\text{RR120} \rightarrow i_p(\text{A}) = -1.06 \times 10^{-9} + 0.039 C (\text{mol l}^{-1}) \quad r = 0.996 \quad n = 5$$

$$\text{RR24} \rightarrow i_p(\text{A}) = 1.14 \times 10^{-9} + 0.027 C (\text{mol l}^{-1}) \quad r = 0.99 \quad n = 6$$



9.5.2 Detection limits

The detection limit under the optimum experimental conditions were estimated to be slightly lower for bisazo RO12 ($8.2 \times 10^{-9} \text{ mol l}^{-1}$) than that for monoazo RY84 ($9.9 \times 10^{-9} \text{ mol l}^{-1}$). However, the detection limits for RR120 and RR24 were found to be around $9.9 \times 10^{-9} \text{ mol l}^{-1}$ and $8.3 \times 10^{-9} \text{ mol l}^{-1}$, respectively. The detection limit was calculated as three times the standard deviation of the determination of the reactive dye at the $1 \times 10^{-7} \text{ mol l}^{-1}$ level. The conditions for the estimation of this detection limit were; supporting electrolyte B-R buffer (pH 6 or pH 8); accumulation time two minutes; accumulation potential 0.0 V and scan rate 6 mV s^{-1} .

9.5.3 Reproducibility and stability

The Reproducibility of the analytical method for the determination of these reactive dyes was evaluated by making successive measurements on eight $1 \times 10^{-7} \text{ mol l}^{-1}$ reactive dye solutions. The relative standard deviation (% RSD) for RY84 and RR120 was 3.2%, whereas it was as low as 2.1% and 2.4% for RR24 and RO12, respectively. Finally, the azo electrochemical response of $1 \times 10^{-7} \text{ mol l}^{-1}$ reactive dye solution appeared to be stable for a period of two hours at least.

The values of correlation coefficients, linear ranges, line slopes and intercepts yielded from the least-squared treatment of the calibration graph of RO12, RY84, RR120 and RR24 are listed in Table 9.4.

Table 9.4: The Least-Square treatment of the calibration graph of the Reactive Dyes.

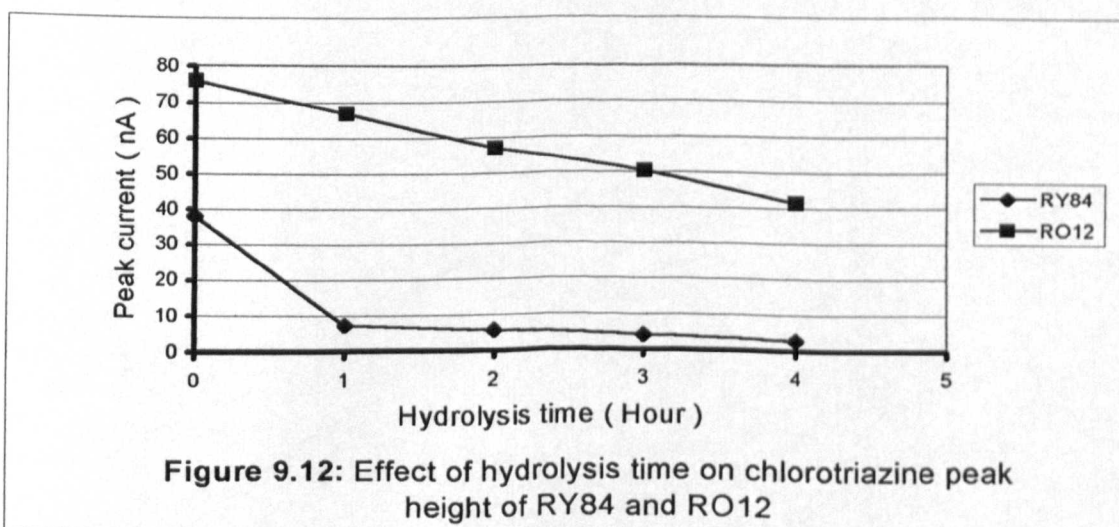
Reactive Dyes	Linear Range (mol l ⁻¹)	Slope (A mol ⁻¹ l)	Intercept (nA)	Correlation Coefficient	Detection Limits (mol l ⁻¹)	%RSD
RO12	1×10 ⁻⁸ -5×10 ⁻⁷	0.063	5.19	0.95	8.2×10 ⁻⁹	2.7
RY84	1×10 ⁻⁸ -1×10 ⁻⁶	0.035	-1.27	0.998	9.9×10 ⁻⁹	3.2
RR120	1×10 ⁻⁸ -1×50 ⁻⁷	0.039	-1.06	0.996	9.9×10 ⁻⁹	3.2
RR24	1×10 ⁻⁸ -1×10 ⁻⁶	0.027	1.14	0.99	6.3×10 ⁻⁹	2.1

9.6 Hydrolysis Studies

The impact of the competition reaction yielded from the hydroxide attack on the chlorotriazine reactive group with the possible discrimination between the original chlorotriazine reactive dyes and their hydrolysed forms were also investigated by AdSV. In fact, the hydrolysis process for these reactive dyes was to some degree comparable to that previously reported for the fluorotriazine reactive dyes. The replacement of the active chlorine atom on the triazine ring by the hydroxide group was attempted by heating 1 × 10⁻⁴ mol l⁻¹ of each reactive dye in 0.1 mol l⁻¹ carbonate buffer at 80°C for 4 hours. The hydrolysis process of these chlorotriazine-based azo reactive dyes can be followed voltammetrically by successive removal of the reactive dye test solutions during the course of hydrolysis process and monitoring the gradual decrease in the chlorotriazine electrochemical response.

For RO12–RY84 system there is no significant change in the peak potential of the chlorotriazine-anchoring group for all the analysed reactive dyes in going from the original reactive dye to the hydrolysed form. In contrast, the peak current of this reactive group exhibited a gradual decrease with the duration of the hydrolysis time.

Consequently, the hydrolysed reactive dye can be differentiated from the original non-hydrolysed reactive dye by monitoring the loss or deterioration of the stripping voltammetric signal corresponding to the cathodic reduction of the chlorotriazine reactive group. However, as can be seen from Fig. 9.12, which illustrates the decrease of the chlorotriazine peak height as a function of the hydrolysis time, the rate of the hydrolysis process for these reactive dyes was very slow. In fact, after 4 hours of the hydrolysis reaction nearly 52% and 8% of the initial peak height remained for RO12 and RY84, respectively. Based on the previous values and findings, it is obvious that the progress of hydrolysis process for RY84 was much faster than that for RO12. After 4 hours hydrolysis times, the peak current for the chlorotriazine group of RY84 substantially decreased, whereas for RO12 nearly half its original value remained after the hydrolysis experiment. The reason for the slow hydrolysis rate for RO12 is probably related to the presence of the double chlorotriazine anchoring systems, which effectively resist the hydrolysis competition reaction compared to the RY84 which has only a mono-chlorotriazine system. Accordingly, RO12 reactive dye with bifunctional chlorotriazine anchoring and reactive systems is probably has higher fixation rate with improved wash-fastness compared to RY84 mono-anchor reactive dye. However, the hydrolysis process has no significant effect on either the azo functional group peak current or potential for both RO12 and RY84.



Nonetheless, the exchange of the halide substituent with hydroxyl groups for other chlorotriazine-based anthraquinone reactive dyes namely Procion Blue MX-R and Cibacron Blue 3GA⁹ and a chlorotriazine-based azo dye¹⁰ was complete and the peak due to the chlorotriazine reduction was completely eliminated after only 1 hour hydrolysis period. However, despite the various experimental investigations and attempts to identify and hence illuminate the reason for such very slow hydrolysis reaction for RO12–RY84 system, the cause for such odd and slow hydrolysis reaction for these reactive dyes compared to other chlorotriazine reactive dyes is not fully understood at this stage (refer to section 7.7).

On the other hand, similar results were obtained for the hydrolysis of RR120 compared to that obtained for RO12. The chlorotriazine reduction signal decreased continuously with the length of the heating time till it reached 50% of its initial peak current after 4 hours of heating. In comparison, the rate of hydrolysis process of RR24 was also very slow i.e. after 4 hours heating period, the peak current due to the cathodic reduction of the chlorotriazine reactive group decreased to about 42% of its original value. Unlike RY84, which was affected considerably by the long hydrolysis process, RR24 behaves similarly (under constant hydrolysis conditions) to the double-anchor bisazo reactive dyes, RR120 and RO12. Finally, a methanolysis process (3% methanol) for the studied reactive dyes over 2 hours experimental duration time at room temperature was also attempted. A slight chlorotriazine peak current reduction was observed suggesting that the rate of methanolysis process is also very slow.

9.7 Conclusions

These chlorotriazine-based azo reactive dyes can be successfully monitored at low trace levels by differential pulse adsorptive stripping voltammetric at a HMDE via the cathodic reduction peaks of azo functional group and/or chlorotriazine reactive system. It was confirmed in the present investigation, that introducing and adding of a further azo functional and chlorotriazine reactive groups to the molecular structure of the chlorotriazine-based bisazo reactive dyes, led to a significant enhancement in their electrochemical signal and adsorption properties compared to the chlorotriazine-based monoazo reactive dye. Optimum experimental conditions were also given for the AdSV determination of the reactive dyes in aqueous solution. A linear range from 1×10^{-8} mol l⁻¹ to 5×10^{-7} or 1×10^{-6} mol l⁻¹ depending on the number of the azo functional systems that exist in the reactive dye molecule with a reasonable detection limits and relative standard deviations were achieved. For RO12-RY84 system, it was found that chlorotriazine-based bisazo reactive dyes with double anchoring systems had higher tolerance and resistance to the competition of hydrolysis attack. Finally, the sensitivity, simplicity and accuracy of this analytical procedure reveal its reliability for the determination of these reactive dyes.

REFERENCES

- 1 Goyal, R.N., Verma, M.S. and Singhal, N.K., *Croat. Chem. Acta*, **71**, (1998), 715.
- 2 Goyal, R.N. and Kumar, A., *India. J. Chem.*, **27**, (1988), 482.
- 3 Malik, W.U., Goyal, R.N. and Mathur, N.C., *J. Electroanal. Chem.*, **235**, (1987), 225.
- 4 Goyal, R.N. and Minocha, A., *J. Electroanal. Chem.*, **193**, (1985), 231.
- 5 Barek, J., Tietzova, B. and Zima, J., *Collect. Czech. Chem. Commun.*, (1987), **52**, 867.
- 6 Barek, J., Balsiene, J., Tietzova, B. and Zima, J., *Collect. Czech. Chem. Commun.*, (1989), **54**, 1538.
- 7 Van den Berg, C.M.G. and Li, N., *Anal. Chim. Acta*, **212**, (1988), 31.
- 8 Gilmartin, M.A.T. and Hart, J.P., *Analyst*, **117**, (1988), 1613.
- 9 Zanoni, M.V.B., Fogg, A.G., Barek, J. and Zima, J., *Anal. Chim. Acta*, **349**, (1997), 101.
- 10 Barek, J., Fogg, A.G., Moreira, J.C., Zanoni, M.V.B. and Zima, J., *Anal. Chim. Acta*, **320**, (1996), 31.

APPLICATION OF AdSV TO THE ANALYSIS OF BISAZO REACTIVE DYES BASED ON THEIR COPPER (II) COMPLEXES AT THE HMDE

10.1 Introduction

Adsorption stripping voltammetry is well suited for the determination of ultratrace amounts of organic compounds and/or inorganic ions through their complexes. Recent studies on the applicability of AdSV for the indirect determination of low concentrations of various synthesised azo dyes such as Reactive Violet 5¹ and Sulfonate azo dyes (Acid Alizarin Violet N and Plasmocorith B)², as well as several azo-based ligands e.g. Beryllon III³, Phenazopyridine⁴ and some heterocyclic azo compounds⁵, had indicated that these azo compounds can be monitored by AdSV preceded by adsorptive collection of their complexes with copper (II) onto the hanging mercury drop electrode (HMDE). As is the case with these azo dyes and ligands, Reactive Blue 171 and Reactive Red 141 which both are chlorotriazine-based bisazo dyes, were found to be determinable indirectly by AdSV after nonelectrolytic accumulation of their copper (II) complexes on the surface of the HMDE followed by measuring the accumulated analyte during the cathodic scan.

10.2 Aim of the Study

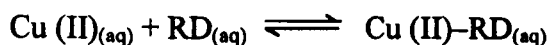
Apart from the study of Reactive Violet 5, no detailed study on the stripping voltammetric behaviour of the copper (II) complexes with azo-based reactive dyes has been reported in the current literature. Considering the above remark and the lack of available data for the indirect determination of bisazo synthetic dyes that contain bifunctional azo systems which both can develop complexes with copper (II) ions, the aim of this work was, therefore, to investigate the electrochemical properties of two chlorotriazine-based bisazo reactive dyes via their copper (II) complexes. Furthermore, a detailed study was carried out to evaluate the effect of the main

experimental variables that control the formation of Copper (II)–Reactive dye complexes and hence their adsorption processes onto the surface of the HMDE.

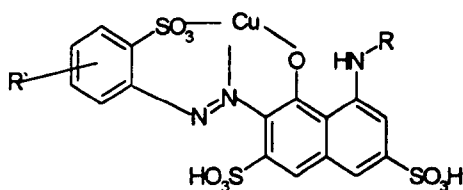
10.3 Electrode Reduction Process

Highly sensitive measurements of synthetic dyes and/or metal ions can be achieved by means of the adsorptive stripping voltammetric procedure based on the spontaneous adsorption of e.g. Cu (II)–Reactive dye complex which can be employed as an effective accumulation step prior to the voltammetric measurements. The reduction paths of the complexes of several azo ligands particularly di-*o*-hydroxyazo compounds with a range of metal ions has been reported and reviewed⁶⁻⁹. However, the overall procedure of this electroanalytical approach involves the formation of an appropriate surface-active/metal ion complex, its interfacial collection onto the HMDE and consequently the stripping voltammetric analysis of the metal-ligand surface bound complex. In fact, the possible electrochemical reduction path for the Copper (II)/Reactive dye complex can be divided into three steps according to the following scheme:

Step 1: Homogeneous reaction in the bulk of the test solution



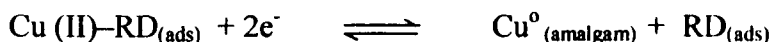
These bisazo-based reactive dyes probably act as tridentate ligands, with the azo nitrogen group forming a co-ordinate link with the copper (II) ions. The proposed structure for the Copper (II)–Reactive dye complex is represented schematically as:



Step 2: Adsorption accumulation. The Cu(II)/Reactive dye chelate can be concentrated and accumulated onto the working electrode surface (HMDE) owing to its surface-active property. The interfacial adsorption process can be expressed as:



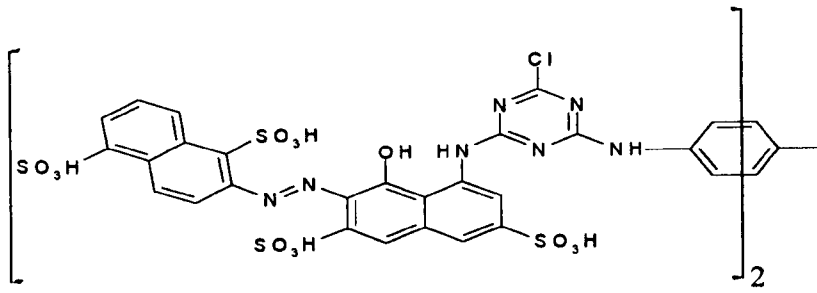
Step 3: Reduction of the adsorbed reactant. The adsorbed Cu(II)/Reactive dye complex is eventually reduced at the HMDE surface and the measurement step consists of electrochemically reducing the copper ion in the adsorbed reactant. This can be described as follows:



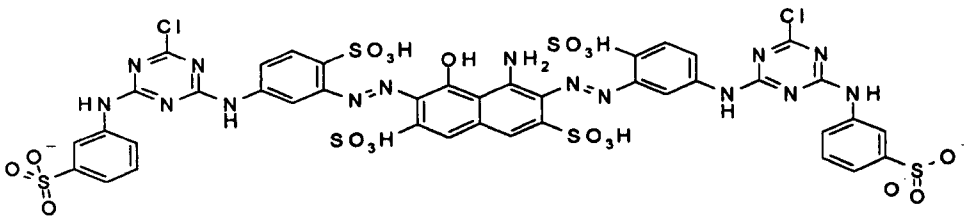
However, the resulting product of this reduction process also has a surface-active property and can undergo further cathodic reduction for the bifunctional azo groups and/or chlorotriazine reactive systems as described in the previous chapters.

10.4 Adsorptive Stripping Peak of Cu (II)-Reactive Dye

The molecular structure of C.I. Reactive Blue 171 (Procion Navy H-ER) and C.I. Reactive Red 141 (Procion Red HE-7B) used in this study are represented in Fig. 10.1. When accumulation was effected at potential 0.0 V, analytically useful reduction peaks were obtained by differential pulse adsorptive stripping voltammetry in B-R buffer (pH 4), acetate buffer (pH 5) and carbonate buffer (pH 10) which all contain $5 \times 10^{-7} \text{ mol l}^{-1}$ RB171 or RR141 solutions with trace concentration of copper (II) ions ($5 \times 10^{-6} \text{ mol l}^{-1}$). Typical adsorptive stripping voltammogram of RB171 at $5 \times 10^{-7} \text{ mol l}^{-1}$ level in B-R buffer is shown in Fig. 10.2. Adsorptive collecting of the reactive dye molecules for 60s, usually resulted in three cathodic reduction peaks. The first cathodic peak at -209 mV peak potential with 33.7 nA peak current was suggested to be due to the electrochemical reduction of copper (II) ions in the Reactive dye/Cu (II) complex to copper amalgam. The second stripping voltammetric response at $E_p = -330 \text{ mV}$ ($i_p = 18.4 \text{ nA}$) is probably associated with the reduction of the two azo chromogen functional moieties. However, the reduction process for the two chlorotriazine reactive systems is thought to be attributed to the third AdSV wave obtained at $E_p = -950 \text{ mV}$ and -1.02 V . In addition, a pre-peak in front of, but unresolved from, the Copper (II)-RB 171 complex wave was apparent at $E_p = -57 \text{ mV}$ ($i_p = 15.8 \text{ nA}$), which is believed to be related to the cathodic reduction of the free copper (II) ions (not complexed by the reactive dye).



Reactive Red 141



Reactive Blue 171

Figure 10.1: The molecular structure of the tested bisazo reactive dyes.

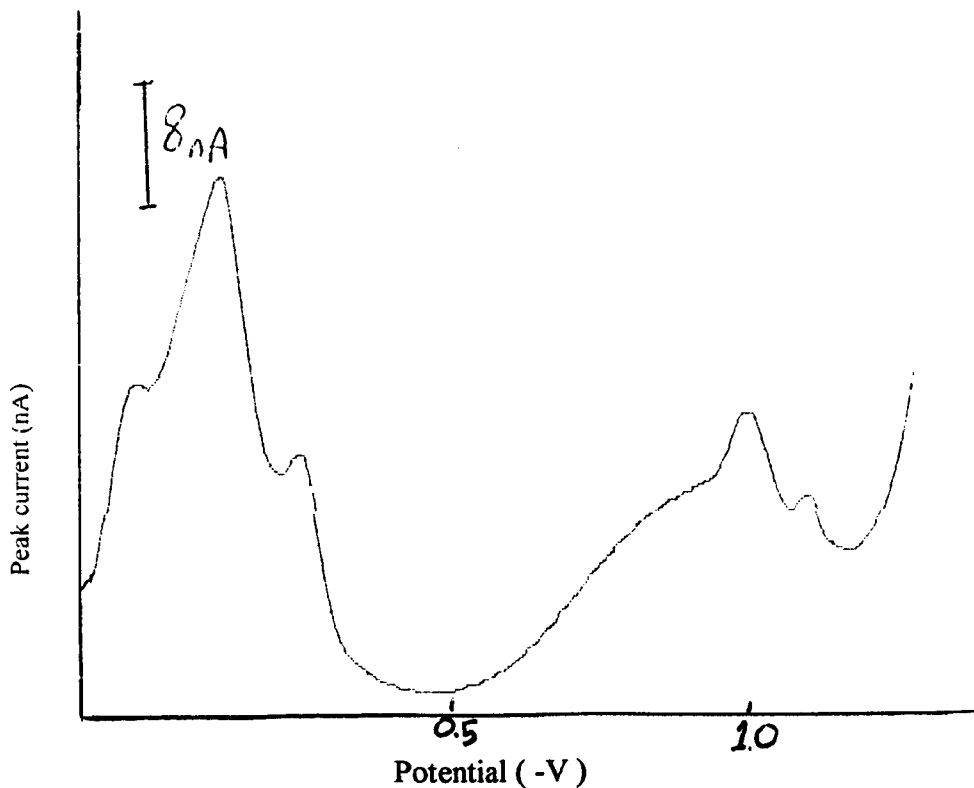


Figure 10.2: AdSV of 5×10^{-7} M Reactive Blue 171 in the presence of 5×10^{-6} M Cu (II), in B-R buffer at pH 4 after accumulating for 2 min at 0.0 V with 6 mV s^{-1} scan rate.

Clearly, this RB171 reactive dye can be monitored directly via the reduction of its azo and/or chlorotriazine groups or alternatively it can be monitored indirectly by its copper (II) complex. Since one azo functional moiety in the RB171 molecular structure has an ortho-amino substitution to the azo system rather than ortho-hydroxy substitution, the copper ions may not be incorporated into an appropriate ring system. Hence this extra azo functional group may not undergo complex reaction with Cu (II) metal ions, and accordingly only one half of the bifunctional azo system present in the bisazo RB171 molecule will act as a chelating agent.

On the other hand, RR141 has a symmetrical molecular structure i.e. both the azo moieties had an ortho-hydroxy substitution, therefore, both the azo functional systems can develop a complex with copper (II) ions. Furthermore, due to the fact that there is no variation in the chemical environment around these azo centres, the AdSV response for the electrochemical reduction of Cu (II)/Reactive dye complexes on both edges of the RR141 molecule will be identical and appeared at the same position on the adsorptive stripping voltammogram. Similar conclusions and outcomes are expected for the stripping voltammetric response of the two azo moieties present in the reactive dye molecules. Confirmation for the above remarks can be extracted from the adsorptive stripping voltammogram of 5×10^{-7} mol l⁻¹ RR141 in B-R buffer (pH 4) given in Fig. 10.3. In acidic solution, it is more often that the AdSV peaks due to the cathodic reduction of azo moiety and Reactive dye/Cu (II) complex are not completely resolved and separated. Therefore, the presence of two large electrochemical signals related to the reduction of the bifunctional azo systems, as well as the reduction of two Metal-Reactive dye chelates in a limited location, will result in one single overlapped AdSV peak as can be observed for the considerable AdSV wave obtained at peak potential = -257 mV with 73.7 nA peak current (see Fig. 10.3). In addition, the consumption of the free copper (II) ions is high in the situation when both the present azo groups for RR141 can develop and form a Metal-Dye complex. This can be proved and verified from the absence of the AdSV peak which, is thought to be corresponded to the cathodic reduction of the free copper (II) ions from the stripping voltammogram of RR141. However, this reactive dye shows a pair of AdSV peaks at peak potential of -950 mV and -1.13 V (the latter signal is a well-defined peak with 109 nA peak current). These adsorptive voltammetric peaks are believed to be due to the reductive elimination of the active chlorine atoms on the triazine ring.

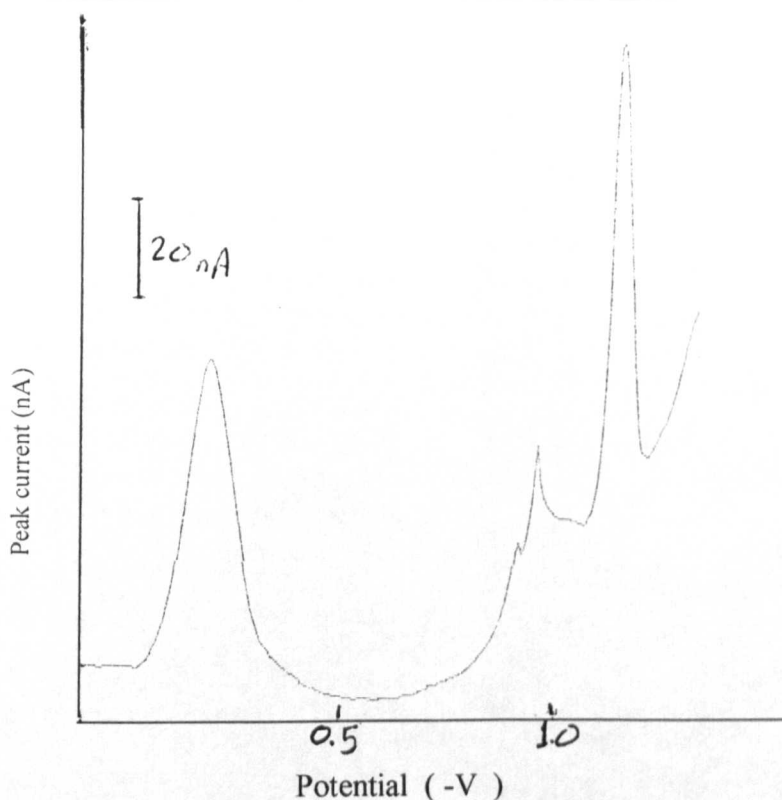


Figure 10.3: AdSV of 5×10^{-7} M Reactive Red 141 in the presence of 5×10^{-6} M Cu (II), in pH 4 B-R buffer. T_{acc} : 2 min, E_{acc} : 0.0 V, scan rate: 6 mV s^{-1} .

10.5 Parameters Affecting Adsorptive Stripping Behaviour

10.5.1 Effect of supporting electrolyte constituent

Preliminary experiments were carried out in various supporting electrolytes in order to examine their utility for the determination of these reactive dyes by AdSV. The chlorotriazine-based bisazo reactive dyes, RB171 and RR141 in acetate buffer (pH 5), yielded a similar AdSV behaviour to that observed with B-R buffer (pH 4). In pH 5 acetate buffer, the stripping voltammogram obtained for RB171 exhibited three AdSV peaks, one for the Cu (II)/RB171 complex at $E_p = -153 \text{ mV}$ with peak current of 19.89 nA. The second electrochemical wave for the azo moiety of the free reactive dye molecules obtained at -249 mV ($i_p = 16.9 \text{ nA}$), whereas the third stripping voltammetric peak related to the cathodic reduction of the chlorotriazine reactive group was observed at -1.06 V . In contrast, RR141 yielded only two AdSV signals, one large electrochemical peak at $E_p = -184 \text{ mV}$ and with 32 nA peak current. This AdSV peak is believed to have resulted from the overlapping of the cathodic reduction of the RR141-Copper (II) complex and the bifunctional azo systems of the free RR141. This electrochemical behaviour is in agreement with the results and findings that were obtained when employing pH 4 B-R buffer as a supporting electrolyte. The

second stripping voltammetric response was a pair of peaks at -995 mV and -1.175 V with peak currents of 64.4 nA and 48.5 nA, respectively. These latter AdSV signals were suggested to be associated with the reduction of the chlorotriazine reactive systems.

However, both RB171 and RR141 measured in pH 10 carbonate buffer, exhibited three well-developed and well-separated AdSV peaks corresponding to the reduction of the adsorbed Copper (II)-Reactive dye complex and to the azo and chlorotriazine systems of the adsorbed free reactive dye. As can be seen from Fig. 10.4, the overlap between the Cu (II)-Reactive dye peak and the azo peak for RR141 was resolved due to the negative shift in the peak potential of the azo functional moiety of RR141 at higher pH solutions. In pH 10 carbonate buffer the resolution of the peak potential between Reactive dye/Cu (II) peak and the free azo peak was 420 mV and 427 mV for RB171 and RR141, respectively. Accordingly, for RR141, the subsequent studies were carried out in pH 10 carbonate buffer solution or alternatively with Britton-Robinson solution at high pH values. However, B-R buffer solutions were a convenient media for the determination of RB171 at various pH values (e.g. pH 2-12). Table 10.1 summarises the influence of the buffer composition on the peak potential and peak current of the adsorbed Cu (II) /Reactive dye complex, azo and chlorotriazine groups for the studied reactive dyes in various supporting electrolytes.

Table 10.1: Influence of supporting electrolyte on reactive dyes' AdSV behaviour.

DYE	Buffer	Cu(II)/Dye peak		Azo peak		Chlorotriazine	
		E_p (-V)	i_p (nA)	E_p (-V)	i_p (nA)	E_p (-V)	i_p (nA)
RB171	B-R Buffer	0.209	33.7	0.330	18.4	1.02	20.5
	Acetate	0.153	19.9	0.249	16.9	1.06	8.4
	Carbonate	0.254	23.7	0.674	7.2	0.851 1.07	37.5 9.1
RR141	B-R Buffer	Overlapped $E_p=0.257$ $i_p=73.7$				0.950 1.13	15 109
	Acetate	Overlapped $E_p=0.184$ $i_p=32$				0.995 1.175	64.4 48.5
	Carbonate	0.263	25.5	0.720	15.9	1.01	47.2

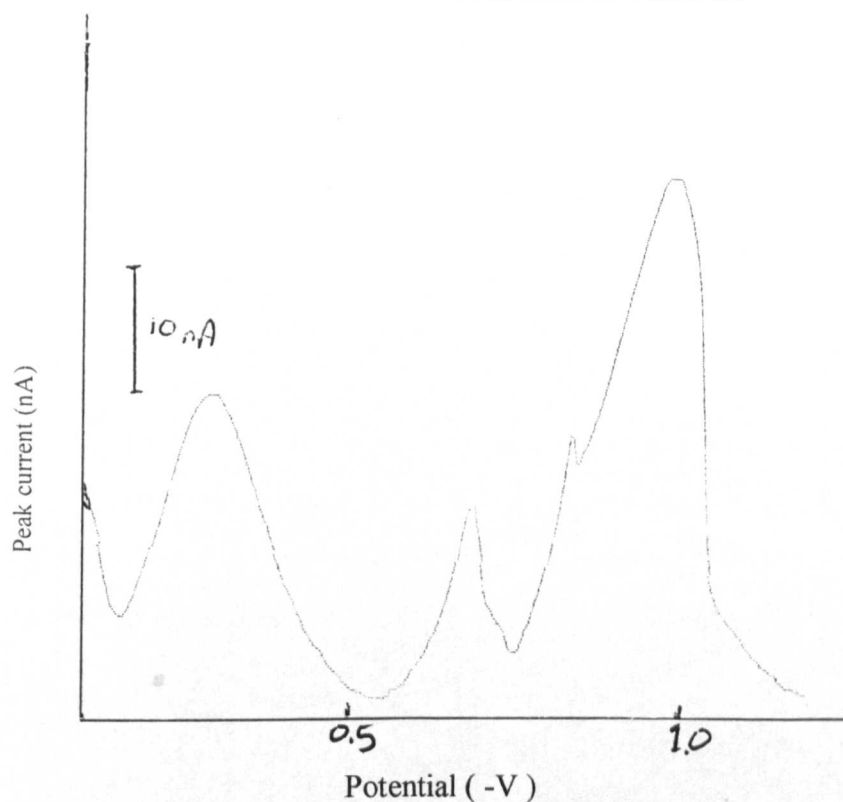


Figure 10.4: AdSV obtained for $5 \times 10^{-7} \text{M}$ RR 141 in the presence of $5 \times 10^{-6} \text{M}$ Cu (II), in pH 10 carbonate buffer. $E_{\text{acc}} = 0.0 \text{ V}$ and $T_{\text{acc}} = 2 \text{ min}$ and scan rate = 6 mV s^{-1} .

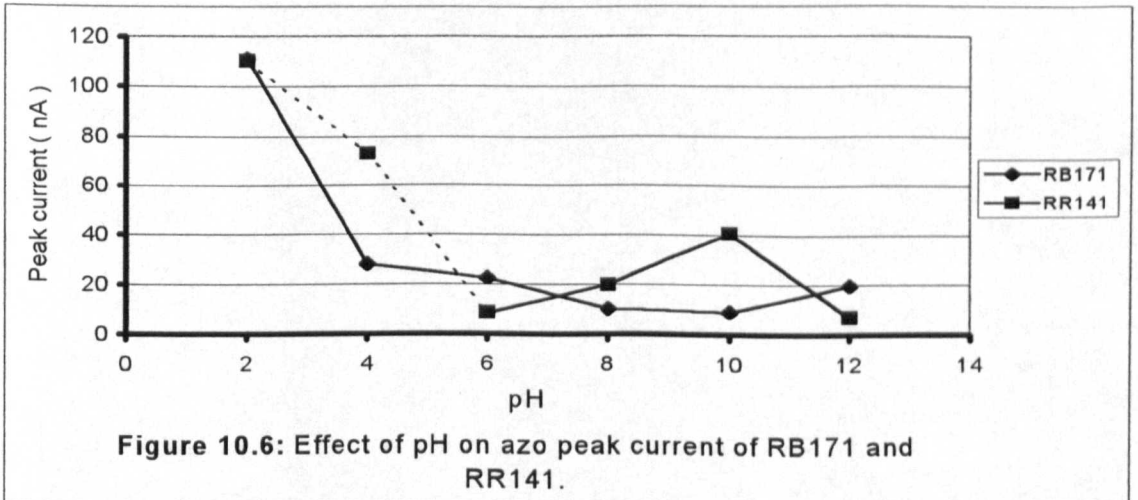
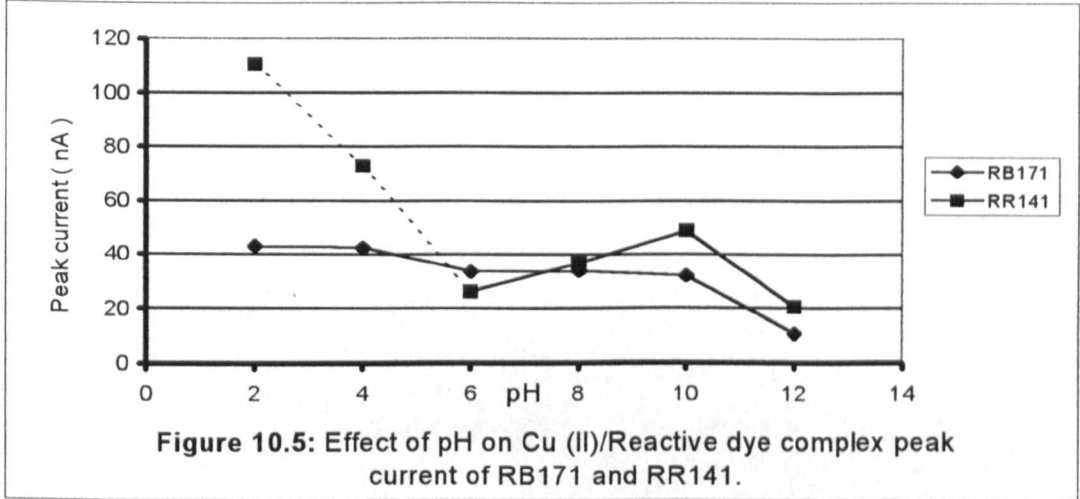
10.5.2 Effect of pH

The test solution pH value is a crucial parameter owing to its influence on the stability of the Reactive dye/Copper (II) complex, and therefore, it affects its peak potential as well as its peak height. Consequently, a detailed study of the effect of pH on the measurement of the free reactive dye ligands and their metal complexes has been performed. This is shown in Fig. 10.5, in which the peak height of Cu (II)-Reactive dye complex of RB171 and RR141 is plotted as a function of pH after two minutes accumulation period at 0.0 V in B-R buffer solution containing $5 \times 10^{-7} \text{ mol l}^{-1}$ reactive dyes. For RB171, the study of the effect of pH on the complex peak current showed that an acidic medium with pH values 2–4 represents the best experimental condition for the analysis of the Cu (II)-RB171 complex. Variations in pH over the range 2–4 did not markedly affect the complex AdSV peak current, whereas at a pH more than 6, the peak current gradually decreased till it rapidly dropped between pH 10 and 12. In comparison, although large electrochemical signals were observed at low pH values for RR141, it appears that the optimal pH value for the monitoring of

RR141-Cu(II) complex signal may be within the pH range 8–10. This alkaline solution provided 300–400 mV peak potential resolution and separation between the complex peak and the free ligand azo peak with reasonable peak currents.

With the exception of the neutral pH solution, for most of the studied pH values, the Cu (II) /Reactive dye complex peak current for RR141 was higher than that obtained for RB171, which supports the assumption that RR141 has two azo functional systems, which both can undergo complex formation with copper (II) ions, whereas RB171 has only one azo functional group applicable for such complex formation. However, the adsorption process and the stability of the formed Reactive dye-Cu (II) complex in alkaline solution are generally low, as can be noticed for RB171 at extreme basic media (pH 12). This substantial peak height reduction is probably due to the copper (II) hydrolysis¹⁰. However, it was found that the peak potential for Cu (II)-RB171 exhibited a shift in the negative direction by 323 mV when pH was varied over the range 2–12. Meanwhile, the peak potentials for the Cu(II)-RR141 complex peak shifted about 33 mV pH⁻¹ unit in the negative direction over the pH range from 2 to 6. The cause for the observed negative shift is not fully understood, nonetheless, it has been suggested that as the concentration of OH⁻ and the ionisation degree of the ortho-hydroxy group nearby to the azo functional system rise with pH, Cu (II) complexes with more negative charges are formed. The repulsion between the negative charges and the HMDE makes the reduction of Cu (II) complexes more difficult¹¹.

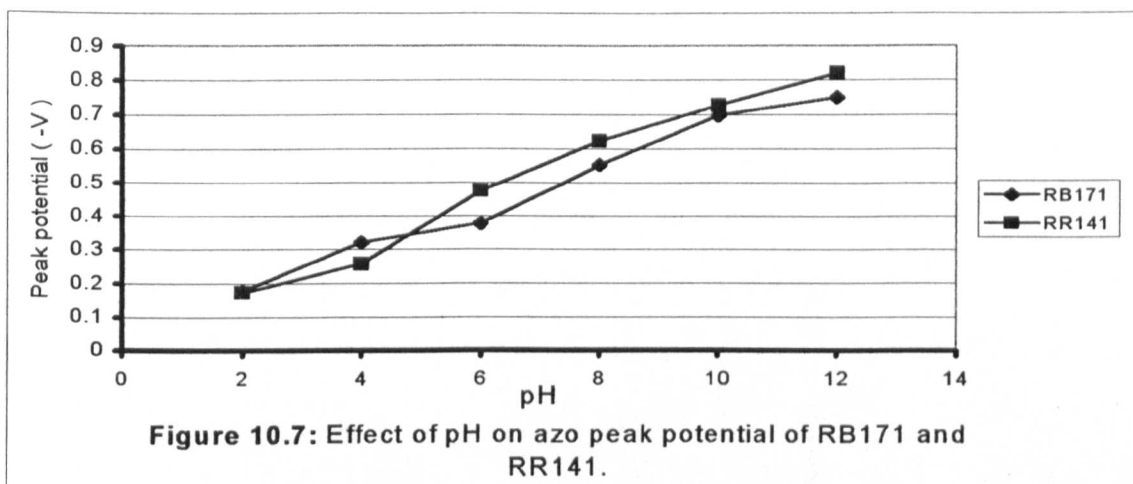
In the same way, the effect of the variation of the test solution pH value on the AdSV behaviour of the azo functional group for RB171 and RR141 was also evaluated. Figure 10.6 illustrates the influence of this experimental parameter (pH) on the azo peak current for the studied reactive dyes. In general, similar results and findings to that recently reported for the effect of pH on the AdSV peak height of Cu(II)/Reactive dye complexes were also obtained for the azo peak height of the free reactive dye ligands. To sum up briefly, the optimum pH value for monitoring both the azo group and the Reactive dye/Cu (II) electrochemical signals for RB171 is at acidic media (pH 2–4). By contrast RR141 is best measured by any of the two stripping voltammetric waves at higher pH values (pH 8–10), which assured good peak potential resolution between the complexed reactive dye and the free azo ligand. Finally, a shift of 60 mV pH⁻¹ and 68 mV pH⁻¹ to a more negative potential for the free reactive dye azo peak potentials for RB171 and RR141, respectively, with the



variation of pH over the range from 2 to 12, was observed and represented in Fig. 10.7. This negative shift in the azo peak potentials indicates a consumption of hydrogen ions in the electrode reaction. Table 10.2 summaries the effect of pH on the peak current and peak potential of Cu (II)-Reactive dye, azo and chlorotriazine signals for RB171 and RR141.

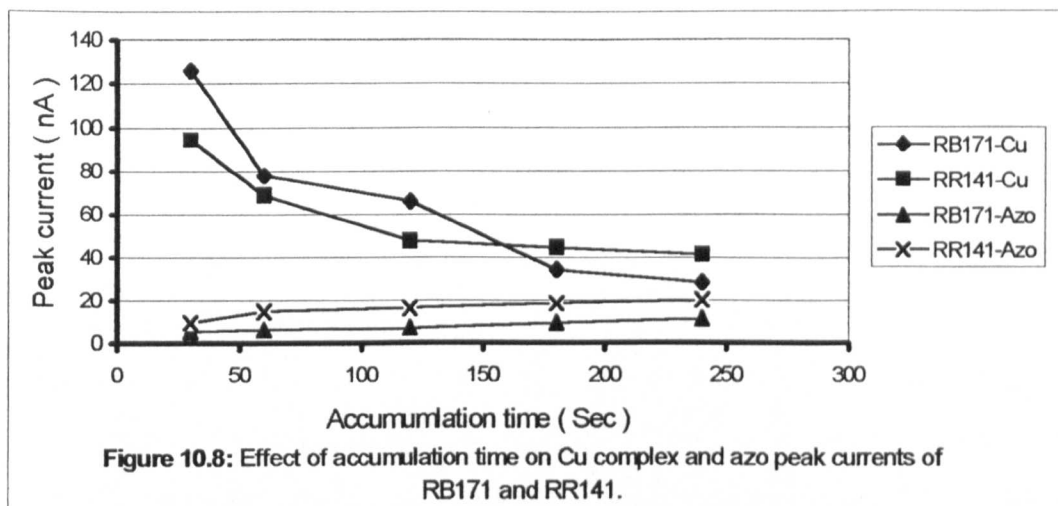
Table 10.2: Effect of pH on the studied bisazo reactive dyes' AdSV behaviour.

pH		Cu (II)/Dye peak		Azo peak		Chlorotriazine	
		E_p (-V)	i_p (nA)	E_p (-V)	i_p (nA)	E_p (-V)	i_p (nA)
RB171	pH 2	0.047	43.1	0.178	111.4	1.11	40.1
	pH 4	0.206	42.4	0.322	28.3	1.1	7.9
	pH 6	0.254	33.5	0.377	22.6	0.773	25.8
	pH 8	0.270	33.9	0.553	10.1	0.790	45.2
	pH 10	0.284	32	0.698	9	0.860	42.5
	pH 12	0.370	10.8	0.750	19.5	0.941	26.6
RR141	pH 2	Overlapped $E_p=0.173$ $i_p=110.5$				1.06	130.7
	pH 4	Overlapped $E_p=0.257$ $i_p=73$				1.15	95.1
	pH 6	0.305	26	0.475	8.5	1.05	26.3
	pH 8	.0305	37	0.622	19.9	1.08	54
	pH 10	0.305	48.7	0.728	40.6	1.08	61
	pH 12	0.305	20.5	0.820	7	1.160	10.3



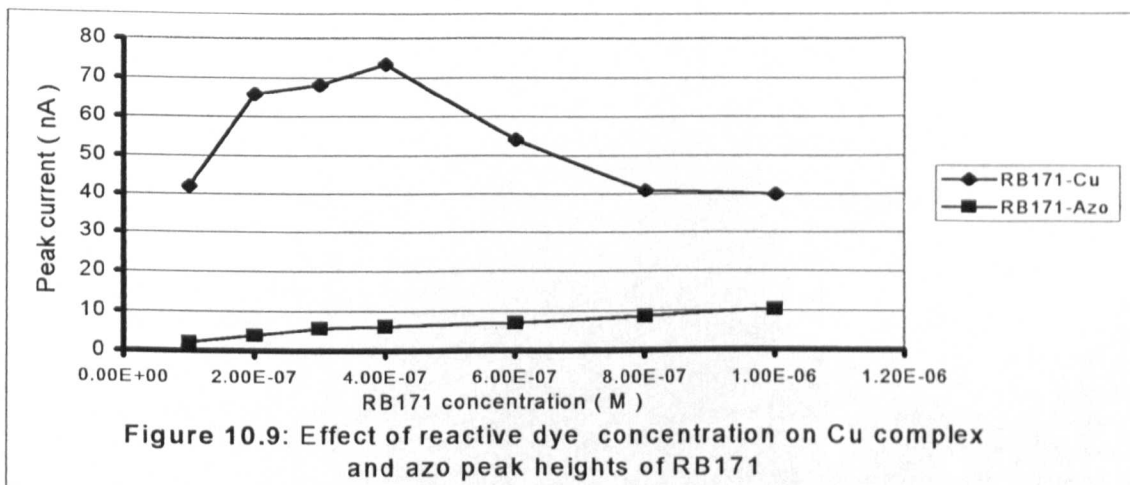
10.5.3 Effect of accumulation time and potential

Figure 10.8 shows the dependence of the adsorptive stripping peak currents of the Copper (II)/Reactive dye complex and the azo functional system for both analysed bisazo reactive dyes on the accumulation time parameter. It is apparent that the Reactive dye/Cu (II) complex was adsorbed effectively, even at very short collection times, compared to the adsorption process of the free ligands (Reactive dye). However, when applying longer accumulation periods, the complex peak height starts to decrease since the free reactive dye molecules are co-adsorbed competitively onto the adsorption sites at the surface of the HMDE. On the other hand, the peak current of the reduction process of the azo functional group increased almost linearly on extending the accumulation times up to 240s and 180s for RB171 and RR141, respectively. Beyond these accumulation times, the increase in the azo peak height levelled off. These deviations at longer accumulation times are due to the total coverage of the surface of the working electrode by a monolayer of the reactive dye deposits. A two-minute accumulation time was adopted for the AdSV analysis of both the investigated RB171 and RR141 compounds. Meanwhile, negligible effects for the accumulation potential on either the peak height or peak potential of Cu (II)/Reactive dye complex and azo group were observed. An accumulation potential of 0.0 V was selected as optimal for the subsequent investigations.



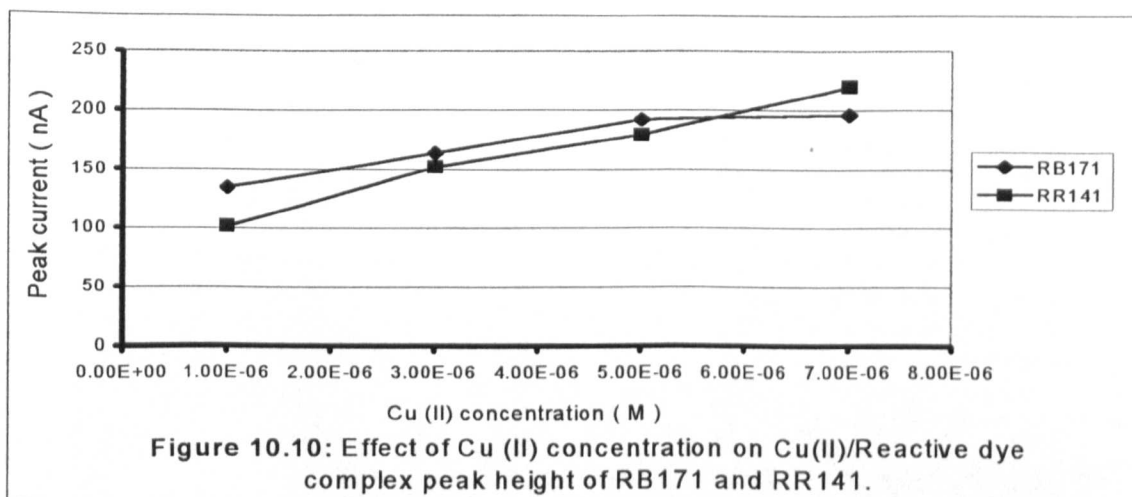
10.5.4 Effect of reactive dye concentration

The reactive dye concentration was varied between 1×10^{-7} and 1×10^{-6} mol Γ^{-1} in the presence of 1×10^{-6} mol Γ^{-1} copper (II) after two minute accumulation period in B-R buffer in order to optimise the analytical procedure. The dependence of the peak height of the azo group of the free RB171 and copper (II) complex AdSV signals on the reactive dye concentration is shown in Fig. 10.9. In the case of the Cu (II)/RB171 stripping voltammetric response, it was found that its peak current increased with RB171 concentration up to 4×10^{-7} mol Γ^{-1} , above which the Copper (II)/Reactive dye complex peak height decreased with the further addition of the reactive dye which compete for the adsorption sites at the HMDE. Whereas, the peak current of the reduction of the azo functional moiety increased linearly over the given RB171 concentration range. On the other hand, the peak potential of the azo systems of the free RB171 was negligibly affected by the variation of the reactive dye concentration, while the peak potential of the Cu (II)/RB171 complex peak exhibits a noticeable shift in the cathodic direction ($\Delta E_p = 182$ mV). Similar results were obtained for the Copper (II)/RR141 complex peak. The optimal reactive dye concentration for the following studies for the determination of copper (II) metal ions is, therefore, in the level of 4×10^{-7} mol Γ^{-1} reactive dye.



10.5.5 Effect of varying Cu (II) concentration

Similarly, the influence of the variation of copper (II) ion concentration over the range 1×10^{-6} to 9×10^{-6} mol l⁻¹ on the electrochemical behaviour of the Copper (II)/Reactive dye complex wave was also investigated. The peak height of these stripping voltammetric peaks for RB171 and RR141 were measured as a function of the Cu (II) concentration and represented in Fig. 10.10. As expected, the copper (II) complex peak heights for both RB171 and RR141 increased linearly with the continuous additions of copper (II) concentration. This increase reflects the increased formation of the Reactive dye/Cu (II) complex. There was no significant variation in the Copper (II)/Reactive dye peak potential for both reactive dyes when the concentration of Cu (II) increased from 1×10^{-6} to 9×10^{-6} mol l⁻¹. However, the test sample solutions were found to be contaminated with trace amounts of Cu (II), hence, the Cu (II)/ Reactive dye complex AdSV signal is observable even when no Cu (II) solution were added to the voltammetric cell.

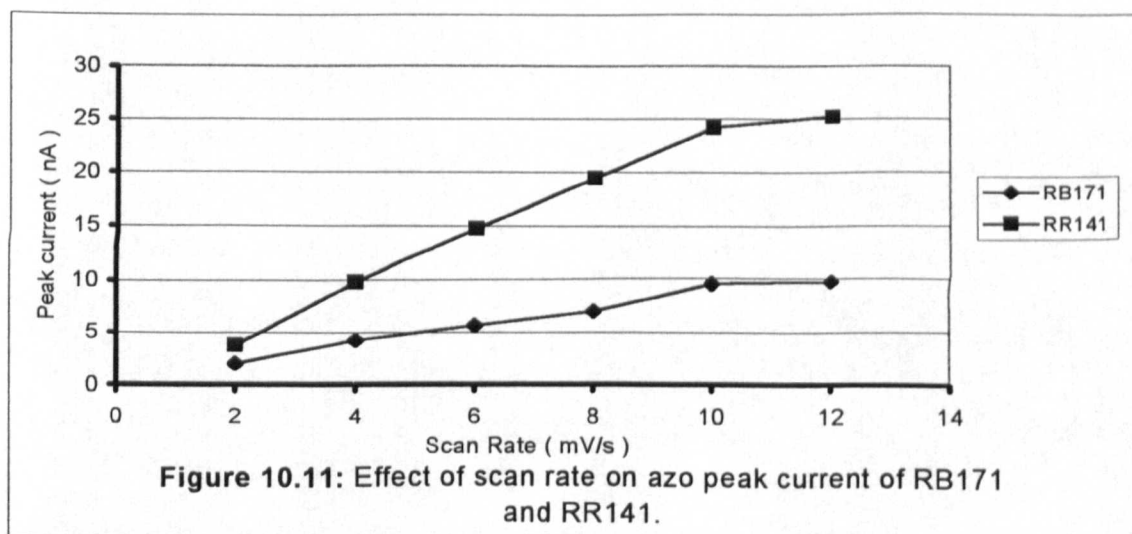


10.5.6 Effect of scan rate

Another experimental condition that affects the AdSV response of the Copper (II)/Reactive dye complex and the azo functional group is the scan rate parameter. The effect of scan rate on the stripping voltammetric peak currents of the Copper-complex and the azo system was examined over the 2-12 mV s^{-1} range and summarised in Table 10.3. It was observed that the cathodic peak height of Cu (II)/Reactive dyes complex for RB171 and RR141 increased linearly at first and then levels off. The linear increase is to be expected for the cathodic reduction for adsorbed material¹². However, the variation of scan rate has no significant effect on the Dye /Cu (II) peak potential for both bisazo reactive dyes. A scan rate of 6 mV s^{-1} was chosen as an optimal condition for the AdSV monitoring of the adsorbed Cu (II)/Reactive dye complex. In addition, this experimental parameter has a profound and considerable influence on the peak height of the second AdSV signal (azo wave) for RB171 and RR141, as can be seen from Fig. 10.11. When the scan rate was increased in steps from 2 to 12 mV s^{-1} , it was observed that the azo peak current enhanced substantially (nearly 5-6 times its initial value), whereas, the azo peak potentials were shifted in the negative direction by 74 mV and 58 mV for RB171 and RR141, respectively.

Table 10.3: Effect of scan rate on peak currents and peak potentials of RB171 and RR141.

Dye			Scan Rate					
			2 mV s ⁻¹	4 mV s ⁻¹	6 mV s ⁻¹	8 mV s ⁻¹	10 mV s ⁻¹	12 mV s ⁻¹
RB171	Cu/Dye peak	E _p (-V)	0.101	0.100	0.101	0.104	0.112	0.112
		i _p (nA)	68.1	78.5	85	89.1	91.5	93
	Azo peak	E _p (-V)	0.518	0.548	0.568	0.577	0.587	0.592
		i _p (nA)	1.97	4.3	5.7	7	9.5	9.7
RR141	Cu/Dye peak	E _p (-V)	0.140	0.140	0.140	0.140	0.140	0.140
		i _p (nA)	67.2	80	81.4	83.3	84.3	87
	Azo peak	E _p (-V)	0.591	0.608	0.620	0.633	0.635	0.649
		i _p (nA)	3.8	9.8	14.7	19.5	24.4	25.3



10.6 Quantitative Utility

The collective adsorption of the Reactive dye/Cu (II) complex can be used as an effective accumulation step prior to the voltammetric measurement. In this approach, highly sensitive measurements of RB171 and RR141 can be achieved by means of AdSV analysis of the Dye/Copper complex. A detection limit of 8.1×10^{-9} and 7.8×10^{-9} mol l⁻¹ for RB171 and RR141, respectively, were estimated from measurements of these reactive dyes at the optimum experimental conditions. Detection limits are calculated based on the signal-to-noise ratio of 3 (S/N=3). Furthermore, the reproducibility and stability of the proposed analytical procedure were also evaluated. For eight successive measurements of 1×10^{-7} mol l⁻¹ of each bisazo reactive dye, a relative standard deviation (RSD %) of 2.7% and 2.6% for RB171 and RR141, respectively, were estimated. Such precise behaviour is attributed to the reproducibility of the adsorption process of the complex, and to the use of a new drop of reproducible working electrode area in each run. The Copper (II)/Reactive dye complexes for RB171 and RR141 were found to be stable for at least two hours.

10.7 Interference Studies

Interference can be caused by co-existing metal ions capable of forming reducible chelates with RB171 or RR141. These may affect the free reactive dye and/or copper (II) complex response via an overlapping peak or may compete for adsorption sites. Hence, such interfering effects arising from various metal ions, organic surfactants, chelating agents and other reactive dyes were examined. Studies of interference were carried out with the recommended procedure in solution containing 1×10^{-6} mol l⁻¹ Cu (II) and after the addition of 10 μM of the interfering metal ions. No significant interferences were observed from the addition of 1×10^{-5} mol l⁻¹ Lead (II), Iron (II), Nickel (II), Cobalt (II), Zinc (II), Manganese (II), Selenium (IV), Tin (II), Indium (II), Aluminium (III), Titanium (IV), Sodium (II), Magnesium (II), Barium (II), Calcium (II) and Lithium (I). In addition, interference by organic surface-active compounds was tested with the model surfactant Triton X-100. The presence of surface-active substance could diminish the surface area of the HMDE available for Cu (II)-reactive dye complexes, and therefore, inhibit the adsorption

process. In the presence of 2 mg l^{-1} of the non-ionic Triton X-100, the height of the Cu (II)/Reactive dye peak was reduced by 31% and 50% for RB171 and RR141, respectively.

However, interfering effects of some chlorotriazine-based azo reactive dyes related to the studied RB171 and RR141 bisazo reactive dyes and which are expected to undergo complex formation with Cu (II) or compete on the adsorption sites, were also investigated. The sensitivity for the determination of $1 \times 10^{-7} \text{ mol l}^{-1}$ RB171 via its Cu (II) complex was reduced by 8%, 13% and 17% after the addition of $2 \times 10^{-7} \text{ mol l}^{-1}$ Reactive Orange 12, Reactive Red 24 and Reactive Red 120, respectively. Similarly, the presence of these interfering reactive dyes lead to a reduction of RR141/Cu (II) peak height by 9%, 13% and 13% respectively. Finally, the possible interfering effects of chelating substances were tested by adding EDTA to the sample solution. The Copper (II)/Reactive dye complex peak currents of $1 \times 10^{-7} \text{ mol l}^{-1}$ RB171 or RR141 were not affected when the ratio of Reactive dye : EDTA was equal to 1. Nonetheless, if the chelating agent was present at relatively high concentrations (e.g. $2 \times 10^{-6} \text{ mol l}^{-1}$), interfering by masking the available Cu (II) ions would be likely. In fact, it yielded nearly 10% reduction in the Cu (II)-Reactive dye peak height for both RB171 and RR141.

10.8 Practical Applications

The suitability of the developed method was tested by determining copper ions in two environmental samples; river water and tap water. Three successive standard additions to the test samples resulted in well-defined AdSV peaks (see Table 10.4). The Copper (II)/Reactive dye peak in the original sample can thus be quantified based on the resulting standard addition plot. The results for the determination of copper ions in river samples by using RB171 and RR141 as chelating agents were 8.2×10^{-6} and $7.5 \times 10^{-6} \text{ mol l}^{-1}$, respectively. However, the content of the copper ions in tap water samples was 7.5×10^{-6} and $8 \times 10^{-6} \text{ mol l}^{-1}$, respectively. These obtained results were approximately equivalent and in agreement with the reported results for the determination of copper ions by AdSV in similar environmental samples after their complexation with heterocyclic azo compounds⁵.

Table 10.4: Standard addition method for the measurement of Cu (II) ion in real practical samples via it Cu (II)/Reactive dye AdSV signal.

Sample	Standard Additions	Cu(II)/Dye Peak Current (nA)	
		RB171	RR141
Tap Water	a = Test Sample	130	183
	a+1 x 10 ⁻⁶ M Cu(II)	138	215
	a+3 x 10 ⁻⁶ M Cu(II)	183	236
	a+5 x 10 ⁻⁶ M Cu(II)	215	302
River Water	b = Test Sample	118	151
	b+1 x 10 ⁻⁶ M Cu(II)	136	156
	b+3 x 10 ⁻⁶ M Cu(II)	149	196
	b+5 x 10 ⁻⁶ M Cu(II)	180	239

10.9 Conclusions

The present study described an effective means for the determination of low levels of two chlorotriazine-based bisazo reactive dyes (RB171 and RR141) based on their copper (II) complexes, by differential-pulse adsorptive stripping voltammetry. The two bisazo reactive dyes formed a Cu(II)-Reactive dye complex which effectively adsorbed onto the HMDE. However, the free reactive dyes can be monitored also via their azo functional and/or chlorotriazine reactive signals. The study pointed out that only one azo functional system of RB171 appears to undergo complex formation with Cu (II) ions, whereas, RR141 has two azo systems that can develop a chelating reaction with Cu (II). Experimental parameters for adsorptive stripping analysis of these reactive dyes have been verified and their conditions have been optimised. Detection limits as low as 8.1×10^{-9} and 7.8×10^{-9} mol l⁻¹ for RB171 and RR141, respectively, can be detected by AdSV in the presence of copper ions. The proposed method is nearly a selective approach for the determination of copper ions since no significant interferences from other metal ions were observed, nonetheless, organic surface-active agents severely interfere by inhibiting the adsorption of the Cu(II)/Reactive dye complex. In addition, chelating agents such as EDTA and other reactive dye molecules would also interfere. Finally, the applicability of the developed procedure for the direct measurement of copper ions in two practical samples was demonstrated.

REFERENCES

1. Fogg, A.G., Rahim, A., Yusoff, H.M and Ahmad, R., *Talanta*, **44**, (1997), 125.
2. Sarzanini, C., Abollino, O., Bruzzoniti, M.C. and Mentasti, E., *J. Chrom.*, **804**, (1998), 241.
3. Zhao, J. and Sun, D., *Anal. Chim. Acta*, **268**, (1992), 293.
4. Farias, P.A., Ferreira, S.L.C., Ohara, A.K., Bastos, M.B. and Goulart, M.S., *Talanta*, **39**, (1992), 1245.
5. Cakir, O. and Bicer, E., *Electroanalysis*, **9**, (1997), 87.
6. George, W. and Latimer, J.R., *Talanta*, **15**, (1968), 1.
7. Florence, T.M., *J. Electroanal. Chem.*, **52**, (1974), 115.
8. Florence, T.M., and Belew, W.L., *J. Electroanal. Chem.*, **21**, (1969), 157.
9. Braininina, K.H. and Neyman, E., *Electroanalytical Stripping Methods*, John Wiley and Sons, NewYork,1993.
10. Van den Berg, C.M.G., Househam, B.C. and Riley, J.P., *J. Electroanal. Chem.*, **239**, (1988), 137.
11. Song, M., Ma, H., Huang, Y. and Liang, S., *Anal. Chim. Acta*, **338**, (1997), 103.
12. Bard, A.J. and Faulkner, L.R., *Electrochemical Methods*, John Wiley and Sons, NewYork,1980.

GENERAL CONCLUSIONS

11.1 Final Conclusions

AdSV is one of the stripping voltammetric techniques that has received considerable attention over the last two decades. The high sensitivity, the wide applicability of the method and the relatively inexpensive instrumentation are some of the attractive features of the AdSV technique over other analytical methods. This electroanalytical method is based on the nonelectrolytic accumulation (adsorption) of the analyte followed by a cathodic reductive scan measurement. In fact, AdSV has shown in recent years its suitability and superiority for monitoring numerous analytes and particularly synthetic dyes that exhibit surface-active properties. The present study has been devoted to investigate the AdSV behaviour and analysis of several reactive dyes with their attempted hydrolysed forms and metal ion complexes at nanomolar concentration levels.

AdSV has been successfully used for monitoring and studying the anthraquinone-based reactive dye (Reactive Blue 19). The stripping voltammograms of this reactive dye exhibited either one or two AdSV peaks depending on the pH value of the supporting electrolyte. The first well-developed cathodic reduction peak was related to the two-electron reversible reduction of the anthraquinone moiety. However, a further AdSV peak was observed when alkaline solutions or carbonate buffer were used, due to the cathodic reduction of anthrone product, which is yielded from a tautomeric rearrangement. Hence, Reactive Blue 19 can be determined directly via its AdSV signals corresponding to the anthraquinone and/or anthrone groups. With respect to the electrochemical reduction of the anthraquinone group, its stripping voltammetric peak is observed when the linear sweep mode is used or when applying the differential pulse mode in the presence of boric acid. The absence of the anthraquinone signal in the differential pulse mode is believed to occur because, when this functional group is reduced in the adsorbed state, it is reduced so rapidly that reduction is complete before the current is monitored at the end of the pulse. This

electrochemical behaviour is in good agreement with the Komorsk-Lovric theory that indicates that for a very fast and reversible reduction of an adsorbed species, which yields an adsorbed product, reduction of the adsorbed species occurs immediately the pulse is applied and that no faradaic current remains when the current is monitored near the end of pulse application. On the other hand, the sulfatoethylsulfone or vinylsulfone reactive systems show no electrochemical activity for all the used supporting buffers.

Meanwhile, the cyclic voltammetric studies of Reactive Blue 19 confirmed that the reduction of the first anthraquinone wave was a reversible process. In contrast, the absence of the anodic peak, coupled with the cathodic peak related to the reduction of anthrone product, indicates the irreversible characteristic of this product. In fact, the differential pulse AdSV and cyclic voltammetric behaviours of Reactive Blue 19 were very similar and identical with the corresponding electrochemical behaviours and results reported for structurally similar anthraquinone-based reactive dyes (Procion Blue MX-R and Cibacron Blue 3GA). The effect of pH over the range 2-12 on the well-defined AdSV peak (anthraquinone peak) was also studied. The anthraquinone signal was observable in all neutral, acidic and alkaline solutions. Clearly, both the peak potential and height of this electrochemical group are pH dependent. Its peak potential shifted to more negative values when pH value was increased. In addition, when measuring the anthraquinone peak current of Reactive Blue19 as a function of accumulation time or reactive dye concentration, a linear relationship was observed. Similarly, the influence of various experimental conditions and instrumental parameters was also evaluated and discussed in detail. The possible differentiation between the original reactive dye and its hydrolysed and intermediate vinylsulfone forms was also attempted. Nonetheless, owing to the absence of stripping voltammetric signal of the sulfatoethylsulfone reactive group, the discrimination between these different forms is limited when direct measurement by AdSV was applied without prior separation.

Furthermore, the present study evaluated the influence of several surfactants on the adsorptive stripping response of anthraquinone group of Reactive Blue 19 molecules adsorbed onto the HMDE. It was found that many surface-active substances interfere severely with the AdSV signal of the analysed reactive dye. Surfactants compete with the analysed reactive dye for the adsorption sites on the HMDE, which can lead to a co-adsorption problem for the AdSV analysis. The

inhibition of the electrode reaction of the anthraquinone group by the presence of Glycerol, Sorbitol, TPPC and Triton-X surfactants was observed, resulting in a decreased peak current. In comparison, the addition of these surfactants has no significant effect on the shape and peak potential of the anthraquinone AdSV signal. On the other hand, the addition of Gelatine at low concentrations leads to a catalytic enhancement influence on the analytical signal, yet another suppressive action was noticed at high Gelatine concentrations. In fact, similar AdSV behaviours of several synthetic dyes in the presence of Gelatine were reported in the literature.

The type and overall charge of the surfactants have a considerable effect on the monitored anthraquinone peak current. The cationic surfactant TPPC exhibited a noticeable inhibition influence on this electrochemical signal. In contrast, the anionic surfactant Aerosol OT enhanced and improved the anthraquinone peak current. The contribution of several experimental conditions on the peak height of the tested reactive dye in the presence of surfactants was also evaluated. As a result, some experimental parameters can be adjusted so that the inhibition action of the surfactant is minimised and a significant recovery of the analytical signal of interest is gained. For instance, short accumulation time (< 3 min), proper choice of pre-concentration potential ($E_{acc} = -0.3$ V) and pH value over the range 8-10 are recommended as an optimal conditions to reduce the surfactants coadsorption problems.

Besides the vinylsulfone-based anthraquinone reactive dye, other reactive dyes with different reactive systems and chromophore groups were also investigated in detail. Fluorotriazine-based azo reactive dyes were monitored in Britton-Robinson buffer (pH 8) after 2 minutes accumulation at 0.0 V. The analysed four fluorotriazine reactive dyes exhibited two adsorptive stripping peaks, which are associated with the reduction of the azo functional group and fluorotriazine reactive system. However, the azo AdSV signal was more favoured for the subsequent electroanalytical application, due to its well-developed peak shape, large AdSV response and its peak potential location far from the electrolyte discharge wave. Apart from the poor and small stripping voltammetric peak for the fluorotriazine reactive group, the AdSV behaviour of these fluorotriazine-based azo reactive dyes was approximately comparable to that for other structurally similar chlorotriazine-based azo reactive dyes. Preliminary studies for these reactive dyes indicated that the variations of the chemical structure around the azo functional group has a significant effect on its peak potential. For instance, fluorotriazine-based azo reactive dye 4 has a weak electron-releasing

NHCONH₂ group on the ortho position to the azo group which slightly increase the electron density and hence relatively facilitates the reduction process of the azo group. In comparison, fluorotriazine reactive dye 1 has a strong electron-releasing methoxy group substituent, which restrains and delays the electrochemical reduction process. This was reflected in the less negative peak potential for fluorotriazine reactive dye 4 compared to fluorotriazine reactive dye 1. As a result of these peak potential variations, the developed AdSV procedure was successfully applied to the simultaneous determination of more than two fluorotriazine reactive dyes in mixtures.

These studied fluorotriazine-based azo reactive dyes can be analysed by the proposed AdSV method down to the ng l⁻¹ level with satisfactory small relative standard deviations (1.2–1.6%). Although the reactivity of the fluorine atom substituent on the triazine group is theoretically high, however, the electrochemical distinction between the original fluorotriazine-based azo reactive dyes and their hydrolysed products was not promising or adequate, due to the continuance of the fluorotriazine AdSV signal after the attempted hydrolysis process. However, despite the various attempts to uncover the reasons for such AdSV behaviour of the fluorotriazine group, the cause for this observation is not fully understood at this stage. In fact, it should be borne in mind and recalled that the electrochemical behaviour of the unhydrolysed (original) reactive dye gave a broad ill-developed AdSV peak for the fluorotriazine reactive system, hence, the attempted hydrolysis reaction may not effect its peak current considerably. Nonetheless, a further more detailed and comprehensive electrochemical and UV spectroscopic studies should be carried out to try to explain the cause for such AdSV behaviour.

In addition to the direct analysis of the fluorotriazine-based azo reactive dyes via their azo and/or fluorotriazine AdSV peaks, these reactive dyes can be monitored by their catalytic-AdSV signals in the presence of nickel (II) ion. The applied procedure is based on the effective interfacial accumulation of Ni (II)/Fluorotriazine dye complex onto the HMDE and the catalytic reduction of the adsorbed complex. After the latter electrochemical reduction process, the initial Reactive dye/Ni (II) complex is regenerated by the homogeneous chemical reaction and undergoes further electrochemical process. Consequently, a favourable peak current enhancement is gained as a result of this catalytic cycle. Indeed, these fluorotriazine reactive dyes in the presence of Ni (II) ion, exhibited a new well-defined catalytic-AdSV peak at -0.82 V, which was suggested to be related to the reduction of Ni (II) in the adsorbed

complex. This observed AdSV peak was much larger and greater than the conventional AdSV peak corresponding to the free ligand (reactive dyes). Various experimental conditions that effect the catalytic-AdSV properties of these fluorotriazine reactive dyes have been evaluated and optimised. Clearly, the catalytic peaks current increased linearly when measured as a function of accumulation time, reactive dye concentration and nickel ion concentration. However, most of the tested metal ions that were present in the test solutions as a co-existing interferences, did not cause any significant effect when existing at low concentrations on the catalytic response of nickel ion. Nevertheless, surface-active substances such as Triton X-100, TPPC and Aerosol OT have a considerable inhibition influence on the electrochemical signal of interest.

In recent years, a new class of bisazo dyes have been developed and introduced to the dye industry. The bichlorotriazine-based bisazo reactive dyes are a representative for this new class of azo dyes, which are composed of bifunctional azo chromogen groups and bifunctional chlorotriazine reactive systems. In view of the importance of investigating the electrochemical characteristic and property of these chlorotriazine reactive dyes, a comparison study between the AdSV behaviour of the double anchor-based bisazo reactive dyes with the AdSV behaviour of a structurally similar monoazo reactive dye with single chlorotriazine anchoring system was carried out. Accordingly, the AdSV behaviour of two double anchor-based bisazo reactive dyes (Reactive Orange 12 and Reactive Red 120) were compared with the AdSV behaviour of two chlorotriazine-based monoazo reactive dyes (Reactive Yellow 84 and Reactive Red 24, respectively). Preliminary studies indicated that for the chlorotriazine reactive dyes when accumulated at 0.0 V for two minutes, their adsorptive stripping voltammograms exhibited two well-separated, well-defined electrochemical waves associated with the reduction of the azo and chlorotriazine groups. However, it appeared that the peak current of the AdSV peaks for the bisazo reactive dyes, Reactive Orange 12 and Reactive Red 120, were more enhanced (nearly twice) that observed for the monoazo reactive dyes, Reactive Yellow 84 and Reactive Red 24, owing to the duplication of the presence of chromophore and anchoring systems. As a result of this enhancement in the peak current of the azo and chlorotriazine groups for the bisazo reactive dyes, a significant improvement on the AdSV detection of the new class reactive dyes at ultratrace-levels measurements via their azo and/or chlorotriazine signals is expected.

It is worthwhile to mention that due to the symmetrical molecular structure of these chlorotriazine bisazo reactive dyes and the invariability of the chemical environment around each azo or chlorotriazine groups, only a large single AdSV peak was observed for the azo functional group or chlorotriazine reactive system. Optimum experimental conditions were also evaluated and reported in detail. On the whole, the hydrolysis studies for these chlorotriazine reactive dyes indicated that the hydrolysis process was slow. In fact, after 4 hours of the hydrolysis, nearly half the initial chlorotriazine reactive group peak heights for most of the tested chlorotriazine reactive dyes remained.

Finally, the preconcentration of the copper (II) complexes of some chlorotriazine-based bisazo reactive dyes (Reactive Blue 171 and Reactive Red 141), followed by a quantitative AdSV measurement, can be used as an indirect analysis method for these chlorotriazine bisazo reactive dyes via their further Cu (II)/Reactive dye complex signal. The Cu (II)/Reactive dye complexes were found to be adsorbed effectively onto the HMDE prior to the cathodic reduction of the copper (II) ion in the adsorbed complex. Both the chlorotriazine-based bisazo reactive dyes, RB171 and RR 141, have at least one azo functional moiety with ortho-hydroxy group capable of undergoing the Ligand/Metal ion complex formation. Accordingly, the adsorptive stripping voltammograms of both chlorotriazine-based bisazo reactive dyes exhibited a new well-defined AdSV peak, which are believed to be related to the reduction of Cu (II) in the formed complexes. However, the free reactive dyes can be monitored also via their azo and/or chlorotriazine AdSV signals. Owing to the symmetrical molecular structure of Reactive Red 141 (i.e. both the azo moieties had an ortho-hydroxy group), both the azo centres can act as a chelating agent and hence undergo Cu (II) complex formation. In contrast, Reactive Blue 171 has only one azo centre with *o*-hydroxy substitution, thus, the second half with *o*-amino group may not be applicable and suitable for the subsequent copper complex formation.

In order to maximise the Cu(II)/Reactive dye electrochemical response, several experimental parameters must be optimised. An acidic solution with pH values 2-4 was found to be an optimal condition that ensured high sensitivity for the analysis of Reactive Blue 171 via its Cu (II) complex. Meanwhile, for Reactive Red 141, it appeared that pH values within the range 8-10 can secure 0.3-0.4 V peak potential resolution between the complex peak and free ligand azo peak with reasonable peak currents. The peak current of Reactive dye/Cu (II) complex increased linearly, when

measured as a function of the chlorotriazine reactive dyes and copper (II) ion concentrations. Nonetheless, deviations from linearity due to the saturation of the HMDE, were observed at higher reactive dye concentrations or when applying long accumulation times. In most cases, no significant interference was observed after the addition of 10-100 fold concentrations of numerous metal ions. However, as was the case with previous AdSV signals associated with the reduction of anthraquinone, azo and halo-triazine groups, surface-active substances severely interfere by inhibiting the adsorption collection of the Cu (II)/Reactive dye complex.

11.2 Further Studies

Clearly, AdSV is sufficiently and satisfactorily useful as a research tool to offer a means for studying and monitoring various reactive dyes (or organic molecules/metal ions). Therefore, the AdSV behaviour and property of a range of new reactive dyes could be investigated in further work. A similar research study and strategy can be extended to other reactive dyes including azo or anthraquinone-based dyes with fluorotriazine, chlorotriazine or sulfatoethylsulfone reactive systems. For instance, fluorotriazine-based reactive dye with anthraquinone chromophore group might be an ideal candidate that can be compared with the chlorotriazine-based anthraquinone reactive dyes (Procion Blue MX-R and Cibacron Blue 3GA), that are well studied in the literature. Similarly, a more detailed electrochemical evaluation of the characteristic of the bifunctional and double-anchoring reactive dyes, is another field of interest. Once again, a double-anchoring system based on a fluorotriazine reactive group will be a preferable example. In addition, it is also intended to study the complexes of these bisazo reactive dyes with various metal ions other than copper (II) ion. In fact, the dual adsorptive-catalytic enhancing action in the presence of nickel (II) for the indirect analysis of bisazo reactive dyes is theoretically expected to improve the analysis of the bisazo reactive dyes substantially and profoundly.

Surely, the slow hydrolysis reaction problem recognised and noticed in this present study for the fluorotriazine and chlorotriazine reactive systems, needs further detailed investigation, in order to identify and define the cause and the source for the obtained odd hydrolysis behaviour. Hence, a comprehensive electrochemical evaluation for all the various hydrolysis experimental conditions applied on a recent and new reactive dye samples, together with a more detailed UV spectroscopic study of the progress of the hydrolysis process, are some of the suggestions and recommendations for further studies.

Likewise, to overcome the limitation in distinguishing between the Reactive Blue-19 and its hydrolysis/methanolysis and/or structurally similar anthraquinone-based reactive dyes, an alternative electroanalytical approach that can secure a desirable discrimination between these different compounds and forms, can be accomplished by applying different square wave frequencies. It is possible that by

employing such a strategy at selected SW frequencies, the stripping voltammetric peak potential shifts for these various forms may be different enough to assure reasonable differentiation between these different compounds and forms. Such expectations are based on the view of observations reported by a research team in Porto University, Portugal (Barros and co-workers). They demonstrated that by applying the mentioned electrochemical procedure, analytical discrimination between two substances with very similar reduction potentials could be achieved.